66082
v2

Ulaanbaatar, Mongolia, Air Monitoring and Health Impact Baseline (AMHIB) Report

Annex A

Particulate Matter Concentrations/Baseline in Ulaanbaatar
June 2008 – May 2009[1]

Introduction

The purpose of this Annex is to present the measurements of particulate matter (PM_{10} and $PM_{2.5}$) that was carried out under the AMHIB study during the period June 2008–May 2009. There were 8 monitoring stations in operation under the AMHIB umbrella during the entire period, although some shorter periods were not covered at some stations due to instrument non-availability or operational problems. In addition, four German donor stations (called GTZ stations) were in operation starting in November/December 2008.

The results of the measurements provide a basis for assessing the ranges of concentrations of PM_{10} and $PM_{2.5}$ that were experienced in Ulaanbaatar (UB) during the AMHIB measurement period, separately for ger and non-ger areas.

The instrumentation for PM measurements at the AMHIB stations was based on what was available in Ulaanbaatar in 2008, owned and operated by various institutions with mandate for and research interest in air pollution monitoring. As a result, the stations were equipped with instruments of different types and measurement principles. Financial and time constraints prevented the complete set up of a state-of-the-art monitoring network with uniform instrumentation. Preparations for the monitoring program revealed that the various instruments gave differing results, which was due to sampling and measurement artifacts of the various instruments. In order to provide a basis for comparable and as correct as possible results from the different stations, instrument inter-comparison campaigns were carried out during 4 different weekly periods during the year. The inter-comparison results could be used to develop data correction procedures to arrive at a common basis for the data from most of the stations.

Nonetheless, these instrument problems cause an uncertainty in the PM monitoring results. Due to these problems and the resulting uncertainty, the appropriate procedure is to first present the data in this Annex as they were measured, without corrections (Chapter A3). Then, after applying the correction procedure, the corrected data are presented and the PM concentration levels in Ulaanbaatar under the AMHIB period is assessed (Chapter A5). The uncertainty caused by the instrument issue has been estimated. It is judged that the quality of the assessment of the PM concentrations in Ulaanbaatar is acceptable, and gives an adequate basis for assessing the health effects of the PM concentrations as well as to support the analysis of the effects of abatement measures.

The corrected results provide a basis for comparison between measured and modeled concentrations using air pollution dispersion models (see Annex C). The air pollution modeling efforts presented in Annex C provide a more complete picture of the spatial variations of the PM concentrations in the UB area, and a more complete basis for the assessment of health effects and effects of abatement measures.

The Annex also contains recommendations regarding continuing air quality monitoring in Ulaanbaatar (Chapter A8).

[1] This report was written by the following World Bank consultants under the AMHIB project: Steinar Larssen, Sereeter Lodoysamba,.Li Liu Dagva Shagjjamba and Gunchin Gerelmaa. It was peer reviewed by Dick van den Hout, Netherlands Organization for Applied research/TNO, Sameer Akbar, World Bank, M. Khaliquzzaman, World Bank consultant and Taizo Yamada, JICA. World Bank Task Team Leaders were Jostein Nygard and Gailius Draugelis.

Table of Contents

A1 AMHIB monitoring network, data collection and data quality assessment

AMHIB monitoring network

Monitoring sites for AMHIB project are shown in Figure A.1. They were selected by UB experts based upon the knowledge of the spatial air pollution distribution in Ulaanbaatar (UB) from data from stationary monitoring stations existing prior to the start of the AMHIB (operated by NAMHEM, CLEM- NAMHEM, NRC-NUM), the geography/topography situation of UB, population density representations and the locations of family hospitals participating in the project. Before AMHIB monitoring started, PM measurements had already been carried out at the CLEM station (PM_{10}), at the NAMHEM site ($PM_{2.5}$ and PM_{10}) and at the NRC site ($PM_{2.5}$ and $PM_{10\text{-}2.5}$). The other sites (3, 4, 6, 7 and 8) were chosen near the family hospitals participating in the health study.

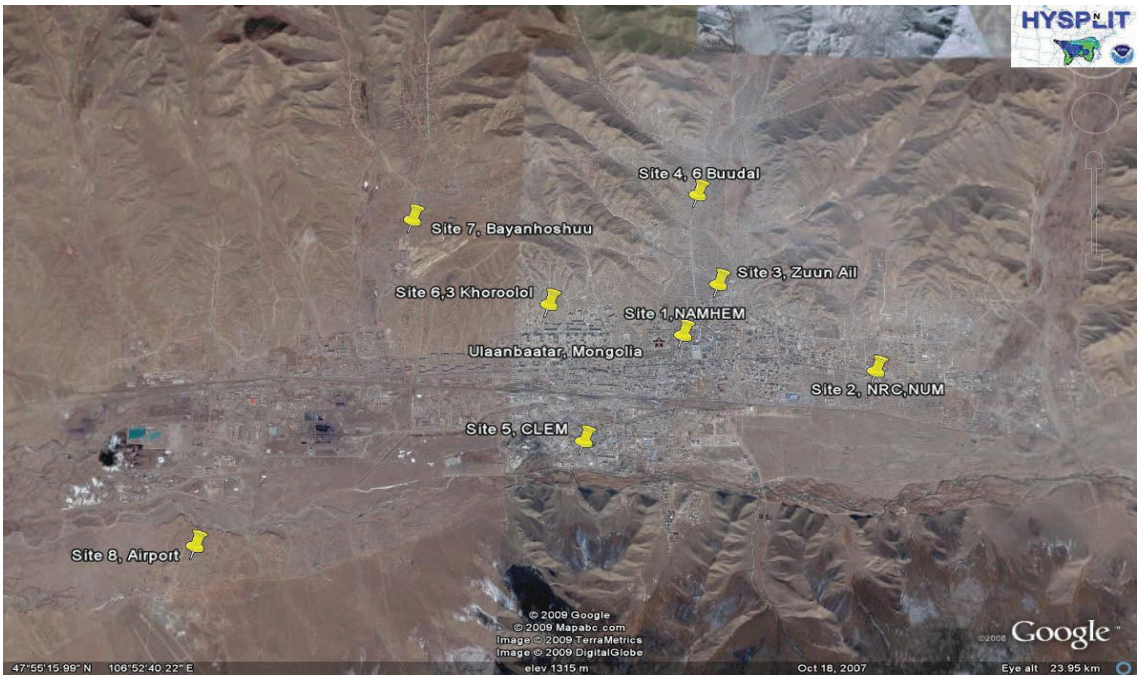

Figure A.1 Location of AMHIB sampling sites.

All monitoring equipment available from various agencies in Ulaanbaatar was collected and mobilized for the measurement of air pollution concentration at the 8 sites. The instruments and samplers are of different makes and utilize different measurement principles. Financial limitations as well as time restrictions prevented the establishment of a monitoring network with state-of-the-art monitors in all locations. It will be clear from the data presentations below that the instruments used have various sampling artifacts and shortcomings, which need to be taken into account when evaluating the results.

Instrument inter-comparison campaigns have been carried out under the AMHIB study. The Data Quality Assessment section below summarizes briefly the results in terms of the corrections that were found and which needed to be introduced for some of the results. This is further referred to in Annex F where the details of the inter-comparisons and the data correction procedures are described.

An additional monitoring network of 4 stations was established by GTZ towards the end of 2008, and the network started to deliver data in late November 2008. This network has provided additional very useful data on the air pollution situation in UB. The data are presented and discussed in section A4.

Table A.1 shows positions of the AMHIB monitoring sites, characteristics of samplers, height of inlet of samplers and PM size fraction collected at each site. Both PM size fractions ($PM_{2.5}$ and PM_{10}) are measured at 3 sites (sites 1, 2, and 3). PM_{10} only is measured at additionally 2 sites (5 and 6) while $PM_{2.5}$ only is measured at additionally 3 sites (4, 7, and 8). At sites 2 and 3, PM_{10} is determined as the sum of the fine ($PM_{2.5}$) and the coarse ($PM_{10\text{-}2.5}$) fractions. Filters from sites 2, 3 and 6 are used for black carbon determination and processed for elemental analysis (see Annex B).

Table A.1 AMHIB monitoring sites, positions, size fractions monitored, and characteristics

Sampling site number	Characteristics	Site position	PM size fraction	Height of sampling head from the ground (m)	Remarks
1	Kosa Monitor (Japanese make), Measures PM_{10} and $PM_{2.5}$. Beta absorption. Continuous monitoring. Gives hourly values. Dust Trak-8520, measures $PM_{2.5}$ or PM_{10}. Laser light scattering. Continuous monitoring. Gives hourly values.	106°54,704 47°55,220	PM_{10} and $PM_{2.5}$	20	From December 2008
2	GENT Sampler, Schulberger Model 250, Measures $PM_{10\text{-}2.5}$ and $PM_{2.5}$. Polycarbonate (nuclepore) filters.	106°58,311 47°54,811	$PM_{10\text{-}2.5}$ and $PM_{2.5}$	1.6	Elemental analysis, Black carbon determination
3	GENT Sampler, Schulberger Model 250. Measures $PM_{10\text{-}2.5}$ and $PM_{2.5}$. Polycarbonate (nuclepore) filters.	106°55,343 47°55,975	$PM_{10\text{-}2.5}$ and $PM_{2.5}$	6	Elemental analysis, Black carbon determination
4	Dust Trak-8520, measures $PM_{2.5}$ or PM_{10}. Laser light scattering. Continuous monitoring; Gives hourly values.	106°54,159 47°54,719	$PM_{2.5}$	3	
5	Rotary Bebicon, Type 35RC-28SD5 (Japanese make). Measures PM_{10}, 15 l/min, filter.	106°52,967 47°53,64	PM_{10}	3	Replaced by EcoTech monitor (beta absorption) from Nov.2008
6	Partisol FRM-Model 2000, Measures PM_{10}, 16.7 l/min, filter (nuclepore).	106°52,167 47°55,582	PM_{10}	4	Fiber filter before December, then Nuclepore filter Elemental analysis, Black carbon determination
7	Dust Trak-8520, measures $PM_{2.5}$ or PM_{10}. Laser light scattering. Continuous monitoring; Gives hourly values.	106°49,485 47°56,732	$PM_{2.5}$	2	
8	Dust Trak-8520, measures $PM_{2.5}$ or PM_{10}. Laser light scattering. Continuous monitoring; Gives hourly values.	106°45,749 47°51,865	$PM_{2.5}$	3	

Description of the station locations:

1. NAMHEM: located at the roof of the NAMHEM building in central UB, about 20 meters above ground. Sample air is drawn through a tube, of a length of about 5 meters, to instruments located inside.
2. NRC: Located at the NRC building, away from direct traffic influence, away from large ger areas. Air intake 1.6 meters above ground. Open soil surfaces and spread out buildings are surrounding the station.
3. Zuun ail: Located at the southern mouth of a low-lying extended valley of ger areas, away from direct traffic influence. Air intake is about 6 meters above ground. Immediate surfaces are mostly grass or asphalt covered. Exposed to emissions from the ger areas as cold air drains down through the valley towards the area of the station.
4. 6 Buudal: Located at a local family health centre well within a ger area, about 50 meters west of a main road. Air intake is about 3 meters above ground. Gers and open soil and road surfaces surrounding.
5. CLEM: Located at the CLEM laboratory, away from traffic influence and ger areas. Air intake is about 3 meters above ground. Grass covered surfaces surrounding.
6. III Khoroolol: Located on the second floor balcony of a small house, well within a ger area. Air intake is about 4 meters above ground. Gers and open soil and road surfaces surrounding.
7. Bayan Hoshoo: Located at a local family health centre well within a ger area, about 100 m east of a main road. Air intake is about 2 meters above ground. Gers and open soil and road surfaces surrounding. A large brick factory nearby, which does not operate during the winter season.
8. Airport: Located at the roof of a small dwelling house, well within a ger area, about 200 m east of a main road. Air intake is about 3 meters above ground. Gers and open soil surfaces surround the location.

Stations 4, 6, 7 and 8 are located within ger areas, at local hospitals with gers and small houses surrounding, except station 6 which was located on a ger house. Typical distances to ger chimneys were 10 meters or further, except at station 6 where the nearest chimney was very near, but its height was sufficiently extended so as to not affect the instrument air intake.

PM sampling

The sampling was conducted on two days per week, Wednesday and Sunday, throughout the project period 1 June 2008 – 31 May 2009. From October 2008 sampling was additionally carried out every day in the last week of every month: 26 October–3 November, 24–30 November, 28 December–03 January, 25–31 January, 27 February–04 March and 25 March–01 April.

Sampling schedule at each site is shown in Table A.2.

Table A.2 Duration of monitoring at each sampling site and samplers used

Years					2008							2009				
Organization	Site name	Site No	Type of Sampler	PM Type	June	July	August	September	October	November	December	January	February	March	April	May
NAMHEM	NAMHEM	1	Kosa	PM_{10}												
				$PM_{2.5}$												
			Dust trak	$PM_{2.5}$												
NUM	NRC	2	GENT	$PM_{10-2.5}$												
				$PM_{2.5}$												
NUM	Zuun Ail	3	GENT	$PM_{10-2.5}$												
				$PM_{2.5}$												
CLEM	6 Buudal	4	Dust trak	$PM_{2.5}$												
UB AQB			Dust trak	$PM_{2.5}$												
CLEM	CLEM	5	Rotary Bebicon	PM_{10}												
			Eco tech	PM_{10}												
NAMHEM	III Khoroolol	6	Partisol	PM_{10}												
CLEM	Bayan Hoshuu	7	Dust trak	$PM_{2.5}$												
CLEM	Airport	8	Dust trak	$PM_{2.5}$												
UB AQB			Dust trak	$PM_{2.5}$												

Measurements at sites No 4 and No 8 were interrupted during July and August, due to sampler problems. Measurements at site No 7 were started from September 2008.

Measurement Data Quality Assessment

QAQC procedures

The PM measurement equipment of the AMHIB network is provided by the various institutions involved, and differs between the various stations. The instruments utilize different measurement principles. Each institution operated the stations and instruments where their own instruments where used. Individual instruments were operated according to their instruction manual. The local AMHIB monitoring team coordinated the monitoring activities and agreed on the procedures for collecting and handling the filters before weighing at the NRC laboratory.

These procedures were followed:

- Before exposure, filters were conditioned being kept at room temperature for 24 hours.
- Filters were then weighed and reweighed, 3 times, taking the average.
- Nucleo pore filters were weighed together with special paper sheet for protection against static charge influence.
- After exposure, same conditioning as before exposure, then weighed 3 times, taking the average.
- The filter weighing results at the NRC laboratory were checked by reweighing some filters at the NILU laboratory, with good agreement, within approximately 10%.
- Sampling volumes are determined by flow rate and sampling time.
- Flow rate of the samplers was checked and found to be within 10% of correct value, using a calibrated, digital flow meter. It was not possible to check the Partisol flow rate this way.

The inter-comparison sampling, see description below, showed that spurious results and large deviations could occur at times. No data has been excluded unless errors have been found, except a few very large outliers.

The QAQC procedures of the GTZ station equipment are not known in detail. They follow procedures developed and used for similar equipment in Germany, and the station operators in UB have been trained by GTZ personnel.

Comparison of samplers and instruments

It is of interest to compare the instruments in terms of the PM concentration data they provide. To investigate this, co-located comparison sampling was carried out during three campaigns in 2008, each of 4-5 days duration: 4-5 and 17-20 April, 1-6 July and 18-22 November. The two first campaigns were carried out at the NAMHEM monitoring station (Station No. 1) at the roof of the NAMHEM building, while the last one in November was carried out at the meteorology station UB3 located in a Ger area to the west and north of UB centre. The inter-comparisons included the following instruments: Gent samplers, Partisol sampler, Kosa instrument, C-20 sampler, Dusttrak instrument. The last campaign in November included an additional instrument: a GRIMM 107 state-of-the-art PM monitor. The Ecotech instrument did not participate in the inter-comparisons.

Details of the results from the monitor and sampler comparisons are presented in Annex F. A summary of the actual adjustments of the concentrations measured with the various instruments is given in section A5. The main conclusions were:

- The Gent samplers (stations 2 and 3) give acceptable results for PM_{10}, while the $PM_{2.5}$ results are uncertain. A first order correction of -25% is applied on the $PM_{2.5}$ results
- The results from the Dusttrak instrument (stations 4,7,8) give acceptable $PM_{2.5}$ results, after they are corrected for the influence of relative humidity (RH) on the instrument's response.
- The Partisol sampler (station 6) gave too low PM_{10} concentrations compared to the Gent sampler. The sampler was run with a non-standard filter (Nuclepore 0.4 μm) after November, to allow for elemental analysis of the filters for source apportionment analysis. A correction factor of the order of 2 is applied. Another sampling problem with the Partisol sampler is that when the Nuclepore filters were used, the filter would clog during heavy pollution days, resulting in substantially reduced flow rate. Because of this, the sampler had to be stopped earlier than after 24 hours, and on polluted days already after a few hours. Since the each day samples were started at 11 AM, the fact that the sampler was stopped after only some hours resulted in that the period with the highest pollution level, usually the late afternoon and evening, was missed. Thus, because of this problem, the Partisol results would be still lower that the 'correct' 24-hour average. Thus, the correction factor should be even larger than 2.0.
- A correction to be applied to the PM data from the Kosa instrument at the NAMHEM station (station 1) could not be developed. During the inter-comparison campaigns, the KOSA instruments gave very low PM concentrations compared to the other instruments, especially in the April and June campaigns. The Kosa results at station 1 are presented as measured, and commented 'as they are'.
- The C-20 instrument operated at the CLEM station (station 5) also gave very low concentrations compared to the other instruments during the inter-comparison campaigns. The C-20 results at station 5 are also presented as measured, and commented 'as they are'.

A2 Air quality standards, limit values and guidelines for PM

Table A.3 summarizes Mongolian air quality standards (AQS) as well as WHO guidelines, US EPA standards and EU limit values (LV) for PM_{10} and $PM_{2.5}$ [2].

WHO Guidelines are the lowest. They should be considered as goals for the future. WHO has established Interim Targets (IT-1-3), realizing that in many developing countries, the WHO guideline cannot be met in the short term.

US EPA standards and EU limit values differ. The EU LV is stricter than the US AQS for PM_{10}, while it is more lax for $PM_{2.5}$. They represent to some extent what is politically and technically feasible to meet presently.

Table A.3 Air Quality Guidelines, Standards, Limit Values

Guidelines, Standards, Limit values (all numbers in µg/m^3)				
	$PM_{2.5}$		**PM_{10}**	
	Annual average	24 hour average (daily)	Annual average	24 hour average (daily)
Mongolian Standards, 2007, MNS 4585:2007	25	50	50	100
WHO Guidelines, 2005	10	25	20	50
WHO Interim Targets (IT)				
IT-1	35	75	70	150
IT-2	25	50	50	100
IT-3	15	37.5	30	75
US EPA AQS, 2006	15	35 [1]	-	150
EU LV	25 [3] 20 [4]	-	40	50 [2]

[1] 7 days above 35 per year is allowed (98th percentile)
[2] 35 days above 50 per year is allowed (90th percentile)
[3] To be met by 2015
[4] Indicative value for 2020

A3 PM ambient air concentrations as measured in the AMHIB project

Individual data from the PM measurements at all the stations are given in the Annex F, for the entire monitoring period 1 June 2008-31 May 2009. The individual data has been quality checked and assured to the extent possible. The data show instances of spurious very high concentrations at certain stations on certain days, some of which are hard to explain. No data has been excluded unless errors have been found, except a few very large outliers.

The very high concentrations measured on some days show up in the time series figures below (Figures A.4-A.8 for PM_{10} and A.11-A.16 for $PM_{2.5}$). These days can represent up to 50-100 µg/m^3, or up to about 25%, of the annual average concentrations at the stations, and are thus important for determining the annual PM pollution level. No

[2] World health organization: Air Quality Guidelines for particulate matter, ozone, nitrogen oxides and sulphur dioxide. Global update 2005. Summary of risk assessment. http://www.epa.gov/air/criteria.html
http://eur-lex.europa.eu/LexUriServ/LexUriServ.do?uri=COM:2005:0447:FIN:EN:PDF

specific reason has been found to doubt these measurements and, although errors cannot be ruled out, they are regarded as examples of very high exposures to PM occurring due to a combination of large local emissions and adverse dispersion conditions.

As described in the Measurement Data Quality Assessment section above, various sampling and measurement artifacts affect the responses of various instruments, and the inter-comparison measurement campaigns give a basis for correcting the data for these artifacts.

It is considered most correct to first present the PM concentrations as they are measured, since the data correction procedures that could be developed have their own uncertainty. Thus, this section presents the PM concentrations as measured. In section A5 below, the concentrations are subjected to a correction procedure which gives a more correct representation of the PM concentrations in Ulaanbaatar.

PM_{10}

Monthly average PM_{10} concentrations at the selected sites are shown in Table A.4 (instrument type in parenthesis). As noted in the section on Data quality above, the comparison sampling indicates that the instruments at the NAMHEM (1), CLEM (5) and III Khoroolol (6) stations give too low PM_{10} values, and results at those stations should be regarded with caution. From Table A.4 can be seen that the PM_{10} concentration was very high in the winter season, especially in January, when the measurements give 1850 μg/m^3 at the site No3 Zuun ail. It should be even higher at the site No7 Bayanhoshuu, according to the measurements of $PM_{2.5}$, see below.

Table A.4 Monthly average PM_{10} concentrations as measured at the AMHIB sites (μg/m^3) [1]

Months	NRC (2) (Gent)	Zuun ail (3) (Gent)	III Khoroolol (6) (Partisol)	NAMHEM (1) (Kosa)	CLEM (5) (C-20/ Ecotech)[2]
Jun-08	160	154	187	29	155
Jul-08	126	113	56	7	18
Aug-08	238	179	85	-	25
Sep-08	221	131	70	-	39
Oct-08	223	128	161	38	80
Nov-08	366	673	801	129	113
Dec-08	180	927	694	277	61
Jan-09	200	1850	932	174	66
Feb-09	302	1007	464	115	86
Mar-09	205	489	358	63	66
Apr-09	316	300	273	34	60
May-09	501	739	183	22	34
Annual aver.	**253**	**558**	**355**	**89 (76)** [3]	**67**

[1] Annual averages are calculated on the basis that the samples taken each month are representative for the month, although all days are not measured, and the number of samples per month varies.
[2] C-20 before November, Ecotech after November.
[3] The number in parenthesis is estimated annual average concentration including months August and September (given an estimated average concentration 10 μg/m^3, with a view to the $PM_{2.5}$ concentrations then, see Table A.5).

Annual average concentrations of PM_{10} at the sites are shown in Figure A.2. The horizontal red line in the figure shows the annual average PM_{10} standard of Mongolia. The standard is exceeded substantially at sites 2, 3 and 6. The NAMHEM and CLEM stations stand out with very low concentrations. Although NAMHEM is located about 20 meters above ground, the inter-comparisons indicate that the instruments give too low values. This is also the case for the case for the instrument at the III Khoroolol station (6). The CLEM station is located south of UB centre in a relatively cleaner area. The inter-comparisons indicate that the C-20 sampler (used until the end of October) give too low values. It was replaced by the Ecotech instrument by the end of October. The Ecotech gave also low PM levels at the station 5. It is a state-of-the-art PM monitor and should give reasonable results. The instrument was not included in inter-comparisons campaigns.

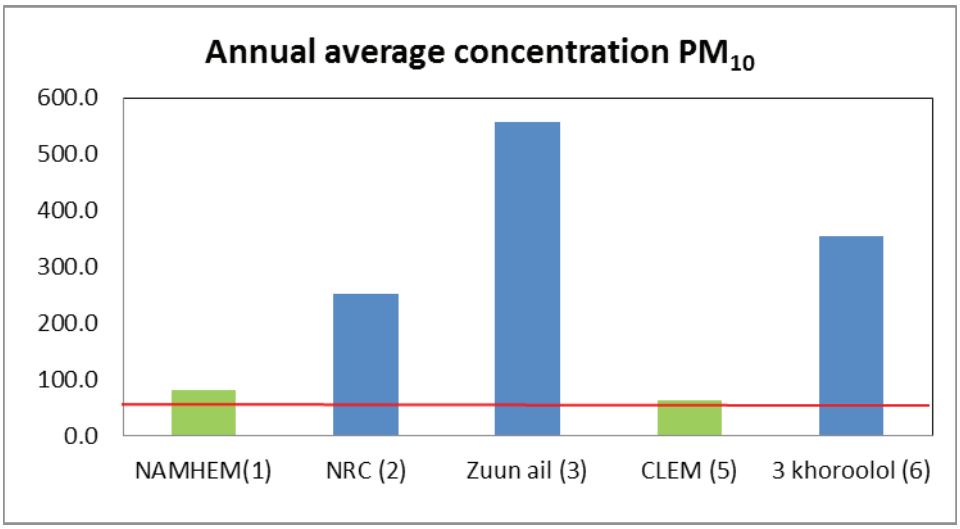

Figure A.2 Annual average PM_{10} concentrations as measured at the AMHIB sites.

Monthly average concentrations at stations 2, 3 and 6 are shown in the Figure A.3. The lower figure is included to represent better the lower concentrations during the summer period (the vertical scale is expanded because concentrations above 1000 at station 3 are peaking above the scale).

PM concentrations are increasing in winter season from November to March mainly due to the residential (gers and houses) heating in the ger areas and coal combustion in Heat-only boilers. High concentrations at some stations in May are probably due to suspended dust from dry surfaces during high wind periods.

Time series of PM_{10} for each of the sites are presented in the Figures A.4–A.8. The horizontal red line shows daily Mongolian standard. Comments on the measurements at each station are included under each figure.

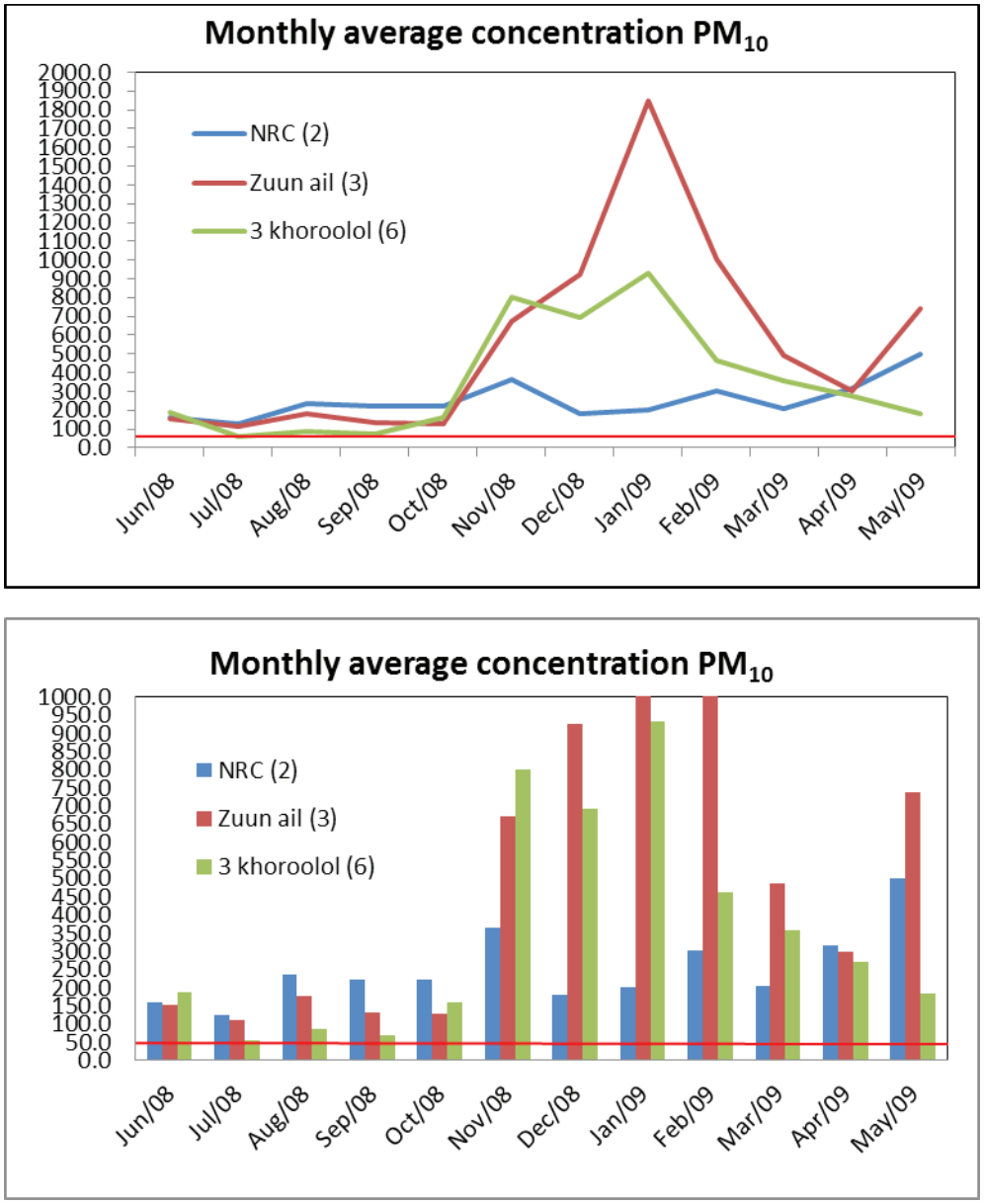

Figure A.3 Monthly average PM_{10} concentrations by site. Red line: Mongolian AQ standard, annual average.

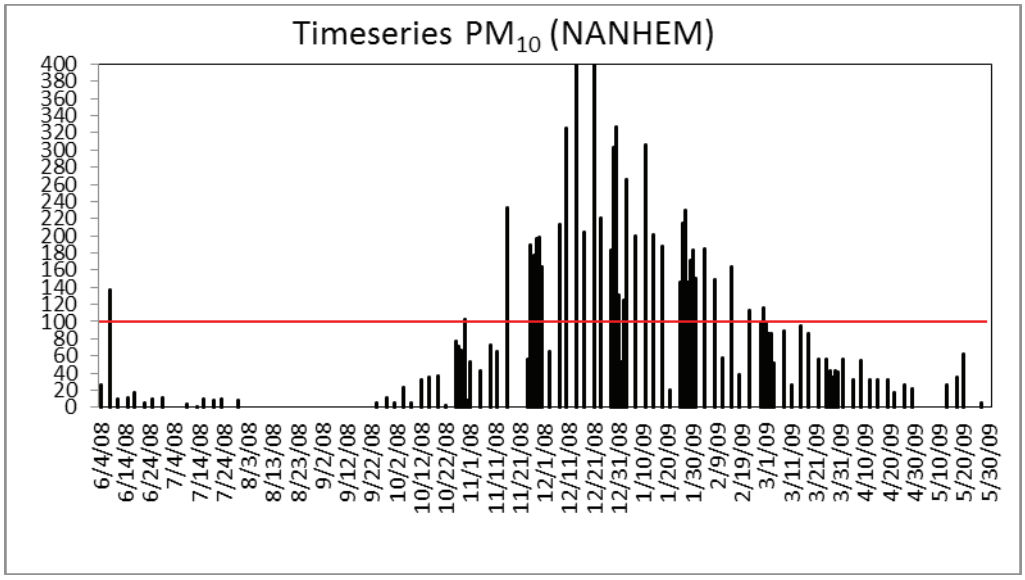

Figure A.4 Time series of PM_{10} concentration in NAMHEM site (AMHIB 1). Two peaks of 426 and 649 μg/m^3 extend above the top of the vertical axis. Red line: Mongolian AQ standard, 24-hour average.

Although the concentrations measured by the instrument (Kosa beta absorption) at this station are too low, as described above, the measured time series shows well the typical seasonal variation of PM_{10} in UB central areas, with very high winter time concentrations, here shown to be building up gradually from mid October, peaking in December and reducing gradually towards March-April. This time sequence indicates that the station is affected mostly by combustion PM; dominated by coal combustion.

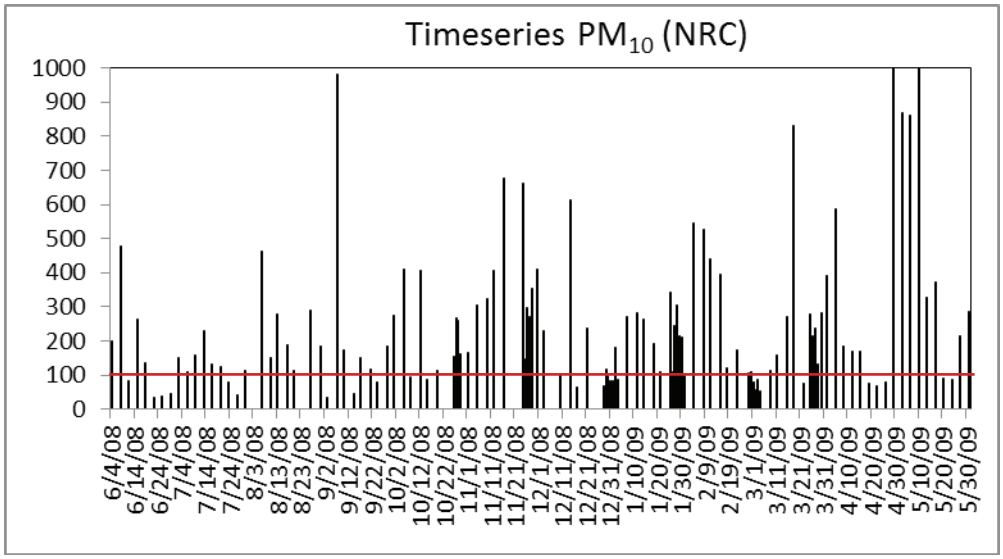

Figure A.5 Time series of PM_{10} concentration in NRC site (AMHIB 2). Two peaks of 1,118 and 1,403 μg/m^3 extend above the top of the vertical axis.

The time sequence at the NRC station does not show the same seasonal variation as at the NAMHEM station. It shows that high concentrations can be met throughout the year. This indicates that the PM_{10} at this station, which is located in an area with open soil surfaces, is affected both by combustion PM as well as by suspended dust from dry soil and road surfaces. The very high concentrations measured during early May are conspicuous. They show up also at the Zuun ail (3) station, see below. Since they don't show up in other stations, they can probably be explained by local dust suspension from dry soil surfaces due to turbulent wind action.

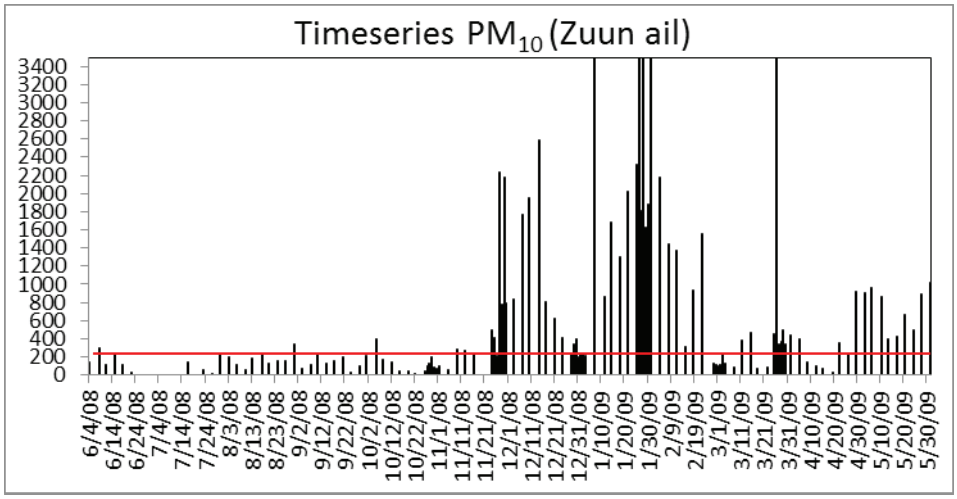

Figure A.6 Time series of PM_{10} concentration in Zuun ail site (AMHIB 3). Four peaks in the range 3,612-4,360 µg/m^3 extend above the top of the vertical axis (the largest outlier has been excluded from further processing).

This station shows the typical seasonal variation. It is located near a ger area, and combustion PM dominates over dust from open soil surfaces.

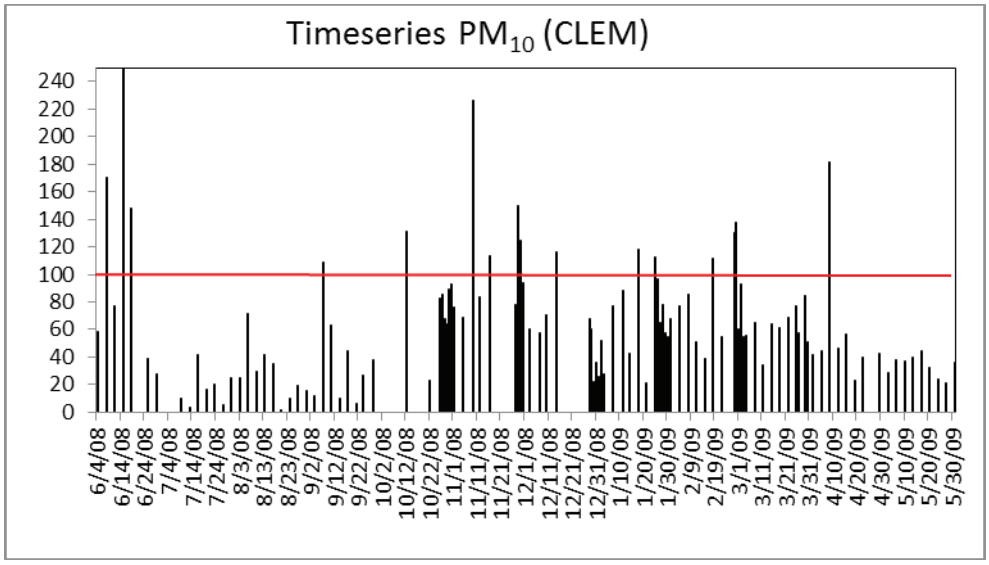

Figure A.7 Time series of PM_{10} concentration in CLEM site (AMHIB 5). One peak of 319 µg/m^3 extends above the top of the vertical axis.

This station is located to the south-west of the main PM source areas, and is thus not much affected by the combustion PM. There are some open soil surfaces in the area, so the station is exposed somewhat to suspended dust. Thus, the time sequence shown is without the typical seasonal variation. As explained above, the instrument used at this station until the end of October gives too low PM_{10} values.

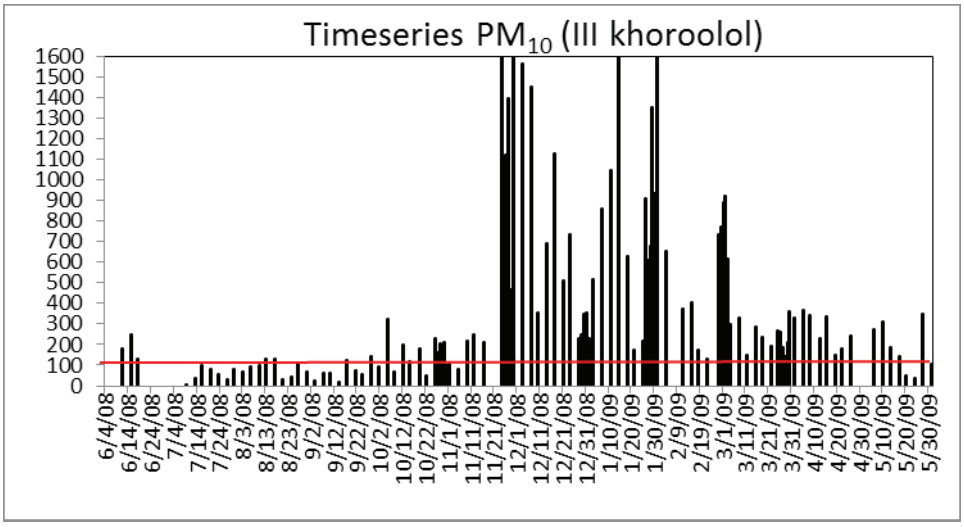

Figure A.8 Time series of PM_{10} concentration at the III Khoroolol site (AMHIB 6). Three peaks in the range 2,725-3,800 μg/m^3 extend above the top of the vertical axis (the largest outlier has been excluded from further processing).

This station is located well within a ger area to the north-west of UB centre. It shows the typical seasonal variation, and concentrations are extremely high during winter. It is also affected by suspended dust from nearby open soil and road surfaces, although the contribution from that source is much less than that from the combustion PM. The comparison sampling indicates that the instrument at this station also measures too low.

$PM_{2.5}$

Monthly average $PM_{2.5}$ concentrations as measured at the sites are shown in Table A.5 (instrument type in parenthesis). All the instruments used for $PM_{2.5}$ determinations are affected by sampling artifacts, as explained above. For instance, the Dusttrak instruments at stations 1, 4, 7 and 8 give too high values on days with high relative humidity, which is the case on many winter days, due to the effect of the relative humidity (RH) of the instrument response. Observed and reported values there could be a factor of 1.5-2 higher on days in the winter months, especially in December and January, than measurements with a standard measurement method would show.

At the NAMHEM site, $PM_{2.5}$ was during October–December measured also with a Dusttrak instrument, at the 2nd floor of the building.

$PM_{2.5}$ concentrations were extremely high in winter, especially in December and January. The January average measured at the site No 7 is 1,536 μg/m^3, at the Zuun ail site No3 it is 1,291 μg/m^3 and at site 4 (6 Buudal) 859 μg/m^3 (note the effects of the sampling and instrument artifacts). The Dusttrak measurements at the NAMHEM station (5 meters above ground level) during October-December indicate that the $PM_{2.5}$ concentration there, in a central area, is quite a bit lower than in the ger areas (stations 3, 4, 7).

Annual average $PM_{2.5}$ concentrations by site are shown in the Figure A.9. The annual average $PM_{2.5}$ standard of Mongolia is 25 μg/m^3.

Table A.5 Monthly average $PM_{2.5}$ concentrations, as measured at the AMHIB sites ($\mu g/m^3$)

Months	NRC (2) (Gent)	Zuun ail (3) (Gent)	6 Buudal (4) (Dusttrak)	Bayan hoshuu (7) (Dusttrak)	Airport (8) (Dusttrak)	NAMHEM (5) (Kosa) 20 m.a.g.	NAMHEM (5) (Dusttrak) 5 m.a.g.
Jun-08	29	26	85		169	17	
Jul-08	22	13				1	
Aug-08	65	49				6	
Sep-08	19	38	37	47	38	8	
Oct-08	46	39	281	498	185	38	119
Nov-08	122	331	527	568	406	81	205
Dec-08	107	576	1205	1421	893	225	384
Jan-09	121	1291	859	1536	515	138	
Feb-09	141	358	342	971	413	100	
Mar-09	80	346	179	321	207	45	
Apr-09	129	120	94	137	92	25	
May-09	279	371	42	59	53	24	
Average	**97**	**296**	**365**	**618**	**297**	**59**	

[1] Annual averages are calculated on the basis that the samples taken each month are representative for the month, although all days are not measured, and the number of samples per month varies.

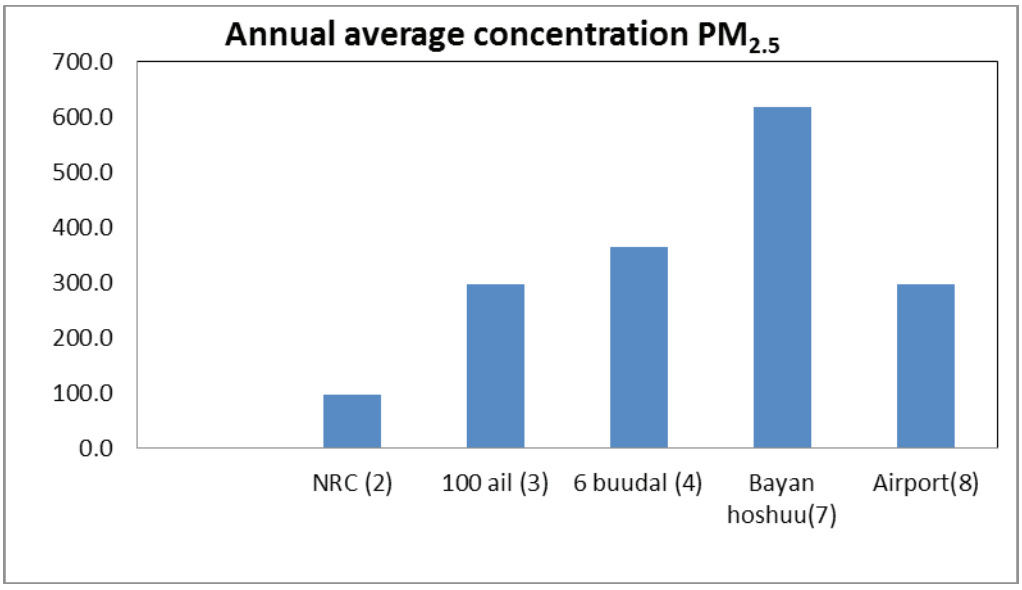

Figure A.9 Annual average concentration of $PM_{2.5}$ as measured at the AMHIB sites

Annual average $PM_{2.5}$ concentration is exceeding the Air Quality Standard at all measured sites by 2-25 times at 5 sampling sites, and it is specially high at site 7 (Bayanhoshuu) which is located well within a ger area to the north-west of UB centre.

Monthly average concentrations by sites are shown in the Figure A.10 in two different representations, to increase clarity.

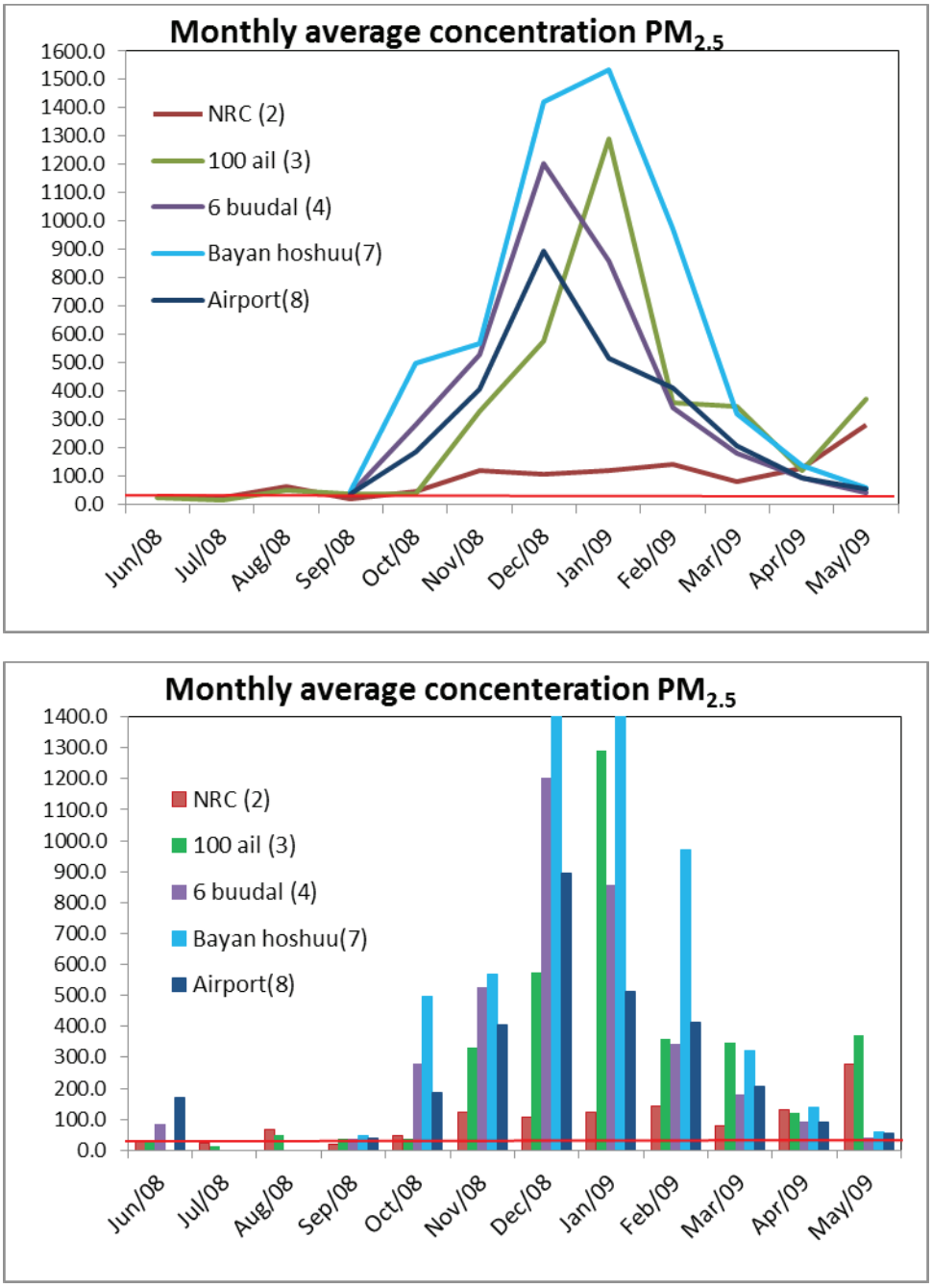

Figure A.10 Monthly average $PM_{2.5}$ concentration at the sites. Red line: Mongolian AQ standard, annual average.

$PM_{2.5}$ pollution is increasing rapidly towards the winter. $PM_{2.5}$ particles are mainly from the coal and to some extent wood combustion. Concentration is especially high at the site 3, 4 and 7, which are located in or near the Ger districts.

Daily $PM_{2.5}$ concentration time series are shown in the Figures A.11–A.16. The horizontal red line shows Mongolian daily standard of $PM_{2.5}$. Comments on the measurements at each station are included under each figure.

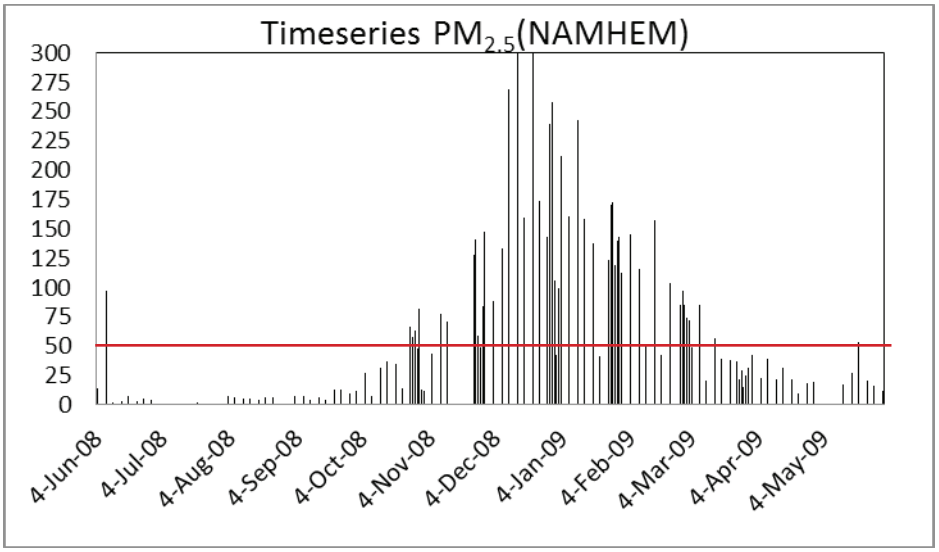

Figure A.11 Time series of $PM_{2.5}$ concentration at the NAMHEM (AMHIB 1) station. Two peaks of 372 and 528 µg/m^3 extend above the top of the vertical axis. Red line: Mongolian AQ standard, 24-hour average.

Again, the concentrations measured by the instrument (Kosa beta absorption) at this station are too low, as described above. Even so, the measured time series shows well, as it does for PM_{10}, the typical seasonal variation of $PM_{2.5}$ in UB central areas, with high winter time concentrations, here shown to be building up gradually from mid October, peaking in December and reducing gradually towards March-April.

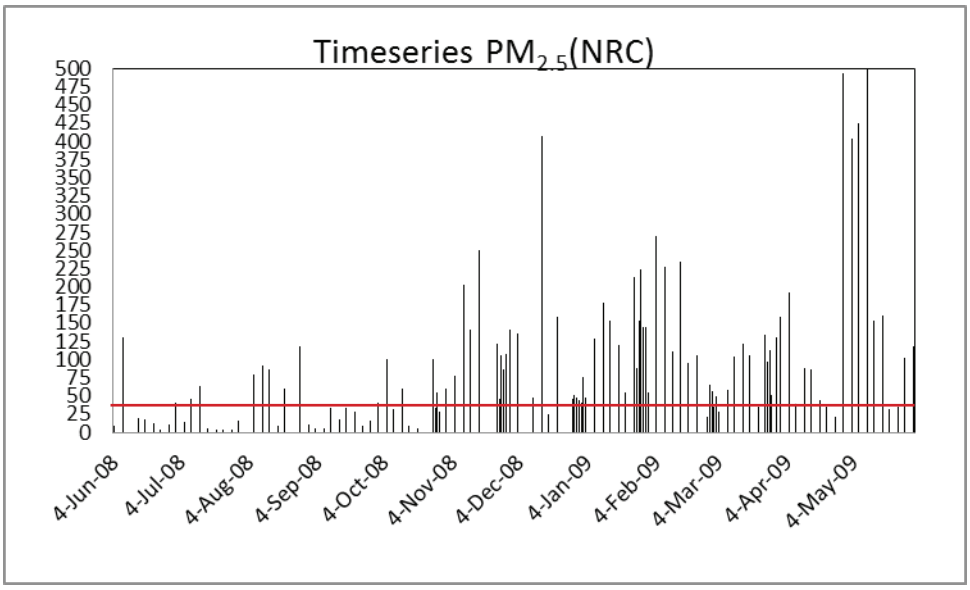

Figure A.12 Time series of $PM_{2.5}$ concentration at the Nuclear Research Center, National University of Mongolia (AMHIB 2). One peak of 1,085 µg/m^3 extends above the top of the vertical axis.

As was the case also for PM_{10}, the time series at the NRC station does not clearly show the same seasonal variation as at the other stations, although increased winter concentrations do show for $PM_{2.5}$. The very high $PM_{2.5}$ concentrations on some days in May, as was the case for PM_{10} also, can probably be explained by wind action suspending local dust from open dry soil surfaces. The wind suspended dust is mainly coarse dust, but a certain part is also in the $PM_{2.5}$ fraction, but a fraction of them show up erroneously on the $PM_{2.5}$ filter in the sampler, see section A5.

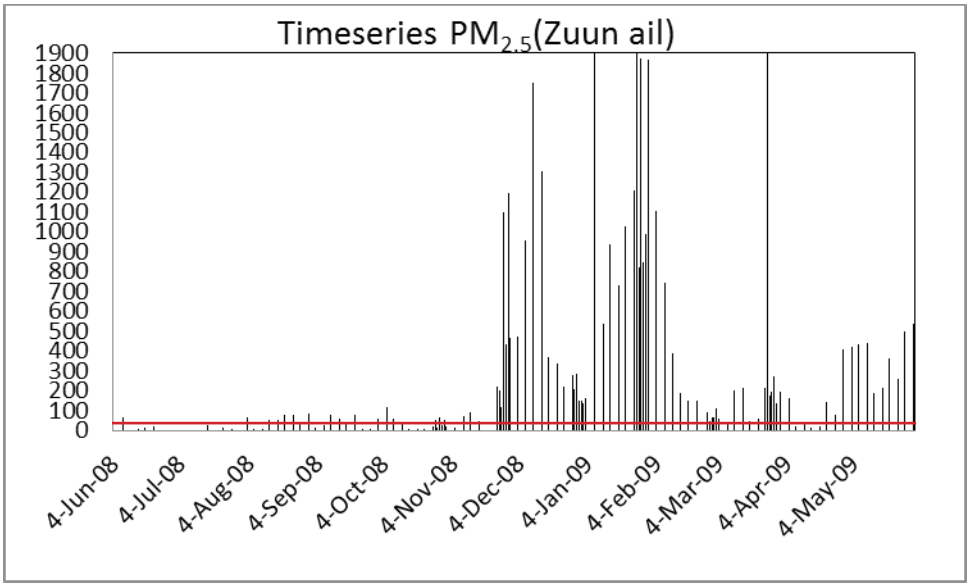

Figure A.13 Time series of $PM_{2.5}$ concentration at the Zuun ail (AMHIB 3). Three peaks in the range 2,434-5,657 µg/m^3 extend above the top of the vertical axis.

This station again shows the typical seasonal variation, with its location near a ger area. It is not much affected by open soil surfaces, although it has similar high concentrations in early May as at NRC (see the explanation above).

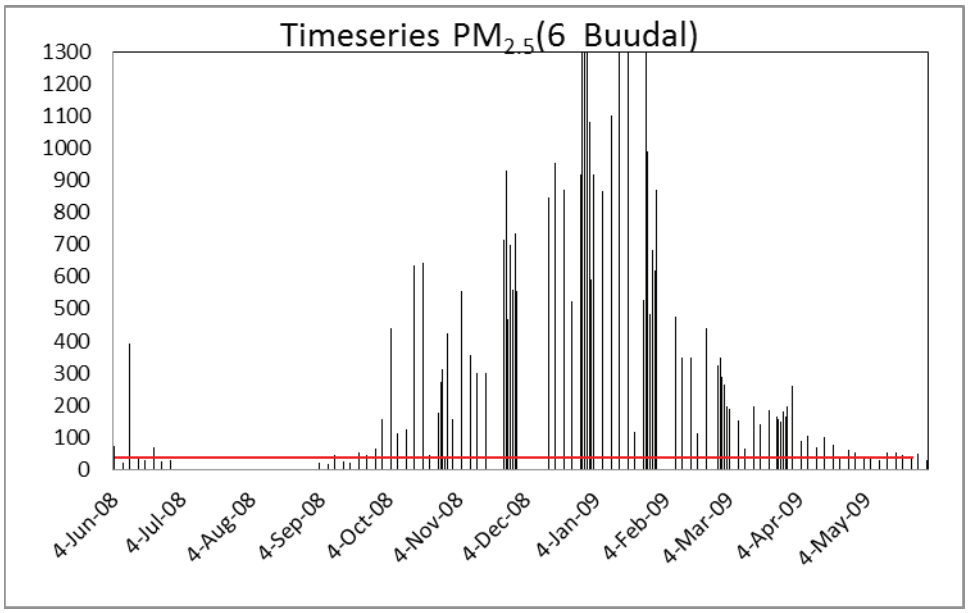

Figure A.14 Time series of $PM_{2.5}$ concentration at the 6 Buudal (AMHIB 4). Six peaks in the range 1,330-2,640 µg/m^3 extend above the top of the vertical axis.

This station is located well within a ger area to the north of UB centre. It shows the typical very pronounced seasonal variation, with very high $PM_{2.5}$ levels during January and February 2009, due mainly to residential coal and to some extent wood combustion in the area. Note that the instrument at this station (Dusttrak) gives too high readings on days with high RH, which occurs mainly during winter.

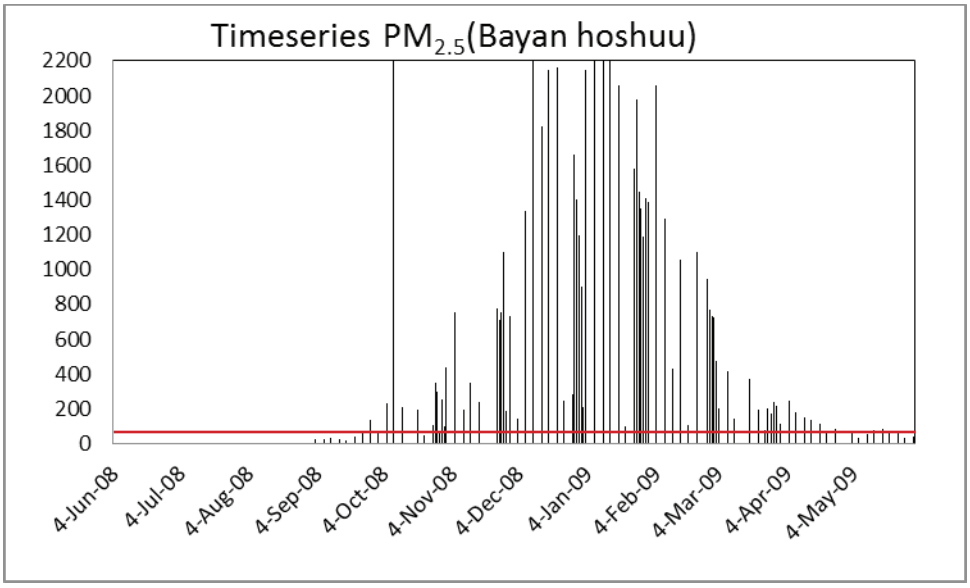

Figure A.15 Time series of $PM_{2.5}$ concentration at the Bayanhoshuu (AMHIB 7). Five peaks in the range 2,310-4,060 µg/m^3 extend above the top of the vertical axis.

As the station 6 above, this station is also located well within a ger area, to the north-west of UB centre. It also shows the typical very pronounced seasonal variation, with extremely high $PM_{2.5}$ levels during January and February 2009, due mainly to residential combustion in the area. As above, the instrument at this station (Dusttrak) also gives too high readings on days with high RH during winter.

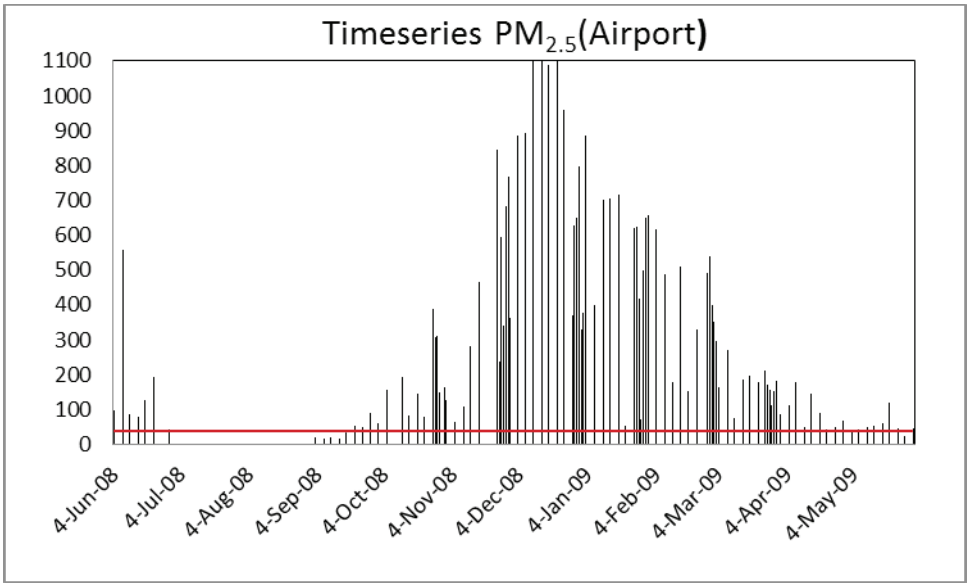

Figure A.16 Time series of $PM_{2.5}$ concentration at the Airport (AMHIB 8). Three peaks in the range 1,110-1,230 µg/m^3 extend above the top of the vertical axis.

This station is located within a smaller ger area near the airport, well to the west of UB centre. It also shows the typical very pronounced seasonal variation, with very high $PM_{2.5}$ levels during January and February 2009, due mainly to residential combustion in the area. As above, the instrument at this station (Dusttrak) gives too high readings on days with high RH during winter.

A4 GTZ measurements

During AMHIB measurement, four stationary Air quality measuring stations were installed and put in operation during November-January in Ulaanbaatar by the GTZ, the Germany institute for Technological Co-operation. Figure A.17 shows position of those GTZ stations as well as the other UB stations. The GTZ stations West and East Junction are located more within the central areas of UB than the AMHIB stations which are more in the ger areas. The GTZ station 'TV Antenna' is fairly close to ger areas. PM monitors of the type GRIMM EDM 180 are used at the GTZ stations. This instrument has been designated as an instrument equivalent to reference instruments for PM measurements, according to European Standards.

Description of the stations:

- West Junction: Located near a large road crossing of two main roads in the western part of UB central area. Asphalted and gravel covered surfaces nearby.
- East Junction: Located about 20 m north of a main road in the eastern part of UB central area, about 5m higher than the road. Grass/brush covered areas nearby.
- TV Antenna: Located in an area with dispersed public buildings, about 20 m west of a main road. Asphalted areas nearby. The area is fairly close to the ger areas to the north-east of the station.
- Airport: Located in the less populated Ger area near to the AMHIB 8 site, but at the river side of the small hill.

Figure A.17 Positions of GTZ stations and CLEM meteorology stations: Yellow marks: AMHIB stations; Red marks: GTZ stations and Blue marks: CLEM meteorology stations

Table A.6 presents the GTZ measurement results, for PM_{10} (A) and $PM_{2.5}$ (B). The tables also show the uncorrected data from the AMHIB stations for the same months. The GTZ measurements have been averaged in two different ways: first the concentrations only for the days with AMHIB measurements (Wednesday and Sunday and every day in the last week of winter months), and second for all the days of GTZ measurements. It can be concluded that the selected days for AMHIB measurements represent the period well in terms of average PM concentration. Direct comparisons of the measurements at the AMHIB and GTZ stations are complicated by the stations not being located in the same areas.

Time series plots of 24-hour averaged concentrations for each station and component are shown separately in Figures A.18-A.25.

Table A.6 A Comparison of AMHIB and GTZ monthly average PM_{10} concentrations

#	**PM_{10} monthly average concentration (ug/m^3)**							**Average Jan-May**
	AMHIB Sites							
		December	January	February	March	April	May	
2	NRC (2)	180	200	302	205	316	501	**305**
3	Zuun ail (3)	927	1850	1007	489	300	739	**877**
5	III Khoroolol (6)	694	932	464	358	273	183	**442**
6	**Average**	**600**	**994**	**591**	**351**	**296**	**474**	**541**
GTZ data Selected for AMHIB measured days								
1	TV antenna		408	249	165	311	97	**246**
2	East junction		275	260	138	198	96	**194**
3	Airport		201	176	107	151	117	**150**
4	West junction	187	205	219	190	249	184	**209**
	Average	**187**	**272**	**226**	**150**	**227**	**123**	**199**
GTZ data all days								
1	TV antenna	272	383	261	149	279	114	**237**
2	East Junction		248	222	163	177	120	**186**
3	Airport		186	156	123	150	119	**147**
4	West junction	226	200	201	210	253	185	**210**
	Average	**249**	**254**	**210**	**161**	**215**	**134**	**195**

Table A.6 B Comparison of AMHIB and GTZ monthly average $PM_{2.5}$ concentrations

#	**$PM_{2.5}$ monthly average concentration (µg/m^3)**							**Average Jan-May**
	AMHIB Sites							
		December	January	February	March	April	May	
2	NRC (2)	107	121	141	80	129	279	**150**
3	Zuun ail (3)	576	1291	358	346	120	371	**497**
4	6 Buudal (4)	1205	859	342	179	94	42	**304**
5	Bayanhoshuu(7)	1421	1536	971	321	137	59	**605**
6	Airport(8)	893	515	413	207	92	53	**256**
	Average	**840**	**864**	**445**	**227**	**114**	**161**	**362**
GTZ data, Selected for AMHIB measured days								
1	TV antenna		369	219	85	99	41	**163**
2	East junction		221	170	70	59	27	**110**
3	Airport		153	130	57	44	32	**83**
4	West junction	137	167	137	80	69	46	**100**
	Average	**137**	**228**	**164**	**73**	**68**	**36**	**114**
GTZ data all days								
	TV antenna	201	349	236	76	79	43	**156**
	East junction		203	150	81	49	38	**104**
	Airport		159	120	64	41	31	**83**
	West junction	166	165	133	87	63	44	**98**
	Average	**183**	**219**	**160**	**77**	**58**	**39**	**110**

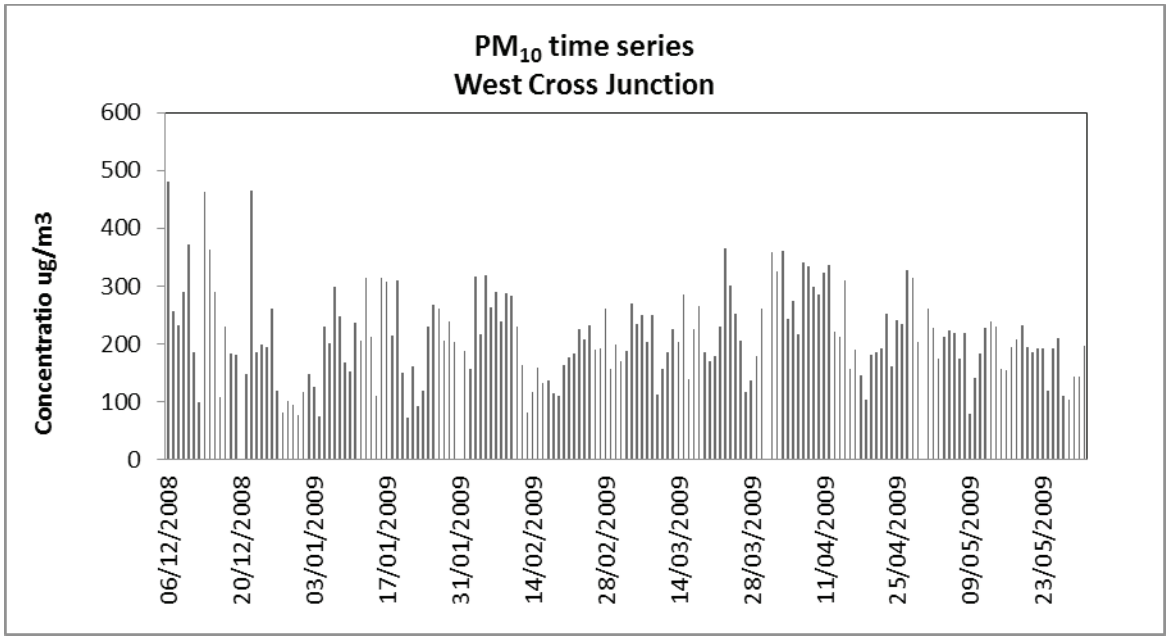

Figure A.18 PM_{10} time series at the GTZ West Junction station.

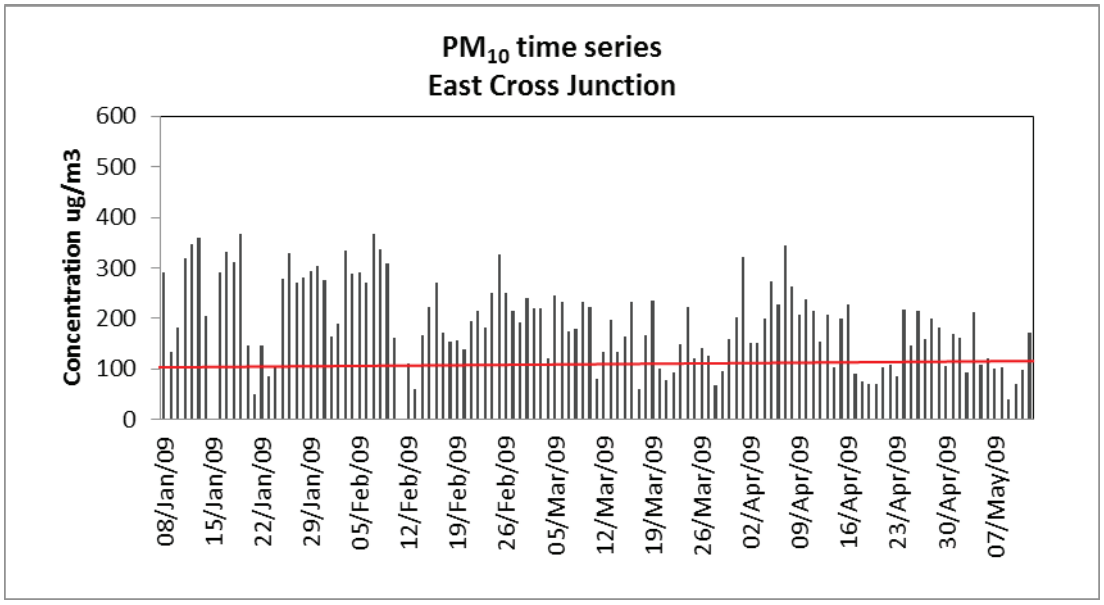

Figure A.19 PM_{10} time series at the GTZ East Junction station.

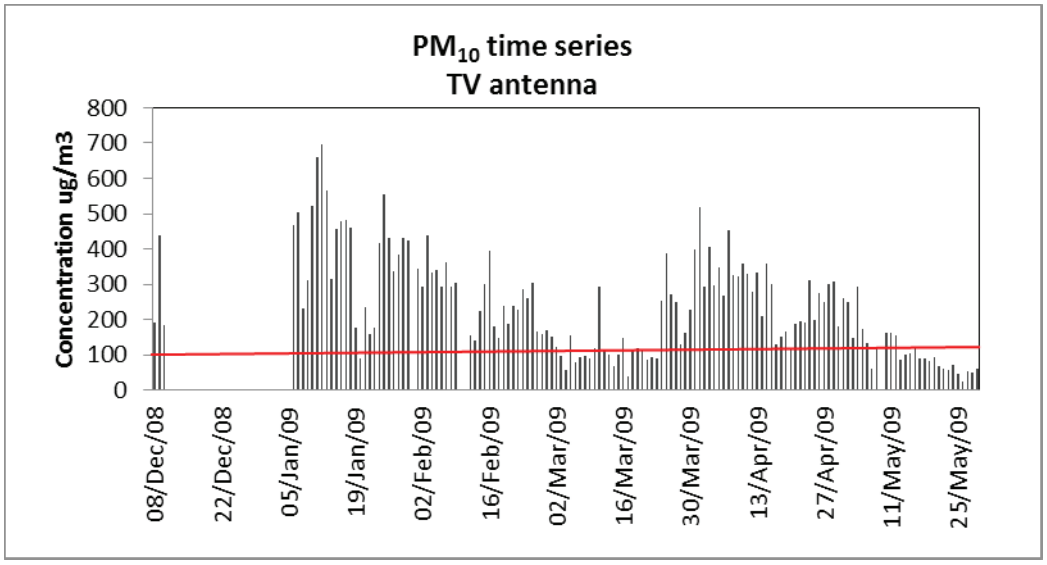

Figure A.20 PM_{10} time series at the GTZ TV Antenna station.

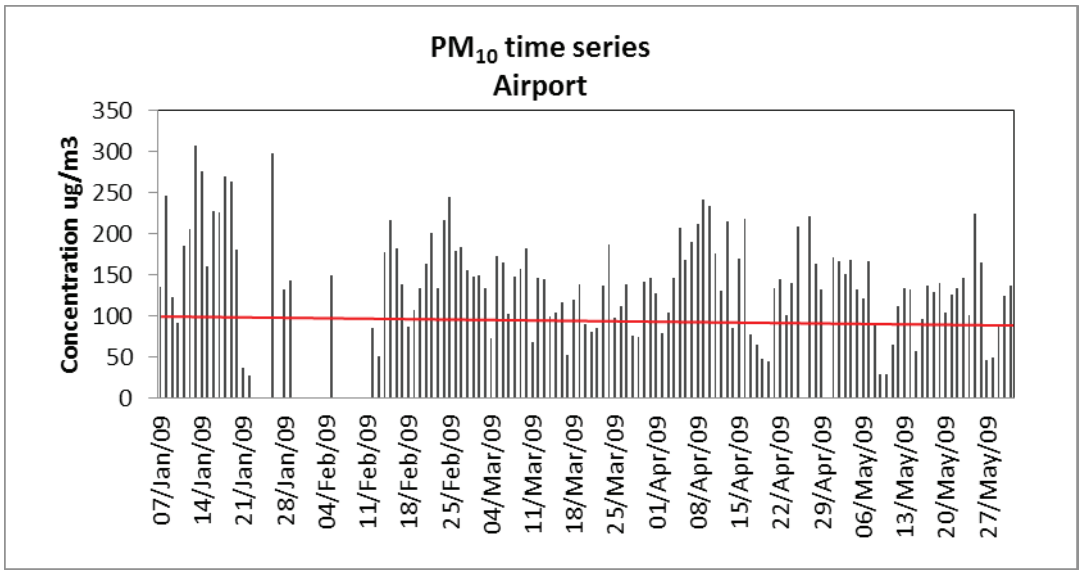

Figure A.21 PM_{10} time series at the GTZ Airport station.

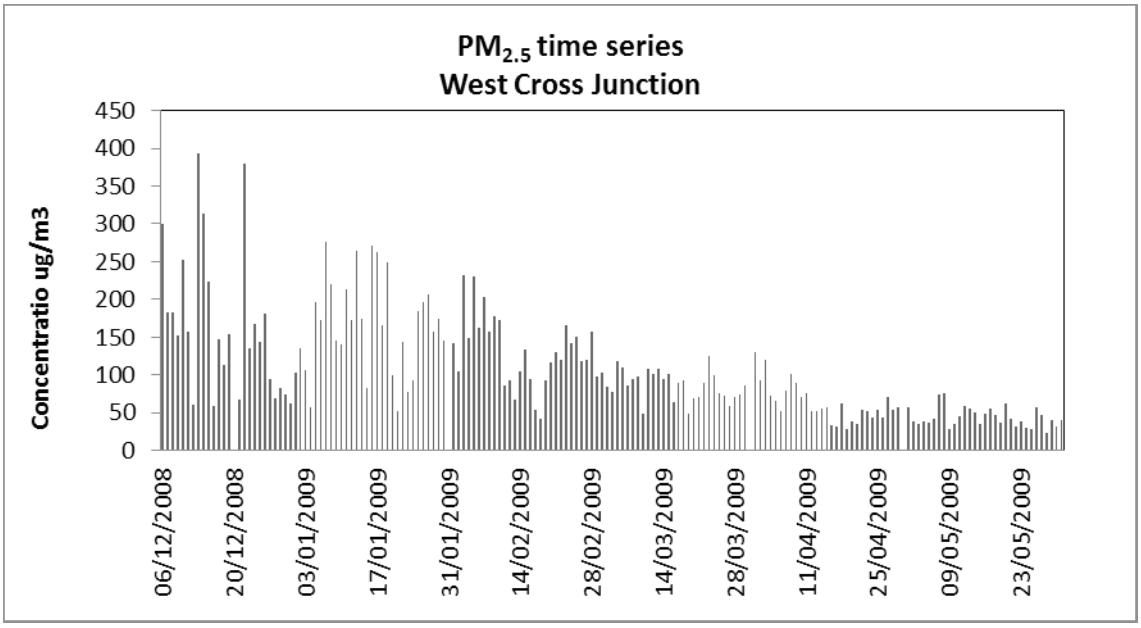

Figure A.22 $PM_{2.5}$ time series at the GTZ West Junction station.

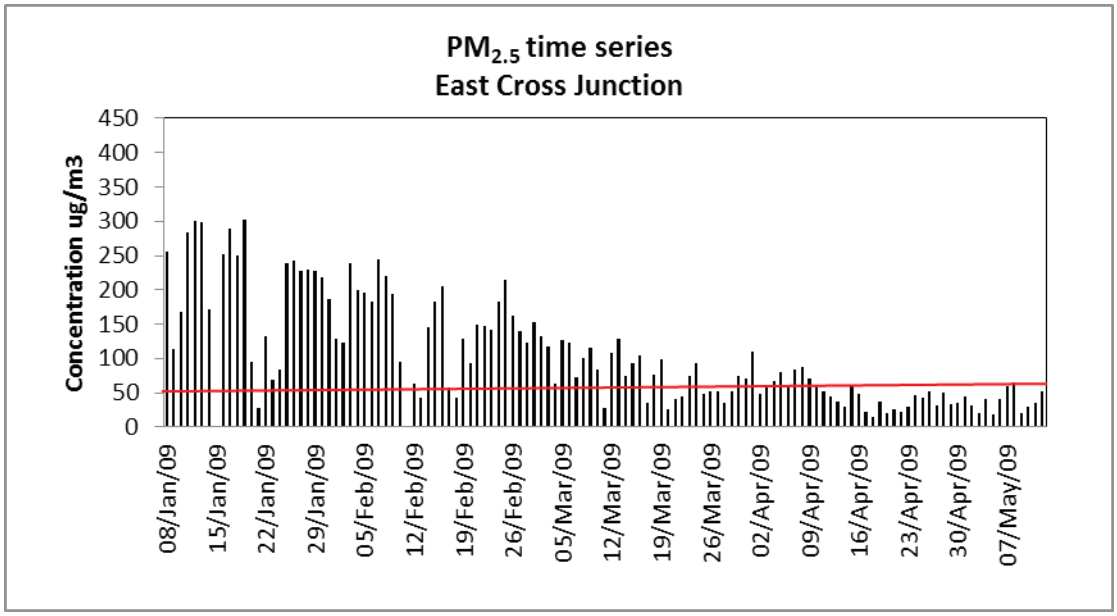

Figure A.23 $PM_{2.5}$ time series at the GTZ East Junction station.

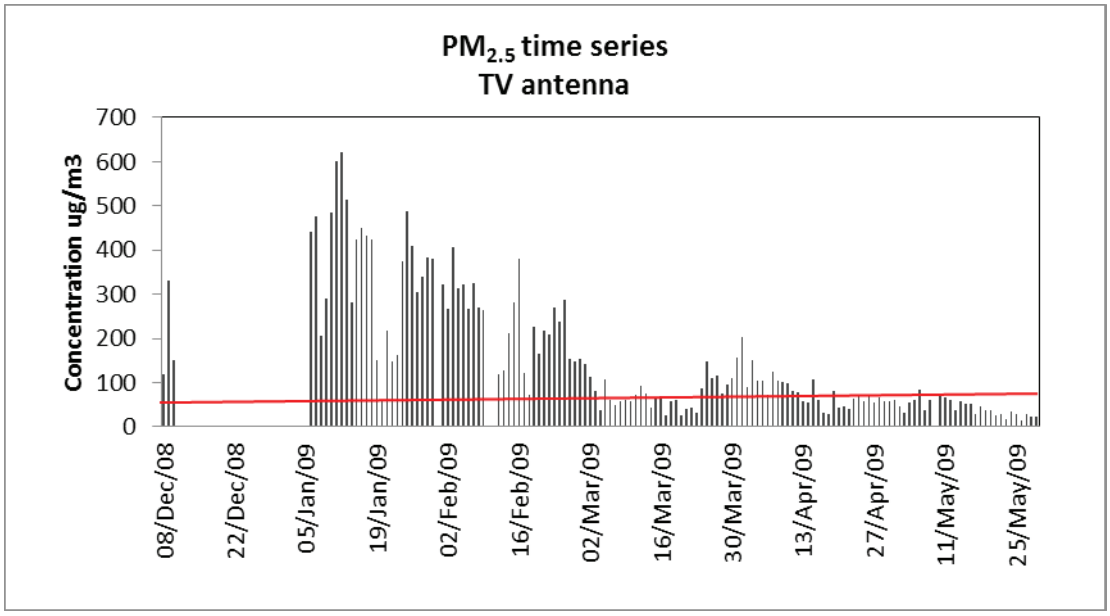

Figure A.24 $PM_{2.5}$ time series at the GTZ TV Antenna station.

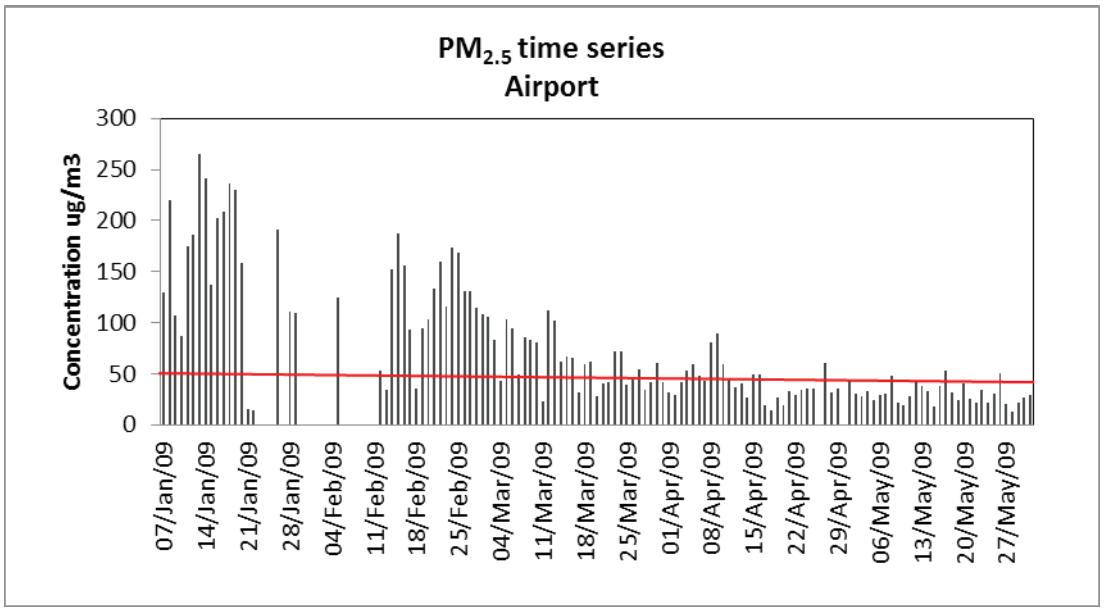

Figure A.25 $PM_{2.5}$ time series at the GTZ Airport station.

A5 PM concentrations in UB from corrected AMHIB data and GTZ data

PM concentrations as measured at the AMHIB stations, given in Table A.4 and Table A.5 above, are summarized in Table A.7.

Table A.7 Annual average PM concentration in Ulaanbaatar city, as measured at the AMHIB stations

Site No	Site name	$PM_{2.5}$	PM_{10}
2	NRC	97	253
3	Zuun ail	296	558
4	6 Buudal	365	-
6	III Khoroolol	-	355
7	Bayanhoshuu	618	-
8	Airport	297	-

Note that PM_{10} and $PM_{2.5}$ is not measured at the same stations. Some $PM_{2.5}$ stations are located in areas with significantly higher PM pollution level than some of the PM_{10} stations.

Due to the discrepancies between the various instruments used, as well as other sampling artifacts, as described in Annex F and in the Data Quality Assessment section above, some of these data needs to be corrected, to give a more correct representation of the PM concentrations in UB. Although the comparison measurement campaigns were rather brief, they still covered a total of up to 20 days dependent upon the instrument. Sometimes good indications of correction factors could be given, but there are uncertainties coupled to the correction factors.

The procedure for correction of the data from the various stations is described in Annex F.

A summary of the corrections is as follows:

PM_{10} at stations 2 and 3:
Gent samplers were used here. They compare well with results from the GRIMM 107 instrument when its response was corrected for the RH effect. No corrections are applied to the PM_{10} results from the Gent samplers.

$PM_{2.5}$ at stations 2 and 3:
On the average, the Gent sampler gave about 25% higher $PM_{2.5}$ concentration than the RH adjusted GRIMM 107, based upon 7 samples (one strong outlier excluded). This corresponds to penetration of a certain part of the coarse fraction particles through the coarse filter and down to the fine filter. There is a large variation in this factor between the 7 samples. The 25% factor is used as a first order correction for the UB data, but it is uncertain.

PM_{10} at station 6:
The Partisol sampler is used here. In the period June-November it was used with the standard fiber filter, and nuclepore filter subsequently. When the nuclepore filter was used, the filter easily clogged, and the sampler had to be stopped often after a few hours, missing the most polluted part of the day. Correction of the data for this sampler is complicated by the use of different filter types during most of the comparisons and during measurements in the AMHIB period. Correction of the Partisol data is uncertain. Based on the information at hand, the data is corrected by a factor larger than 2.0, a factor with a relatively large uncertainty.

$PM_{2.5}$ at stations 4, 7 and 8:
The Dusttrak instrument is used on these stations. Data from the Dusttraks are corrected for the effect of the RH on the instrument response:
- RH >65%: correction factor: 0.55
- RH of 50-65%: correction factor: 0.65
- RH <50%: correction factor: 1.0.

During the October-February period, 55% of the days had average RH>65%, and 38% of the days had RH of 50-65%. This leads to a correction factor for $PM_{2.5}$ data from the Dusttraks of 0.68 to be applied to the average $PM_{2.5}$ concentration measured during that period.

An additional correction needs to be applied because data from the Dusttraks are missing for the months June/ July-August, see Table A.5. Using the same monthly variability as for the stations with data for these months, this gives a correction factor of 0.85 for stations 4 and 8, and 0.75 for station 7.

Applying these corrections to the measured concentrations given in Table A.7 gives the corrected PM concentrations presented in Table A.8. The uncertainty of the corrected numbers is indicated with indices 1-3, 1 the least uncertain and 3 the most uncertain. Statistics for assessing the uncertainty is not available. It is judged it to be of the order of +-10-15% for index 1, +- 15-20% for index 2, and +-40-50% for index 3.

The NAMHEM and CLEM stations are included in the table for completeness. The sampler inter-comparisons showed that the instruments at those stations gave much too low values, although the instrument at the NAMHEM station gave more reasonable results for the winter period. They stand out in the table with very low levels for PM_{10}. The $PM_{2.5}$ at the NAMHEM station is not so much lower than at NRC. The NAMHEM station is located 20 meters above ground, where concentrations would be lower than a few meters above ground level.

Table A.9 shows the results from the measurements at the GTZ stations, for the period January-May 2008. Corrected concentrations at non-ger AMHIB stations are also shown there, for the same period, for comparison. The relations between PM concentrations at the various stations can be described as follows:

The East and West Junction stations are located in the central UB area, outside of the ger areas. The West station is very close to a heavy traffic junction. Their $PM_{2.5}$ concentration is similar to the NRC station, which is located more to the east, but also outside large ger areas. The PM_{10} concentration at those GTZ stations is lower than at the NRC station. The NRC station is more exposed to suspended soil dust than the GTZ stations. The GTZ station 'TV antenna' is located closer to ger areas, and probably for this reason has higher PM concentrations than the other more centrally located stations. The GTZ Airport station has significantly lower $PM_{2.5}$ than the AMHIB Airport station. The AMHIB station is located within ger areas close to the airport, while the GTZ airport station is located in a cleaner area. As above, NAMHEM (Kosa at 20 meters) and CLEM are included for completeness; see the comment related to Table A.8 above. In addition, please note that Dusttrak measurements at the 2nd floor of the NAMHEM building during October-December (see Table A.5) confirm, when corrected for the RH effect, to the $PM_{2.5}$ levels in non-ger central UB areas measured by the GTZ stations.

The stations are located in various parts of the ger areas and in more central areas in UB. The results show that the PM concentrations vary significantly between the areas, dependent upon their closeness to main source areas. It is clear that the concentrations are significantly higher in the ger areas than in the more central areas.

Table A.8 Annual average PM concentration of Ulaanbaatar city, corrected according to results from sampler comparisons. Indices 1-3 indicate the uncertainty of the numbers, with 1 the least uncertain and 3 the most uncertain. Index 4: The instruments at these stations were shown to give too low values. They are included here for completeness.

Site No	Site name	$PM_{2.5}$	PM_{10}
2	NRC	78 [3]	253 [1]
3	Zuun ail	236 [3]	558 [1]
4	6 Buudal	225 [2]	
6	III Khoroolol		>700 [3]
7	Bayanhoshuu	338 [2]	
8	Airport	190 [2]	
1	NAMHEM	59 [4]	76 [4]
5	CLEM		67 [4]

Table A.9 PM concentrations measured at the GTZ stations, period January-May, 2008, compared with AMHIB stations NRC and Airport. This has the same uncertainty estimation as in Table A.8.

Site No	Site name	$PM_{2.5}$	PM_{10}
AMHIB			
2	NRC	120	305
8	Airport	150	
1	NAMHEM	66	82
5	CLEM		62
GTZ			
	East Junction	110	194
	West Junction	100	209
	TV antenna	163	246
	Airport	83	150

Based upon the data and evaluations related to Tables A.8 and A.9, the following estimation of the ranges of annual average PM concentrations in UB can be given in Table A.10, for ger areas and non-ger areas. In addition to the basis in Tables A.8 and A.9, a ratio of 0.55 between $PM_{2.5}$ and PM_{10} has been assumed. This is the ratio measured as an average at the four GTZ stations, varying between 0.66 at the 'TV antenna' station near ger areas and 0.48 at the West Junction station.

Table A.10 Estimated range of $PM_{2.5}$ and PM_{10} concentrations (annual average) at ground level, in ger areas and in central UB areas, AMHIB period

	$PM_{2.5}$	PM_{10}
In ger areas	200-350	350-700
In UB central areas	75-150	150-250

The ranges are applicable to the areas where measurements were actually taken. The monitoring network included stations in probably the most exposed parts of the ger areas. This is supported by the air pollution modeling results (see Annex C). Thus, the estimated ger area ranges probably cover the highest parts of the PM exposure in UB. Some of the outer parts of the ger areas have lower exposure than indicated by the ranges. The same is probably true for the central, non-ger areas: the ranges cover well the most exposed areas, while cleaner parts of the non-ger areas, e.g. to the south of central UB, have lower concentrations. The concentrations would be lower as one moves higher above ground level, as could be indicated by the measurements at the NAMHEM station about 20 meters above ground.

These indicated PM level ranges represent the situation in the AMHIB period, June 2008-May 2009. PM has been measured at the NRC station since 2006, see Figure A.26, which shows monthly time series of PM concentration at the NRC site for 2006-2009. This time series shows a development towards increased concentrations over the period, both during the summer and winter periods. The highest winter concentrations of PM_{10} occurred during 2007-08, and they were higher also during the last winter than in the first two winters. For $PM_{2.5}$, the highest levels were measured during the last winter, significantly higher than in earlier winters. Explanations for this increase must be sought in possible increased polluting activities resulting in higher emissions and/or in changes in meteorological conditions.

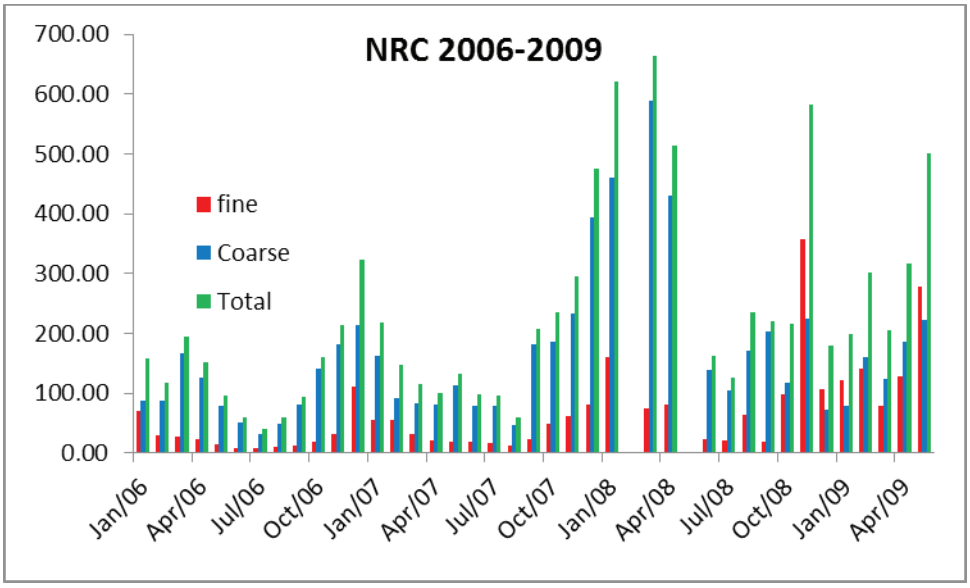

Figure A.26 PM_{10}, $PM_{10\text{-}2.5}$ and $PM_{2.5}$ concentrations at the NRC site (AMHIB station 2) for 2006-2009.

A6 Contributions to PM from emission sources

The main sources to PM concentrations in air in Ulaanbaatar have been assessed to be emissions from the burning of coal and wood for heating of individual residences in ger areas (ger stoves) and suspension of dry dust from roads and other surfaces (World Bank, 2009). Emissions from power plants, heat-only boilers (HOB) and vehicle exhaust are also sources of importance, although they were assessed to give less important contributions to ground level PM concentrations.

Quantitative assessment of the contributions from various pollution sources to concentrations levels are best done using methods like dispersion modeling and receptor modeling (as used and described in Annexes B and C). However, concentration measurements can give their own useful indications on source contributions. Such indications can be extracted from the AMHIB and GTZ measurements reported here. Starting with the PM situation in central UB areas, the hourly measurements of PM_{10} and $PM_{2.5}$ at the GTZ West Junction station can be used as an illustration (see Figure A.27).

$PM_{2.5}$ concentrations during summer (June in the Figure) should represent the contribution from vehicle exhaust to concentrations near the heavily trafficked road crossing, since the ger heating sources are very small at that time. Concentrations during the morning hours as well as during the afternoon rush hour and evening hours are increased (not very visible with the scale used in Figure A.27). This is the result of combined influences from the typical daily wind speed variation (increased day-time wind speed), the daily variation in traffic volume with rush hours as well as influence from the evening cooking in gers.

These variations and source influences are very small compared to the very much higher winter time concentrations. The curves show morning and evening increases. The periods of increase correspond with periods with ger heating. The prolonged evening/night peaks can be explained by the typically reduced wind speed at night combined with often strong ground level temperature inversions causing reduced dispersion and increased concentrations, together with the prolonged periods of heating during the evenings. The fact that the afternoon traffic rush hours are not pronounced in the winter months indicate that the vehicle exhaust contribution to the $PM_{2.5}$ concentrations is limited compared to other sources, even at the West Junction station in a non-ger area.

The much higher PM_{10} concentrations show that there is a large influence from sources of the coarse PM fraction (particle sizes between 2.5 and 10 micrometer). This is so even in the summer (June). Sources to coarse PM are suspension of dry dust from surfaces, such as open dry ground as well as roads and their surroundings. Combustion of coal and wood in gers and other combustion sources also contribute somewhat with coarse PM. The average daily variation shown in Figure A.27, which shows significant increases both in the morning, a bit

less during mid-day and a strong evening peak, indicates that road dust and other coarse PM sources are involved. The course fraction is especially large during spring time (March-May). This is a clear indication that suspension of dust from dry surfaces (roads and open soil surfaces) is an important source.

The similar analysis from the GTZ station 'TV Station', see section A7 below, located close to ger areas, show similar variations as at the West Cross station, but much more pronounced, indicating the importance of ger area emissions.

The much higher concentrations measured at the stations in the ger areas, as described in Section A5, is a strong indication of the large contribution from the ger heating sources to the PM concentrations at those locations.

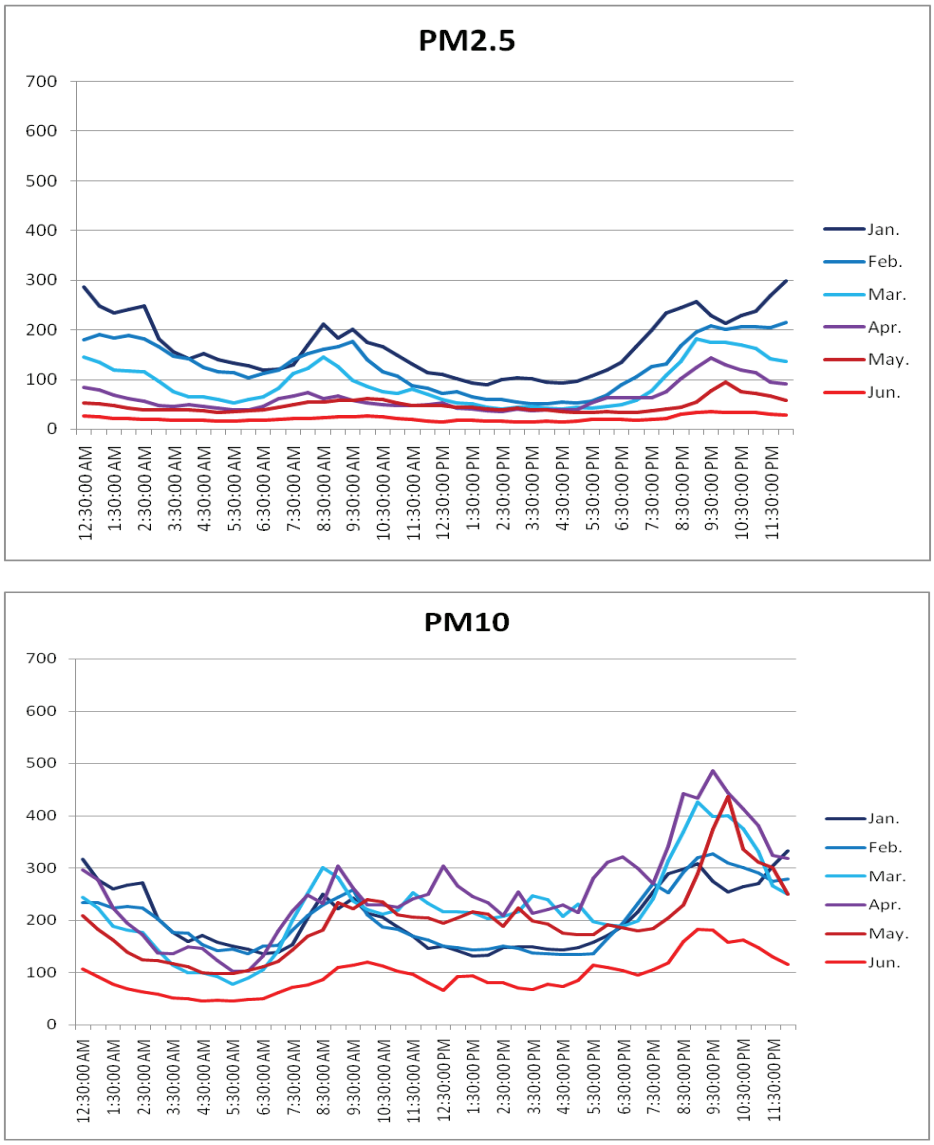

Figure A.27 Monthly average daily variation of PM_{10} and $PM_{2.5}$ at the GTZ West Junction Station, during work days.

Such evaluations can only be used to indicate PM source contributions and their importance. The measurements presented in this Annex indicate that ger heating sources is a major contributor to $PM_{2.5}$ concentrations in the ger areas. It also contributes to PM in UB central areas. Dust suspension from open soil surfaces and roads is another major source. The influence from road vehicle exhaust is limited even in central traffic areas.

The contribution from power plants and HOBs to PM concentrations in UB cannot be quantified by means of the data presented in this Appendix.

A7 Causes of variability in the PM Concentrations in UB

Meteorological variations

Smoke pollution from combustion for heating is mainly dependent on the temperature, since consumption of coal and wood for heating increases with lower temperature. Wind speed is also important, since the dispersion of the emissions increases with increased wind speed, resulting in lower concentrations in air. PM and its dependence on meteorological parameters is shown in Annex F. Figures A.28 and A.29 show examples, where the AMHIB station at the airport has been arbitrarily chosen together with meteorological data from the UB3 station.

Figure A.28 shows how the $PM_{2.5}$ concentration increases as the temperature decreases towards the winter (and opposite towards the spring), because the amount of coal and wood used for residential heating in the area increases. This relationship is modified by the influence of other meteorological conditions, such as wind speed. Figure A.29 shows periods when increased wind speed on some days reduces the concentrations, and vice versa. The very high concentrations during the first half of December are caused by a combination of low temperature and low wind speed. This occurs typically during anti-cyclonic (high pressure) meteorological conditions that are often the cause of very local pollution concentrations anywhere. In such periods it is also typical that ground level temperature inversions occur (increased temperature with height above ground) which traps ground level emissions and causes high pollution concentrations.

Another effect of increased wind speed is increased suspension of soil dust from open surfaces and roads. This mostly affects the coarse $PM_{10-2.5}$ fraction, and thus increases the PM_{10} level, although to some extent also the $PM_{2.5}$ level. This effect is probably the cause of the very high PM_{10} concentrations at the NRC (2) station during the end of April and early May, when the wind speed in UB was rather high, combined with dry soil conditions.

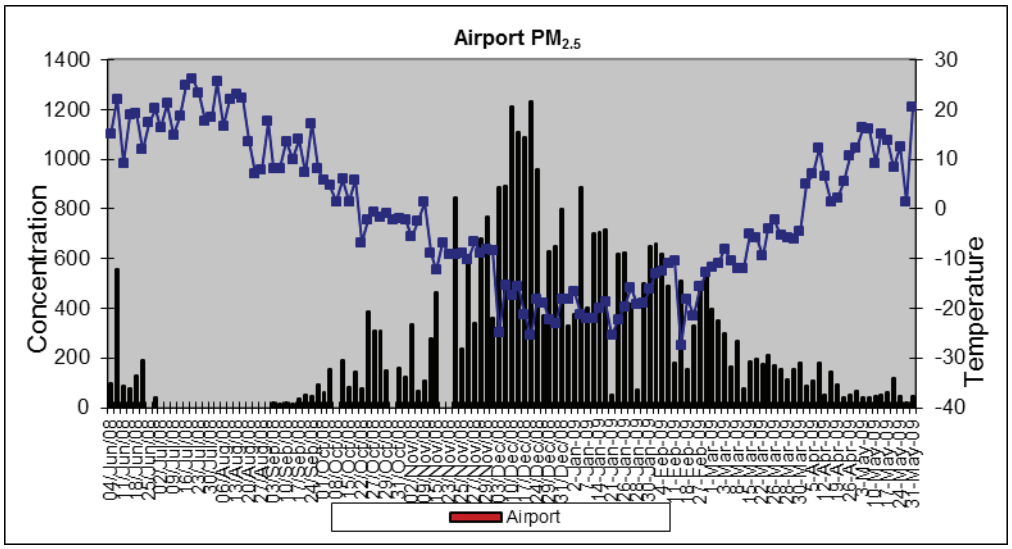

Figure A.28 Time series of $PM_{2.5}$ pollution and temperature at the site 8 Airport.

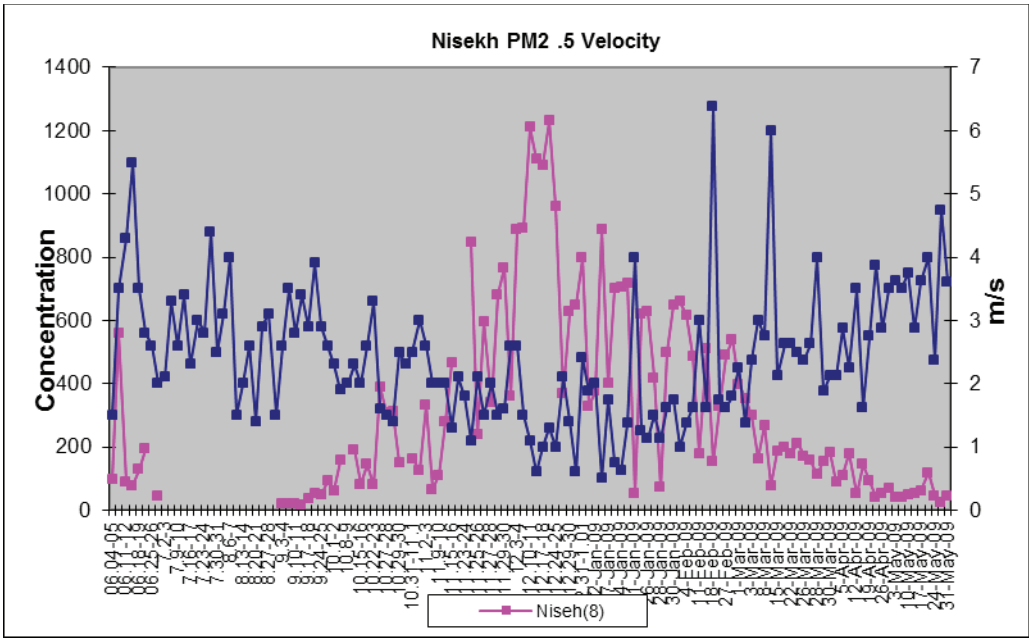

Figure A.29 $PM_{2.5}$ and wind speed dependence at the site 8 Airport.

Firing practices in ger stoves

It is interesting that smoke pollution tends to be higher in December early in the winter than later (see e.g. Figure A.28 and Figure A.29). This occurred during 2008-2009 despite the daytime average temperature being slightly lower in January. This could be caused by the fact that at the beginning of the winter people keep the stoves cold, and fire the stoves two or more times a day. This generates more pollution than when the stoves are kept hot in the mid and late winter.

This can be further substantiated by Figure A.30 where a time series of PM air pollution obtained at the Takhilt meteorology station (UB 3) on a day at the end of November 2008 is shown. This illustrates the beginning of the winter, and shows clear peaks in the time series of PM near Ger district sites.

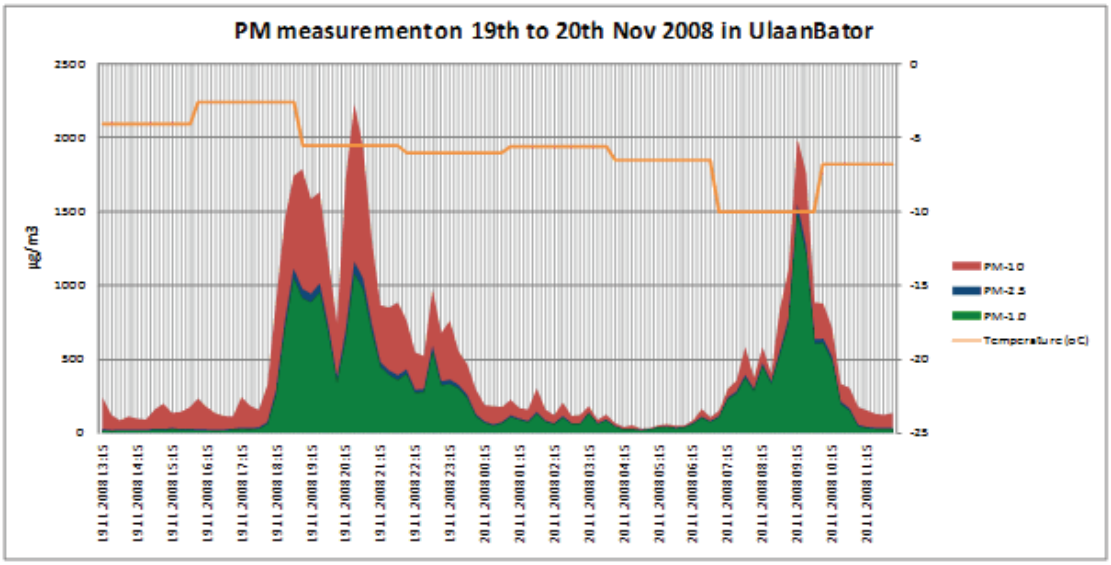

Figure A.30 Example of time series of $PM_{2.5}$ for one day at the beginning of winter.

The peak from 07.15-11.15 corresponds to morning firing and peak 18.15-20.15 corresponds to evening fire reloading and partially to fugitive road dust, which is caused by the increasing traffic after work.

It can be estimated that about 50% of PM concentrations corresponds to ignition phase (cold start) in the mornings 8.30-9.30, in the evening 18.30-19.30 and during the reloading of stoves 20.30-21.30.

The main size fraction of the $PM_{2.5}$ in the winter is PM1.0 (Figure A.30), which means the main component of smoke PM pollution is PM1.0, rather than PM2.5-1.0 pollution.

The influence of the firing practices is presented as an example of the averaged daily concentration variations on a monthly basis (months January-June) measured at the GTZ TV station.

The morning peak in those figures corresponds to morning ignition of stoves but in the evening it has two close peaks. Probably earlier peak corresponds to evening firing and the later peak from 8.30pm corresponds to the sum of firing and road dust. It can be clearly seen from the March and April curves of PM_{10} concentration. Smoke in the morning disperses rapidly and remains longer in the night due to the temperature inversion.

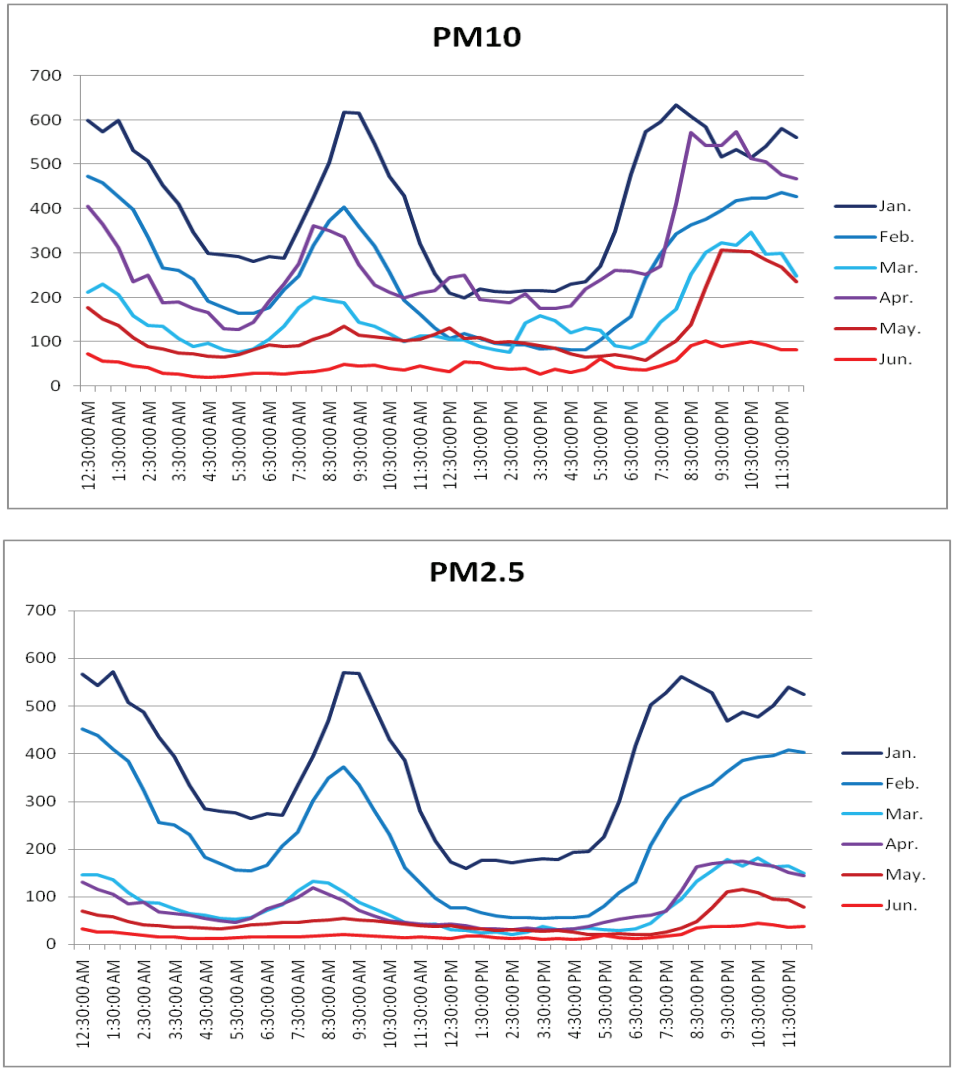

Figure A.31 Daily variation of PM concentration at the GTZ TV station site for PM_{10} and $PM_{2.5}$, for work days.

A8 On a long-term air quality monitoring network in UB

The introductory part of this chapter deals with principles for air quality network design, and establishes some general criteria.

In the second part, recommendations are made for the design of the long-term Ulaanbaatar monitoring network, and a specific network is suggested. This suggestion is a proposal for discussion between the parties involved, especially those with local knowledge of the pollution situation in Ulaanbaatar.

The recommendations are based largely upon recommendations and requirements to air quality monitoring networks set forth in the European air quality directives (http://ec.europa.eu/environment/air/legis.htm). These directives give a good example of rules that are based upon and represent state-of-the-art knowledge regarding the assessment of air quality based upon monitoring activities. Although Mongolia is in a relatively early stage in its efforts to assess its urban air quality, it is considered appropriate to base such recommendations upon state-of-the-art air quality monitoring principles and practices, when developing recommendations for improving the air quality monitoring in UB for long term operation.

Principles for air quality monitoring network design

There are no specific and detailed rules for network design which are valid and applicable in all situations. Network design is determined mainly by the overall monitoring objectives and resources availability. The description below gives a description of network design considerations developed for monitoring networks in European cities.

Although monitoring systems can have just a single, specific objective, it is more common for them to have a broad range of targeted programme functions. Typical monitoring objectives listed below:

Monitoring objectives

- Determining compliance with national limit values/standards.
- Determining population exposure and health impact assessment.
- Informing the public about air quality and raising awareness.
- Identifying threats to natural ecosystems.
- Providing objective inputs to Air Quality Management, land-use and traffic planning.
- Source apportionment and identification of source contributions.
- Policy development and prioritization of management actions.
- Development/validation of management tools (models, Geographical Information Systems etc.).
- Assessing point or area source impacts.
- Trend quantification, to identify future problems or progress against management/control targets.

The first monitoring objective for networks in most cities/countries is to determine compliance with national air quality limit values or standards, as highlighted above. For the UB AMHIB project, the second objective above, to determine health impact, is obviously also directly relevant. To comply with this objective, the monitoring network must be designed with a view to assess the population exposure.

Network design

The design of an AQ monitoring network basically involves determining the number of stations and their location, and monitoring methods, with a view to the objectives, costs and available resources.

There are two *main basic approaches* to determine the number of stations and locations:

- to locate stations in a regular geometric grid covering the city. The grid size thus determines the number of stations;

- to locate stations at sites considered to be representative for more defined local environments, exposure situations or source activities, such as urban background.

While the first approach was used earlier, e.g. in Germany, the latter approach is now in more general use.

The typical approach to network design, appropriate over city-wide or national scale, thus involves siting monitoring stations or sampling points at carefully selected representative locations, chosen on the basis of required data and known emission/dispersion patterns of the pollutants under study. This approach to network design requires considerably fewer sites than grid strategies and is, in consequence, cheaper to implement. However, sites must be carefully selected if measured data are to be useful. Moreover, dispersion modeling and other objective assessment techniques may need to be utilized to ''fill in the gaps'' in any such monitoring strategy.

A consideration in the basic approach to network design is *the scale of the air pollution problem.* For urban monitoring networks the main issue is whether the air pollution is of predominantly local origin, or if there is also a significant contribution from areas outside the city. In UB the anthropogenic air pollution is predominantly from local origin, from sources within the city. Suspension of dust from dry soil surfaces, a natural source of air pollution, is one of the main sources of PM in UB. This means that the network can be concentrated to locations within the city, with one or may be two stations in areas outside the city, to check for the external mainly soil dust contribution.

The *number of sites* depends of course upon the size and topography of the urban area, the complexity of the source mix, and again upon the monitoring objectives.

The European AQ Directives specify a minimum number of stations to be established dependent upon the size of the urban population, and it also indicates what types of areas should be monitored (representing average as well as hot-spot exposure situations).

For a city of UB size (approx. 1 million inhabitants), the European AQ Directive would require at least 6 PM stations, of which some could be for PM_{10} and some could be for $PM_{2.5}$.

A minimum effort should be invested into the determination of number and location, to ensure that the network, which will normally be established to be operated over a long period (many years), will serve its purpose most effectively. A basic procedure of several steps should be followed:

- Start with a map showing main pollution related features such as urban central district, residential areas, areas of dense traffic, the main road network, large industrial plants and areas;
- Use a (preliminary) emissions inventory as a support to find the most polluted areas;
- Carry out preliminary dispersion modelling to identify polluted areas;
- Carry out surveys using inexpensive methods, such as passive samplers;
- Consider that different pollutants have different spatial scales of variability (e.g. CO concentrated near streets; NO_2 ozone and PM more evenly distributed).

For the UB case, the AMHIB study activities have provided a sound basis for designing a long term UB air pollution monitoring network.

The *site classification scheme* used in the European AQ Directives is a useful guide to be used in the network design, so that any station can be classed according to that scheme, and such that the network covers as many as possible of the station classes:

Classification Level 1: Type of station: traffic, industrial, background;
Classification Level 2: Type of area: urban, suburban, rural.

For UB the dominating sources are small scale heating/cooking sources in residential (ger) areas, and suspended soil dust. The soil dust source is active throughout most of the non-built-up areas in UB, and its strength is dependent upon the degree of open soil surfaces locally. Road traffic (suspension of road dust and also vehicle exhaust) is also a significant source near the main road network. On the basis of this, the monitoring network should concentrate on the following types of stations:

- Urban and suburban background (residential area) stations (locations which are not dominated by traffic and industrial sources). Both ger areas and non-ger areas should be covered.
- Urban traffic stations (close to roads/streets with high traffic).
- One (some) station location(s) may need to cover special dust suspension sources, such as areas with known intense soil suspension (based upon local knowledge), and possibly the ash ponds of the power plants.
- The need to cover areas near brick factories should be considered by local experts. The brick factories operate mainly in the summer season when other pollution sources are low.
- Areas with much refuse burning may also need to be covered.

Monitoring involves *assessing pollutant behavior in both space and time*. A good network design should therefore seek to optimize both spatial and temporal coverage, within available resource constraints. The first target is to maximize spatial coverage and obtain spatially representative measurements. Once priority pollutants are selected, the sampling methods must be capable of a time resolution consistent with the pollutant averaging times specified in air quality standards and guidelines.

The *compounds* to be measured and the *reference methods* used in Europe are prescribed by the European AQ Directives.

An air quality monitoring network must in addition to the air pollution monitoring part also include a *meteorology (dispersion parameter) monitoring* part.

The meteorological data are needed for at least two reasons:

1. For the interpretation of the temporal and spatial variation of the data from the air quality monitoring, there is an obvious need for meteorological data: wind speed and direction; parameters describing atmospheric turbulence and stability, such as temperature profiles (measurements at two or more heights), or direct turbulence measurements; mixing height; and ground air temperature.

2. An air pollution assessment and management program should consist of both pollutant monitoring activities as well the use of methods such a dispersion modelling and source apportionment methods. Such modelling methods are needed both for the assessment of contributions from the various main source in the area, as well as to assess the effects of various abatement and control measures to improve the pollution situation. Meteorological data are needed input for dispersion models.

The meteorological data should provide hourly spatial fields of the meteorological/dispersion parameters, either by interpolation, or using a wind-field model. The calculation of dispersion parameters from the meteorological parameter measurements to be used in the dispersion models usually requires the use of a meteorological pre-processor.

Monitoring network design for Ulaanbaatar

The following recommendations on air pollution monitoring network design for Ulaanbaatar is limited to particular matter, PM, since the AMHIB study concentrates on PM. Other pollutants that are already monitored in UB, such as SO_2, NO_2, ozone, should be continued. The networks of those stations in UB have not been evaluated here.

Locations of present PM monitoring stations in UB

Figure A.32 shows the locations of existing and planned monitoring stations in Ulaanbaatar. There are the following sub-networks:

- The AMHIB network. Locations marked with yellow points.
  These stations exist. Various institutions and instrument methods are involved, see Table A.1.

- Two new automatic stations operated by NAMHEM/CLEM, installed in July, 2008.
  These are located at the sites 'Station 5-CLEM' and 'Western Cross' in the Figure (marked with blue points there).

- The German donor (GTZ) monitoring stations, marked with red points (G). The stations started in November-December 2008.

- NAMHEM/CLEM stations for SO_2 and NO_2 monitoring, as well as meteorology (marked with blue points).

- Lately (mid-2010) 4 new stationary donor monitoring stations financed by France have been established. They are located (ref to the map Figure A.32) at Western Cross, at the AMHIB station 3 (Zuun Ail), at UB4 station as well as at a location outside UB, towards south-east. A mobile instrumented unit is kept at the CLEM station, for use in various places according to need.

Figure A.33 shows the isolines of PM_{10} concentrations as modeled, as an input to the location of stations in high or average exposed areas.

Recommended design criteria for a UB air quality monitoring network

Based on the general criteria described above, and based upon the situation in UB, the following criteria should apply for the PM monitoring network design in UB:

- The number of stations should be at least 6 (according to European criteria).
  The number of stations available in UB is 8 AMHIB stations, 2 new NAMHEM/CLEM stations (1 of them is co-located with AMHIB station 5, the CLEM lab), and 4 GTZ stations, totally 13 stations. This is 'more than enough', and provides the possibility to monitor many areas.

- The stations should be in operation over several years.
  One of the objectives is to show the results of various abatement actions.

- The stations should cover the following areas:
  1. The most polluted areas, see Figure A.33.
  2. Residential areas, both in the city centre (non-ger) and the ger areas.
  3. Areas with high traffic, stations located fairly close to the streets/roads.
     Such traffic stations should cover both
     - city centre (highly trafficked, but with paved roads), and
     - highly trafficked roads in ger areas.
  4. Possibly other high PM and dust exposed residential areas, such as areas with much soil suspension, close to the ash ponds, or close to places with much refuse burning, based upon local knowledge.
  5. One station could be established to check for high ground level concentrations occurring due to the power plant emissions.
  6. One station should be reserved for relatively clean external areas, as a reference.

- The long-term monitoring network should be based upon automatic monitors at most stations, but with filter samplers at some of the stations. All equipment used must comply with the requirements to reference methods, or be shown to be comparable to reference methods. The automatic monitors must be compared with reference methods, and correction factors for UB conditions established.

- Filter samplers at some stations provide the possibility for chemical analysis of the filters, to be used for statistical analysis for source apportionment. At present the two AMHIB stations #2 and 3 have such equipment. The operation of these samplers should continue to provide continued possibilities for chemical analysis of the particles and statistical analysis of source contributions.

- Topography considerations:
  UB is located in a wide valley, with hills to the North and South of the valley. Winds are predominantly along the valley axis during autumn and winter, when the air pollution is highest, while during spring and summer it is turned more from the northerly direction. Due to these topography/wind patterns, the wide UB valley is to a large extent separated from the parallel valleys behind the hills during the high pollution periods, and the emissions flow mostly along the valley axis.
  The ger areas which are expanding behind the hills are thus to a large extent separated pollution-wise from the main valley. Those ger areas thus have to some extent their own air pollution domain.
  With more monitoring equipment available, it would be of interest to check on the air pollution concentrations also in those areas.

- Indoor air pollution considerations
  The air pollution inside the gers have been studied to some extent in UB. One report has found extremely high concentrations, using passive samplers, while the report from the Public Health Institute found moderate PM concentrations, using active samplers (the NUM samplers).
  There is no doubt that the indoor pollution is higher than outdoor, but more work is needed to establish exactly how much higher.
  Such work should be carried out in parallel with the monitoring network discussed in this note. In such work, it would be important to monitor indoor and outdoor pollution simultaneously.

In order to establish a link between the baseline monitoring done at the AMHIB network until mid 2009 and the continuing, long-term monitoring with the German, French and NAMHEM/CLEM equipment , this new equipment should be co-located at a number of the AMHIB stations.

Suggested monitoring network

From these recommended criteria, the following design of a long-term AQ monitoring network in Ulaanbaatar is suggested, as shown in Figure A.34, as input to a discussion with local experts. It is considered that the GTZ stations will continue long term operation in their present locations (red points, G). Green triangles are suggested locations for additional stations. These are described as follows:

- AMHIB site 1, NAMHEM: This is an urban background station. Should be continued, with automatic reference equipment.

- AMHIB site 4, 6 Buudal: Monitoring near this site should be continued. It is suggested that the site be moved fairly close to the main road going North-South near the station. Then this site will be classified as a traffic (T) site in an otherwise heavily polluted residential area.

- AMHIB site 6, III Khoroolol: Monitoring near this site should be continued. This is a heavily polluted densely populated residential area. It should be considered to move the site a bit northward, to be more securely located within the most polluted area, away from the gradient towards lower concentrations towards the city centre. This is an urban background site.

- AMHIB site 7, Bayanhoshoo: This site is similar to site 6. Urban background site. Monitoring should be continued at this densely populated area.

- AMHIB site 3, Zuun ail: Similar to sites 6 and 7. Urban background site. Should be continued. It should be considered to move the site a bit further east, since the modeling indicates higher concentrations there. A French donor station has now been located here, with automatic instrumentation.

- AMHIB site 2, NRC: This site has been operated since 2006. Urban background site. It is located in a fairly low polluted area with low population density. Because of the long time series with data at this site, it should be considered for continuation.

- Reference site in a relatively clean area: The GTZ Airport site is considered well suited for this purpose.

- Other sites to be considered:
  - 1-2 more sites within the urbanized central UB areas should be considered, to get better knowledge of the pollution levels in central areas.
  - A site to be located to check for high ground level concentrations from the power plants.

- This suggested network will provide:
  - 3 urban background stations in the most polluted ger areas (AMHIB Sites 3, 6, 7).
  - 1-3 urban background stations in central areas (Site 1 NAMHEM and 1-2 more sites)
  - 1 station between ger and central areas, somewhat traffic exposed (GTZ TV station).
  - 3 traffic stations (GTZ West Cross and East Cross, and modified AMHIB site 4).
  - 1 reference station in relatively clean area (GTZ Airport site).
  - Some additional specialized sites.

Many stations should be equipped with automatic monitors, dependent upon availability and funding. The automatic equipment at the CLEM station (AMHIB site 5) and at the CLEM site near West Cross should be considered to be moved to some of the sites suggested above. The rest of the stations should be equipped with reference or comparable samplers. The Gent samplers should be operated to provide filters for chemical and source contribution analysis. They can also be used for PM_{10} concentration measurements, when operated so as to avoid the clogging problem.

The need to continue sampling for source apportionment analysis should be considered, and at which stations this should be done. At these stations, the Gent samplers or other similar samplers must be used.

This suggestion should be considered a proposal for discussion between all partners.

Data quality considerations

It is of paramount importance that proper and uniform data quality control and assurance (QA/QC) procedures are established, documented and in operation for the monitoring network, and that the necessary training is provided to local operators. This training should be followed up regularly. The operation of the QA/QC procedures should be audited regularly by expert institutions.

Figure A.32 Location of monitoring stations in Ulaanbaatar. Yellow points: AMHIB stations; Red G: GTZ stations; Blue: CLEM stations.

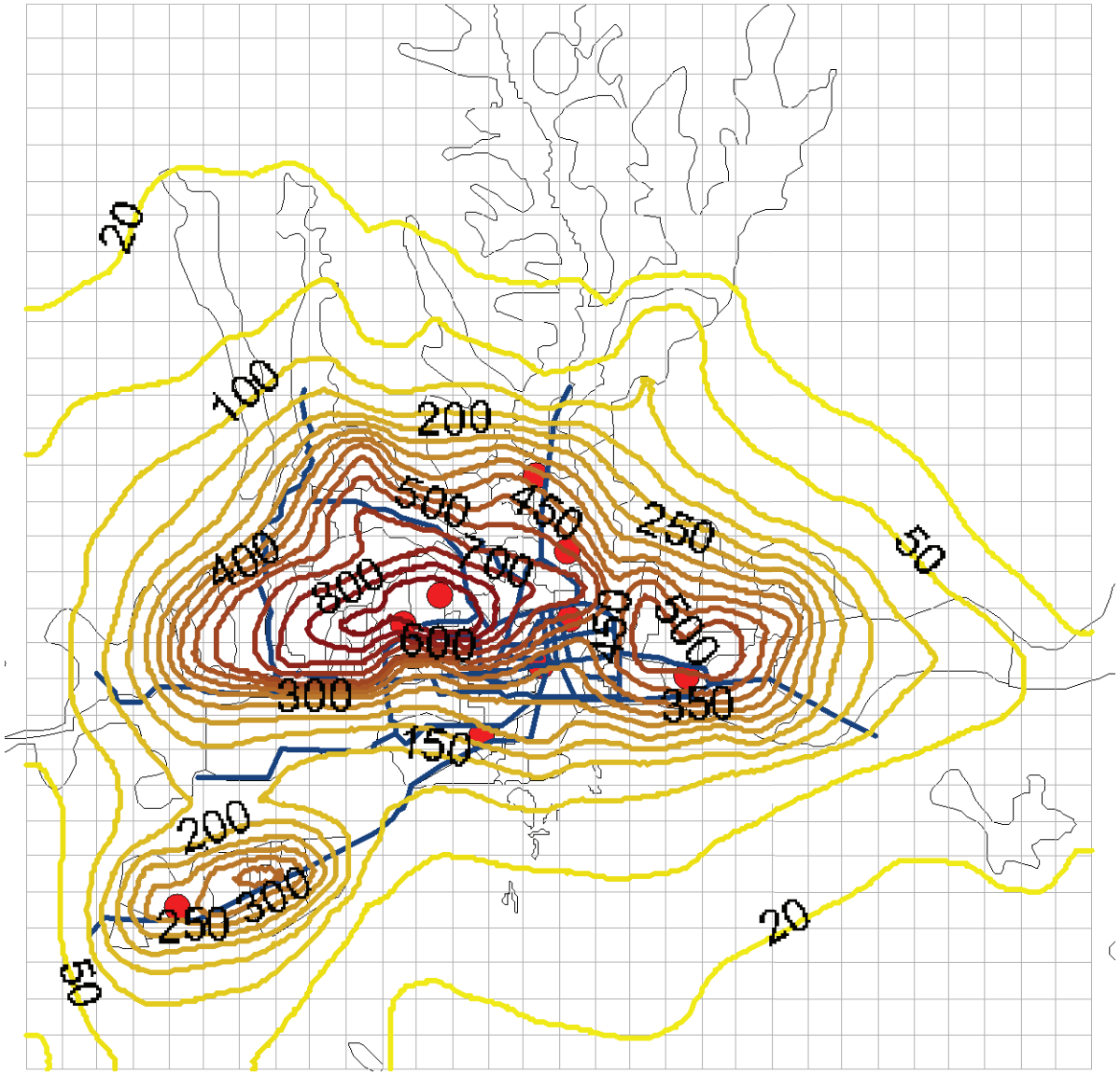

Figure A.33 Modeled PM_{10} concentration distribution in Ulaanbaatar (see Annex C).

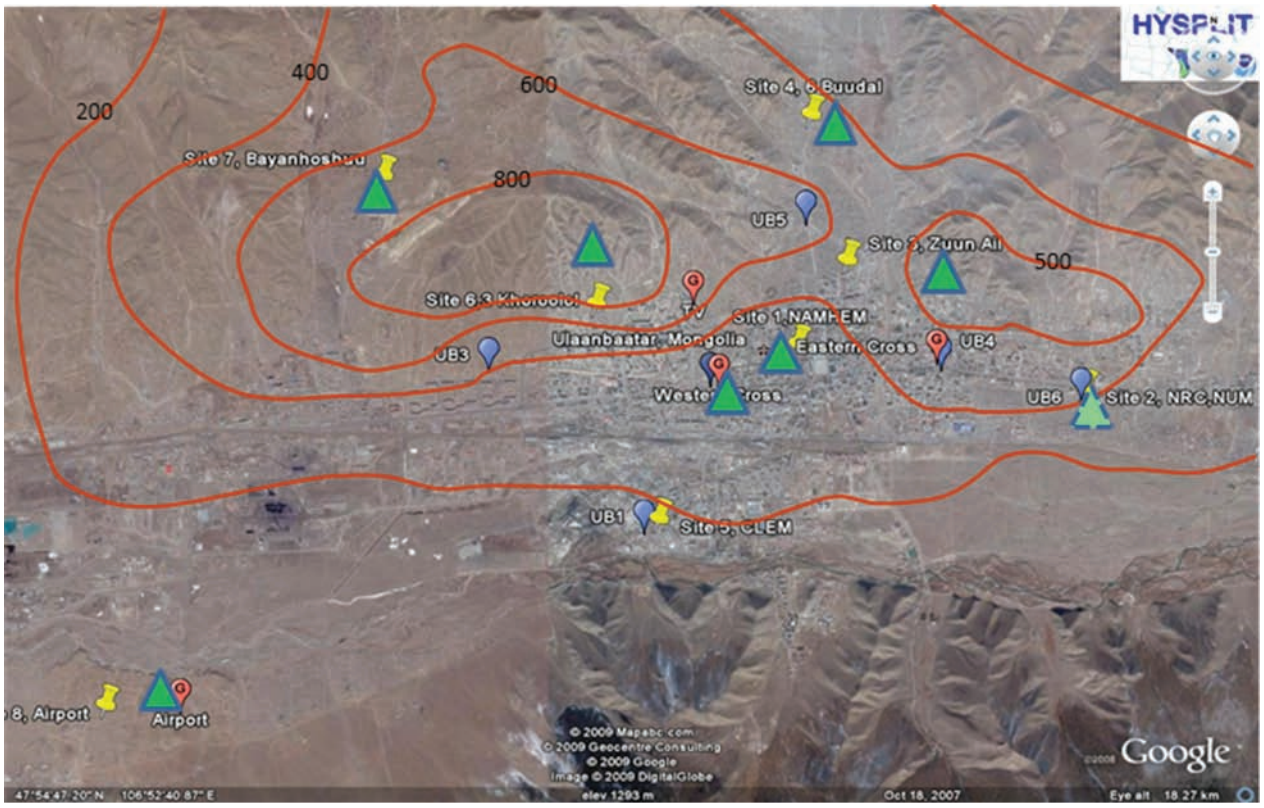

Figure A.34 Suggested location of AQ monitoring stations for the long-term Ulaanbaatar network.

Nomenclature as in Figure A.32. Green triangles and red points (G): Suggested locations for long-term monitoring stations.

Ulaanbaatar, Mongolia, Air Monitoring and Health Impact Baseline (AMHIB) Report

Annex B

Identification and Apportionment of Particle (PM) Pollution Sources by Receptor Modeling[1]

Introduction

The purpose of Annex B is to present the results of the source apportionment analysis that has been carried out based upon PM data from the three AMHIB stations 2 (NRC), 3 (Zuun ail) and 6 (III Khoroolol). The Nuclear Research Centre (NRC) of the National University of Mongolia (NUM) has been participating in an international project during many years, where particulate matter samples have been taken at the NRC station and been subjected to multi-elemental analysis at the Institute of Geological and Nuclear Sciences (GNS) in New Zealand. Receptor modeling has also been carried out on the data, lately using the PMF methodology (see below). Under the AMHIB project, this activity was enhanced so that PM samples suitable for receptor modeling were taken also at the AMHIB stations 3 and 6.

The Annex presents the methodology and the detailed results of the source apportionment (SA) for each of the PM size fractions sampled at the stations (fine PM fraction—$PM_{2.5}$, coarse PM fraction—$PM_{10-2.5}$, and the sum of fine and coarse—PM_{10}).

The results provide a separate basis for assessing source contributions to PM in Ulaanbaatar. They can also be studied together with results of source contributions that can be extracted from the air pollution dispersion modeling work that has been carried out for Ulaanbaatar as a part of the AMHIB project, based upon an inventory of PM emissions from the sources in Ulaanbaatar and upon meteorological data. Annex C describes the dispersion modeling work and the comparison with the SA results from the receptor modeling described in this Annex.

[1] This report was written by the following World Bank consultants under the AMHIB project: Steinar Larssen, Sereeter Lodoysamba, Dagva Shagjjamba and Gunchin Gerelma. Andreas Markwitz of Geological and Nuclear Sciences (GNS) in Gracefield, Lower Hutt, New Zealand also contributed to this report. It was peer reviewed by Dick van den Hout, Netherlands Organization for Applied research/TNO, Sameer Akbar, World Bank, M. Khaliquzzaman, World Bank consultant and Taizo Yamada, JICA. World Bank Task Team Leaders were Jostein Nygard and Gailius Draugelis.

Table of Contents

B1 Source apportionment by receptor modeling

The fundamental principle of source/receptor relationships is that mass conservation can be assumed and a mass balance analysis can be used to identify and apportion sources of airborne particulate matter in the atmosphere. This methodology has generally been referred to within the air pollution research community as *receptor modeling* [Hopke, 1985; 1991]. The approach to obtaining a data set for receptor modeling is to determine a large number of chemical constituents such as elemental concentrations in a number of samples. Alternatively, automated electron microscopy can be used to characterize the composition and shape of particles in a series of particle samples. In either case, a set of mass balance equations can be written to account for all m chemical species in the n samples as contributions from p independent sources. The solution of this set of equations provides a set of 'profiles' with different elemental compositions. These profiles can be interpreted as emission sources of particles, to the extent that the elemental composition of the PM emissions from the sources can be linked to the calculated elemental profiles. This provides the basis for calculating the contributions from the specified factors/sources to the measured PM concentrations.

Sample collection and analytical methods

Samples of particulate matter, PM, in air were taken at the AMHIB stations NRC (station 3), Zuun ail (station 3) and III Khoroolol (station 6). See Annex A for details regarding their location and characteristics.

The sampler used at stations 2 and 3, the Gent sampler (http://www.informaworld.com/smpp/content~db=all~content=a779035212) consists of a PM_{10} impactor-type size selective inlet and stacked filter unit assembly connected to a pump and gas meter (Maenhout and Francois et. al. 1993). The stacked filter unit (SFU) is made up of two filters in series, the top filter (polycarbonate) collects the particulate size fraction between 10 microns and 2.5 microns in aerodynamic diameter ($PM_{10-2.5}$ or coarse fraction), the bottom filter (polycarbonate) collects particulate matter 2.5 microns and less in aerodynamic diameter ($PM_{2.5}$ or fine fraction). The performance of the SFU and the size selective inlet has been assessed against other particle monitoring systems (Hopke, Xie et al. 1997). Hopke et al. found that the SFU has a 50 % collection efficiency for PM2.2, but the effective size selectivity range was 2.0–2.5 μm. For the purpose of this work the particle collection size of the fine filter is assumed to be 2.5 μm and below and is reported as $PM_{2.5}$ accordingly.

The sampler has a non-ideal behavior when the PM concentration is very high, such as in Ulaanbaatar. This has been shown and discussed in Annex A. At high PM concentrations a part of the coarse fraction penetrates the top filter and ends up on the fine fraction filter. The result is that the elemental composition, and thus the source apportionment (SA) of the fine fraction, the $PM_{2.5}$, partly reflects the coarse fraction composition. This should be noted, for example, when the SA finds a significant fraction of soil dust in $PM_{2.5}$. The real soil contribution to $PM_{2.5}$ would most probably be smaller than found as a result of the SA analysis of the $PM_{2.5}$ filters.

Generally, the samples were collected continuously for a 24 hour period, but on some days particularly in the winter it was not possible to collect the sample over the entire 24 hours as the high particulate matter concentrations lead to clogging of the top, coarse fraction filter. Thus, the sampler was operated alternating on and off (e.g., 1 hour on followed by 1 hour off) over the course of the 24 hours period to provide a representative sample for that day. On extremely polluted days, even on-off sampling lead to early clogging, and on those days sampling had to be stopped after 6–8 hours.

The sampler used at station 6, the Partisol 2000 sampler (http://thermoscientific.com/wps/portal/ts/products/detail?navigationId=L10405&categoryId=89579&productId=11960560), has a 10μm size selective inlet excluding particles larger than 10 μm from the sample. The PM_{10} particle fraction was collected on a Nuclepore filter of 0.4 μm pore size. This sampler also clogged on polluted days, and the instrument had to be stopped after some hours.

Samples were analyzed at the New Zealand ion beam analysis (IBA) Facility operated by the Institute of Geological and Nuclear Sciences (GNS) in Gracefield, Lower Hutt, New Zealand. Ion Beam Analysis (IBA) was used to measure the concentrations of elements with atomic number above neon in particulate matter on the filter samples (Figure B.1) (Trompetter, Markwitz et al. 2005).

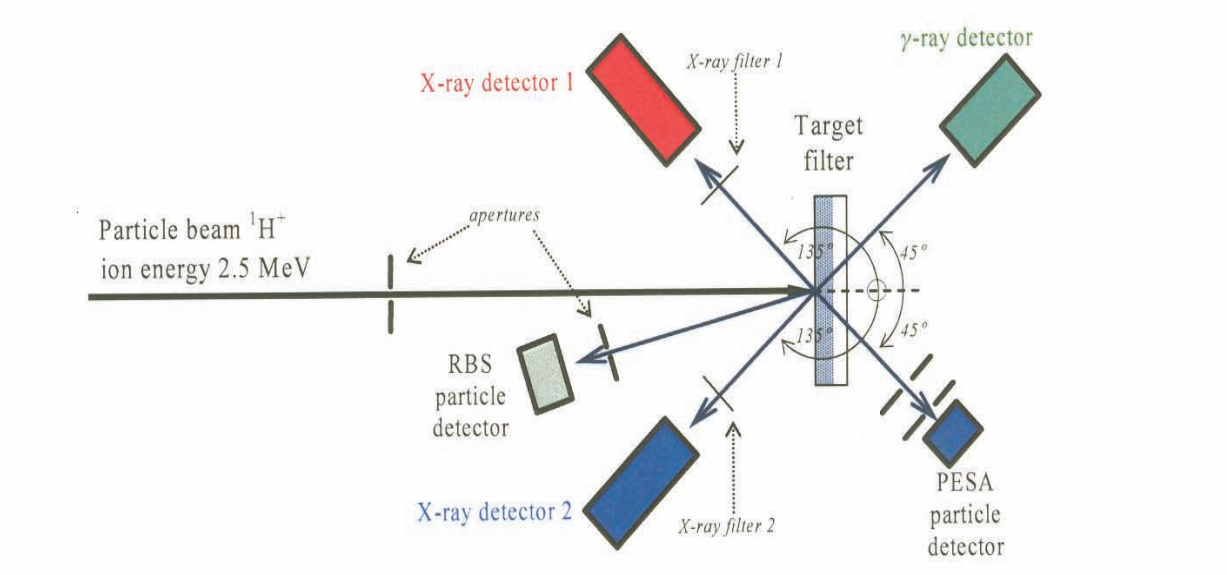

Figure B.1 Schematics of experimental set-up.

Black carbon (BC) concentrations on filters were determined by light reflection using a M43D Digital Smoke Stain Reflectometer. For atmospheric particles, BC is the most highly absorbing component in the visible light spectrum with very much smaller absorption coming from soils, sulfates and nitrate (Horvath 1993; Horvath 1997). Hence, to the first order it is assumed for the purposes of this study that all the absorption by particles on filters is due to BC.

Receptor modeling by PMF

Receptor modeling and apportionment of PM mass by PMF was performed using the PMF2 program (Paatero 1997). With PMF, sources are constrained to have non-negative species concentrations, and no sample can have a negative source contribution and error estimates for each observed data point are used as point-by-point weights. This feature is a distinct advantage, in that it can accommodate missing and below detection limit data that is a common feature of environmental monitoring results (Song, Polissar et al. 2001). The signal-to-noise ratio for an individual elemental measurement can have a significant influence on a receptor model and modeling results. For the weakest (closest to detection limit) species the variance may be entirely due to noise (Paatero and Hopke 2002). Paatero and Hopke strongly suggest down-weighting or discarding noisy variables (as measured by their signal-to-noise ratio) that are always below their detection limit or species that have a lot of uncertainty in their measurements relative to the magnitude of their concentrations (Paatero and Hopke 2003). Therefore, the data were screened by their signal-to-noise ratio (S/N ratio). Variables with very low S/N ratios (< 0.2) were excluded from the analysis, while weak variables (0.2 < S/N < 2) were down-weighted. Rotational freedom in solutions were explored and controlled using FPEAK (Paatero, Hopke et al. 2002) and observing the effect on the Q values (chi-squared), G-vector plots and residual plots (Paatero, Hopke et al. 2005). Only those solutions that could be related to physical sources were considered acceptable.

B2 Identification of main sources to PM in UB atmosphere by receptor modeling

A total of 545 particulate matter samples were included in the receptor modeling analyses of AMHIB data, the period June 2008–May 2009, collected at the three sites NRC (site 2), Zuun Ail (site 3) and III Khoroolol (site 6). Samples from the Site 2 and Site 3 were collected in two fractions, $PM_{2.5}$ (Fine) and $PM_{10\text{-}2.5}$ (Coarse), samples from site 6 was collected only in one fraction, PM_{10}. Figure 3.1.1 in chapter 3.1 shows their locations.

Analysis has also been carried out on the data for the entire 2004–2009 time series obtained at the site 2 (NRC), for $PM_{10-2.5}$, $PM_{2.5}$ and PM_{10} separately. Results of the analysis of this series of data covering a long time had good statistics (5 years data) and are also included in this chapter. The time series analysis adds to the understanding of pollution sources and their contribution.

Output from the PMF analysis is a number of 'factors' defined by their specific and separate element composition, or profile. From this elemental profile it is often possible to allocate the 'factor' to a certain pollution source, based upon knowledge of tracer elements or the elemental composition of the emissions from the source type. From the PMF analysis of the AMHIB data, it was possible to allocate factors to sources associated with coal combustion, motor vehicles/road dust, and soil.

The statistical significance of the factors appearing out of the PMF analysis is determined by their 'Eigenvalue'. The higher the eigenvalue, the better are the factors assessed in statistical terms. The ranking of the eigenvalues of the factors is not necessarily the same as the ranking of the contributions from the factors, in mass terms. A factor with a relatively low eigenvalue can have a large contribution, and vice versa. In the descriptions of the results for each site and PM fraction below, factors, expressed as sources, are listed according to their eigenvalues, while the value of their contribution have a different ranking.

Source identifications are described in more detail in the discussion section of this annex. Generally, it involves the following:

Soil: airborne soil originating from crustal matter as the profile is dominated by Al and Si along with Ca, Ti and Fe. It has been possible to identify two different sources to airborne soil in UB—the source identified by the above elements (named Soil 1) and a Soil 2 source which in addition includes a significantly higher BC component. The difference between the two crustal matter sources is most likely the source location, with the Soil 2 source originating more locally in Ulaanbaatar where there is likely to be a greater concentration of settled combustion particles and coal dusts mixed into the crustal matter, hence the higher presence of BC in the source profile. Soil 1 represents the general crustal matter in the area around Ulaanbaatar. The soil sources contribute to PM in air through the action of wind and turbulence to suspend the particles in the soil surface into air. The nature of soil surfaces varies widely between areas in terms of the size distribution of the particles in the top soil surface. The finer they are, the easier they will be suspended by wind and turbulence. The very dry and cold climate in Mongolia probably leads to a size distribution leaning towards a higher fraction of very fine particles, compared to areas with more humid and mild climates. The soil sources in UB contribute mostly to the coarse PM fraction ($PM_{10-2.5}$), but it also contributes to the fine PM fraction ($PM_{2.5}$).

Combustion: For some of the cases, it was possible to identify two distinct coal combustion source types present in the Ulaanbaatar airshed. One has black carbon as well as a significant sulfur component (called Combustion 1), and another also has black carbon but also has relatively lower sulfur and higher soil elements associated with it (called Combustion 2). The high sulfur profile could be associated with high-temperature combustion (such as in power plants and boilers) while the low sulfur could be associated with low-temperature combustion such as in small-scale residential stoves. The combustion sources contribute mostly to the fine PM fraction ($PM_{2.5}$) while they also make a smaller contribution to the coarse PM fraction.

Motor vehicles/road dust: The profile which can be associated with a local motor vehicle and road dust component contains BC, most of the zinc and lead along with elements typical of crustal matter. Mongolia has phased out the use of leaded petrol over the past few years, although there is likely to be residual lead in local road dusts. This is a mixed profile consisting of exhaust particles in the fine fraction ($PM_{2.5}$) and suspended road dust mainly in the coarse PM fraction ($PM_{10-2.5}$). These two parts of the profile are highly correlated in time since they both originate from the road traffic with its specific time variation, and thus they show up in the analysis as one source.

Biomass burning: The profile associated with biomass burning contains black carbon and most of the potassium in the samples. Biomass burning contributes in UB mostly to the fine PM fraction ($PM_{2.5}$).

This profile/source contribute differently to the coarse and the fine fractions of the PM at the different sites.

The four identified profiles that were associated with main PM sources, coal combustion, biomass combustion, motor vehicles and soil, dominated the contributions to the PM concentrations measured. The mass associated

with these factors accounted for more than 90% of the total mass, except for the case of the NRC station for the 5-year data series, where it was about 85%, and was based upon a reconstructed mass calculation procedure. The unaccounted mass, which is rather small, could be water, or smaller sources that are not large or specific enough to show up as factor profiles as a result of the PMF analysis. Although the PMF analysis is based upon analysis of inorganic components of the mass, the mass of the organic PM constituents is, as a result of the PMF analysis, included in the mass contributions that were found to be associated with the various sources, since the organic constituents in the source contributions vary in time and space in the same manner as the inorganic constituents.

The four main factors/sources summed up to the following fraction of the total mass for the 1-year AMHIB period analysis:

- Station 2 (NRC): $PM_{2.5}$: 91.64%; $PM_{10-2.5}$: 95.13%
- Station 3 (Zuun ail): $PM_{2.5}$: 95.71%; $PM_{10-2.5}$: 93.07%
- Station 6 (III Khoroolol): PM_{10}: 99.13%

Station characteristics and source contributions: The three sites represent different locations and positions relative to main PM sources in UB, and thus give a degree of spatial understanding of the source contributions to PM in air:

- Site 2, NRC, is located a few kilometers to the east of central UB. It is away from ger areas in an area with open soil surfaces in the neighborhood. It is several hundred meters away from any main road, but there are unpaved roads with low traffic nearby the site. There are some heat-only boilers in the area. Sampler height is about 1.6 meters above ground. It is expected that the soil sources will give significant contributions to this site.

- Site 3, Zuun Ail, is located a few kilometers north-east of central UB, at the juncture of some small northern valleys (Chingeltei, Hailaast and Selbe). Extensive ger areas are located in those valleys and expose the site to emissions from ger heating systems when air is drained down the valleys towards the south. There are few open soil surfaces surrounding the site, and the site is also removed from the main roads, while there are unpaved roads carrying little traffic. Sampling height at the site 3 is 6m above the ground, which might reduce the influence of local dust suspension. It is expected that ger area emissions will contribute significantly to this site.

- Site 6, III Khoroolol, is located well within a ger area surrounded by local unpaved roads. The sampler was placed at a height of 4m above the ground on a balcony on the second floor of a residential house. The chimney of the house is located about 5 meters from the sampler inlet, not in the main wind direction and about a meter higher than the sampler inlet. There were several chimneys on nearby houses surrounding the sampler location, typical of the situation in the ger areas. It is expected that ger area emissions and soil and unpaved road dust will contribute significantly to this site.

In the following sections, results are first presented from an analysis of the 5-year long data series at Site 2 (NRC). This large data base enables a detailed evaluation of source contributions to be made, not least by analyzing the time series and the contributions on a seasonal basis, underpinning the explanations of the contributions from the various sources.

Next, the results from the analysis of the AMHIB data are presented, from the 3 stations—Site 2 (NRC), Site 3 (Zuun Ail) and Site 6 (III Khoroolol)—giving a better understanding of the source contributions in different areas in UB.

Regarding the analysis of contributions to $PM_{2.5}$, it is important to note the non-ideal behavior of the Gent sampler, and that the $PM_{2.5}$ fraction has a certain coarse PM fraction embedded in it. Therefore, for example, soil contribution to $PM_{2.5}$ would be somewhat smaller than resulting from the SA analysis.

B3 Apportionment of main PM sources in UB at the NRC site, based upon a 5-year data series

2004–2009 study of coarse fraction PM ($PM_{10-2.5}$) at NRC

The NRC study 2004–2009, made at the AMHIB site 2 based upon samples taken over the years from 2004 to 2009, is presented here. Table B.1 presents the mean, standard deviation, median, maximum, minimum, and number of samples above LOD and S/N ratio for individual species.

Table B.1 Summary statistics for $PM_{10-2.5}$ and elemental concentrations at AMHIB site 2 (ng/m^3)

ng/m^{-3}	Arithmetic Mean	Std Dev	Median	Maximum	Minimum	Samples > LOD[a]	S/N
$PM_{10-2.5}$	144000	122000	110000	955000	5000		
BC	4401	3394	3550	25617	483	224	3.1
Na	843	829	614	4434	0	173	0.3
Mg	936	769	736	4781	70	195	0.5
Al	5524	4832	3800	23436	191	223	3.4
Si	13579	10877	10696	61060	507	225	26.0
P	211	285	130	2087	0	189	0.6
S	1458	1659	965	13831	129	225	15.1
Cl	331	244	264	1284	34	225	6.0
K	1760	1441	1340	7813	72	225	18.0
Ca	4604	3443	3616	20023	257	225	20.6
Ti	298	324	197	2981	7	225	8.1
V	10	14	5	115	0	45	0.1
Mn	80	66	60	364	3	224	3.1
Fe	3338	2707	2493	14214	116	225	1.0
Cu	21	38	9	372	0	126	0.4
Zn	99	180	58	2415	0	211	2.5
Pb	34	66	11	489	0	56	0.1

[a] Limit of detection

A total of 300 particulate matter samples were included in the receptor modeling analyses of these data. While more than 25 elemental constituents were detected above their respective LOD, 18 species were selected for PMF modeling ($PM_{10-2.5}$, BC, Na , Mg, Al, Si, P, S, Cl, K, Ca, Ti, V, Mn, Fe, Cu, Zn, Pb) as other elements were only present in a few samples and/or in low concentrations (the S/N ratio was lower than 0.2).

A four-source model was found to be the most appropriate solution which, on average, explained 85% of the gravimetric mass. Figure B.2 shows the comparison between modeled (PMF) $PM_{10-2.5}$ and measured $PM_{10-2.5}$ concentrations.

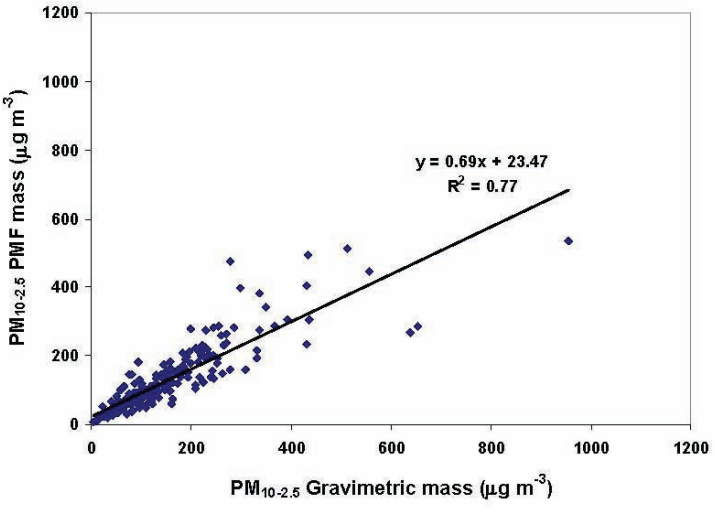

Figure B.2 Comparison between modeled (PMF) $PM_{10\text{-}2.5}$ mass concentrations and measured $PM_{10\text{-}2.5}$ mass concentrations.

Average mass contributions from sources to $PM_{10\text{-}2.5}$ at AMHIB site 2 for 2004–2009 is presented in Table B.2, source profiles are shown in Figure B.3 and their contributions in Figure B.4.

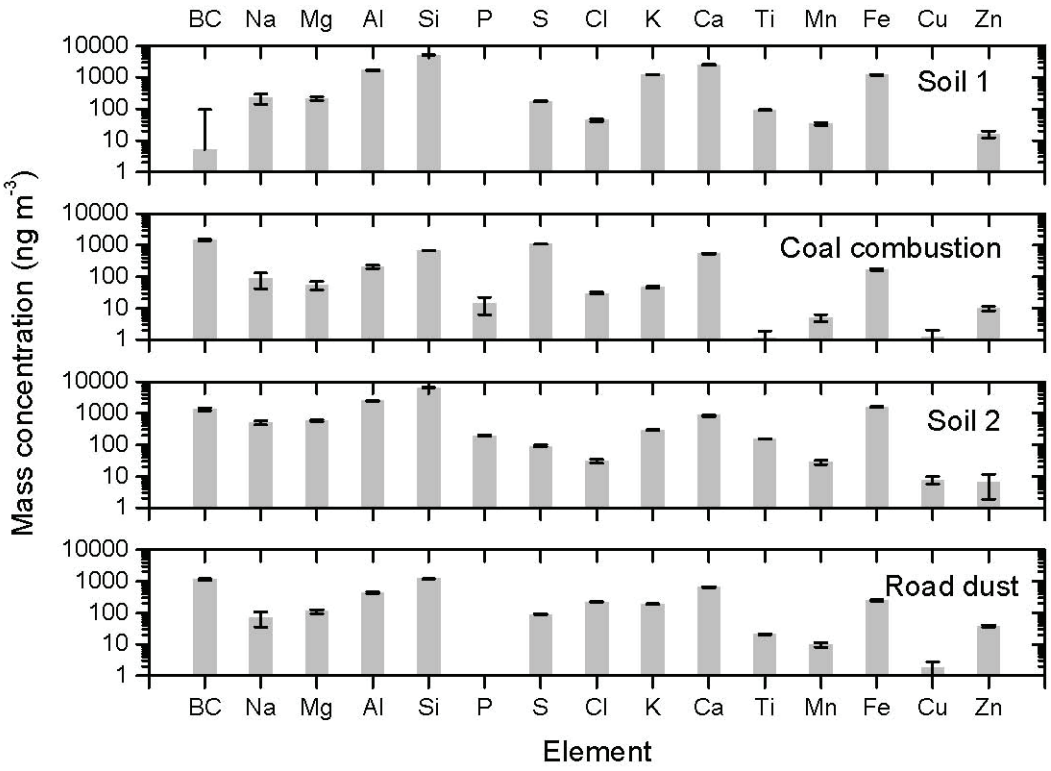

Figure B.3 Elemental source profiles derived by PMF for $PM_{10\text{-}2.5}$ samples (predicted ± StdDev), for the NRC 2004–2009 data.

Table B.2 Average source mass contributions to $PM_{10-2.5}$ at AMHIB site 2

Source	$PM_{10-2.5}$ mass ($\mu g/m^3$)	Percent
Soil 1	54.7 (3.3)	45
Soil 2	42.4 (2.5)	34
Combustion	11.7(1.1)	10
Road dust	14.0(0.8)	14

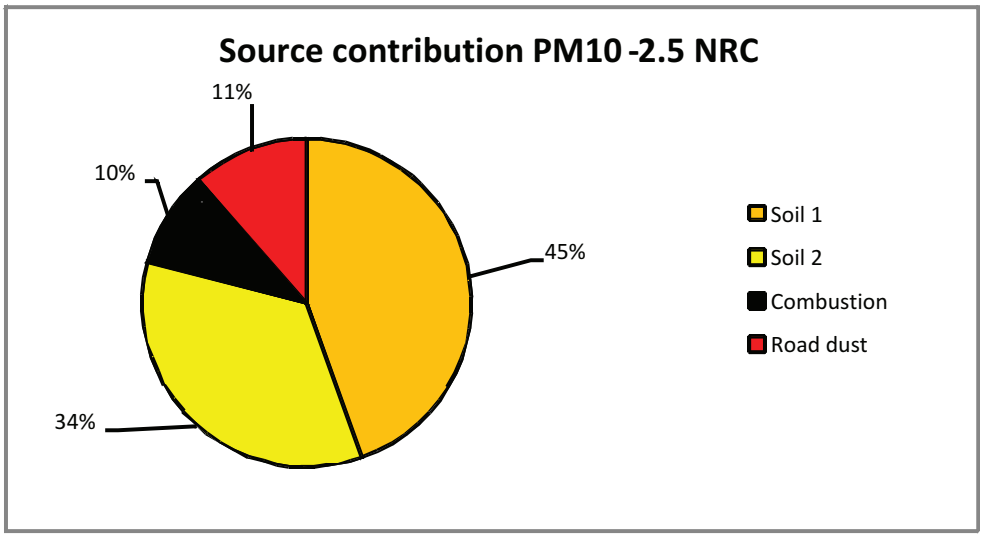

Figure B.4 2004–2009 average $PM_{10-2.5}$ mass contribution diagram at AMHIB site 2.

The first source profile, labeled as Soil 1, is identified as airborne soil originating from crustal matter as the profile is dominated by Al and Si along with Ca, Ti and Fe. The Si:Al ratio was found to be 2.6:1, typical of crustal matter composition (aluminosilicates) (Lide 1992). The second source, labeled as Soil 2, has also been identified as originating from crustal matter with the primary distinction between the two profiles being that the Soil 2 source has a significantly higher BC component, originating more locally in Ulaanbaatar where there is likely to be a greater concentration of settled combustion particles and coal dusts mixed into the crustal matter, hence the higher presence of BC in the source profile. Analysis shows that the two soil sources are correlated ($r^2 = 0.8$). However, a three factor PMF solution which essentially combined the two crustal matter sources yields unsatisfactory results, primarily due to significant skews in the residual plots (more highly positive or negative for a number of elements) and a poorer correlation between predicted (PMF mass) and measured (gravimetric) $PM_{10-2.5}$ mass concentrations. The third factor has been identified as a coal combustion source contribution for the coarse fraction and this contains the majority of black carbon and a significant sulfur component. The fourth source has been identified as a local motor vehicle and road dust component as this profile contains BC, most of the zinc and lead along with elements typical of crustal matter. Mongolia has recently phased out the use of leaded petrol years although there is likely to be residual lead in local road dusts. It is also evident that at least some lead is emitted from coal combustion sources as found in studies at locations elsewhere in Asia where coal combustion is a major source of air particulate matter (Mukai, Furuta et al. 1993; Mukai, Tanaka et al. 2001; Song, Zhang et al. 2006).

Time series analysis of contributions (see Figure B.6) underpins the above explanations of the various source contributions. Figure B.5 shows that the $PM_{10-2.5}$ coal burning source contribution peaks during winter indicating that it is likely to be due to emissions from local power generation and solid fuel fires for domestic heating.

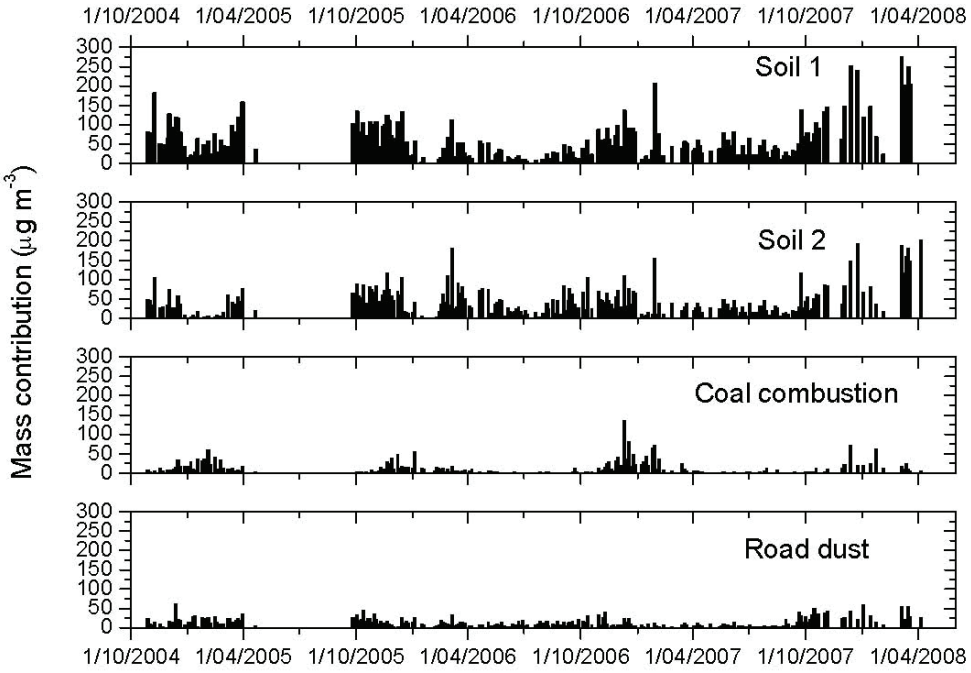

Figure B.5 Contribution time series of resolved sources for $PM_{10-2.5}$ at AMHIB site 2.

Figure B.6 further shows that the crustal matter (soil) contributions are highest during spring and autumn with significant contributions during winter from the Soil 1 crustal matter source. The temporal variations in crustal matter contributions are consistent with precipitation patterns in Ulaanbaatar as most rain fails during summer and a consequent suppression of dust generation. Spring, autumn and winter in Mongolia are generally dry with spring and autumn the windiest seasons (Xuan, Sokolik et al. 2004). This variation with the dryness and wind of the season is consistent with the understanding that soil particles appear in the airborne PM due to wind as turbulence action suspending particles from the top soil surface into the air.

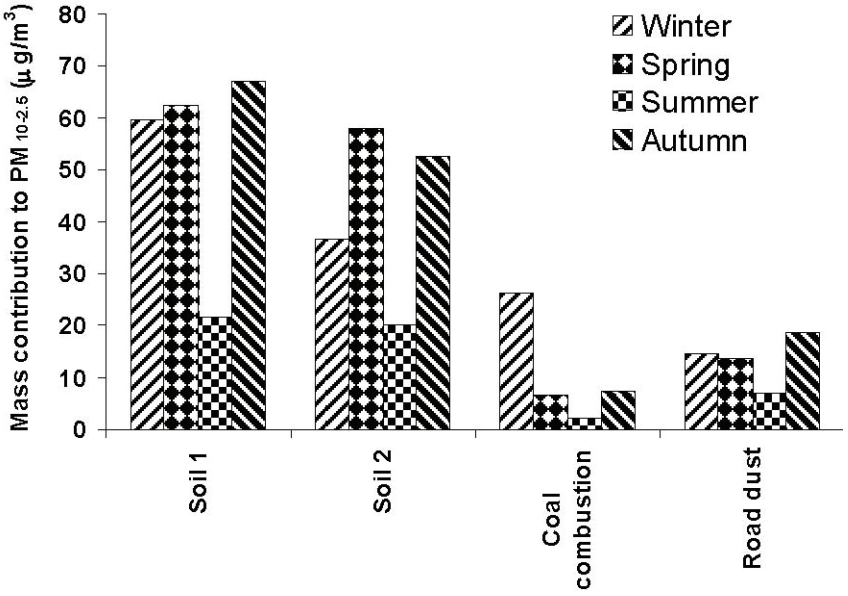

Figure B.6 Seasonal source mass contributions to coarse fraction PM ($PM_{10-2.5}$) at NRC.

2004–2009 study of fine fraction PM ($PM_{2.5}$) at NRC

A total of 232 fine particulate matter samples were included in the receptor modeling analyses of NRC data from 2004–2009. While a total of 25 elemental constituents were detected above their respective LOD, 16 species were selected for PMF modeling ($PM_{2.5}$, BC, Na , Mg, Al, Si, S, Cl, K, Ca, Ti, Mn, Fe, Cu, Zn, Pb) as other elements were only present in a few samples and/or the S/N ratio was low. Table B.3 presents the mean, standard deviation, median, maximum, minimum, number of samples above LOD and S/N ratio for individual species.

Table B.3 Summary statistics for $PM_{2.5}$ and elemental concentrations at AMHIB site 2 (ng/m^3)

ng/m^3	Arithmetic Mean	StdDev	Median	Maximum	Minimum	Samples > LOD[a]	S/N
$PM_{2.5}$	51800	91400	28200	1210000	5700		
BC	7290	10454	4242	94206	680	235	2.75
Na	290	425	112	2642	0	88	0.13
Mg	326	276	235	2083	31	200	0.62
Al	1150	1224	745	7627	0	227	0.81
Si	2305	1740	1871	10554	129	236	17.2
S	1969	3978	900	40079	125	236	17.55
Cl	139	133	88	849	12	236	2.14
K	324	239	243	1558	35	235	7
Ca	789	559	652	3194	50	236	11.92
Ti	37	33	28	156	0	191	0.27
Mn	15	14	11	65	0	178	0.18
Fe	523	388	416	2150	26	236	0.62
Cu	10	29	3	373	0	105	0.21
Zn	44	54	30	400	0	213	0.55
Pb	31	73	7	525	0	50	0.08

[a]Limit of detection

A seven-source model was found and Figure B.7 shows the comparison between modeled (PMF) $PM_{2.5}$ and measured $PM_{2.5}$ concentrations. The elemental source profiles are presented in Figure B.8. The derived source profiles were compared to measured source profiles and/or those reported in other studies to ensure they made physical sense. The average mass contributions of each of the sources to ambient fine particle concentrations are shown in Table B.4, mass contribution diagram is shown in Figure B.9.

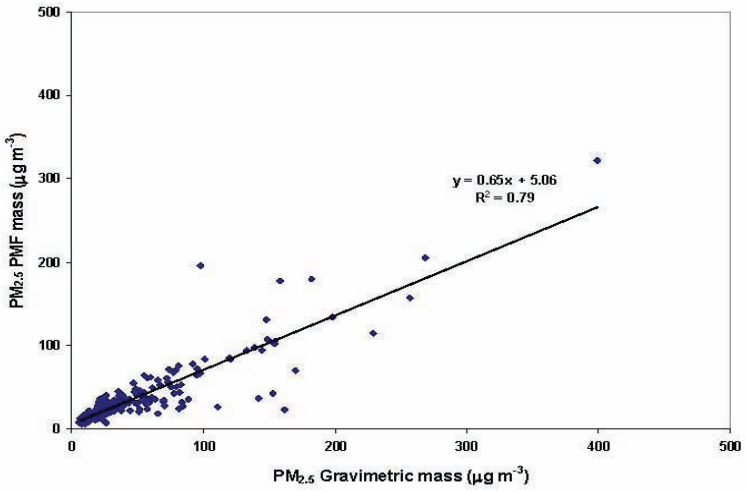

Figure B.7 Comparison between modeled (PMF) $PM_{2.5}$ mass concentrations and measured (gravimetric) $PM_{2.5}$ mass concentrations.

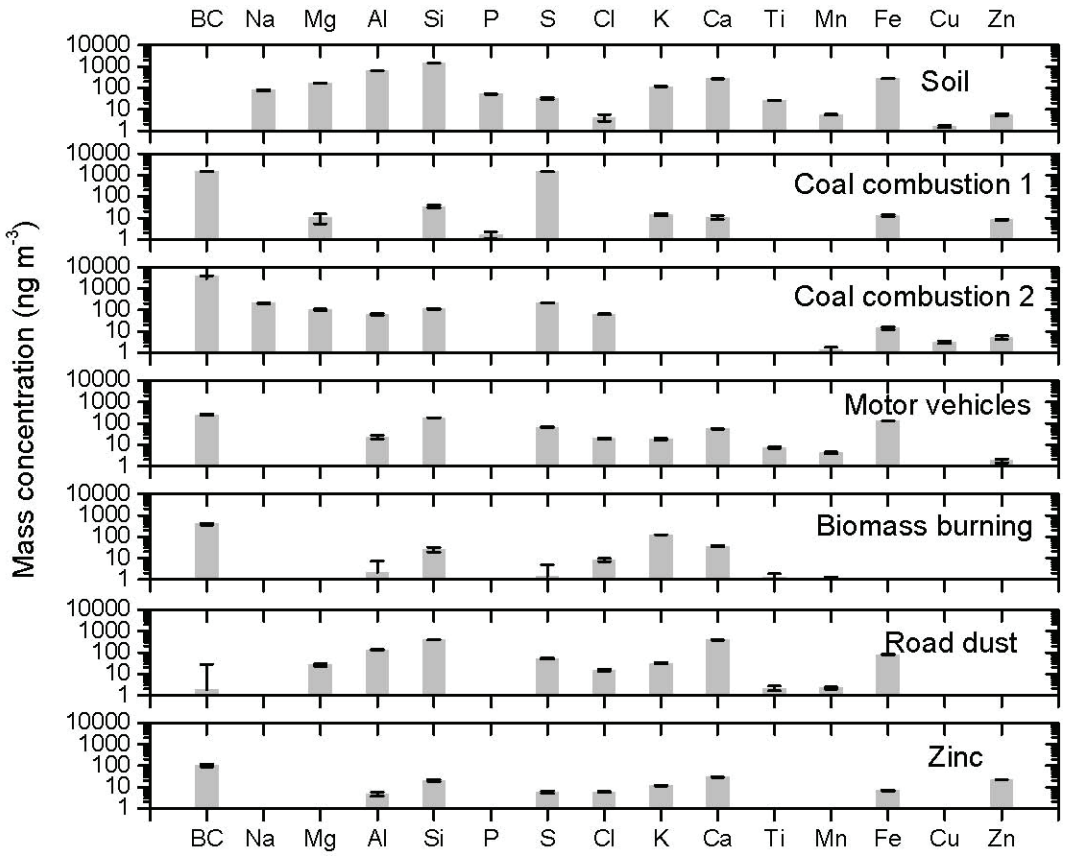

Figure B.8 Elemental source profiles derived by PMF for $PM_{2.5}$ samples (predicted ± StdDev) (ng/m^3).

Table B.4 Average source mass contributions to $PM_{2.5}$ at AMHIB site 2

Source	$PM_{2.5}$ mass µg/m^3	Percent
Soil	5.0 (0.3)[a]	14
Coal combustion 1	12.2(1.6)	35
Coal combustion 2	11.5(0.9)	33
Motor vehicles	1.9(0.2)	1.9
Biomass burning	1.1 (0.1)	1.1
Road dust	2.9 (0.2)	2.9
Zinc	0.6(0.1)	0.6

[a]Standard error

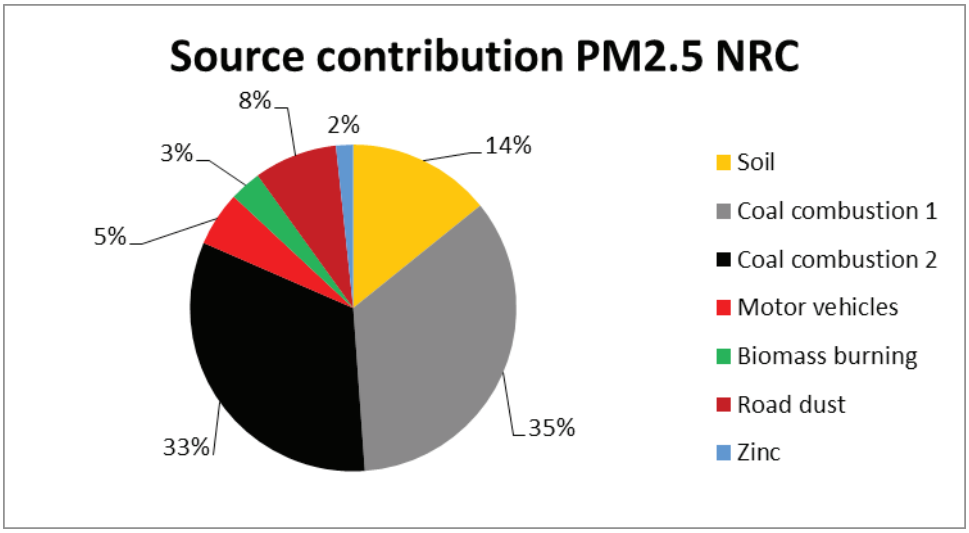

Figure B.9 2004–2009 average $PM_{2.5}$ mass contribution diagram at AMHIB site 2.

The temporal variation on source contributions to $PM_{2.5}$ is presented in Figure B.10. It is important to note that the scales for the coal combustion sources are an order of magnitude higher than the other plots. The temporal variation in source contributions shows that coal combustion peaks during winter in Ulaanbaatar. Seasonal contributions by $PM_{2.5}$ sources are presented in Figure B.11. The $PM_{2.5}$ crustal matter and road dust sources had peak contributions during spring and autumn corresponding with the driest seasons as did the biomass burning source. The crustal matter and road dust contributions are a bit overestimated, due to the mentioned non-ideal behavior of the sampler.

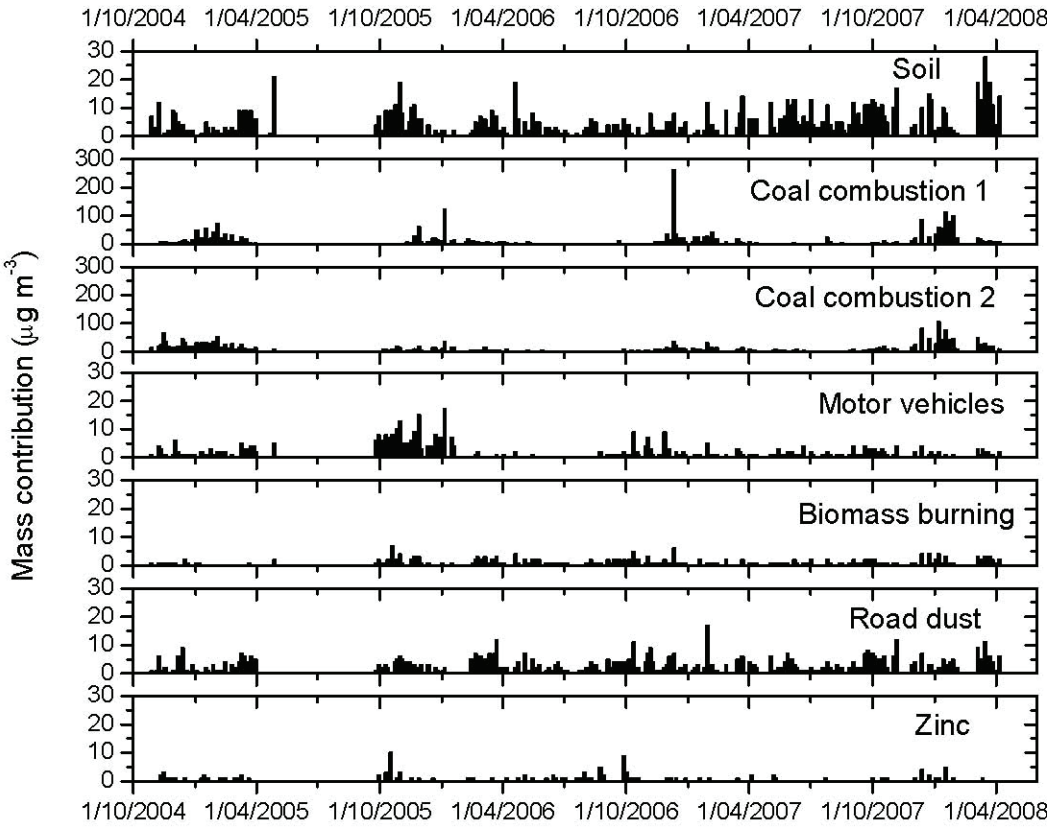

Figure B.10 Contribution time series of resolved sources for $PM_{2.5}$ at NRC.

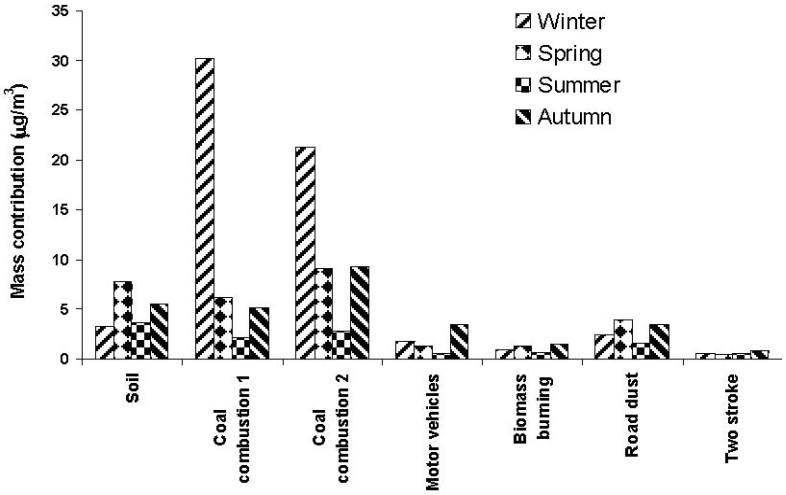

Figure B.11 Source contributions to $PM_{2.5}$ by season at the AMHIB site 2.

2004–2009 study of PM_{10} at NRC

The PM_{10} pollution source apportionment was carried out based on the analysis $PM_{2.5}$ and $PM_{10\text{-}2.5}$ data analysis for 2004–2009 for site 2. This introduces the calculations for PM_{10} source contributions from those calculations (see Table B.5 and Figure B.12).

Table B.5 Average source contribution to PM_{10} at the site 2 (2004-2009 years average) (percent)

No	Source	Mass (µg/m^3)	Percentage
1	Soil	102.1	64
2	Combustion	35.4	22
3	Motor vehicles + Road dust	18.8	12
4	Biomass burning	2.9	2
5	Zinc	0.6	0.4

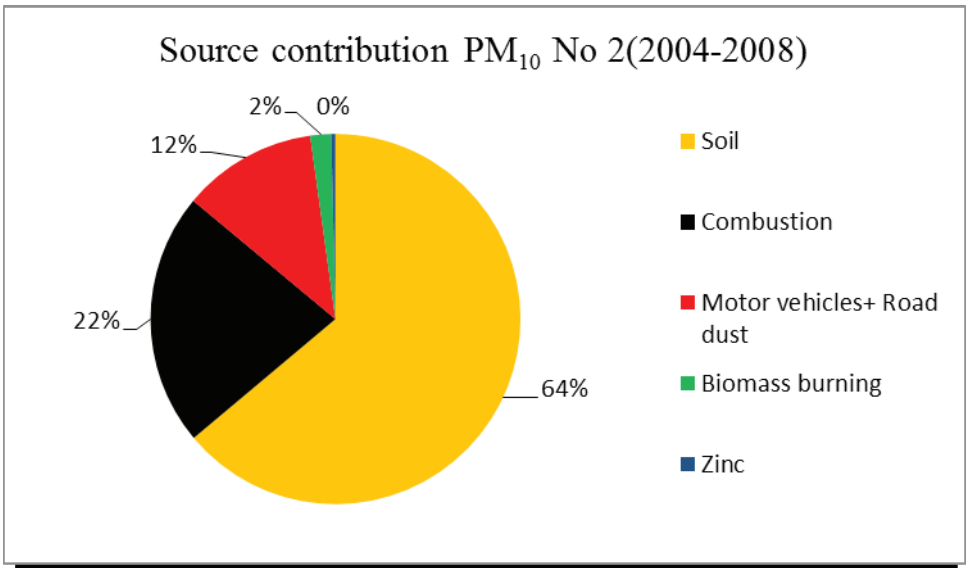

Figure B.12 Diagram of 2004–2009 average source apportionment for PM_{10} at the AMHIB site 2.

The largest contributor to source for site 2 for period 2004–2009 is soil with 64%. This is a similar result at this site for the AMHIB period. Second is coal combustion (combustion1 and combustion2 combined), third is motor vehicle emissions and road dust at approximately 12%.

Summary of the 2004–2009 study at the NRC site

The NRC site gets, as expected, a dominating contribution from soil suspension to the coarse PM fraction, which also contributes to the fine PM fraction ($PM_{2.5}$) (14%). Coal combustion dominates completely the $PM_{2.5}$ fraction, and it also gives a small (10%) contribution to the coarse fraction. Motor vehicles exhaust gives only a small contribution (5%) to $PM_{2.5}$, while dust particles defined as road dust contributes 11% to the coarse fraction and even a certain contribution to the fine fraction ($PM_{2.5}$). Biomass burning is found to have a very small contribution (3%) to $PM_{2.5}$.

The time series analysis underpins these explanations of source contributions, in that the contributions follow a seasonal variation consistent with seasonal variation of the emissions from the sources as well as climatic conditions. The analysis thus presents a consistent picture of the contributions to PM in air from the various main sources in this part of UB, some kilometers east of the central UB areas.

The AMHIB data presented below will extend this analysis of source contributions to other areas in UB.

B4 Apportionment of main PM sources in UB based upon AMHIB data

B4.1 $PM_{10-2.5}$ (coarse fraction) data analysis

$PM_{10-2.5}$ or coarse particle samples for source apportionment were collected at the site 2 (NRC) and site 3 (Zuun Ail). The data annex part E, Table 1 and Table 2 presents the mean, standard deviation, median, maximum, minimum, number of samples analyzed for $PM_{10-2.5}$ and elemental concentrations at the site 2 and site 3.

A total of 115 (for Site 2) and 121 (for Site 3) coarse particulate matter samples were included in the receptor modeling analyses. More than 30 elemental constituents were detected above their respective detection limits (LOD), 14 species were selected for PMF modeling ($PM_{10-2.5}$, BC, Na , Mg, Al, Si, S, Cl, K, Ca, Ti, V, Mn, Fe, Zn, Pb) as other elements were only present in a few samples and/or in low concentrations (the S/N ratio was lower than 0.2 for those sites for $PM_{10-2.5}$).

Site 2 (NRC)

The average mass contributions of each of the sources to $PM_{10-2.5}$ ambient coarse particle concentrations and the elemental source profiles at the NRC site are presented in Table B.6 and its diagram is shown in Figure B.13.

Table B.6 Average mass contributions of each source to $PM_{10-2.5}$ ambient particle concentrations at the site 2 (NRC) (ng/m^3)

	Motor vehicles+Road dust	Soil1	Coal combustion	Soil2
BC	10.9	0.0	2235.0	1897.9
Na	0.0	449.2	0.0	935.2
Mg	223.9	492.2	163.0	70.6
AL	356.8	2347.4	276.0	1103.1
SI	792.8	6339.5	736.5	3808.6
S	47.4	275.8	810.5	0.0
Cl	138.0	0.0	3.4	176.9
K	72.6	711.4	40.8	553.8
Ca	248.1	1256.7	445.3	1457.7
Ti	9.7	105.2	10.3	110.3
Mn	4.0	22.3	7.0	24.5
Fe	138.1	1199.6	227.4	924.6
Zn	4.5	4.3	6.9	21.6
Pb	30.4	26.3	34.7	0.0
MassC	29005.0	31285.0	14952.0	74058.0

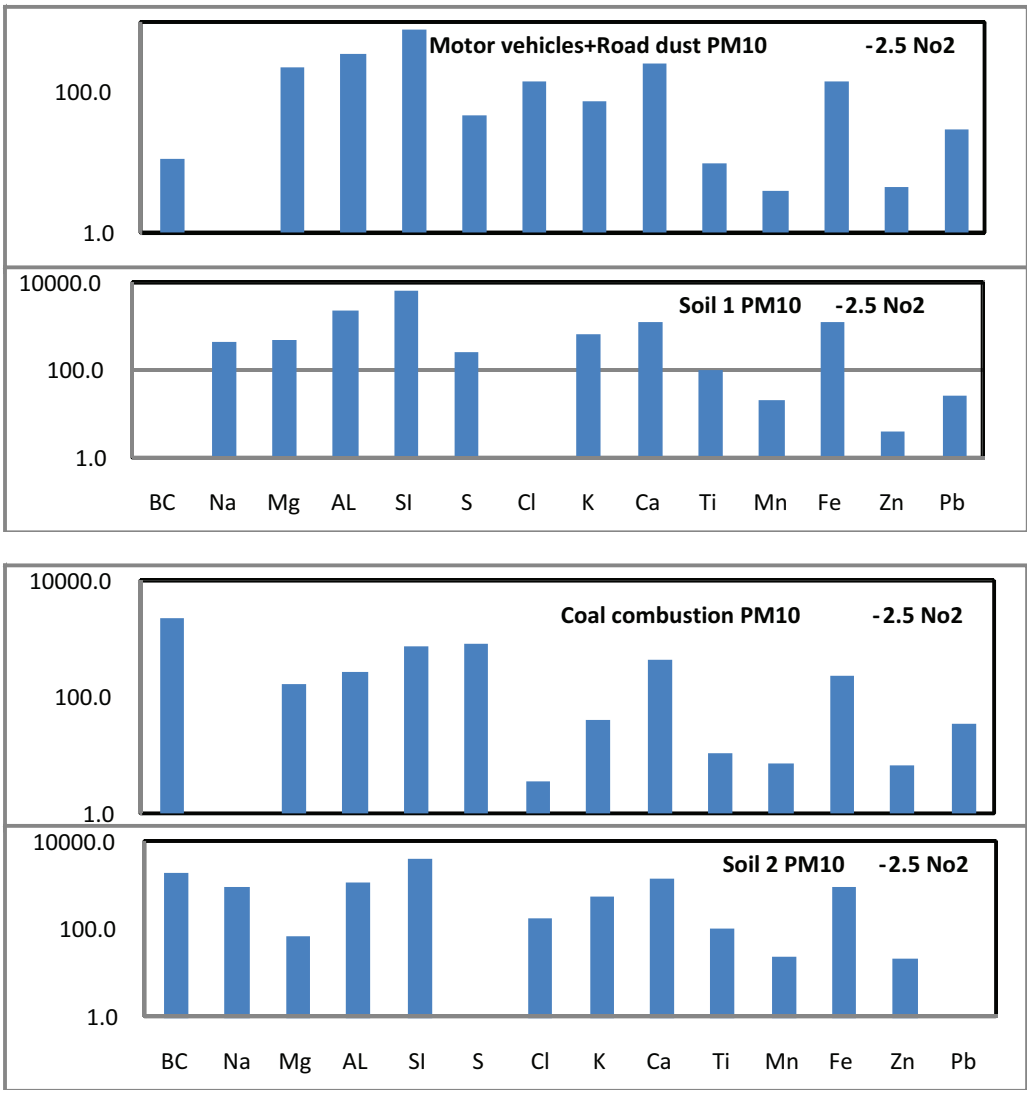

Figure B.13 Elemental source profiles derived by PMF for $PM_{10-2.5}$ samples at NRC (site 2) (ng/m^3).

The relative source contributions to the $PM_{10-2.5}$ pollution at NRC (site 2), as a result of PMF analysis is shown in Table B.7 and its diagram is shown in Figure B.14.

Table B.7 Average relative source contribution to $PM_{10-2.5}$ at the site 2 NRC (mass and percent)

Source	Mass $PM_{10-2.5}$(µg/m^3)	Percent
Motor vehicles+Road dust	29.005	19
Soil1	31.285	21
Coal combustion	14.952	10
Soil2	74.058	50

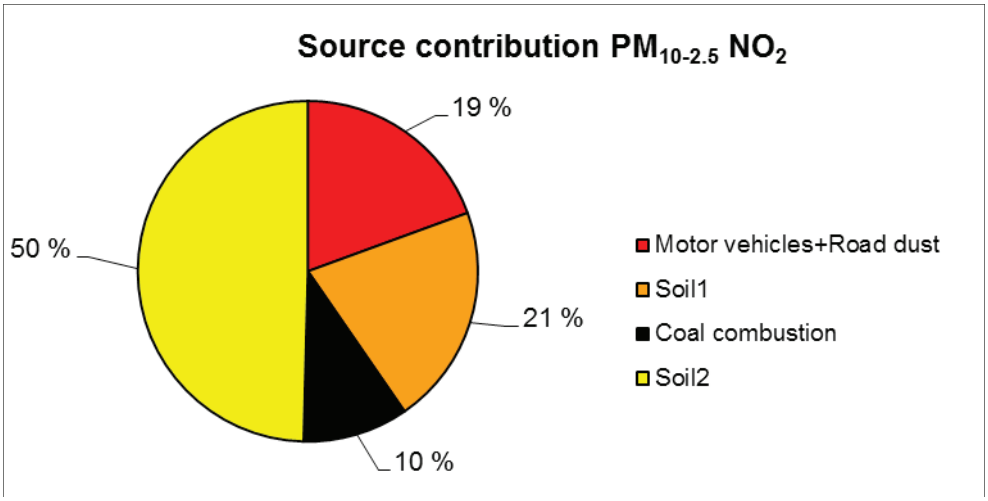

Figure B.14 Diagram of Source apportionment to $PM_{10-2.5}$ at site 2 (NRC).

For site 2 the first distinct source profile, i.e. the one which has highest Eigenvalue (see Data Annex part E) is identified as a motor vehicle and local road dust component as this profile contains BC, most of the zinc and lead along with elements. The second profile is identified as airborne soil originating from crustal matter (labeled as Soil 1) as the profile is dominated by Al and Si along with Ca, Ti and Fe. The Si:Al ratio was found to be 2.6:1, typical of crustal matter composition (aluminosilicates) (Lide 1992). The fourth profile is a combination of natural soil surrounded the city with the soil source originating more locally in Ulaanbaatar (labeled as Soil 2) where there is likely to be a greater concentration of settled combustion waste particles and coal dusts mixed into the crustal matter, hence the higher presence of BC in the source profile. The third factor is identified as a coal combustion source contribution for the coarse fraction and this contains the majority of black carbon and a sulfur component. The two combustion profiles could not be distinguished here.

As expected the soil sources completely dominate the coarse PM fraction, with 71%. This agrees favorably with the results from the 5-year analysis above, where the soil contributed 79%.

Site 3 (Zuun Ail)

The average mass contribution of each of the sources to $PM_{10-2.5}$ (coarse particles) at the Zuun Ail site 3 is presented in Table B.8 and the elemental source profiles are shown in Figure B.15.

Table B.8 Average mass contributions of each sources to $PM_{10-2.5}$ ambient particle concentrations at the site 3 (Zuun Ail) (ng/m^3).

	Combustion	Motor vehicles+Road dust	Soil	Biomass burning
BC	2524.6	1506.5	377.4	0.8
Na	67.1	405.6	52.2	627.0
Mg	127.8	210.4	100.5	328.8
Al	62.0	717.9	141.5	2109.8
Si	136.0	1996.8	344.0	5815.9
S	1056.2	0.0	144.8	153.0
Cl	37.4	233.1	49.3	0.5
K	3.1	266.9	28.7	687.8
Ca	260.3	542.2	180.6	1453.1
Ti	4.4	40.0	6.8	117.8
Mn	3.7	9.9	3.1	29.7
Fe	87.6	426.0	84.9	1222.6
Zn	11.4	12.5	0.9	10.2
Pb	41.2	26.8	15.5	0.0
MassC	11739.0	16610.0	314420.0	3313.3

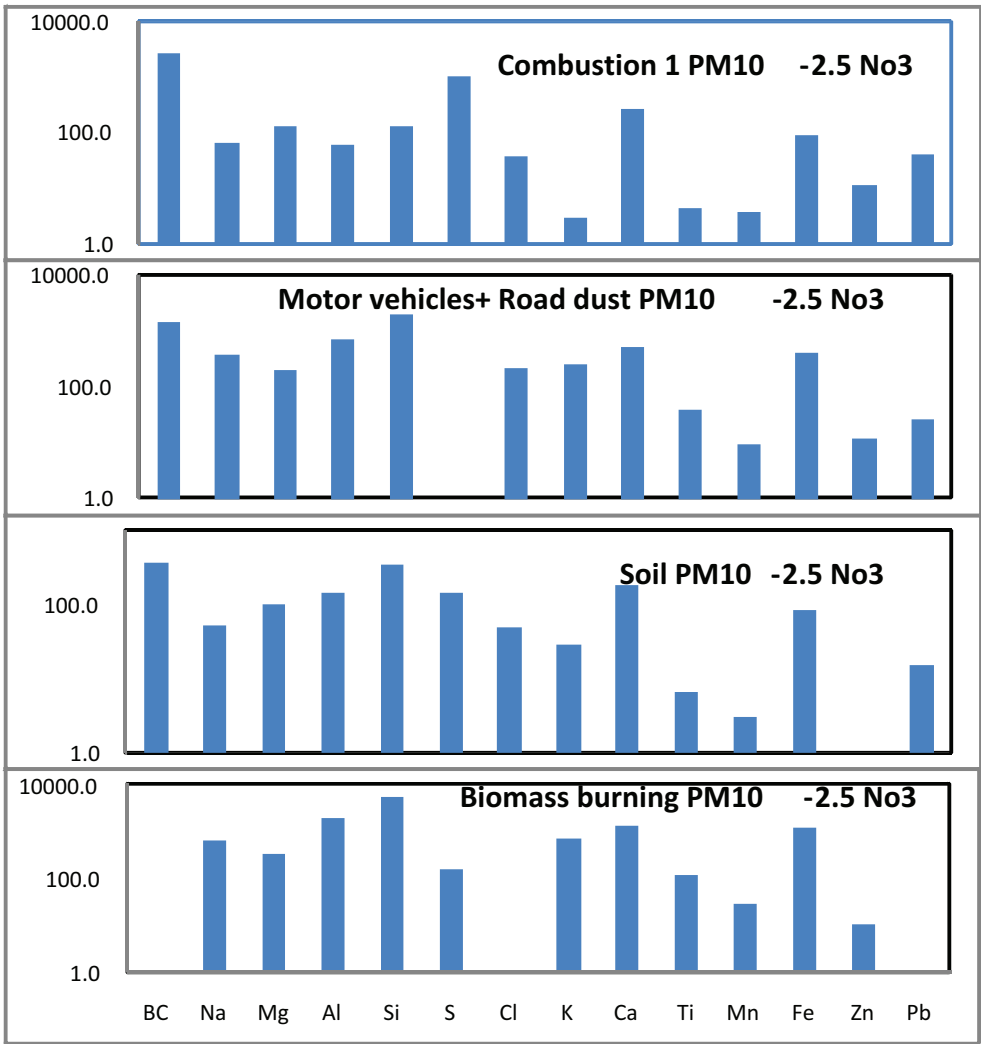

Fig B.15 Elemental source profiles for $PM_{10-2.5}$ site 3 Zuun Ail (ng/m^3).

The average source contributions to the $PM_{10-2.5}$ pollution at the site 3, as a result of PMF analysis, are shown in Table B.9 and its diagram is shown in Figure B.16.

Table B.9 Average relative source contribution to $PM_{10-2.5}$ at the site 3 Zuun Ail (mass and percent)

Source	Mass $PM_{10-2.5}$ (μg/m^3)	Percent
Motor vehicles+Road dust	16.610	5
Soil	314.420	91
Coal combustion	11.739	3
Biomass burning	3.313	1

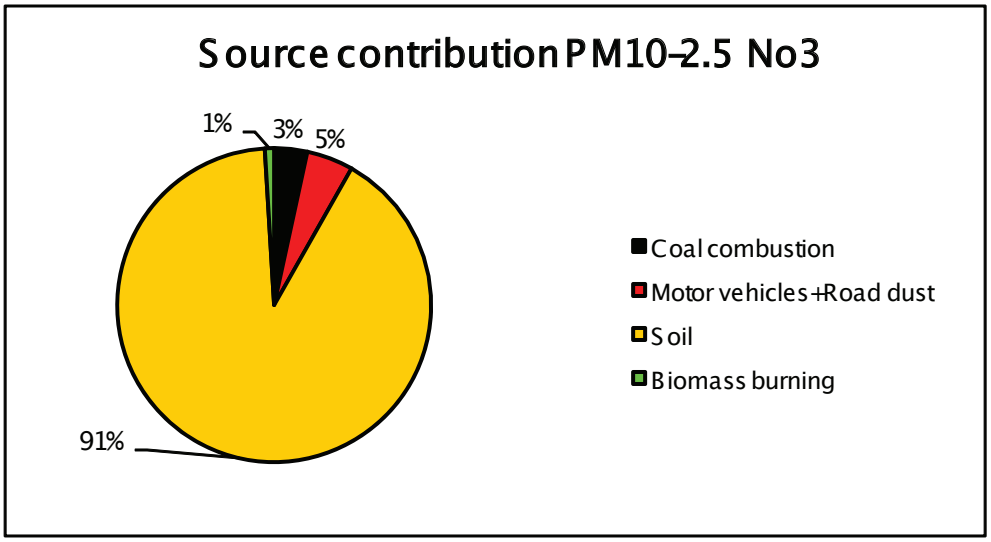

Figure B.16 Diagram of source apportionment to $PM_{10-2.5}$ at site 3 (Zuun Ail).

For the Site 3 (Zuun Ail) the first source profile is identified as coal combustion (the two combustion profiles could not be distinguished), the second is identified as a motor vehicle and local road dust component.

The third and most contributing source profile is identified as airborne soil originating from crustal matter as the profile is dominated by Al and Si along with Ca, Ti and Fe and some black carbon. In this site the difference between soil1 (natural soil) and soil2 (waste from the soil) could not be clearly separated. As a result it is referred to as a general soil profile.

The fourth profile is identified as biomass burning because it contains BC and potassium.

Although there are only small areas of open soil surfaces surrounding the site, and also little traffic on unpaved roads, the large coarse PM fraction at site 3 could be explained by fugitive dust being transferred from north-east ger areas and surrounding valleys through a local wind regime of air drainage down the valleys

B4.2 $PM_{2.5}$ data analysis of AMHIB data

$PM_{2.5}$ or fine fraction particle samples for source apportionment were collected at the site 2 (NRC) and site 3 (Zuun Ail). Data Annex part E table 3 and table 4 presents the mean, standard deviation, median, maximum, minimum, number of samples for $PM_{2.5}$ and elemental concentrations at the site 2 and site 3.

A total of 115 (for Site 2) and 121 (for Site 3) fine particulate matter samples were included in the receptor modeling analyses of AMHIB data. While a total of 33 elemental constituents were detected above their respective LOD, 14 species were selected for PMF modeling ($PM_{2.5}$, BC, Na , Mg, Al, Si, S, Cl, K, Ca, Ti, Mn, Fe, Cu, Zn, Pb) as other elements were only present in a few samples and/or the S/N ratio was low.

Site 2 (NRC)

The average mass contributions of each of the identified factors/sources to $PM_{2.5}$ ambient fine particle concentrations is presented in the Table B.10 and the elemental source profiles presented in Figure B.17.

Table B.10 Average mass contributions of each sources to $PM_{2.5}$ ambient particle concentrations at the site 2 (NRC) (ng/m^3).

	Combustion2	Motor vehicles+Road dust	Soil	Biomass burning	Combustion1
BC	4198.6	0.0	0.0	2000.4	4616.9
Na	45.2	32.1	380.4	12.6	2.5
Mg	11.7	146.7	91.5	98.7	24.9
Al	22.3	677.3	56.9	256.0	0.2
Si	126.1	1716.6	121.4	663.3	0.0
S	0.0	62.2	187.7	289.1	2269.6
Cl	0.0	0.0	67.9	115.2	19.5
K	40.4	191.9	19.1	74.3	15.8
Ca	67.4	461.4	0.0	255.2	10.4
Ti	0.0	38.2	0.0	0.0	3.9
Mn	0.0	6.5	1.2	4.1	1.1
Fe	41.9	345.8	10.9	140.5	0.6
Zn	21.7	2.2	3.1	0.1	5.9
Pb	12.2	15.1	15.2	0.0	8.8
MassFine	16422.0	10625.0	37933.0	3500.3	11491.0

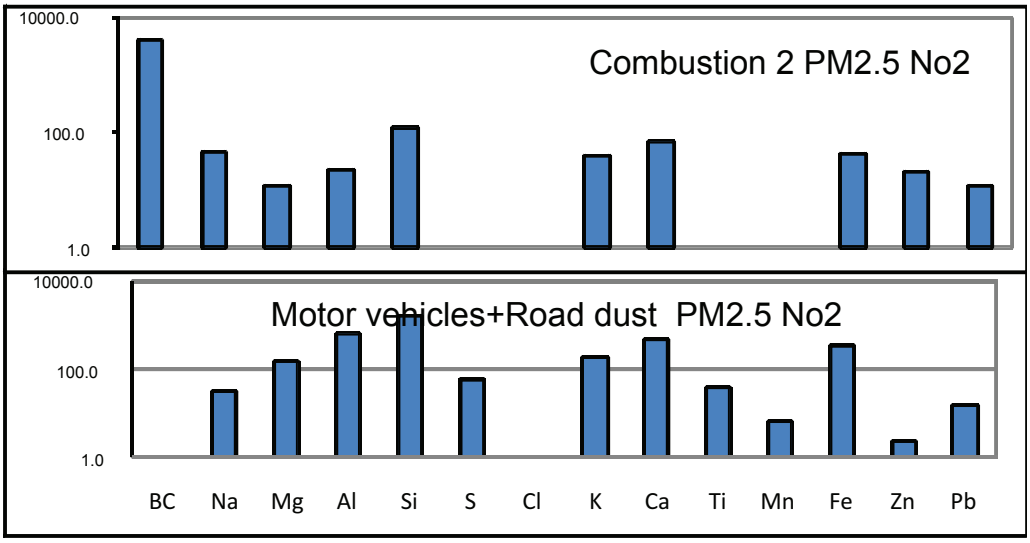

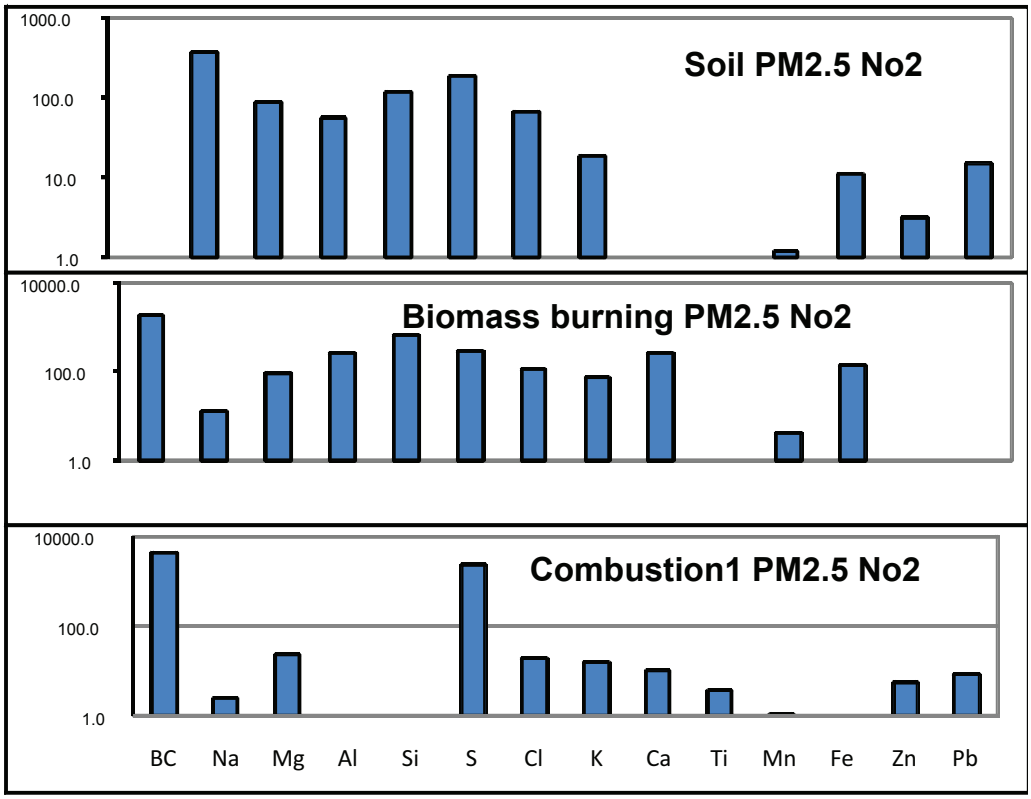

Figure B.17 Elemental source profiles derived by PMF for $PM_{2.5}$ at site 2 (NRC) (ng/m^3).

The average source contributions to the $PM_{2.5}$ pollution at the site 2, as a result of PMF analysis is shown in Table B.11 and its diagram is shown in Figure B.18.

Table B.11 Average source contribution to $PM_{2.5}$ at the site 2 NRC (percent)

Source	$PM_{2.5}$ mass (μg/m^3)	Percent
Soil	37.9	47
Combustion2	16.4	21
Motor vehicles+Road dust	10.6	13
Biomass burning	3.5	4
Combustion1	11.5	14

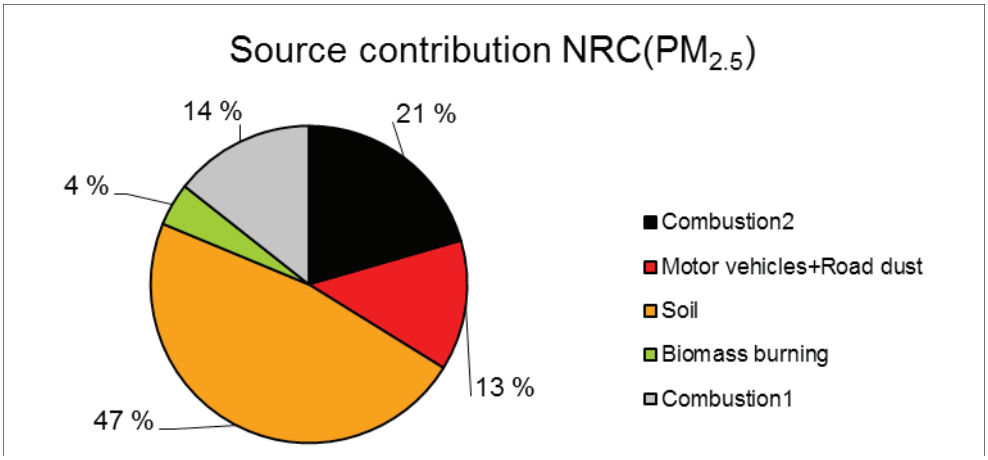

Figure B.18 Diagram of sources apportionment to $PM_{2.5}$ at the site 2 (NRC).

For $PM_{2.5}$ sources at the site 2 (NRC), the first factor is attributed to coal combustion sources. The two distinct coal combustion source types, with high/low sulfur contents respectively, could be distinguished at this site. The third source profile is identified as originating from motor vehicles and road dust, by the soil elements as well as black carbon, lead and zinc.

The fourth profile and most contributing source is identified as airborne soil originating from crustal matter as the profile contains the majority of Al and Si with an Si:Al ratio approximately 2.5:1. The two soil types cannot be distinguished in $PM_{2.5}$ at this site (NRC).

The fifth profile is identified as biomass burning contributions to $PM_{2.5}$ ambient mass concentrations due to the association of black carbon and potassium in the profile. Wood burning for cooking is used all year in Ulaanbaatar but there was also evidence that forest fire events to the north of the region can contribute at certain times.

According to the analysis, suspended soil particles constitute the most contributing source to the fine PM fraction, with 47%. In the 5-year analysis for this site (see the previous section), soil particles contributed only 14% to this fraction. Because of the previously mentioned non-ideal behavior of the sampler, the real contribution is less than this. However, the AMHIB year (June 2008–May 2009), and especially the winter months, had a fairly high average wind speed and it was also a dry year/winter, compared to the previous 2 years. Thus, the climate conditions could explain partly the high soil contribution in the AMHIB year.

Site 3 (Zuun Ail)

The average mass contributions of each of the sources to $PM_{2.5}$ ambient fine particle concentrations at the site 3 is presented in Table B.12 and elemental source profiles are shown in Figure B.19.

Table B.12 Average mass contributions of each source to $PM_{2.5}$ ambient particle concentrations at the site 3 (Zuun Ail) (ng/m^3)

	Motor vehicles+Road dust	Combustion1	Soil	Biomass burning	Combustion 2
BC	4900.2	5893.4	397.9	662.7	1596.4
Na	0.0	0.0	58.9	387.0	24.9
Mg	68.0	17.4	148.7	46.2	42.9
Al	41.3	0.0	573.2	52.5	10.8
Si	107.1	60.9	1458.6	96.0	10.4
S	415.3	2732.8	16.8	311.4	310.0
Cl	78.5	47.3	48.9	2.3	22.1
K	53.4	21.3	161.3	27.6	7.2
Ca	22.5	37.2	426.3	0.0	4.1
Ti	0.0	2.8	24.1	0.6	1.0
Mn	2.0	2.7	7.2	0.8	0.0
Fe	16.4	18.0	304.2	12.2	1.3
Zn	8.0	12.1	0.0	16.7	6.1
Pb	24.7	34.4	8.9	11.5	12.2
$PM_{2.5}$	10327.0	16408.0	10562.0	5579.2	292900.0

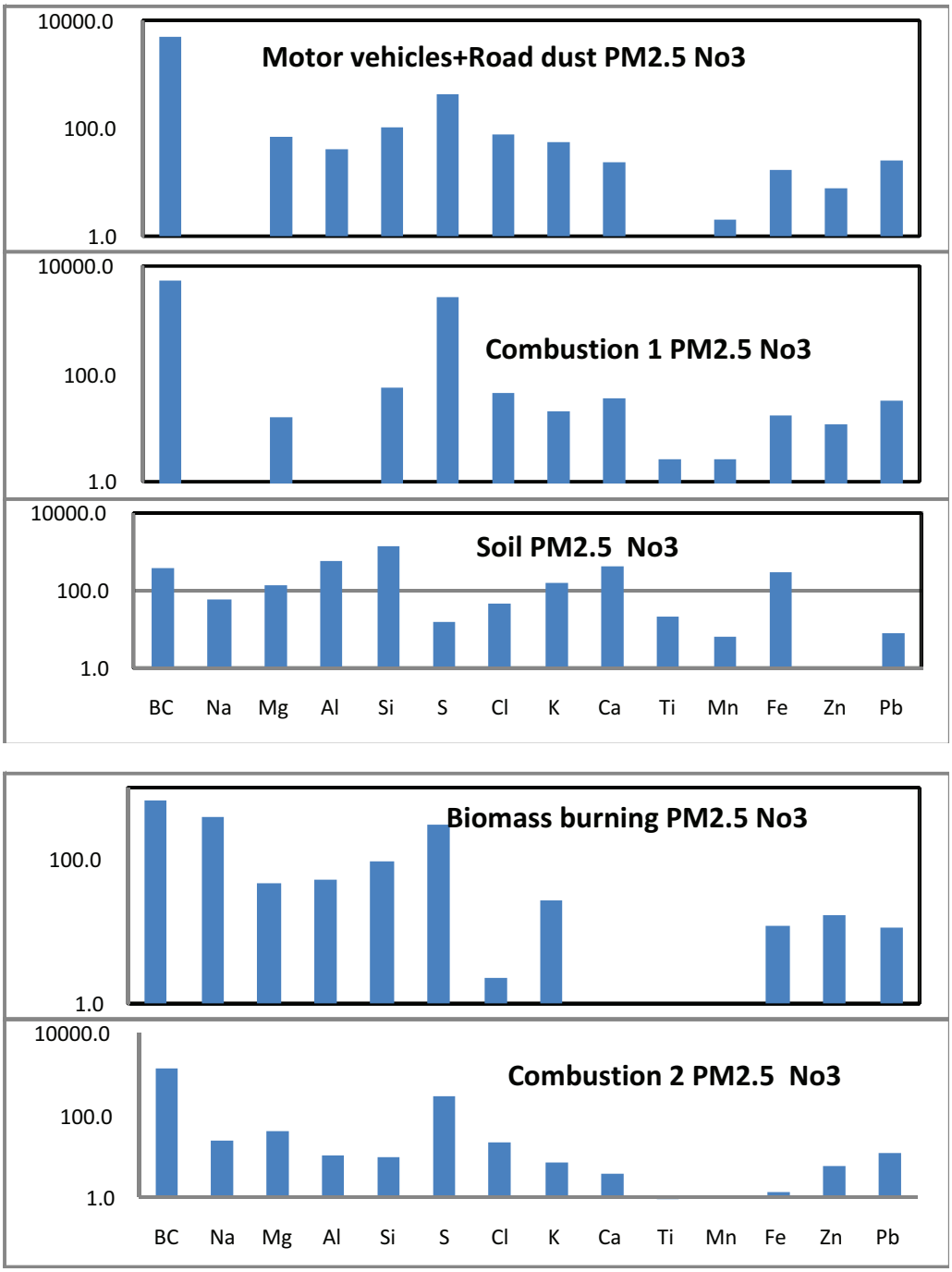

Figure B.19 Elemental source profiles derived by PMF for $PM_{2.5}$ at site 3 (Zuun Ail) (ng/m^3).

The average source contributions to the $PM_{2.5}$ pollution at the site 3, as a result of PMF analysis is shown in Table B.13 and its diagram is shown in Figure B.20.

Table B.13 Average source contribution to $PM_{2.5}$ at the site 3 (Zuun ail) (mass and percent)

Source	$PM_{2.5}$ mass (μg/m^3)	Percent
Soil	10.6	3
Combustion1	16.4	5
Combustion2	292.9	87
Motor vehicles+Road dust	10.3	3
Biomass burning	5.6	2

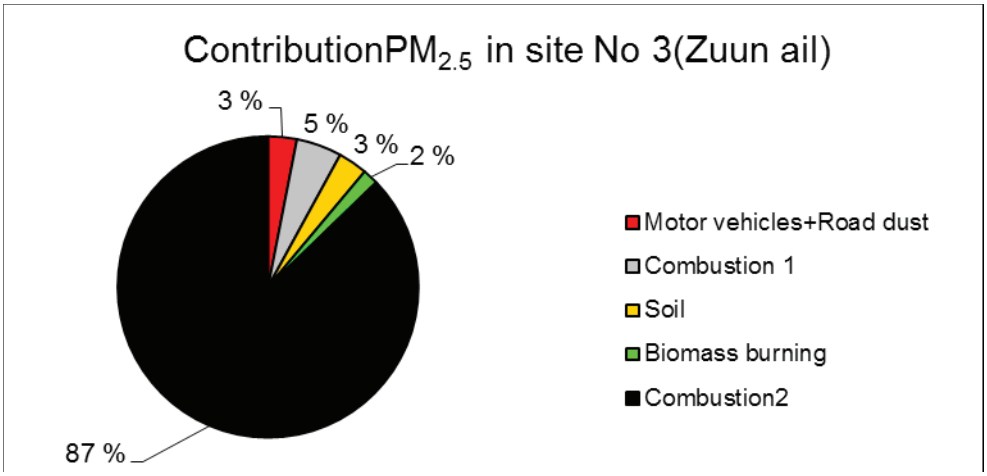

Figure B.20 Diagram of source apportionment to $PM_{2.5}$ at the site 3 (Zuun Ail).

For $PM_{2.5}$ sources at the site 3 (Zuun ail) the first factor is identified as motor vehicle and road dust. The second factor is attributed to coal combustion sources with black carbon and sulfur component, labeled combustion 1, and the fifth is also identified as combustion, labeled combustion 2, with low sulfur and soil elements and significant amounts of black carbon.

The third profile is airborne soil. As for the $PM_{2.5}$ fraction at NRC site, the two different soil profiles cannot be distinguished at site 3. The fourth profile is identified as biomass burning.

The combustion source completely dominates the fine PM fraction at site 3.

B4.3 PM_{10} data analysis of AMHIB data

Site 6 (III Khoroolol)

In the AMHIB project PM10 samples for source apportionment were collected at site 6 (III Khoroolol) for the period December 2008–May 2009. The Partisol sampler was used for this purpose and the same Nuclear pore filter which was used for GENT sampler for $PM_{2.5}$ was used in this sampler. Data Annex part E table 5, table 6 and table 7 present the mean, standard deviation, median, maximum, minimum, number of samples for PM_{10} and elemental concentrations at site 6.

A total of 73 PM_{10} particulate matter samples were included in the receptor modeling analyses of AMHIB data. While a total of 30 elemental constituents were detected above their respective LOD, 14 species were selected for PMF modeling ($PM_{2.5}$, BC, Na , Mg, Al, Si, S, Cl, K, Ca, Ti, Mn, Fe, Cu, Zn, Pb) as other elements were only present in a few samples and/or the S/N ratio was low.

The average mass contributions of each of the sources to PM_{10} ambient particle concentrations are presented in Table B.14 and the elemental source profiles at the site 3 are shown in Figure B.21.

Table B.14 Average mass contributions of each sources to PM_{10} ambient particle concentrations at the site 6 (3 Khoroolol) (ng/m^3)

	Soil	Biomass burning	Motor vehicles+Road dust	Combustion
BC	748.4	0.0	11239.0	15539.0
Na	1398.6	457.1	391.9	0.0
Mg	813.8	0.0	400.7	120.2
Al	4556.4	295.7	856.5	162.8
Si	12178.0	1255.4	1802.2	559.7
S	0.0	1421.1	0.0	5865.3
Cl	123.7	810.3	327.3	97.6
K	1183.1	312.7	355.6	95.6
Ca	4420.3	1231.4	72.0	474.3
Ti	272.0	57.4	0.0	17.9
Mn	53.3	23.2	0.0	12.2
Fe	2734.7	582.8	188.4	205.8
Zn	18.2	28.5	19.4	57.1
Pb	0.0	0.0	73.2	37.1
PM_{10}	58513.0	75462.0	124250.0	210840.0

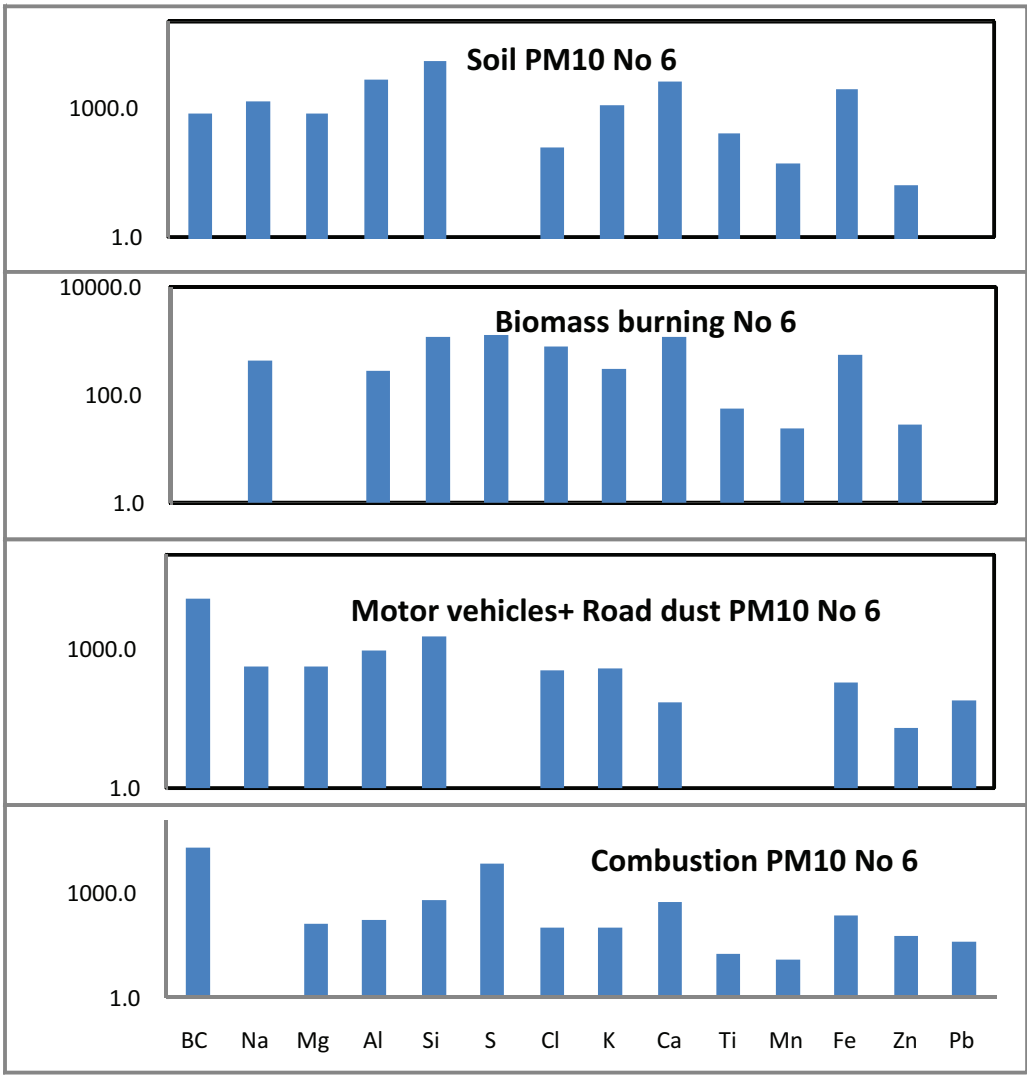

Figure B.21 Elemental source profiles derived by PMF for PM_{10} at site 6 (III Khoroolol) (ng/m^3).

The average source contributions to the PM_{10} pollution at the site 6, as a result of PMF analysis, are shown in Table B.15 and its diagram is shown in Figure B.22.

Table B.15 Average source contribution to PM_{10} at the site 6, III Khoroolol (mass and percent)

No	Source	Mass (μg/m^3)	Percent
1	Motor vehicles +Road dust	124.2	26
2	Soil	58.5	12
3	Combustion	210.8	45
4	Biomass burning	75.5	16

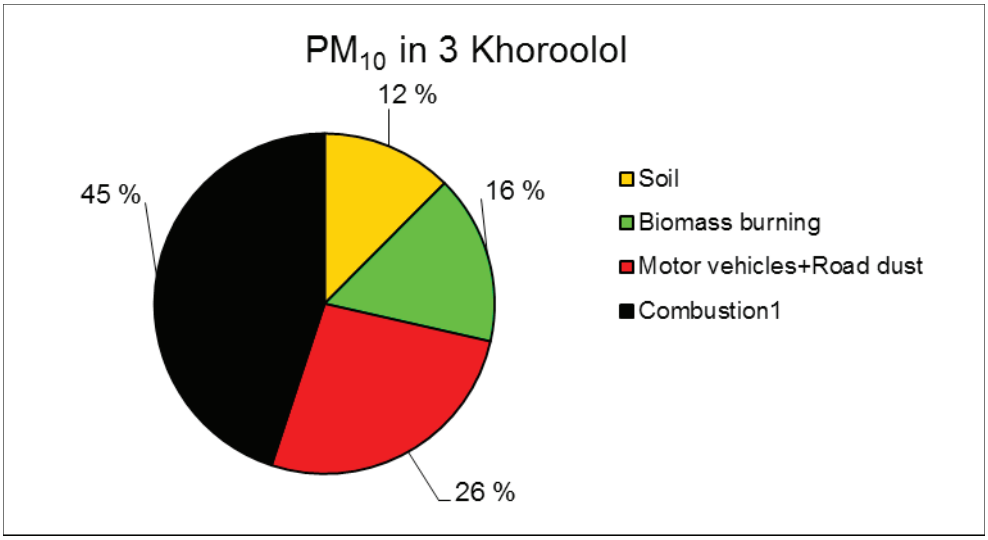

Figure B.22 Diagram of source apportionment to PM_{10} at the site 6 (III Khoroolol).

The first profile for this site is the soil, the second is biomass burning, third profile is motor vehicle + road dust and fourth and most contributing profile is combustion.

As this analysis covers only part of the year (period December 2008–May 2009, 73 days) the results here are less representative than the analysis at sites 2 and 3. Also, the samples do not cover the whole day (24 hours) during high pollution days, and may miss the most polluted hours of such day, in the late afternoon/evening.

This profile of contributions corresponds with the location of the site, within a ger area with unpaved roads surrounding it.

Site 2 (NRC)

The source contributions for total PM_{10} pollution were calculated based on the $PM_{2.5}$ and $PM_{10-2.5}$ source contribution tables for the site 2 and the site 3.

The average source contributions to the PM_{10} pollution at site 2, as a result of PMF analysis from the $PM_{10-2.5}$ and $PM_{2.5}$ particles, is shown in Table B.16 and its diagram is shown in Figure B.23.

Table B.16 Average source contribution to PM_{10} at the site 2 NRC (mass and percent)

No	Source	Mass (μg/m^3)	Percent
1	Motor vehicles + Road dust	39.6	17
2	Soil	143.3	62
3	Combustion	42.9	19
4	Biomass burning	3.5	2

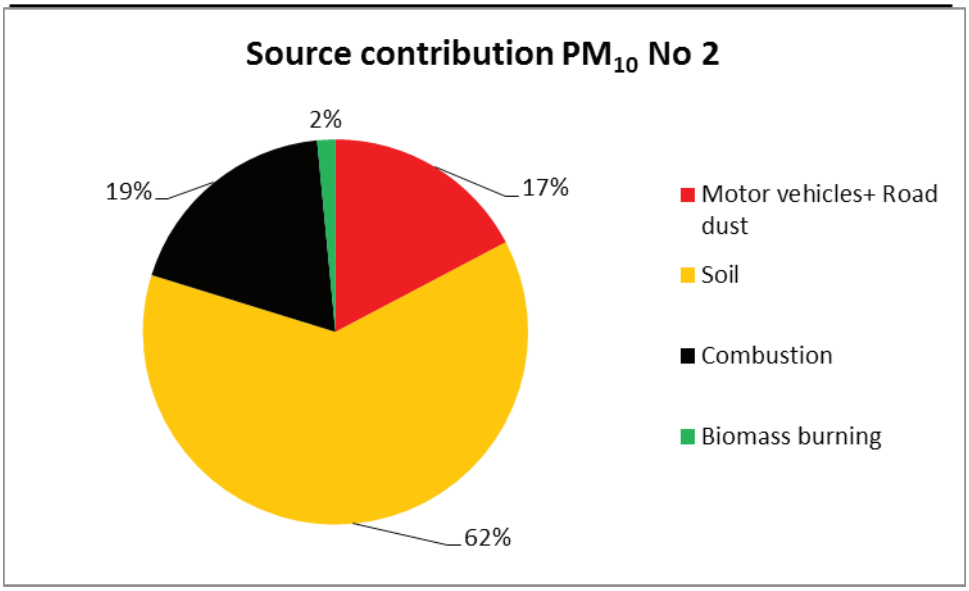

Figure B.23 Diagram of source apportionment to PM_{10} at the site 2 (NRC).

Corresponding with the results from the separate fine and coarse PM fraction analysis above, the most dominant source for PM_{10} at site 2 is soil. The second most important source is the coal combustion source. Third is motor vehicles and road dust.

This analysis of PM_{10} for the AMHIB period agrees well with the 5-year analysis described in the section above.

Site 3 (Zuun Ail)

The average source contributions to the PM_{10} pollution at the site 3, as a result of PMF analysis from the $PM_{10\text{-}2.5}$ and $PM_{2.5}$ particles is shown in Table B.17 and its diagram is shown in Figure B.24.

Table B.17 Average source contribution to $PM_{2.5}$ at the site 3 (Zuun Ail) (mass and percent)

No	Source	Mass (μg/m^3)	Percent
1	Motor vehicles + Road dust	26.9	4
2	Soil	325.0	48
3	Combustion	321.1	47
4	Biomass burning	8.9	1

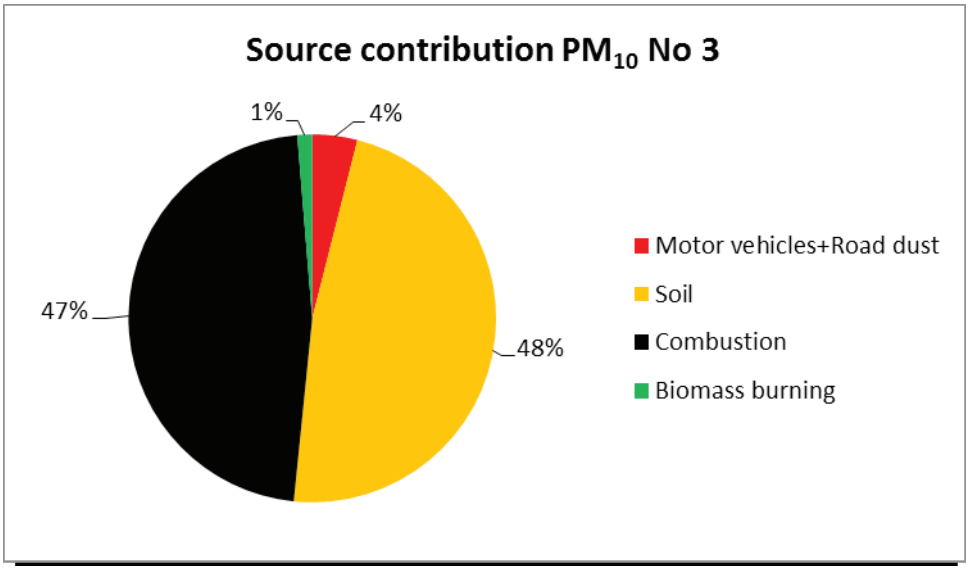

Figure B.24 Diagram of source apportionment to PM_{10} at site 3 (Zuun Ail).

Corresponding with the separate analyses of the fine and coarse PM fractions above, this composite analysis shows that the soil and combustion sources contribute equally to PM_{10} at site 3 and together dominate completely. The motor vehicles and road dust source has a small contribution, and biomass burning is hardly visible.

B5 Discussion

Figure B.25 and B.26 summarize the source contribution assessments described above. Figure B.25 shows the PM concentrations contributions, in µg/m^3, at the three stations where source apportionment was carried out. Figure B.26 shows the contributions as a percentage of the total PM concentration.

The general picture is that the combustion source is the largest contributor to the fine PM fraction ($PM_{2.5}$) concentrations, both in terms of concentrations and percentage, especially at site 3 (Figure B.25). Likewise, the suspended soil particles dominate the coarse fraction ($PM_{10\text{-}2.5}$), while it also contributes to $PM_{2.5}$, particularly at the NRC site 2, although the real soil contribution to $PM_{2.5}$ is less than shown in the figure, as a result of the mentioned non-ideal behavior of the sampler. Soil and combustion both contributes to PM_{10}, but varies between sites: soil dominates at site 2 (NRC), combustion dominates at site 6 (III Khoroolol), while they contribute about equally at site 3 (Zuun ail).

The motor vehicles/road dust source gives a certain contribution to the coarse PM fraction and a very small contribution to $PM_{2.5}$. The biomass contribution is very small except for PM_{10} at the site 6, which is located in a ger area. This profile is very clear when looking at percentage contributions (see Figure B.28). The motor vehicles/road dust source contributes about 10% to $PM_{2.5}$ at the 3 sites, and 5–20% to the coarse PM fraction, due to suspended road dust.

The contributions and their variations are presented below.

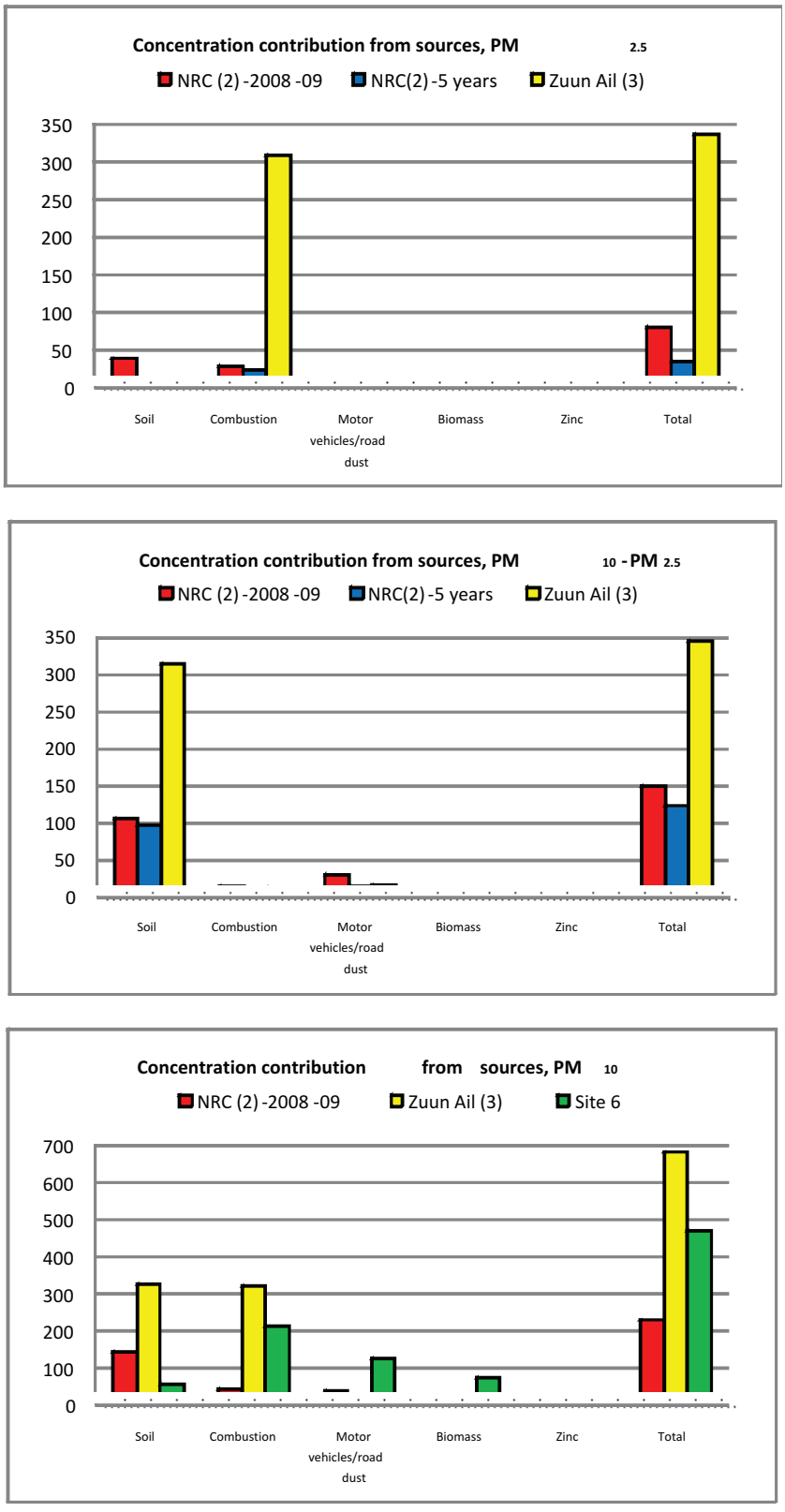

Figure B.25 Concentration contributions to PM in air from main sources in UB (μg/m^3).

Top: $PM_{2.5}$; Mid: $PM_{10\text{-}2.5}$; Bottom: PM_{10}.

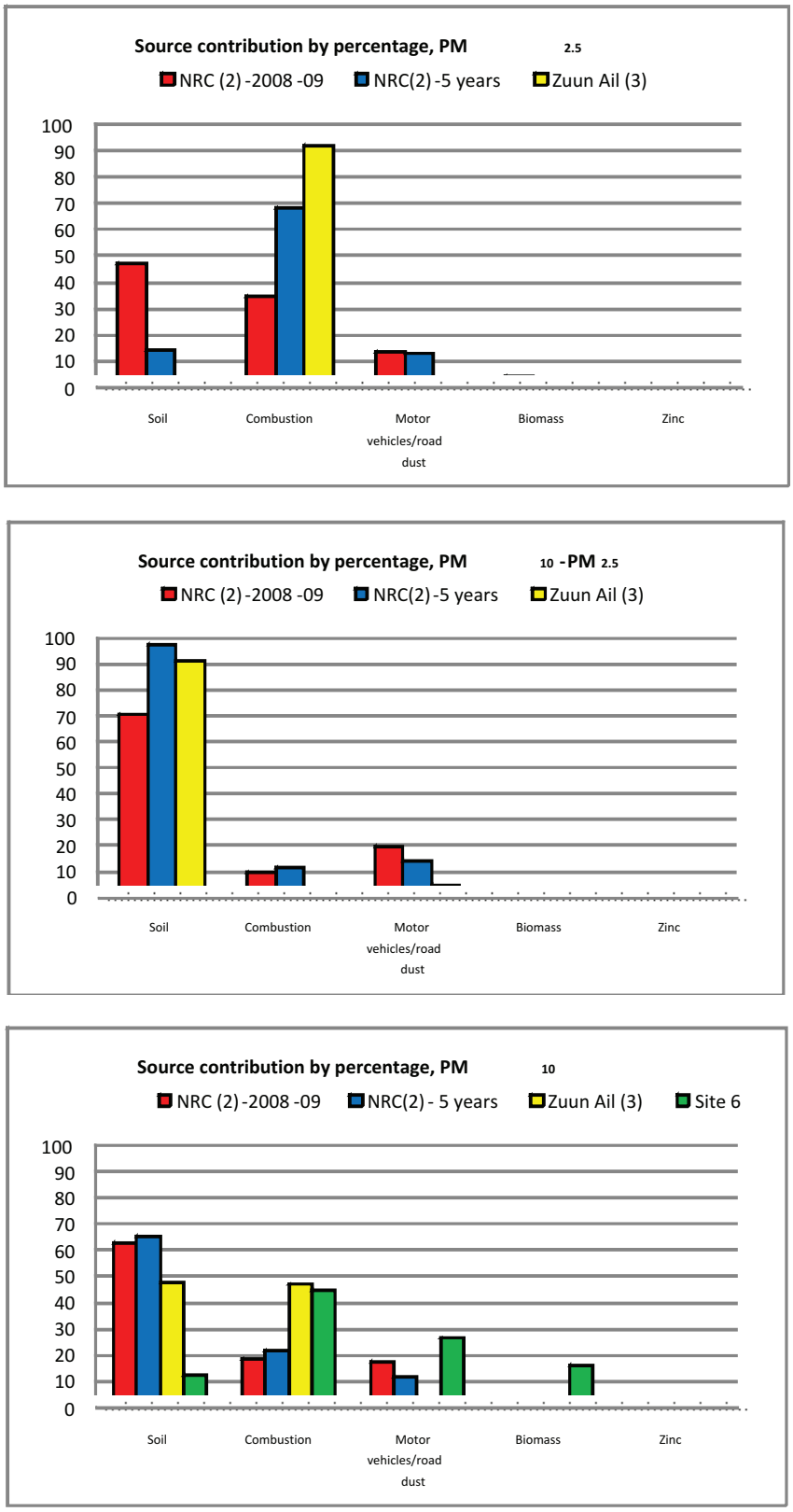

Figure B.26 Relative contributions to PM in air from main sources in UB (percent).

Top: $PM_{2.5}$; Mid: $PM_{10\text{-}2.5}$; Bottom: PM_{10}.

The percentage contributions from the main sources are summarized in Table B.18, for each station and PM fraction.

Table B.18 Summary of source contributions for sites and PM fractions (percent)

PM fraction	Soil suspension 1 & 2	Coal combustion 1 & 2	Motor vehicles exhaust and road dust	Biomass	Zinc
$PM_{2.5}$					
NRC (2)	47[1]	35 (14/21)[2]	13[4]	4	
NRC-5year	14[1]	68 (35/33)[2]	13[4]	3	2
Zuun Ail (3)	3[1]	92 (5/87)[2]	3[4]	2	
$PM_{10-2.5}$					
NRC (2)	71 (21/50)[3]	10	19[5]		
NRC-5year	79 (45/34)[3]	10	11[5]		
Zuun Ail (3)	91	3	5[5]	1	
PM_{10}					
NRC (2)	62	19	17	2	
NRC-5year	64	22	12	2	0.4
Zuun Ail (3)	48	47	4	1	
Site 6	12	45	27	16	

[1]The real soil contribution is somewhat less than this, due to the non-ideal behavior of the sampler
[2]In parenthesis: Comb 1 / Comb 2
[3]In Parenthesis: Soil 1 / Soil 2
[4]Mostly exhaust particles
[5]Mostly road dust particles

Source contributions at the sites

Combustion sources

Two source profiles related to coal combustion have been found. The coal combustion 1 source profile is dominated by BC and S (most likely present as sulfate species). This source profile could represent high temperature coal combustion characteristic of power stations (Polissar, Hopke et al. 2001) and large Heat Only boilers. The coal combustion 2 source profile, with less sulfur in it, could represent more low-temperature coal combustion with significant ash and crustal matter components (Na, Mg, AL, Si) (Zheng, Salmon et.al. 2005). This profile could then represent the emissions from coal fires used in small stoves for domestic heating.

The coal combustion contribution to $PM_{2.5}$ is large: 35% at site 2 and 92% at site 3.

Coal combustion contributes less than 10% to the coarse PM fraction.

For PM_{10} the coal combustion source contribution varies between sites: 19% at site 2, 47% at site 3 and 45% at site 6.

Combustion 1 vs. combustion 2
The two combustion related profiles could be distinguished in the analysis of the fine PM fraction ($PM_{2.5}$) both at sites 2 (NRC) and 3 (Zuun ail). At site 2 (NRC) the two sources contribute about equally, reflecting the location of the site 2: away from ger areas but in an area with heat-only boilers around. Also, the power plant emissions could make a contribution to this site. At site 3, which is exposed to ger emissions, the Combustion 2 source (combustion in ger stoves) dominates completely. At site 6 located within a ger area it is found that the combustion factor is completely dominant, but the analysis could not distinguish the two profiles.

Crustal matter sources
Two crustal matter elemental profiles have been identified (Soil 1 and Soil 2) and it is suggested that they originate from different source areas based on the BC content in the profile. The Soil 1 source most likely represents the general crustal matter in the area around Ulaanbaatar, and the Soil 2 source is likely to originate more locally in Ulaanbaatar where there is a greater concentration of settled combustion particles and coal dust mixed into the crustal matter, hence the higher presence of BC in the source profile.

Sites 2 and 3 (NRC and Zuun ail)
The soil contribution dominates the coarse particle fraction ($PM_{10-2.5}$).

- It is 71% at the site 2 NRC and 91% at the site 3 Zuun Ail.
- The Soil 1 and Soil 2 separation could be seen clearly only at site 2 NRC, and the local soil source dominates here.

For the $PM_{2.5}$ fine particle fraction the contribution from soil is smaller.

- For site 2 NRC the soil contribution is 47% (14% for the 5-yr series) and at site 3 it is 3%. The real contribution is smaller due to the non-ideal behavior of the sampler.
- Soil at site 2 has more sulfur in it, and it is possible that the fugitive dust contains more coal waste than at site 3.
- The soil at site 3 has no sulfur content, corresponding more to natural fugitive dust.

Suspended soil particles give the largest contribution to the PM_{10} concentrations.

- 48% at the site 3 Zuun ail and approximately 62% for the site 2 NRC for the AMHIB period.
- It averages 64% at the site 2 for the 5-year (2004–2009) measurements.

Site 6 (III Khoroolol), PM_{10} only
At site 6 the relative contribution from soil is much lower—12% to PM_{10} according to the analysis, while coal combustion dominates. Samples from this site were collected from December to May, and thus do not represent year round results, but more of a winter picture.

Soil 1 vs soil 2
The two soil profiles could be separated in the analysis only for the coarse fraction at site 2 (NRC) where they contribute roughly equally to coarse PM for the 5-year period, while local soil dust is twice as large as the general dust source in the AMHIB period. Thus, the general (Soil 1) and the more local (Soil 2) dust suspension sources appear to be of equal importance. This indicates that control of local soil suspension, e.g. by covering open surfaces, will only address part of that problem.

Motor vehicle exhaust particles and road dust
Motor vehicle and road dust do not make a large contribution to the PM_{10} pollution at sites 2, 3 and 6.

The motor vehicle and road dust contribution to PM_{10} pollution at site 2 is 17% (the 5 years average at site 2 is 12%), 4% at site 3 and 27% at site 6. The road dust portion of the source dominates its PM_{10} contribution.

Contribution of motor vehicle exhaust particles and road dust to the $PM_{2.5}$ fraction is 13% at site 2 (same as the 5 years average) and 3% at site 3. Although the percentage contribution is different at the sites, the mass of the contribution is very similar, 10.6 µg/m^3 at site 2 and 10.3 µg/m^3 at site 3.

Biomass burning

The biomass burning source originates from domestic cooking activities in Ulaanbaatar with peak contributions from forest fires to the north during spring and autumn. Forest fires are a common occurrence during the dry spring and autumn months in Mongolia (Nyamjav, Goldammer et al. 2007). Air-mass back trajectory analysis for peak biomass burning events shows that source emissions originate north of Ulaanbaatar. For example, a peak in biomass burning source contribution to $PM_{2.5}$ occurred on 20 April 2006 (4 µg/m^3). The back trajectory presented in Figure B.28 shows the air mass arriving at Ulaanbaatar from the north and satellite records show significant fires burning in southern Russia and northern Mongolia over the same period.

Figure B.29 presents the satellite image for April 23, 2006, showing that large fires were burning in the foothills of the mountains that separate Russia (north) from Mongolia (south). The Moderate Resolution Imaging Spectroradiometer (MODIS) on NASA's Terra satellite captured the image of the fires (actively burning areas outlined in red) and their accompanying large burn scars (dark brown). The smoke is blowing southeastward across Mongolia (from http://earthobservatory.nasa.gov/NaturalHazards/view.php?id=16493).

The biomass burning contribution to the PM_{10} pollution is small according to the analysis, 2% at site 2 (the same for the 5 years analysis), 1% at site 3 and 16% at site 6.
Contribution to the $PM_{2.5}$ pollution is 4% at site 2 (5 years average at the site 2 is 3%) and 2% at site 3.

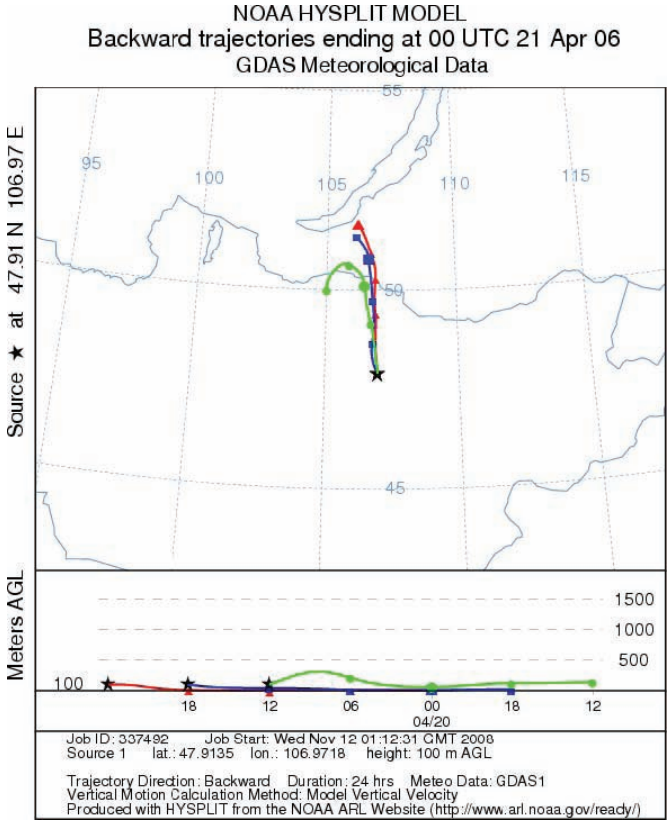

Figure B.28 Air mass back trajectory (24 hr) for 20 April 2006 (Source: NOAA HYSPLIT).

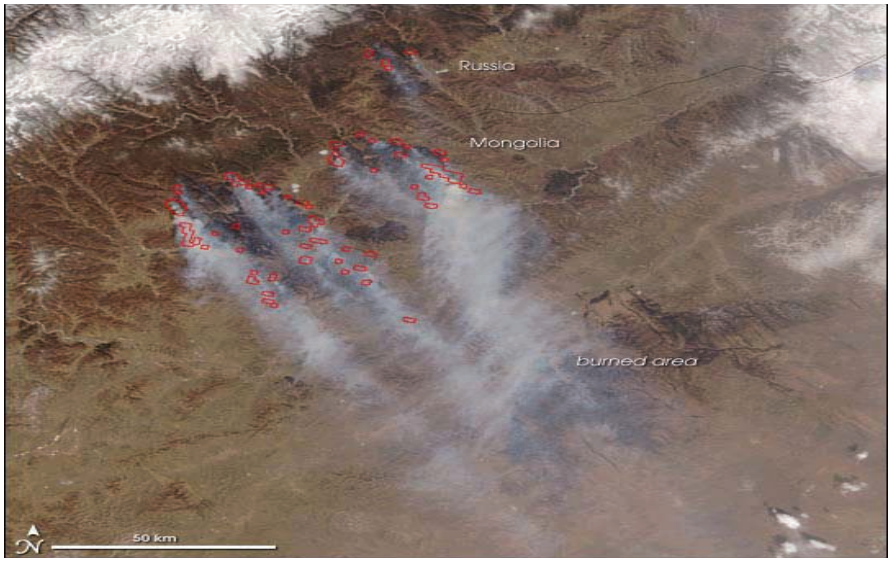

Figure B.29 Satellite image of forest fires burning in southern Russia and northern Mongolia on 23 April 2006 (Source: NASA Earth Observatory at http://earthobservatory.nasa.gov/NaturalHazards/view.php?id=16493).

B6 Summary

The main result from the source apportionment analysis is that coal combustion and soil suspension dominates as sources to PM at the investigated stations 2, 3 and 6, and that motor vehicles and biomass burning made smaller contributions. There are significant differences between stations in the amount of contribution to the different PM size fractions.

$PM_{2.5}$ (fine particle fraction)

Coal combustion and soil suspension both give substantial contributions to $PM_{2.5}$ at site 2 (NRC) while coal combustion dominates completely at site 3 (Zuun Ail). This can be explained by the differences in site locations: NRC is located away from ger areas but within an area with open and often dry soil surfaces, while Zuun Ail is exposed to ger area emissions there are no extensive dry soil surfaces close to the station. Both are located well away from paved main roads, but there is traffic on smaller unpaved roads nearby the sites. However, the motor vehicle contribution to $PM_{2.5}$ is small at both sites. At NRC, there is some discrepancy between the AMHIB period and the 5-year period analysis, with relatively more soil in the AMHIB period at the expense of the coal combustion source, while the opposite is true for the 5-year period. Annex A shows that the $PM_{2.5}$ fraction was very high in the AMHIB period compared to earlier. The source apportionment indicates that this increase is linked to a larger contribution from the soil source. Possibly this can be linked to drier conditions in the AMHIB period that leads to more fine particle suspension.

$PM_{10\text{-}2.5}$ (coarse particle fraction)

Soil suspension dominates at both sites 2 and 3. The motor vehicle source gives a measurable contribution to both sites, due to road dust suspension. The distance to main roads is large, but there is traffic on smaller unpaved roads nearby the sites. In addition, traffic in the whole area causes road dust concentrations in the entire UB air shed.

PM_{10}

PM_{10} is the sum of $PM_{2.5}$ and $PM_{10\text{-}2.5}$. As shown in Annex A of this report, the $PM_{10\text{-}2.5}$ (coarse fraction) concentration is generally substantially higher than the $PM_{2.5}$ concentration. As a consequence of this and the above, soil dust suspension gives the largest contribution to PM_{10} at sites 2 and 3. Coal combustion is also a very large source at site 3, while road dust gives a significant contribution to site 2.

For site 6, only PM_{10} apportionment has been carried out, and the samples cover only the winter period. Site 6 is located well within a ger area with surrounding small unpaved roads surrounding. Hence coal combustion

dominates at this location and road dust gives a significant contribution, while biomass (wood) burning and soil suspension are also noticed as a sources.

Instrument problems influence the results to some degree. The Gent samplers used at stations 2 and 3 allow some penetration of coarse PM to the $PM_{2.5}$ fraction, resulting in the assessed soil contribution to $PM_{2.5}$ to be slightly too high. The Partisol instrument at station 6 did not operate during evenings on highly polluted days, resulting in a slightly too low assessment of the coal combustion contribution.

References

Draxler, R. R. and G. D. Rolph (2003). HYSPLIT (HYbrid Single-Particle Lagrangian Integrated Trajectory) Model, NOAA Air Resources Laboratory, Silver Spring, MD.

Hopke, P. K. (1985). "The use of chemometrics in apportionment of air pollution sources." Trends in analytical chemistry. Vol. 4, No. 4: 104–106.

Hopke, P. K. (1991). An introduction to receptor modeling. Chemometrics and Intelligent Laboratory Systems: 21–43.

Hopke, P. K., Y. Xie, et al. (1997). "Characterization of the Gent stacked filter unit PM_{10} sampler." *Aerosol Sci. Technol.* **27**(6): 726–735.

Hopke, P. K., D. D. Cohen, et al. (2008). "Urban air quality in the Asian region." *Science of the Total Environment* **404**(1): 103–112.

Horvath, H. (1993). "Atmospheric Light Absorption—A Review." *Atmos. Environ,* **27A**: 293–317.

Horvath, H. (1997). "Experimental calibration for aerosol light absorption measurements using the integrating plate method—Summary of the data." *Aerosol Science* **28**: 2885–2887.

Kim, E. and P. K. Hopke (2006). "Characterization of fine particle sources in the Great Smoky Mountains area." *Science of the Total Environment* **368**(2–3): 781–794.

Lide, D. R (1992). *CRC Handbook of Chemistry and Physics*, CRC Press Inc.

Maenhaut, W., F. Francois, et al. (1993). The "Gent" Stacked Filter Unit Sampler for the Collection of Atmospheric Aerosols in Two Size Fractions: Description and Instructions for Installation and Use. *Co-ordinated Research Programme: CRP E4.10.08*. Vienna, International Atomic Energy Agency.

Markwitz, A. (2005). "An overview of the RCA/IAEA activities in the Australasian Region using nuclear analysis techniques for monitoring air pollution." *International Journal of PIXE* **15**(3/4): 271–276.

Mukai, H., N. Furuta, et al. (1993). "Characterization of sources of lead in the urban air of Asia using ratios of stable lead isotopes." *Environmental Science and Technology* **27**(7): 1347–1356.

Mukai, H., A. Tanaka, et al. (2001). "Regional characteristics of sulfur and lead isotope ratios in atmosphere at several Chinese urban sites." *Environmental Science and Technology* **35(6)**: 1064–1071.

Nyamjav, B., J. G. Goldammer, et al. (2007) "The Forest Fire Situation in Mongolia." *International Forest Fire News* **Volume**, DOI:

Paatero, P. (1997). "Least squares formulation of robust non-negative factor analysis." *Chemom. Intell. Lab. Syst.* **18**: 183–194.

Paatero, P. and P. K. Hopke (2003). "Discarding or downweighting high-noise variables in factor analytic models." *Anal. Chim. Acta* **490**(1–2): 277–289.

Paatero, P., P. K. Hopke, et al. (2002). "Understanding and controlling rotations in factor analytic models." *Chemomet. Intellig. Lab. Syst.* **60**(1–2): 253–264.

Paatero, P., P. K. Hopke, B. A. Begum, S. K. Biswas (2005). "A graphical diagnostic method for assessing the rotation in factor analytical models of atmospheric pollution." *Atmos. Environ*. **39**: 193–201.

Polissar, A. V., P. K. Hopke, et al. (2001). "Atmospheric Aerosol over Vermont: Chemical Composition and Sources." *Environ. Sci. Technol.* **35**(23): 4604–4621.

Song, X. H., A. V. Polissar, et al. (2001). "Sources of fine particle composition in the northeastern US." *Atmos. Environ.* **35**(31): 5277–5286.

Song, Y., Y. Zhang, et al. (2006). "Source apportionment of $PM_{2.5}$ in Beijing by positive matrix factorization." *Atmospheric Environment* **40**(8): 1526–1537.

Trompetter, W. J., A. Markwitz, et al. (2005). "Air Particulate Research Capability at the New Zealand Ion Beam Analysis Facility Using PIXE and IBA Techniques." *International Journal of PIXE*.

Wang, Y. Q., X. Y. Zhang, et al. (2006). "The contribution from distant dust sources to the atmospheric particulate matter loadings at Xi'an, China during spring." *Science of the Total Environment* **368**(2–3): 875–883.

Xuan, J., I. N. Sokolik, et al. (2004). "Identification and characterization of sources of atmospheric mineral dust in East Asia." *Atmospheric Environment* **38**(36): 6239–6252.

Zheng, M., L. G. Salmon, et al. (2005). "Seasonal trends in $PM_{2.5}$ source contributions in Beijing, China." *Atmospheric Environment* **39**(22): 3967–3976.

Ulaanbaatar, Mongolia, Air Monitoring and Health Impact Baseline (AMHIB) Report

Annex C

Air Pollution Dispersion Modeling for Ulaanbaatar: Assessment of Source Contributions and Population Exposure[1]

Introduction

The purpose of Annex C is to present the basis for the dispersion model calculations, the models, and the results. The dispersion models were used also in the preliminary assessment of concentrations and contributions from sources that were presented in the Discussion Paper (World Bank, 2009). New data has become available, and as a result the emissions inventory (EI) was updated. The Annex gives details on the updating of the EI. The measurements carried out by the AMHIB study (see Annex A) provided a better basis for evaluating the model calculations, and this is presented in the Annex. The Annex also compares the results regarding source contributions to PM that come from the two methodologies: the statistical source apportionment based upon the elemental analysis of PM samples (described in Annex B) and the dispersion modeling described in this Annex, and develops conclusions on this issue.

The dispersion model calculations provide the spatial distribution of the PM concentrations across the 30×30 km^2 grid used, on an hourly basis. When validated by the measurements, this spatial distribution provides the basis for the calculation of the exposure of the population to PM pollution, e.g. in terms of the population averaged exposure. The methods and results of this calculation are presented. This population exposure figure is the input to the estimation of the health effects of the PM pollution in UB.

[1]This report is drafted by the following World Bank consultants under the AMHIB project: Steinar Larssen, Sereeter Lodoysamba, Li Liu, Dagva Shagjjamba and Gunchin Gerelmaa. It was peer reviewed by Dick van den Hout, Netherlands Organization for Applied research/TNO, Sameer Akbar, World Bank, M. Khaliquzzaman, World Bank consultant and Taizo Yamada, JICA. World Bank Task Team Leaders were Jostein Nygard and Gailius Draugelis.

Table of Contents

C1 The dispersion model system, data input and its application in the AMHIB study

A state-of-the-art Eulerian grid model established for urban scale applications (Slørdal et al., 2003) was used to model the spatial and temporal air pollution concentrations in Ulaanbaatar for the AMHIB study. A diagnostic wind field model was used to provide the hourly meteorological data fields that are needed for input to the dispersion model. An emission inventory for Ulaanbaatar was used as input to an emissions model that provides hourly gridded emissions as input to the dispersion calculations. The models are described below. The model calculations for Ulaanbaatar have concentrated on particulate matter, PM.

The Eulerian grid model

The dispersion model used, named the EPISODE model (Slørdal et al., 2003) is a Eulerian grid model with embedded sub-grid models for calculation of pollutant concentrations resulting from different types of sources (area-, line- and point sources). EPISODE solves the time dependent advection/-diffusion equation on a 3 dimensional grid. The EPISODE model has been applied for the calculation of pollution compounds such as SO_2, CO, O_3, NO_2, NOx, PM_{10} and $PM_{2.5}$.

In addition to the Eulerian grid model, EPISODE also contains different sub-grid models for refined calculations in areas close to important line or point sources. Two different types of point-source sub-grid models can be applied optionally in the EPISODE. One is based on a segmented plume/trajectory model, while the other is the puff/trajectory model INPUFF. In both models the emissions from individual sources are treated as a temporal sequence of instantaneous releases of a specified pollutant mass. The air pollution resulting from the power plant emissions in UB was calculated using the embedded INPUFF model.

The line source sub-grid model was not applied in Ulaanbaatar, since the road traffic does not stand out as an important source to PM in Ulaanbaatar and there was no need to specify concentrations close to the main roads in UB.

The meteorological field model

The wind-field model implemented in AirQUIS is a model called CG-MATHEW (Conjugated-Gradient Mass Adjusted Three Dimensional Wind field). MATHEW (Sugiyama, 1997) is a diagnostic model designed to produce a gridded three-dimensional mass-conserving mean wind field from hourly averaged measured meteorological data. The wind field model has the main characteristics:

- it incorporates terrain explicitly, in order to be site independent;
- it uses available meteorological measurements;
- it is computationally stable;
- it calculates a three-dimensional velocity field with a relatively large number of grid points in relative short computer time.

MATHEW generates mass consistent wind fields by minimal adjustment of input fields derived from observations. The adjustments are performed by a constrained variational minimization using finite-difference methods and a conjugate gradient solution (Sugiyama, 1994) based on the theoretical framework of Sasaki, 1958; 1970. The requirement of minimal adjustment maintains consistency with available meteorological measurements, while the use of observed atmospheric stability parameters governs the relative amounts of change in the vertical and horizontal wind components. It should be noted that the velocity components are defined on staggered grid faces so that the mass-consistency constraint is cell-flux rather than grid point based.

Figure C.1 shows an example of the wind field as calculated by the Mathew model for a certain hour, represented by wind arrows giving the direction and strength (length of arrows) in each of the model grid cells.

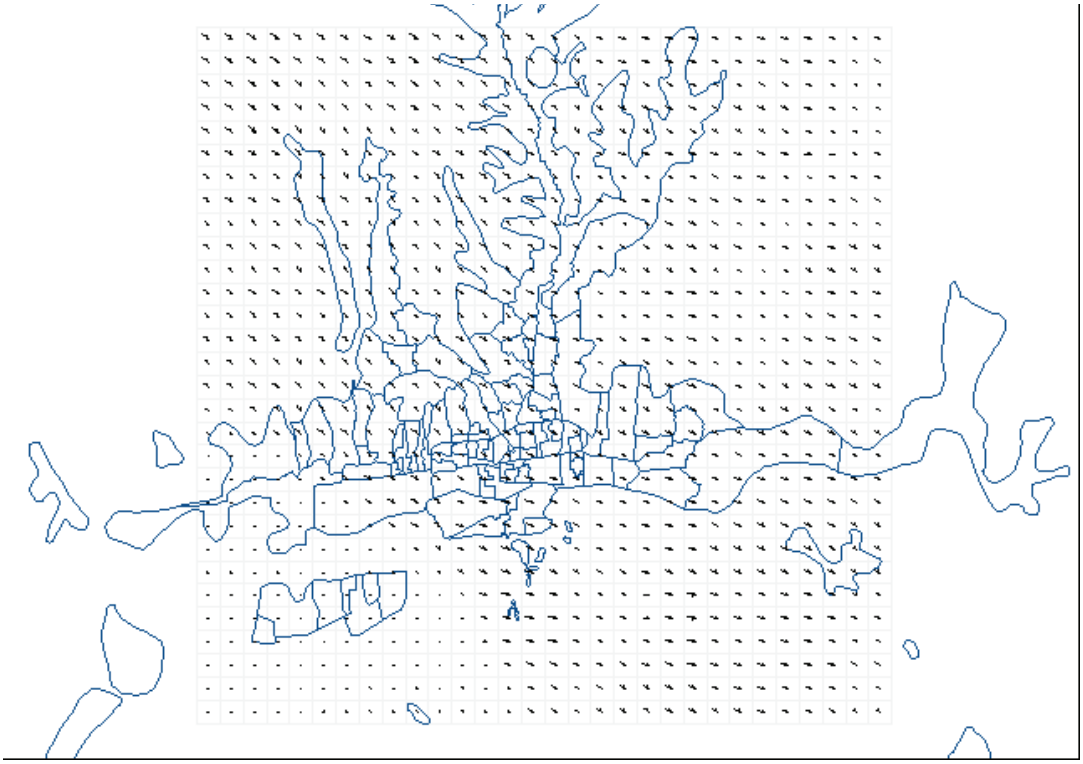

Figure C.1 Example of wind field produced by the Mathew model, for a certain hour.

Input data required by EPISODE

1. Emissions Inventory

The emissions inventory module contains data such as fuel consumption, emission factors, physical description of stacks and processes, traffic load etc. Estimates of hourly emissions of the different air pollutants are calculated by application of the emission model. The emission inventory includes three categories of sources:

- Point source emissions: Emissions from power plants, large industrial sources and significant single sources (e.g. larger boilers).

- Line source emissions: Emissions from road traffic. In the calculation, roads with annual daily traffic above a user defined limit value are included as line sources. The emissions from the roads with lower annual daily traffic are treated as area sources.

- Area source emissions: Both stationary sources that are too small to be treated as separate point sources as well as road traffic emissions from roads with low traffic loads.

2. Meteorological data

Meteorological data is prepared for input to the EPISODE model. The meteorological data can be acquired from local meteorological stations, or simulated by meteorological models. The required meteorological parameters are: wind (speed and direction), temperature, atmospheric stability, horizontal and vertical turbulence and mixing height. Cloud cover, relative humidity and precipitation are asked as optional. Wind data are input to the model from the Mathew model and observational data from NAMHIB, as well as data from the meteorological model TAPM (see section C3 below).

3. Background concentrations

The pollutants in the air transported into the urban area (the regional air pollution component from sources outside the city and transported from larger distances) are specified at the open boundaries of the model domain as a spatially constant value. This value can be specified by the user or taken from a background measurement station.

Application of the dispersion model in the AMHIB study in Ulaanbaatar
The software system platform AirQUIS was used to perform the modeling work for UB effectively. The GIS based AirQUIS system (AirQUIS, 2008) is an integrated air quality management system that contains different modules for treating and combining various data such as emission inventory data, geographical information data, measurement data, as well as the various models needed to perform dispersion and exposure calculations.
The models included in the present AirQUIS system that was used for the calculations in UB include:

- Emissions model
- Wind field model—The diagnostic wind field model (Mathew)
- Pollution dispersion model—The urban dispersion model (EPISODE)
- Exposure model—For stationary population exposure assessment

All models provide hourly spatial fields on a 1×1 km^2 basis, for the entire 30×30 km^2 grid defined for the model calculations. The system has been tested and used in several cities including Oslo, Norway (Slørdal et al., 2008) and Taiyuan in Shanxi Province, China (Daisheng et al., 2010).

The AirQUIS software system with the embedded models was run for Ulaanbaatar to calculate the present PM spatial distribution and the contributions from the main sources. It was also run for some selected source control scenarios to calculate the resulting reductions in PM concentrations across the UB area. Chapter C3 describes the set-up of the AirQUIS system for the UB modeling for the AMHIB period (June 2008–May 2009), including specifications of the input data used, and the evaluation of the model against measured concentrations.

Dispersion calculations using the system were carried out for UB in 2008–09, for the year 2007, as part of the preliminary assessment of PM pollution (World Bank, 2009). The calculations were carried out before the AMHIB PM measurement data were available, so only few data were available for model evaluation. New and updated emissions distribution data have since become available. Thus, updated model calculations are carried out to reflect the new data and present a better validated picture of the spatial distribution of PM pollution across UB.

C2 Updated AMHIB emissions inventory for Ulaanbaatar

C2.1 Updated total PM emissions in Ulaanbaatar in 2008
The main sources considered for PM in Ulaanbaatar are:

1. Stoves in households in Ger areas
2. Stoves in Kiosks and Food shops
3. Power plants
4. Heat only boilers
5. Vehicle exhaust emissions
6. Fugitive dust—Transport and Non-transport
7. Construction industry—Bricks
8. Garbage burning

The inventory of the PM emissions in UB for 2007, which was used as a basis for the Discussion Paper on air pollution in UB and published in 2009 (World Bank, 2009) was described in detail in that report. For the fugitive dust source, only the transport portion, which is suspension of dust from road surfaces, was included in the previous report. A method for including non-transport dust suspension, mainly dust suspension from open soil surfaces was lacking, although it is considered as a significant source of PM_{10} in air in UB. For this present report a method has been introduced and the non-transport dust suspension is included in the air pollution assessment.

The emissions from the brick industry and from garbage burning were, and are still, considered small on a total basis compared to the other sources, although such sources could have significant influence on the air pollution concentrations nearby. The brick industry is operated mainly during the summer season when the PM pollution in UB is low.

The inventory of each of the sources was described in the Discussion Paper in terms of:

- Description of the source
- Calculation method
- Emission factor(s)
- Total emissions
- Spatial distribution
- Time variation
- Uncertainties

The emission inventory has been updated, valid for 2008, as a preparation for the work of this report. The updating was mainly based upon new and updated data on population and its spatial distribution, as well as a better spatial distribution of the heat-only boilers (HOB). Also there has been a development towards less use of wood in gers during the later years. The updated data and the resulting emissions calculations are described in section C2.2 below. Regarding the emissions from the power plants (CHPs), the emissions used in this work are those provided from the Capacity Development Project for Air Pollution Control in Ulaanbaatar City, Mongolia Summary Report of 2nd JICA Detailed Planning Survey (March 15–May 13, 2009), based upon emission testing they carried out on CHP 2 and 4, after the cleaning equipment. The total emissions from the CHPs are uncertain, due to the limited amount of emission data from the plants, and also due to the cleaning equipment not being in proper operation during some periods (see Appendix 1). Since the cleaning equipment of CHP no. 2 was not functioning properly during the JICA emission testing period (a cleaning efficiency of only about 25% could be indicated (Appendix 1), the indication is that the total PM emissions used for the CHPs is on the high side of a real value.

Table C.1 shows the PM emissions in 2008, as resulting from the updating of the emissions inventory. Details are given in section C2.2.

The main change in the total emissions as a result of the updating is that the emissions of PM ger households and kiosks increased by 20.5%, as a result of the number of households increasing from 130,000 in the 2007 inventory to 155,285 in the 2008 inventory. Also, the CHP emissions have been increased significantly.

The even more significant result of the updating is the change in the spatial distribution of the ger households, concentrating the emissions more towards the near-central ger areas, as a result of the updated population distribution. Figure C.2 compares the spatial distribution of ger emissions used in the 2007 work and the distribution used for this report.

Table C.1 Summary of the emissions inventory for Ulaanbaatar, 2008 (tons/year)

Source	**PM_{10}**	**$PM_{2.5}$**	**Height of emissions, meters**	**Spatial distribution**
Ger households	19,731	15,785	3–5	Throughout ger areas
HOBs	1,077	646	10–20	Dispersed over UB surroundings
CHPs	18,589	7,436	100–200	3 point sources to the west of UB centre
Vehicle exhaust	1,161	1,161	<1	Dispersed along main road system mainly throughout the central city areas
Dry dust from roads				
Paved roads	5,142	771	<1	Mainly throughout the central city areas
Unpaved roads	4,812	722	<1	Mainly throughout the ger areas

The significance of these source-wise emissions for the PM_{10} pollution concentrations in UB can be summarized as follows:

The Ger households are the largest source of PM emissions. The ger and the HOB sources emit at fairly low heights and are distributed throughout large parts of the urban area, thus giving important contributions to the population's exposure to PM pollution. The CHPs, which have PM cleaning equipment, have about the same total emissions as the HOBs. Their emissions take place at large heights (through the CHP stacks of 100–200 meters), which limits their contribution to population exposure.

Vehicle exhaust is a less important PM source than gers, HOBs and CHPs in terms of mass of emissions. The vehicle related suspension of dry particles from roads is, however, a more important PM_{10} source, with a total emission mass about 50% larger than HOBs. The suspended particles are mainly in the coarse fraction. PM suspension is much less important for $PM_{2.5}$.

As mentioned, the suspension of soil particles through wind action from open surfaces, apart from the roads, is not included in the emissions table above. Source apportionment indicates this as an important PM_{10} source. In this work, the emission strength of the soil suspension source is not calculated as a total emission figure (tons/year). The soil suspension is included in the dispersion model through an algorithm calculating the suspension and its resulting contribution to airborne PM concentrations as a function of wind speed and other parameters (see sections 3.3 and 3.4).

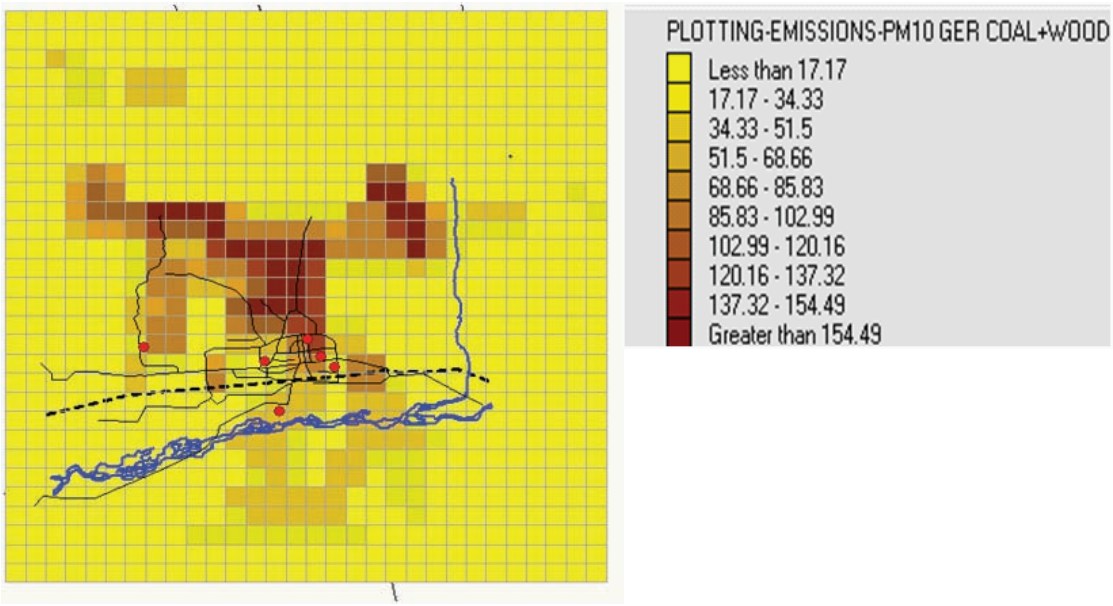

Figure C.2 Spatial distribution of ger household emissions of PM_{10}. tons/km^2.year.

A: The emissions distribution used in the Discussion Paper (World Bank, 2009).

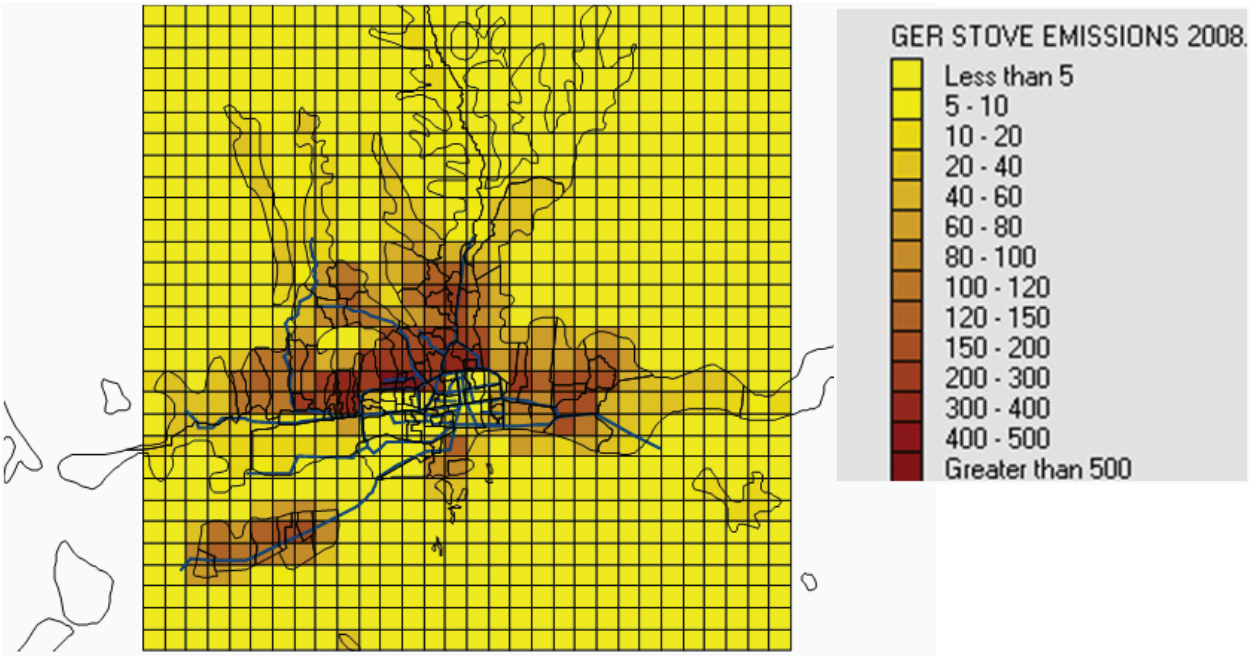

B: The distribution used for this report.

C2.2 Updated emission inventory for ger households and HOBs

Based on the new available information on population and number of families as well as their distribution in Khoroos in Ulaanbaatar, the ger emission inventory has been modified.

Population distribution

The population data provided through Dr. S. Lodoysamba includes the population and family numbers in Khoroo areas and its distribution, the data is available from 2000 to 2008. There are a total of 126 Khoroos in 6 administrative districts in Ulaanbaatar. The distribution of the population in 2008 is shown in Figure C.3. Figure C.4 shows the population distribution in the model grid (30×30 km). The model grid contain over 95% of the total population in Ulaanbaatar.

The coal and wood consumption from ger areas was estimated based upon the consumption for each household. Therefore, the availability of the number of the households can improve the estimation on the total fuel consumption and emissions from ger households. Table C.2 shows the population and family numbers for 2008 in each of the Khoroos in those regions and administrative districts. The population has increased rapidly in Ulaanbaatar in recent years. From 2005 to 2008, the total increase in the population is 99,863, representing 33,693 families immigrating into Ulaanbaatar, with most of those new immigrants living in the ger areas. From 2005 to 2008, the population increased by 3.6%, and households increased about 1.2% every year.

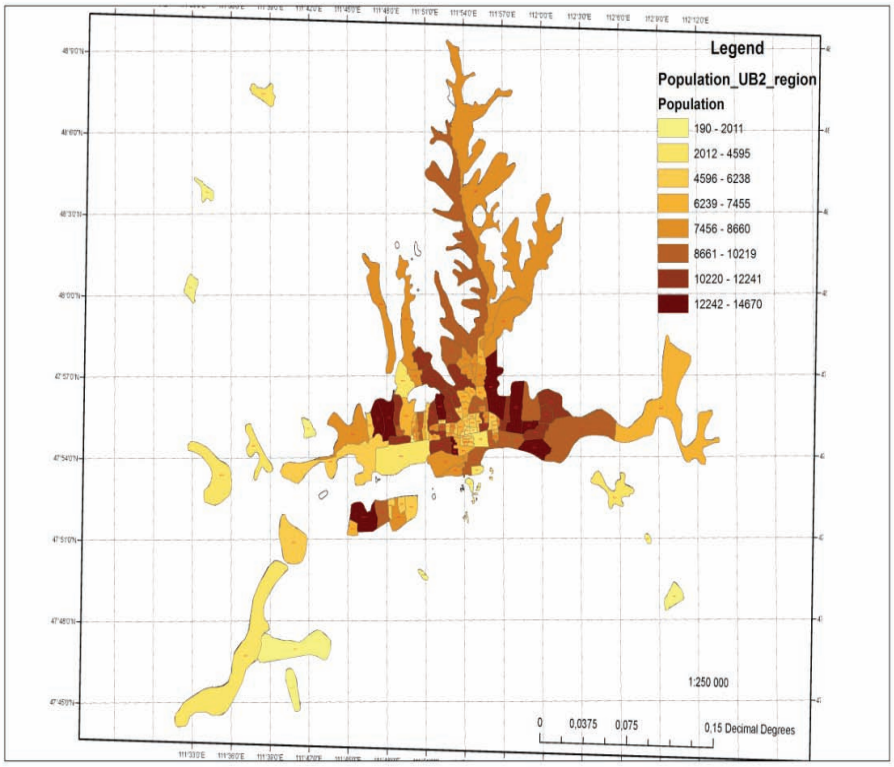

Figure C.3 Population distribution in Khoroos in Ulaanbaatar, 2008.

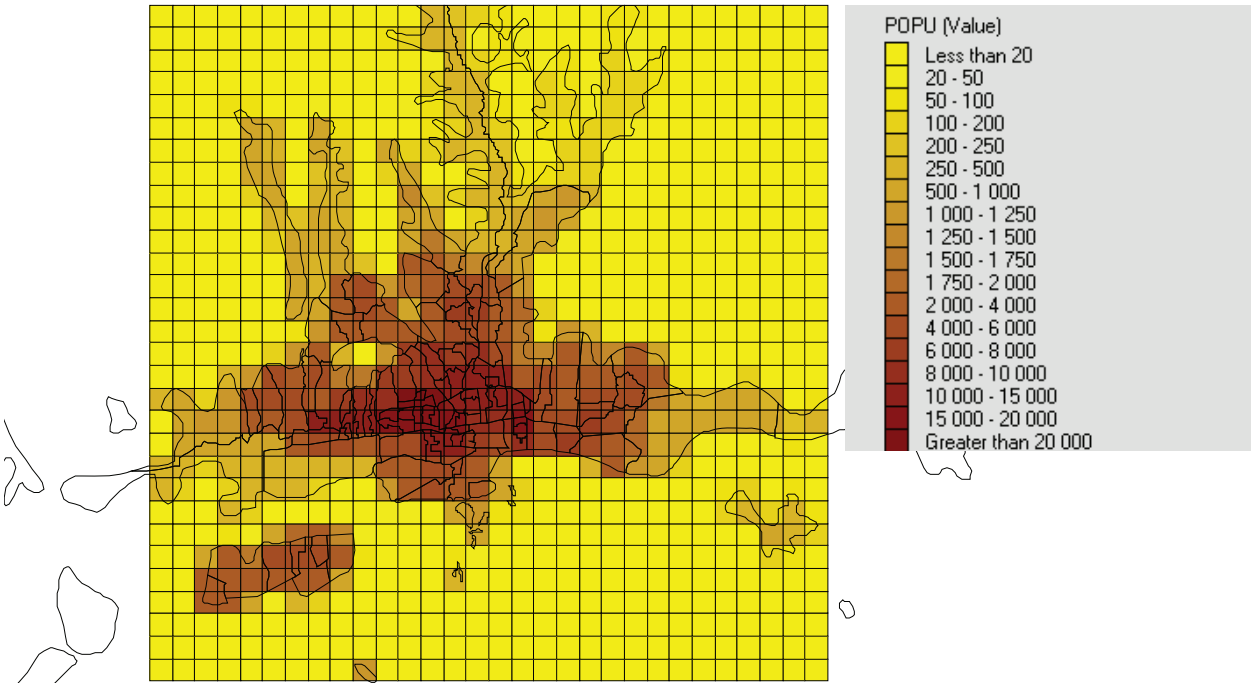

Figure C.4 Population distribution in grids in Ulaanbaatar, 2008.

Table C.2 Population and household numbers in Khoroos in Ulaanbaatar, 2008

Ulaanbaatar districts																	
Bayangol dist.			**Bayanzurkh**			**Songinokhairhan**			**Sukhbaatar**			**Khan-Uul**			**Chingeltei**		
Khoroo	**Popu.**	**Family**	**Khoroo**	**Popu.**	**Family**	**Khoroo**	**Popu.**	**Family**	**Khoroo**	**Popu.**	**Family**	**Khoroo**	**Popu.**	**Family**	**Khoroo**	**Popu.**	**Family**
BG01	12817	2734	BZ01	5753	1524	SH01	13907	3177	SB01	4512	1190	KH01	10176	2909	CH01	3931	960
BG02	6800	1198	BZ02	14670	3200	SH02	5381	1150	SB02	5850	1395	KH02	8076	1885	CH02	4028	846
BG03	7275	1685	BZ03	5040	1493	SH03	13033	2769	SB03	6885	1514	KH03	7786	1848	CH03	4595	1275
BG04	10798	2311	BZ04	11122	2776	SH04	12955	2683	SB04	4019	1229	KH04	6822	1812	CH04	5249	1200
BG05	6574	1705	BZ05	13083	3170	SH05	10881	2356	SB05	5253	1254	KH05	5855	1356	CH05	5231	1141
BG06	11614	2625	BZ06	9810	2180	SH06	7279	1729	SB06	6238	1394	KH06	7846	1685	CH06	5972	1477
BG07	8660	1799	BZ07	7698	1800	SH07	11480	2611	SB07	7874	1980	KH07	5610	1458	CH07	12025	2372
BG08	9825	2250	BZ08	10841	2342	SH08	7797	1677	SB08	10981	2697	KH08	9138	2420	CH08	4834	1157
BG09	12037	3007	BZ09	11160	2567	SH09	7938	1796	SB09	9427	2050	KH09	13374	3765	CH09	7455	1593
BG10	14495	3715	BZ10	9953	2525	SH10	12191	2397	SB10	8473	1896	KH10	6939	1830	CH10	7328	1448
BG11	12241	2979	BZ11	4215	1116	SH11	11800	2562	SB11	10219	2040	KH11	5660	1469	CH11	6309	1435
BG12	10992	2421	BZ12	12484	2800	SH12	7188	1862	SB12	7302	1963	KH12	5587	1580	CH12	12212	2457
BG13	4560	1004	BZ13	9042	1912	SH13	7455	1715	SB13	7734	1760	KH13	3452	1006	CH13	7856	1671
BG14	4939	1106	BZ14	8914	2550	SH14	9341	2327	SB14	6610	1581	KH14	2494	875	CH14	8561	1660
BG15	5016	1312	BZ15	5696	1356	SH15	7882	1642	SB15	8374	1840				CH15	8461	1674
BG16	6787	1642	BZ16	13216	2650	SH16	7153	1576	SB16	8387	2009				CH16	9629	2160
BG17	5611	1040	BZ17	10531	2484	SH17	6826	1684							CH17	10187	2382
BG18	8067	1693	BZ18	8207	2254	SH18	11268	2633							CH18	10040	2175
BG19	6137	1486	BZ19	9240	2100	SH19	9931	1936									
BG20	4033	960	BZ20	6596	2100	SH20	9894	2186									
						SH21	5500	1643									
Sum	**169278**	**38672**	**Sum**	**187271**	**44899**	**Sum**	**197080**	**44111**	**Sum**	**118138**	**27792**	**Sum**	**98815**	**25898**	**Sum**	**133903**	**29083**

Updated ger emissions using the updated population distribution

The latest official data regarding the coal/wood consumption per ger household are used in the preliminary emission inventory presented in the Discussion Paper (World Bank, 2009): 4.18 ton/yr coal and 3.18 ton/yr wood consumption as an average per household. These consumption figures are based upon a questionnaire study and are valid for the 2006–07 winter season (World Bank, 2008).

The population in the central areas of Ulaanbaatar lives mostly in apartments, and about 80% of them are covered by central heating and hot water supplied by three heat-and-power plants (CHPs). The rest of the apartments are heated by heating boilers, and a few use stoves. Since the coal/wood consumption from stoves is concentrated in ger areas, we identified the central areas as ger-free areas, and then calculated the coal/wood consumption and its distribution based on the distribution of the households located in the ger areas. The specification of the ger-free area distribution is based on a ger distribution map from R.Oyun (Risk Study Center, Ulaanbaatar Master Plan for Air Pollution Reduction Working Group) see Figure C.5. With this data processing, there are 151,285 households in ger areas, which is about 64.2% of the total households in Ulaanbaatar.

The emission factors used in the preliminary emission inventory are, for PM_{10}, 16 kg/ton of coal and 18.5 kg/ton of wood (see World Bank 2009). The ratio used between $PM_{2.5}$ and PM_{10} was 0.8.

The updated population amount and distribution coupled with the consumption and emission factor data above give the distributions of the PM_{10} emissions from coal and wood burning in ger areas shown in Figure C.6.

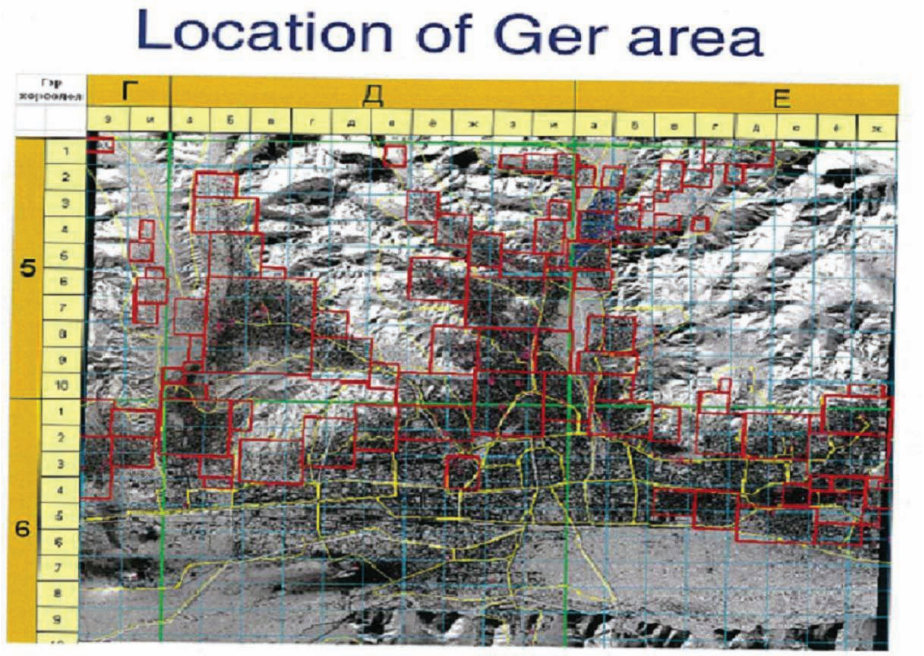

Figure C.5 Location of ger areas, represented by red squares. (Source: R.Oyun, Risk Study Center, Ulaanbaatar Master Plan for Air Pollution Reduction Working Group)

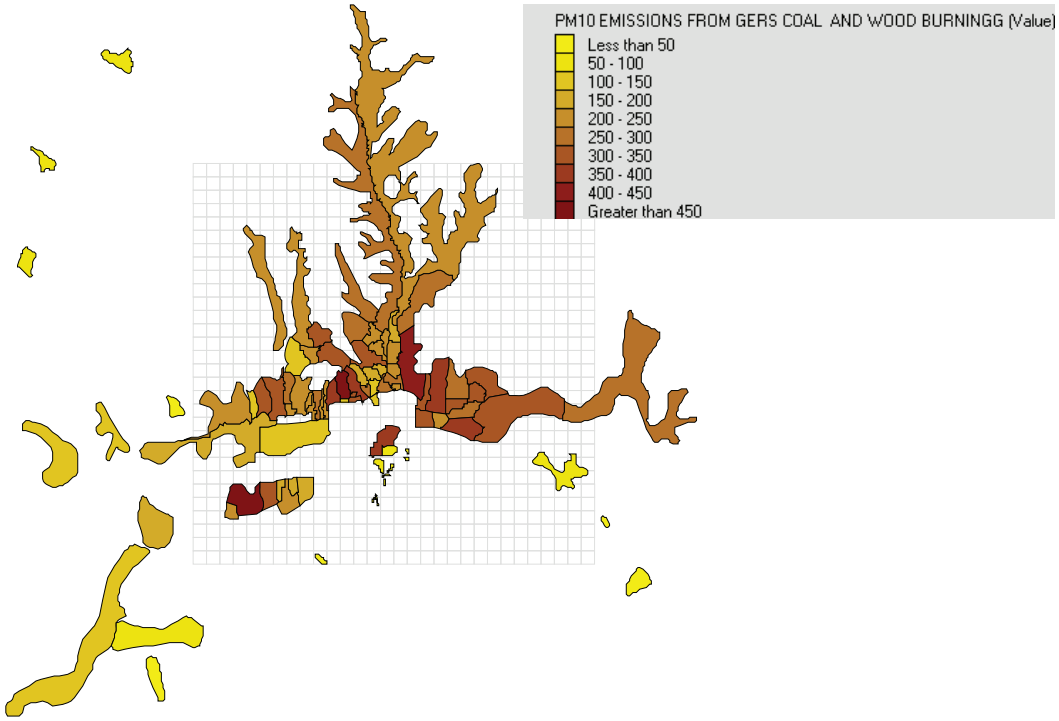

Figure C.6 Distribution of PM_{10} emissions from coal and wood burning from Ger stoves, 2008. tons/km^2

It is assumed that the number of kiosks and food shops increase in proportional with the Ger population. 4,500 kiosks were estimated for the year 2005 (Guttikunda, 2008). Since the population increased by 16.8% between 2005 and 2008, 5,255 kiosks and food shops are estimated for 2008. The estimated coal consumption for each kiosk is 8.2 ton/yr (Guttikunda, 2008).

The total PM_{10} emissions from the ger heating systems during the AMHIB (2008–09) winter, as resulting from the same specific coal and wood consumption and emission factors as assessed for the winter 2006–07 and an updated population distribution, are 19,042 tons, with a 53/47% split between coal and wood emissions (see World Bank 2009). In addition, kiosks and food shops in ger areas contribute a small amount, calculated to 690 tons. As mentioned, the $PM_{2.5}$ emissions are 0.8 times the PM_{10} emissions.

New information regarding wood consumption and ger stove emissions, presented in the section below, give reason to re-evaluate this inventory, especially regarding the coal/wood split.

New information on ger household coal and wood consumption and emission factors

Coal and wood consumption in gers

The present experience (as per autumn 2010) is that ger households use much less wood now than was used in the preliminary inventory. The previous data was based upon the questionnaire study that was applicable for the winter season 2006/07. A higher price of wood is one of the reasons for less amounts of wood burned now. Some of the wood was burned for cooking during the summer season. Currently, it appears as though electricity is predominantly used for cooking during the summer season, thus there are very little ger emissions during the summer.

This trend towards substantially less wood consumption seems real, and it has taken place over a short time, after the 2006–07 winter season when the questionnaire data were obtained. The AMHIB period covered the 2008–09 winter season, i.e. two years after the questionnaire study. No data are available to support an estimate of how much wood was burned during the AMHIB winter, as compared to the previous estimate of about 3 tons per winter. A reasonable assumption is that less wood consumption would mean larger coal consumption to keep the gers warm. If wood is replaced by coal, it should not affect the total emissions significantly.

Emission factors

Some very preliminary data on emission factors for ger stoves is available from the testing of stoves in the new ADB financed emissions laboratory (Reference to paper: 'Early Conclusions from Emission Testing (Ger stoves, Kalakh coal)'.

One stove has been tested, with emissions measured continuously during a complete firing cycle. The test showed that the absolute majority of the PM emissions took place during the cold start-up phase, with emissions being small during the warm/hot burning phase of the full cycle. Thus, the total emissions from the combustion of coal (and wood) over a period from ger and similar stoves is mainly a function of the number of re-starts of the fire from cold stove during the period rather than the amount of fuel used, although the emissions from the warm phase do give a contribution. This is a confirmation of previous experience regarding small stove combustion. Emission factors for coal (and wood) consumption in small stoves (like the factors used in the preliminary emission inventory for UB) always represent average emissions over a longer period (like a winter season) based upon typical firing practices.

The one test reported covered a full burning cycle, assumed to be a typical/average firing cycle for UB winter conditions. Results from that test combined with an estimate of the number of restarts during 6 winter months (estimated 360 restarts) give the following first order-of-magnitude estimate of emissions from the coal use in one stove: 36 kg of $PM_{2.5}$ per winter (6 months). Combined with the updated number of ger households (151,285) this gives a figure for the winter emissions from coal in gers of 5,446 tons. In comparison, the updated $PM_{2.5}$ emissions from coal use in ger households based upon the previous consumption and emission factor is 8,114 tons.

There is a question of the representative nature of the one stove tested. The stove was purchased on the market and is representative of the type and quality found today. It appears that many people have replaced their stove in the recent past. Still, there is a multitude of stove makes and qualities used in the gers, so the question of representativeness for present average stove emissions is unresolved.

However, that notwithstanding, emissions from different models of stoves can be reduced by a large amount. A full burn cycle for a traditional stove emits about 300 mg of $PM_{2.5}$ per MJ of heat produced, and the same stove with slight modification + a different lighting technique shows only 60 mg of $PM_{2.5}$ per MJ produced.

Conclusion on updating of the ger emissions

The new information on wood consumption, although undoubtedly correct, is not specific enough presently to support an estimate of how much wood was actually used during the AMHIB winter 2008–09. When replaced by coal, the shift probably does not significantly affect the total emission amount. The one stove test could be used to give an estimate of the winter emissions per stove which is less than used previously. However, more data from testing of ger stoves over the types of stoves dominating in the UB gers is needed to support a modification of the previously used emission factors. Another factor is that the PM pollution level in UB has not been reduced from the 2006–07 winter towards the AMHIB year (2008–09). On the contrary it has increased (see Figure A.26 in Annex A). Indeed several factors in combination determine such trends, like climate as well as combustion amount and practices, but the increasing PM trend does not provide support for an argument of a large PM reduction from a shift from wood to coal consumption and emissions.

We conclude that is it clear, now as earlier, that the estimated emission amount from gers is uncertain. The new information regarding wood consumption and how it is replaced by coal is not yet specific enough to support a modification of the ger emissions. The indication that the PM concentrations in UB did not decline from 2006 towards 2009 supports this position. The one stove emission test might indicate that the emission factor for coal burning in gers that has been used previously is too high, but no conclusion can be drawn about the representative nature of the one test. Further testing of representative stoves is needed to support a modification of the total ger emissions in this report.

Thus, the total ger emissions from household combustion are retained as calculated above, based upon updated population data, while the split between emissions from coal and wood, now about 50/50, should lean more towards the coal side.

The source apportionment (SA) analysis from the receptor modeling on data from the AMHIB year gives the result that the contribution to PM concentrations in air from coal combustion is much larger than the contribution from wood burning (see Annex B). This appears to support a significant shift from wood to coal in gers. However, the similar analysis on the 5-year data series 2004–2009 gives the same result. Thus it seems likely that the SA analysis results do not reflect a shift from wood to coal that has taken place since 2006–07. This result is not easily explained. It could be that the chemical composition of the particles that has been analyzed as a basis for the SA analysis do not sufficiently clearly separate out the wood chemical profile in the particles, and that the analysis only partly associates wood particles with the 'biomass' emission profile. In any case, the SA results cannot be used to further specify the coal/wood split during the AMHIB winter, other than to support that the split should lean much more towards coal.

Updated spatial distribution of HOBs

Heat only boilers are distributed mostly in ger areas but also on the edge of the center of Ulaanbaatar city where the district heating system is not available. To locate the HOBs in Ulaanbaatar, we also refer to a map from R.Oyun where the location of the 'individual heating stoves' (HOBs) are marked (see Figure C.7). New information on the consumption of coal in the heat only boilers in UB is now available (see Chapter 8.3 in the Final UB Assessment Report). The previously used and the new information is shown in Table C.3. It seems clear that the previous estimate of HOB coal consumption, which was taken from the latest report available, was too high. The large number of HOBs used previously might have included boilers outside the 6 districts close to UB which are enclosed by the model area. Also the average consumption per HOB is lower in the new data. The emission factor is kept, as there is no new data.

Figure C.8 shows the updated emission distribution from HOBs in Ulaanbaatar.

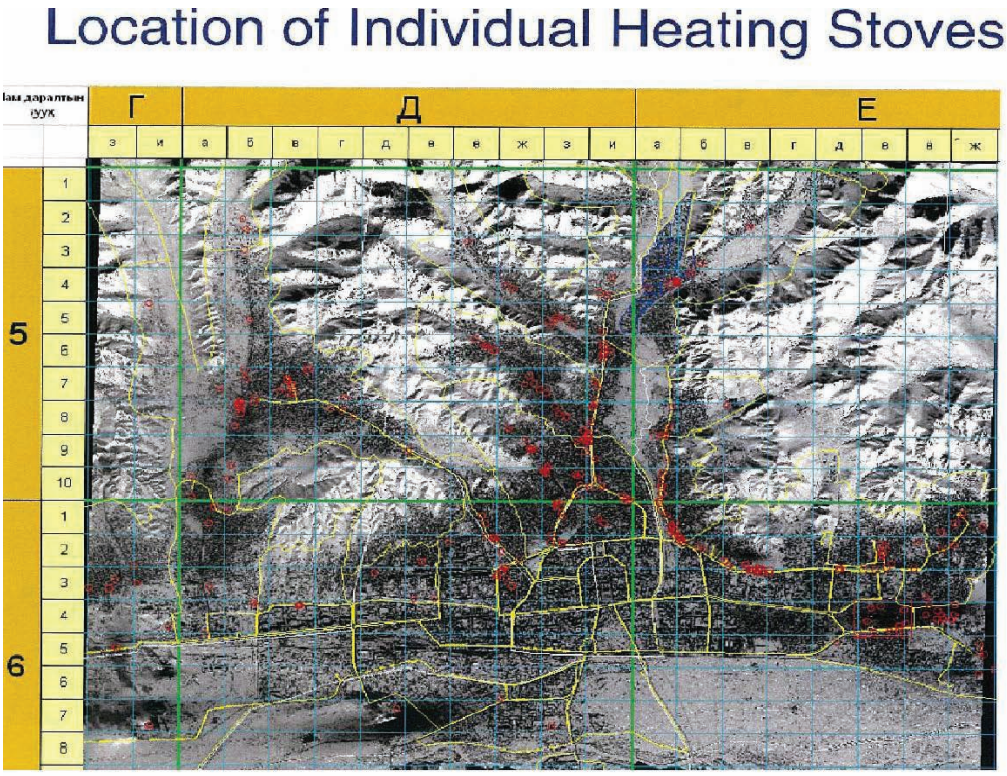

Figure C.7 Location of individual heating stoves, red dots indicates the locations if HOBs. (Sources: R.Oyun, Risk Study Center, Ulaanbaatar Master Plan for Air Pollution Reduction Working Group)

Table C.3 PM_{10} emissions inventory for HOBs, winter season 2008/9

	Number of HOB	**Specific consumption**	**Total consumption**	**Emission factor, PM_{10}**	**Total emissions**
		tons/winter	tons	kg/ton	tons/year
Previously used data	>267		400,000	16.2	6,480
New information	160		66,500	16.2	1,077

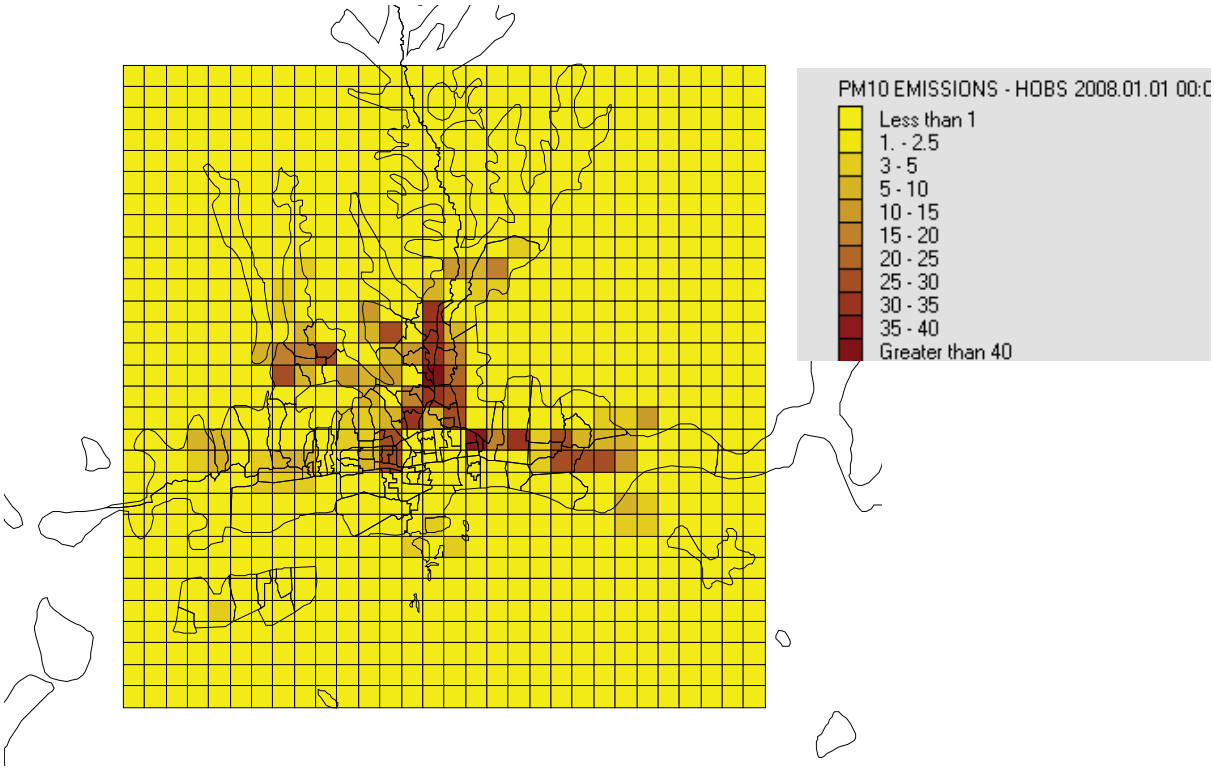

Figure C.8 Distribution of PM_{10} emissions from coal burning from HOBs.

C3 Dispersion model set-up and data input for 2008

Model domain and grid

The modeling work was performed with the model integrated within AirQUIS system. In this GIS based system, UTM coordinates are applied. In order to have all information consistent, all collected information based on Lat/Lon coordinates have been converted to UTM coordinates. The model domain lower left point coordinates is as same as Guttikunda's (2007) model domain, and covers the urban area of Ulaanbaatar and its surroundings (Figure C.9). The model domain has 30×30 grid cells on a 1 km resolution, covering a 900 km^2 area.

Topography

The terrain information has been downloaded from http://www.esri.com/data/resources/geographic-data.html and prepared for modeling domain on the 1 km resolution.

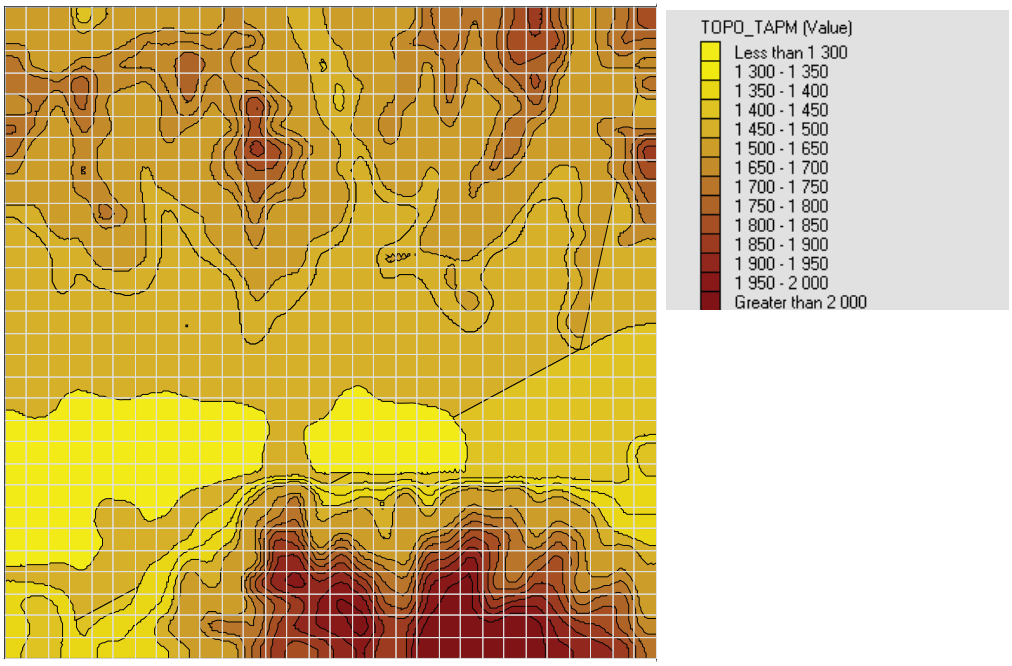

Figure C.9 The domain used for air pollution modeling in this work. 1×1 km^2 grid cells. Topography in meters.

Emission data and inputs

The details of the emissions inventory used for UB in this work are given in Appendix E of the Discussion Paper (World Bank, 2009), with the modifications described in section C2.2 above. The UB sources are introduced into the model system as point sources, area sources and line sources. In the import of the vehicle emissions, the traffic source is treated as line sources (road sections), while in the modeling set-up, most of the traffic source emissions are treated as area sources. When the receptor points are located within influence distance (which is $\Delta x/2$, Δx as grid size which is 1,000 meter in this work) from the road links, the emissions from road links are treated as line sources.

Point sources

The stacks of the 3 power plants located in the southwest of Ulaanbaatar city are the only sources inserted as point sources in the modeling set-up. The physical data of the stacks, such as exact coordinates, stack height, diameter, flow rates and cleaning efficiencies is input for the simulation. There is a certain variation in the power plants' loads over the year, and also over each day, as was described briefly in the Discussion Paper (World Bank, 2009) based upon a reference (PREGA, 2006). There is an obvious variation in monthly load of approx ±30% from the average, higher in winter and lower in summer. As a simplification, in the model calculations the CHP load is kept constant over the year, as this will introduce only a limited error in the calculations of PM contributions, considering also the relatively small contribution to total PM concentrations from the CHPs.

Area sources

In Ulaanbaatar, based on the pollution release height, emissions from households in gers, kiosks, heat only boilers (HOBs) and waste burning are considered as area sources.

The coal and wood consumption in gers and HOBs is used for heating and cooking, and therefore, an obvious seasonal variation is applied. This emission time variation is based on the estimated energy consumption during a year. No time variation factors were applied to the kiosks and waste.

Line sources

Traffic related emissions include both direct exhaust emissions and the fugitive dust from the roads (dry dust on the roads suspended in air due to the action of the turbulence created by passing vehicles).

Meteorological data

One year's meteorological observation data for Ulaanbaatar (year 2008) from 3 stations were provided by NAMHEM. The meteorological data is available for most of the year with 3-hourly observations, while hourly meteorological data is available from one of the stations.

The meteorological parameters available are wind speed, wind direction, surface temperature, and precipitation.

Figure C.10 shows the wind rose made from the meteorological station which provided hourly meteorological data for the period 01/06/2008 to 31/05/2009. The wind rose for the heating season in Ulaanbaatar from 1/10/2008 to 01/04/2009 is also shown.

It is necessary to obtain information on the atmospheric stability in order to model the dispersion of the air pollutants. This information is not available from measurements in Ulaanbaatar. The missing local meteorological data were supplemented by data calculated by the TAPM model ('The Air Pollution Model', Hurley et al., 2005). TAPM was run to calculate the vertical thermal structure over the model domain as the input for the EPISODE model. In this work, TAPM was set up on a 300km × 300km horizontal domain, and nested for Ulaanbaatar region on finer scales (10km × 10km, 3km × 3km, and 1km × 1km). Six-hourly synoptic analyses data on a longitude/ latitude grid at 0.75- or 1.0-degree grid spacing (approximately 75 km or 100 km) was used for driving TAPM, prepared from LAPS or GASP analysis data. Meteorological data simulated for Ulaanbaatar by TAPM has been evaluated through comparing with the surface meteorological measurements for the modeling period, and the results show that TAPM generally agree well with the measured meteorological parameters.

The stability is decided by the temperature differences calculated by TAPM between the first two vertical layers in the model, at 10 and 25 meters separately.

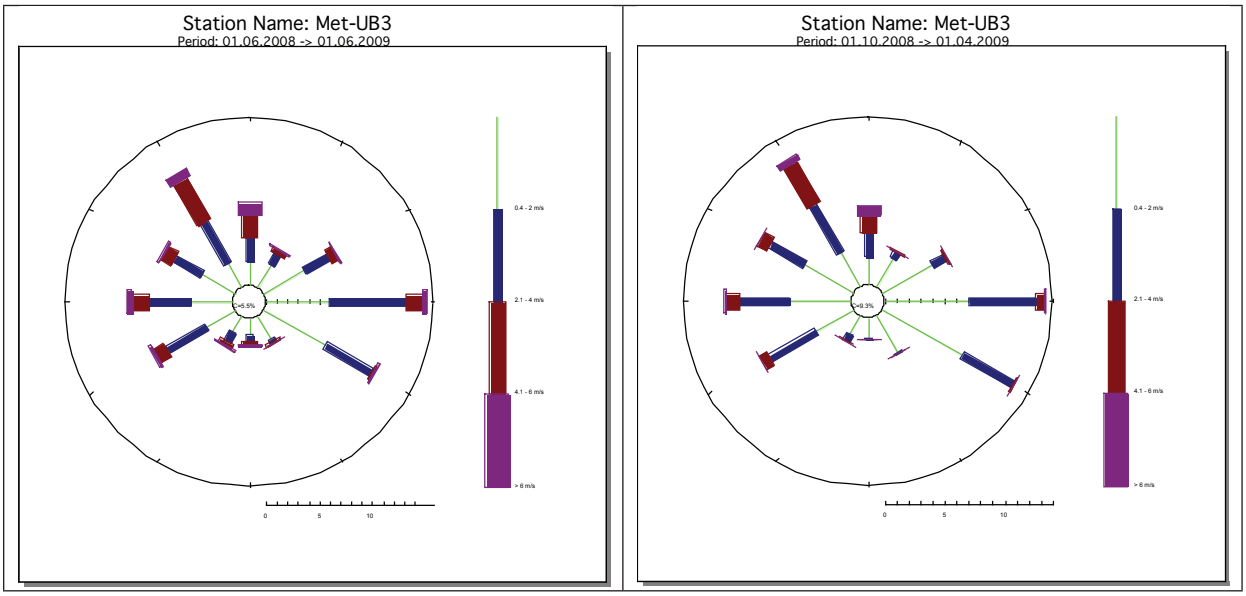

Figure C.10 Wind direction and speed distribution for the NAMHEM meteorological station in UB, 2008.

Soil suspension model

The model for soil suspension in AirQUIS is based on the suspension of soil particles from the surface due to wind and the turbulence of the wind. The understanding is that soil particles are suspended when the wind velocity/ turbulence exceeds a certain starting level and when dust is available on the surface to be released. The suspension of dust by wind action is decided by wind speed, surface load of the dust and precipitation.

In this module, a scheme from Sehmel is applied (Sehmel, 1980). It is defined that the wind speed must be at least 4 m/s for the dust to be released, when the precipitation does not exceed 0.4 mm/hour. If the suspension of dust initially has occurred, it will continue until the wind speed falls below 1m/s or there is precipitation of 0.4 mm/hour.

Release of stored PM_{10} at the grid surface will be calculated when the conditions with respect to wind speed and precipitation are satisfied. The equation for calculating emissions is as below:

(1) $Q(i,j) = M(i,j) * Sdep(i,j) * (4 * 10^{-8} * V(i,j)^{2.5})$

Q = emissions in g/s

M = mass of the deposit of PM_{10} in kg

Sdep = proportion of surface that is able to release dust in each grid

V (i, j) = wind speed in m/s

The constants have been empirically determined.

The proportion of grids that have surfaces from which dust can be released is determined based on land use data. In Ulaanbaatar, we assume all the ger areas are allowing dust suspension from the entire area, and in ger-free areas in the city center 50% of the surface is available for dust release.

The emission of PM_{10} (Q) in each grid is calculated as an area emission in grams per second. It is necessary to know the amount (mass M) of PM_{10} that is available for suspension from the surface in each grid cell. In the method used here, lacking data on the surface soil particle size distribution, this is calculated based on the PM_{10} in air which is deposited to the surface over a whole winter, using a deposition velocity of 0.3 cm/s. This gives the amount of deposited PM_{10} in kg in grid cells available for suspension. The equation used is shown below (see Table C.5 and associated text). This method gives a reasonably good average representation of the soil particle suspension in UB. Calculation of soil suspension based upon size distribution data of the top soil would give a more correct spatial distribution of the soil suspension. In the method used, the population distribution steers the soil suspension distribution to an excessive degree. However, in calculations of the population weighted exposure (PWE) the difference between the method used and a method based upon surface soil size distribution would largely even out.

(2) $M(i,j) = C(i,j) * V_{dep} * T * A * (10^{-6}\ kg/\mu g)$

M = mass of PM_{10} in kg

C = average concentration of PM_{10} in $\mu g/m^3$

V_{dep} = deposition velocity in m/s

T = deposition time through the winter (6 months, 15,552,000 seconds)

A = the grid area in m^2

In the episode model, emission from the release of stored PM_{10} is treated as surface emissions.

Model set-up for this report

The air quality model was run for the 12 months of the AMHIB baseline study period: 1 June, 2008–31 May, 2009. The model calculates hourly average concentrations over the full year in the center point of all the 30×30 km^2 grid cells. Because all measurements from Ulaanbaatar are daily averages, the model results have to be averaged giving 24 hour average concentrations and compared with measurements on the daily basis. The model has a 1km horizontal resolution, and vertically there are 10 modeling layers, from surface to 2,750 m height. The first (lowest) layer is 20 meters, and there are in total 3 layers in the lowest 100 meter (of 20, 30 and 50 meter depths).

The 2008 emission inventory is the basis for the emissions input to the model, and used as total emissions over the AMHIB period. The emissions vary with the different time variations, over the AMHIB period. The time variation applied for CHPs and HOBs are the same as in the Discussion Paper (World Bank, 2009). For ger coal/wood burning the time variation is calculated based on the temperature variation during the heating season.

The starting wind speed for suspension of PM_{10} particles from soil surfaces in UB is set at 4 m/s, based on Sehmel (1980). The ratio between $PM_{2.5}$ and PM_{10} of the suspended soil particles was estimated based upon the source apportionment results for $PM_{2.5}$ and PM_{10} (Annex B), using the data from monitoring station 3 (Zuun Ail). Those data gave a $PM_{2.5}$ /PM_{10} ratio for the suspended soil source of 0.3. This is a fairly high fraction of small particles, indicating that the particles in the surface soil of UB have a fairly high fraction of small particles. This in itself indicates that soil suspension is an important PM source in air in UB.

C4 Evaluation of the model by comparison with PM measurements

C4.1 Modeled and measured PM concentrations

Figure C.11 shows the spatial distribution of PM_{10} and $PM_{2.5}$ concentrations in Ulaanbaatar for the period June 2008–May 2009, as calculated with the described model system, using the updated population distribution and emissions inventory. The figure shows the large variations in concentrations across UB, with very high concentrations in the ger areas, especially those fairly close to the central UB areas. There are very steep gradients when moving out from the ger areas, especially moving south from the ger areas just north of UB central areas and into the city. The steep gradient is due to the equally steep gradient in emission density, very high in the ger areas and much lower in the city. The Figures C.12–C.14 show the spatial contributions as modeled for the sources heat-only boilers (HOBs), road traffic (exhaust particles and road dust combined) and the power plant (CHPs).

To identify explain the large difference in the spatial concentration distribution caused by the updated population distribution, Figure C.15 shows, for comparison, the preliminary concentration maps for 2007 provided in the Discussion Paper (World Bank, 2009). The differences between the maps are mainly due to the updated ger population distribution, as well as the higher total population, used for the AMHIB period maps. The correct and much more concentrated ger population in areas closer to UB central areas results in much higher concentrations than modeled for 2007, when the preliminary population distribution was used (Guttikunda, 2007).

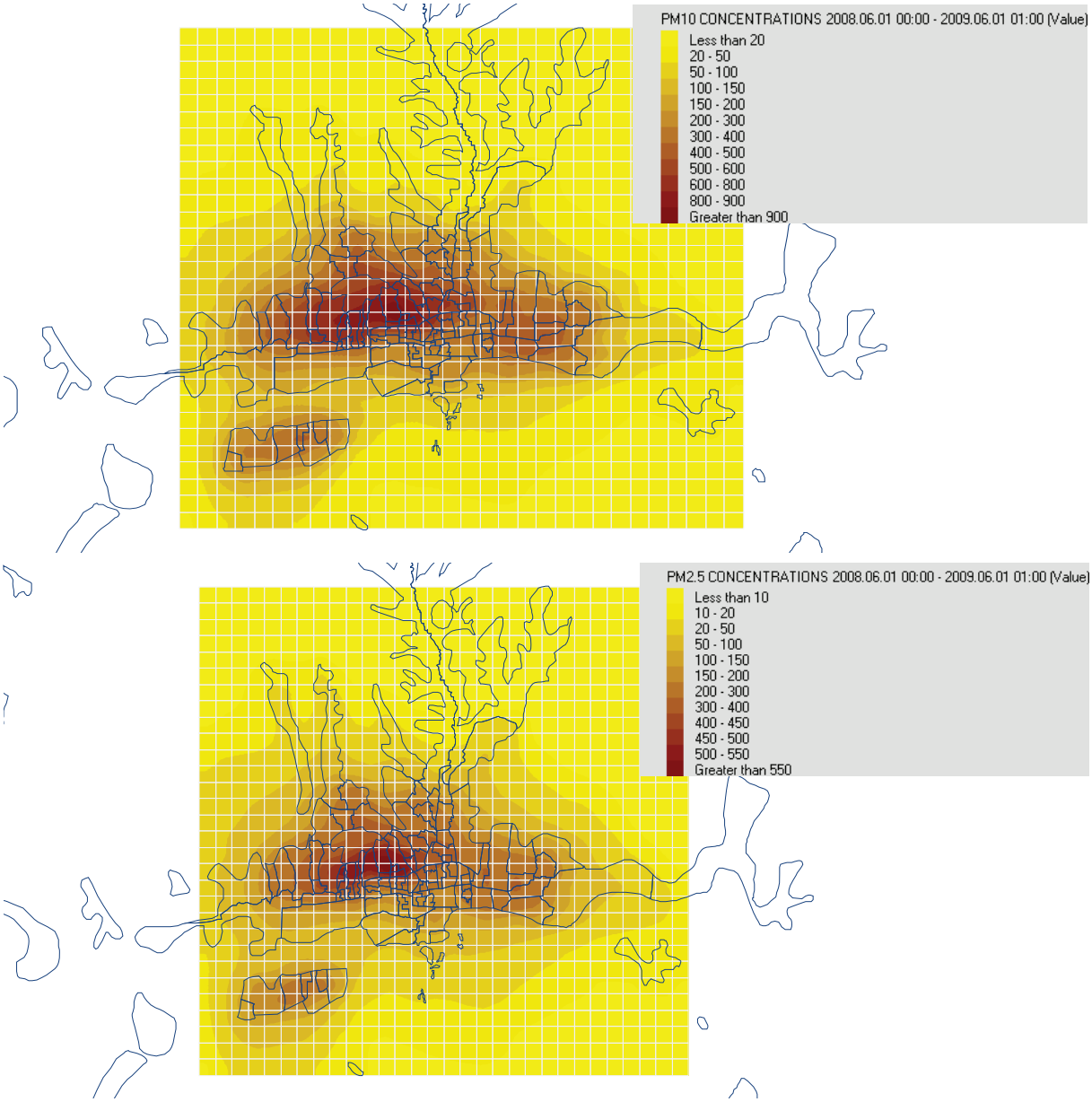

Figure C.11 Modeled PM_{10} (top) and $PM_{2.5}$ (bottom) concentrations in Ulaanbaatar for the AMHIB baseline period, June 2008–May 2009. The figure shows iso-lines of annual average concentrations, $\mu g/m^3$.

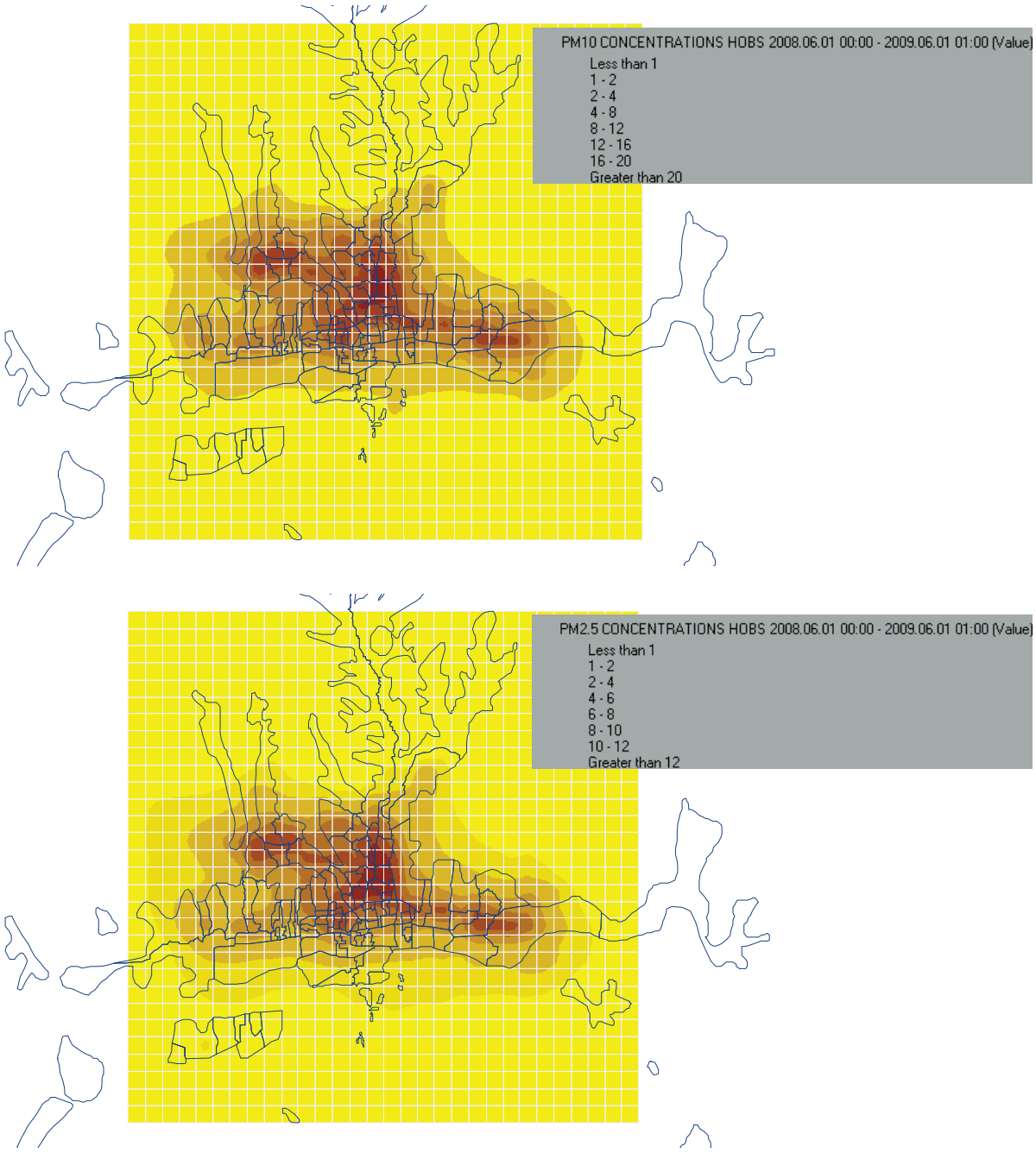

Figure C.12 Modeled PM_{10} (top) and $PM_{2.5}$ (bottom) contribution from HOBs, AMHIB baseline period, June 2008–May 2009. The figure shows iso-lines of annual average concentrations, µg/m^3.

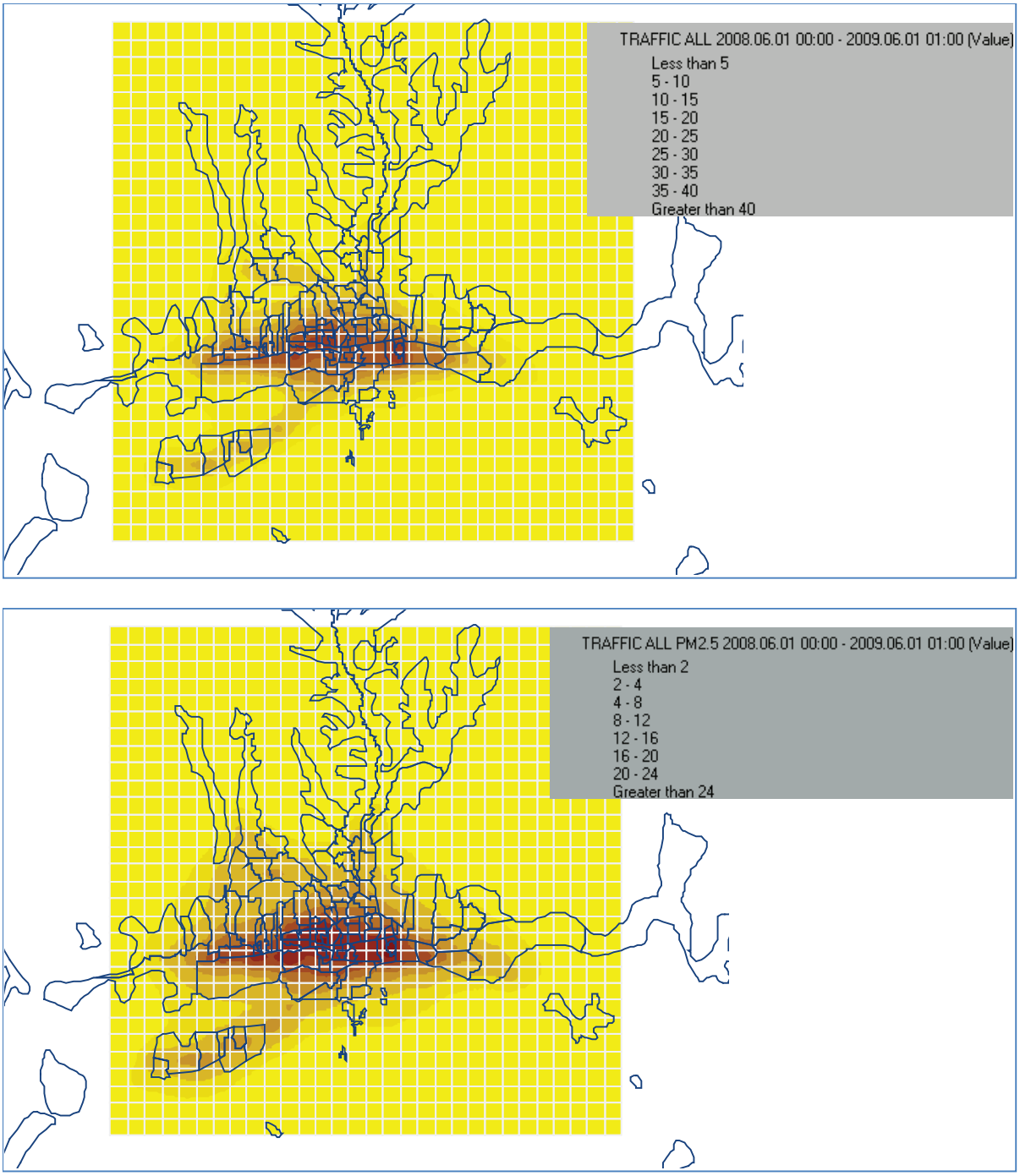

Figure C.13 Modeled PM_{10} (top) and $PM_{2.5}$ (bottom) contribution from road traffic, AMHIB baseline period, June 2008–May 2009. The figure shows iso-lines of annual average concentrations, µg/m^3.

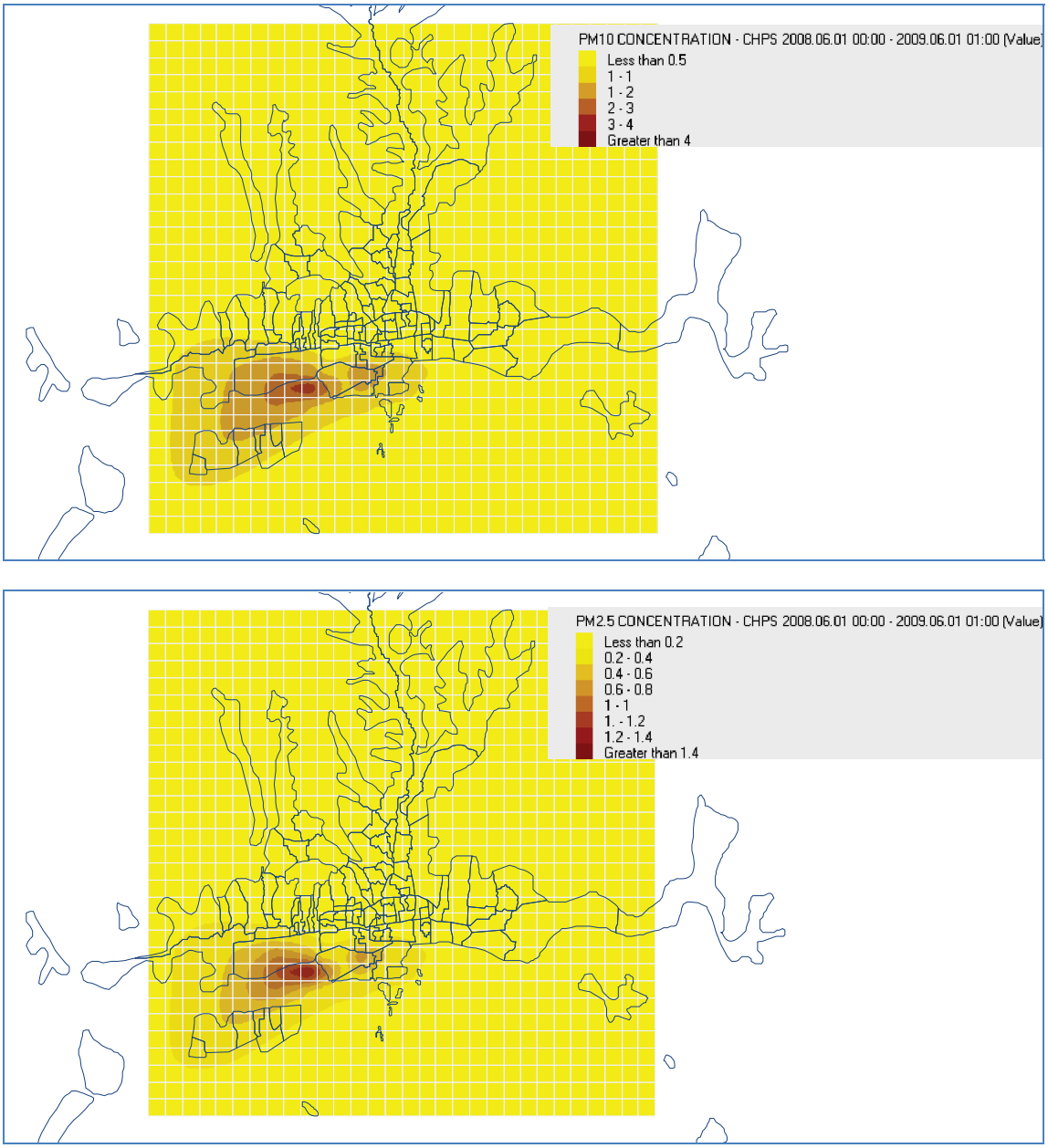

Figure C.14 Modeled PM_{10} (top) and $PM_{2.5}$ (bottom) contribution from power plants (CHPs), AMHIB baseline period, June 2008–May 2009. The figure shows iso-lines of annual average concentrations, μg/m^3.

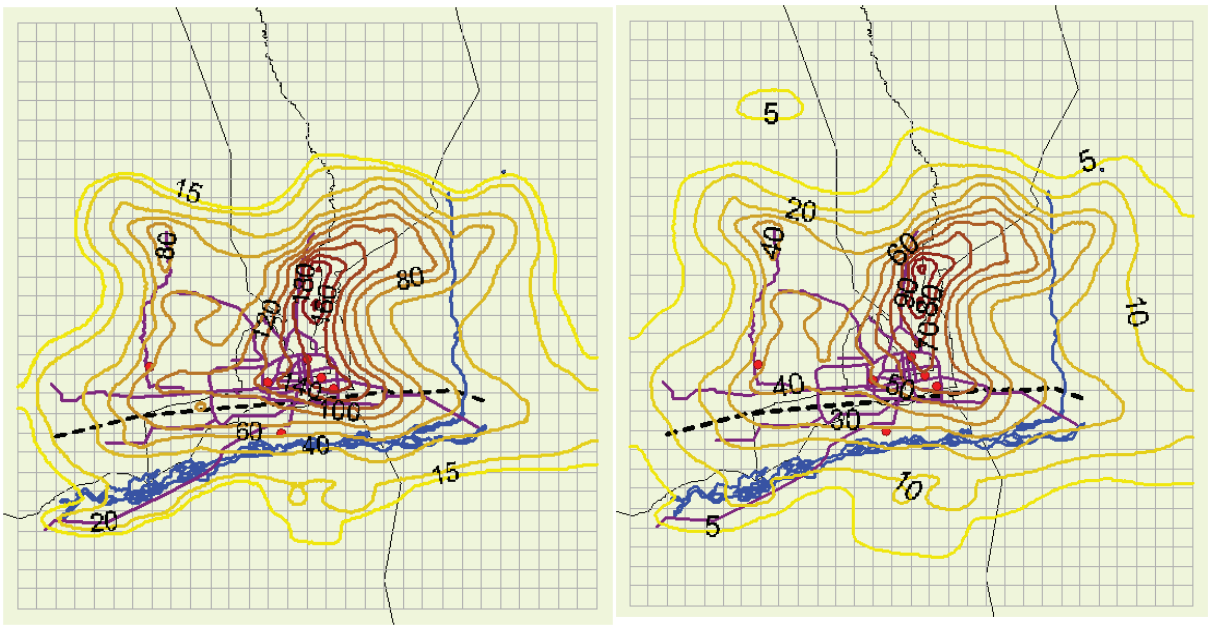

Figure C.15 Modeled PM_{10} (left) and $PM_{2.5}$ (right) concentrations in Ulaanbaatar for 2007 based upon the previously used emissions inventory and population distribution (World Bank, 2009). The figure shows iso-lines of annual average concentration, μg/m^3.

This model is evaluated by comparing the annual averaged modeled concentrations for the grids where the monitoring stations are located, with the measured annual averages. The instruments used, and the conditions they were used in during AMHIB, had problems associated with all of them, due to sampling artifacts. The problems appeared as a result of sampling comparisons of the instruments. The instrument comparisons and associated data enabled a correction of the results from the instruments as well as an assessment of the resulting uncertainty of the data coming from each of the instruments (see Annex A).

The fact that the measurements were carried out on only 38% of the days in the year is another source of uncertainty associated with the annual average estimate from the measurements. The uncertainty associated with this has been estimated to ±20% (World Bank, 2009).

Figure C.16 shows an example of measured and modeled time series for PM_{10} at station 3. Note that measurements were carried out only on 2 days per week except during one week per month when measurements were done every day. The figure shows that the model simulates the seasonal variations that are indicated by the measurements, while week-to-week there are differences between measured and modeled concentrations. At the location of this station 3, the model overestimates concentrations during October-November and underestimates during February and in May. The high concentrations in May are due to dust suspension caused by a combination of very dry and windy conditions that the model does not reflect.

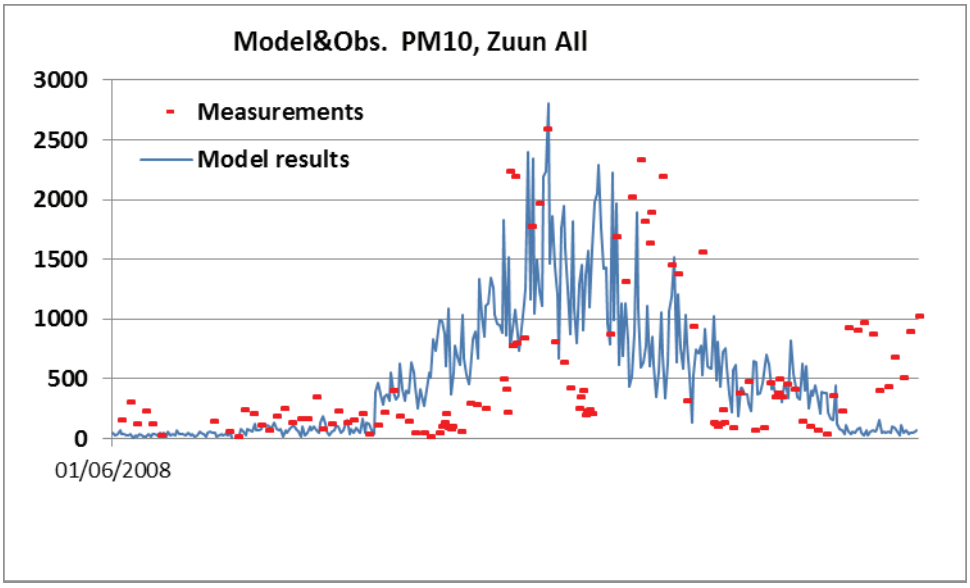

Figure C.16 Modeled and measured time series of PM_{10} at station 3 (Zuun Ail).

The discussion below shows that in terms of annual averages, the model reflects the measurements and their spatial variation.

Table C.4 shows comparison of modeled concentrations with the corrected measured concentrations in the grids where the AMHIB stations are located. The estimated uncertainty of the measured concentrations is indicated.

Table C.4 Measured and modeled PM concentrations at AMHIB stations, average for June 2008–May 2009 (μg/m^3)

Monitoring station	Station name	Modeled concentration	Measured concentration
PM_{10}			
Station 2	NRC	557	253 [1]
Station 3	Zuun Ail	499	558 [1]
Station 6	III Khoroolol	1022	> 710 [3]
$PM_{2.5}$			
Station 2	NRC	254	78 [3]
Station 3	Zuun Ail	259	236 [3]
Station 4	6 Buudal	215	225 [2]
Station 7	Bayan Hoshoo	366	338 [2]
Station 8	Airport	172	190 [2]

Indexes of measurement uncertainty estimates:
[1] ±10–15%
[2] ±15–20%
[3] ±40–50%

The comparison shows that the model performs very well in terms of annual $PM_{2.5}$ concentrations at stations 3, 4, 7 and 8. Modeled concentration is also within the uncertainty range for PM_{10} measured at station 3. The same is true for PM_{10} at station 6, although the measured concentration is quite uncertain. Station 2, NRC, is located a couple of km east of UB central area. The model substantially overestimates the concentrations at this location, for PM_{10} and even more so for $PM_{2.5}$. The model grids surrounding station 2 are, according to the population distribution, located within the ger areas with a high emission density. The emissions might be overestimated for this area. Another explanatory factor could be that the model underestimates the more windy conditions along the river valley area where station 2 is located. More detailed wind measurements are needed to look further into this aspect.

C4.2 Modeled and measured source contributions

Comparison between measured and modeled source apportionment (SA) provides further insight. Figure C.17 illustrates this example for $PM_{2.5}$ at station 2 (NRC), where source contributions were measured. The methods behind measured and modeled source contributions are different. The measured SA is based upon chemical and statistical analysis of PM sampled on the filters at the stations (see Annex B), while modeled source contributions are the result of the dispersion model (DM) runs with the emissions of each of the sources separately. Obviously there are uncertainties associated with both methods.

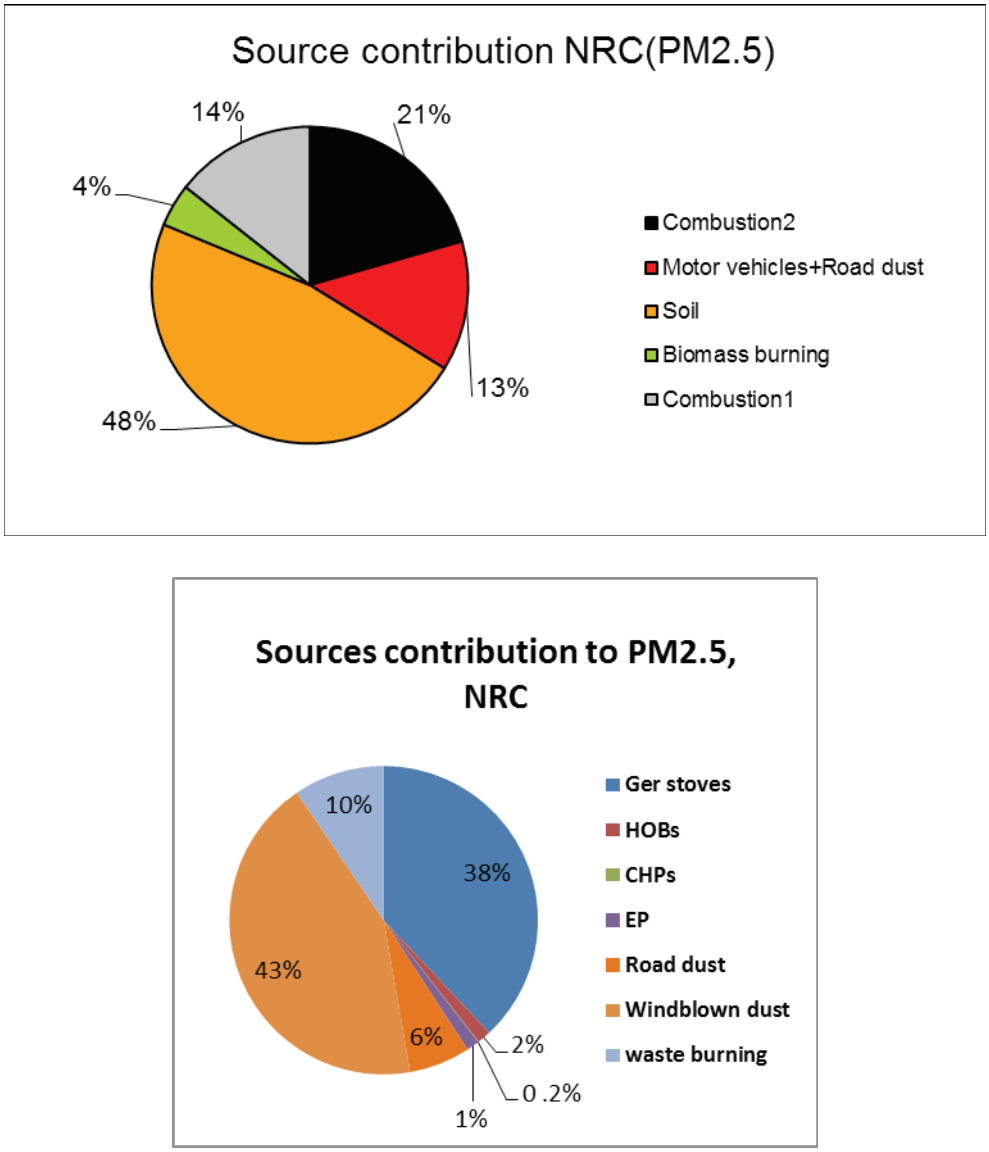

Figure C.17 Source apportionment. Comparison of measured (top) and modeled (bottom) source contributions. Example: $PM_{2.5}$ at station 2 (NRC).

Table C.5 compares the measured and modeled SA for all available cases. The 'sources' in the measured SA are: combustion, soil, biomass burning, and motor vehicle exhaust and road dust (MV+RD) as one source. In Table C.5 biomass is included in the combustion row.

The sources in the dispersion model (DM) results are: ger stoves (coal and wood), HOBs, CHPs, windblown (soil) dust, road dust, exhaust particles (EP) and waste burning. The combustion row for DM includes the ger stoves, HOBs and CHPs. The 'combustion' row is also split between coal and biomass/wood.

The 'soil' row represents suspension of dry dust from open surfaces. So road dust is included together with exhaust particles (MV+RD) in the SA analysis, MV+RD, road dust and EP are compared separately at the bottom of Table C.5.

Table C.5 Comparison of measured (SA) and modeled (DM) source apportionment, UB June 2008–May 2009

	NRC (station 2)				**Zuun Ail (station 3)**				**III Khoroolol (station 6)**	
Source	**$PM_{2.5}$**		**PM_{10}**		**$PM_{2.5}$**		**PM_{10}**		**PM_{10}**	
	SA	**DM**	**SA**	**DM**	**SA**	**DM**	**SA**	**DM**	**SA**	**DM**
Combustion	39	40	21	44	94	51	48	56	61	45
Coal	35	23	19	25	92	28	47	31	45	25
Wood	4	17	2	19	2	23	1	25	16	20
Soil	47	43	62	29	3	33	48	22	12	37
Sum	**86**	**83**	**83**	**73**	**98**	**84**	**96**	**78**	**73**	**83**
Waste		10		11		12		13		11
MV+RD	13		17		3		4		26	
Road dust		6		14		3		8		6
EP		1		2		1		1		1

Combustion (coal and wood) and soil suspension are the two dominating sources both in the measured (SA) and modeled (DM) source apportionment. The sum of the contributions from these two sources is on the average, for $PM_{2.5}$ 85% for the SA method and 78% for the DM method, and for PM_{10} it is 92% for SA and 84% for DM, i.e. a bit larger for PM_{10} than for $PM_{2.5}$, and larger for the SA method than for DM.

The DM model gives sometimes higher, sometimes lower combustion contribution than the SA model, and correspondingly vice versa for soil contribution. In particular, the measured (SA) combustion contribution to $PM_{2.5}$ at Zuun Ail (station 3) is very large and the soil contribution very low compared to the modelled (DM) contributions. 'Waste' represents burning of waste in the ger areas. It does not appear as a separate source in the measured SA, and it cannot be said in which source(s) it is included in the measured SA. Adding the waste contribution to combustion-plus-soil in the SA method, SA and DM give very similar sums of contributions.

For each of the combustion and soil sources, the SA and DM assessed contributions agree reasonable well, within 15% absolute on the average across 3 stations, when the differences between source definitions in the two methods are accounted for.

The split between coal and biomass/wood tends much more towards coal in the measured SA, while in the modelled DM the split is about 50/50 as a result of the similar split between the coal/wood emissions used in the model. Keeping the reservations explained in emission section C2.2 above, it still seems clear that the wood contribution is considerably less than the coal contribution, and that this should be reflected in the emissions inventory.

The road traffic (MV+RD) source in the measured SA compares fairly well with the sum of the modelled EP+Road dust sources, except for PM_{10} at III Khoroolol (station 6). However, at this location the sum of soil and road dust agrees well between measured and modeled.

C4.3 Summary on model evaluation and source contributions

In summary, the evaluation of the model is somewhat hampered by the problems associated with the instruments used to measure PM. When the sampler problems have been accounted for by the correction process, the model compares very well with measurements of $PM_{2.5}$ at 4 of 5 stations, covering a modelled concentration range of

190–340 μg/m^3. It compares also well with PM_{10} measurements at 1 of 3 stations, while the model is at the very high end of the measured uncertainty range at another of the PM_{10} stations. At the remaining station (station 2, NRC), the model overestimates the measured concentration substantially. Regarding relative source contributions to concentrations at 3 locations, the model captures the main features of the measured source apportionment, reflecting the main contributions from the coal combustion and the soil suspension within 10–15% of the measured relative contributions. The overestimation of the concentration at station 2, NRC, is not easily explained. It might be due to the population distribution allocating overly large PM emissions in that area, and/or the model underestimating the windy conditions in the river valley area. The high modelled concentrations at station 6 (III Khoroolol) compared to measurements might similarly be explained by excessively large emissions also. Another reason could be the very steep concentration gradient from north to south across the grid where the station is located, as one moves from inside the ger area towards the city.

The main conclusions of the AMHIB study regarding cost effectiveness and cost benefit comparisons related to control options are based upon the calculation of population weighted average exposure (PWE) to PM concentrations (see section C5). The model's overestimation at station 2, NRC, will not affect the PWE significantly, since the population is not large in that area. The possible overestimation at station 6, which is located in one of the areas with highest concentration and population density, will lead to a certain, but limited, overestimation in PWE.

The air quality model, including its sub-modules concerning road and soil dust suspension, established and set up according to scientifically based estimations of parameters, based upon measurements concerning meteorological conditions and dispersion, and run directly with the emissions calculated from the emissions inventory, gives PM concentrations that agree well with the measured concentrations (from Annex A) at most of the monitoring stations. The air quality model's assessment of source contributions agrees also, on the average across 3 stations, reasonably well (within 15% absolute) with those measured (from Annex B), when the differences between source definitions in the two methods are accounted for. This agreement supports that the measurements and the air quality model reflect well the real air pollution situation in Ulaanbaatar, concerning concentration levels as well as source contributions. It seems also clear that the model gives overly large contributions from wood combustion, and that the split between coal and wood in the emissions inventory should be shifted towards the coal side, although specific data on coal and wood consumption in ger areas both during the AMHIB period and presently are needed.

C5 Assessment of the exposure of the population to PM pollution and its source contributions

In air pollution analysis worldwide, a lot of attention is paid to *population exposure,* i.e. what is the actual concentration level that people are exposed to. It is of importance to assess the specific contributions of each key pollution source to population exposure. This is a good indicator for comparing the importance of each source to the health effects of the population, as opposed to simply comparing emissions amount per source, or even the average ground level concentration contributed by each source. The population exposure should ideally be calculated based upon data on each person's movements within the various parts of the city day-be-day, or even hour-by-hour. Obviously, such data are not available in for Ulaanbaatar, and this detail of population exposure assessment has rarely been carried out anywhere in the world.

In this report we use a population exposure assessment typically used when the data described above is unavailable, and that can be supported by data available in Ulaanbaatar. This is *the population weighted average exposure, PWE,* which sums up the average pollution concentrations in 1 km^2 cells on a distribution map (a grid of 1 km^2 cells in the six central districts of UB) multiplied by the total number of persons in each cell and divided by the total population. Because pollution and people are unevenly distributed across UB, their exposure levels vary depending on where they live. The result of this calculation is the exposure summarized as this one number, PWE, as representing the whole population. This PWE exposure number is based on the outdoor concentration in the grid cell where each individual lives, and does not, as mentioned above, take account of the difference in exposure that occurs when people are moving outside their area when going to work and school etc. A time-activity pattern would need to be established which is unavailable. In UB this may be less important, since the highest concentrations occur during early morning and late afternoon/evening hours when people tend to be mostly around home.

Table C.6 gives the calculated PWE for PM_{10} and $PM_{2.5}$ for UB for the AMHIB period June 2008–May 2009. The contributions to the PWE from the various main sources have been calculated and are given in the table.

Table C.6 Population weighted exposure (PWE) to PM in Ulaanbaatar as calculated by the air pollution model. Contributions from main PM sources (μg/m^3).

	PM_{10}	$PM_{2.5}$
Gers stoves	195.6	156.5
HOBs	9.0	5.4
CHPs	0.3	0.1
EP	9.2	9.2
Road dust	29.9	9.0
Windblown dust	134.4	40.3
waste burning	48.9	39.1
total	427.3	259.6

The emissions from the ger heating systems (burning of coal and wood in stoves and small boilers in ger housing units and kiosks in the ger areas) give the largest contribution to the PWE, 46% for PM_{10} and 60% for $PM_{2.5}$. Windblown dust from open surfaces in the city represents the second largest source (31% for PM_{10} and 16% for $PM_{2.5}$). Power plants, although representing a large emission source, give only a small contribution because of their tall chimneys that lift the power plant plumes away from influencing the ground level most of the time, according to the model calculations. Also, the vehicle exhaust give only a small contribution, since the total PM emissions from the road traffic is relatively small, while the suspension of road dust gives a noticeable contribution to PM_{10}.

References

AirQUIS (2008) AirQUIS 2003, URL: www.airquis.com

Daisheng Zhang, Kristin Aunan, Hans Martin Seip, Steinar Larssen, Jianhui Liu and Dingsheng Zhang (2010). *The assessment of health damage caused by air pollution and its implication for policy making in Taiyuan, Shanxi, China.* Energy Policy 38 (2010), pp. 491–502

Hurley et al., (2005). The Air Pollution Model (TAPM) Version 3, Part 1: Technical Description, CSIRO Atmospheric Research Technical Paper, No. 71, 54 pp.

Leiv Håvard Slørdal, Sam-Erik Walker and Sverre Solberg, (2003). The urban air dispersion model EPISODE applied in AorQUIS2003, Technical Description, No. TR12/2003. NILU.

PREGA, (2006). *Energy efficiency study of thermal power plant #4 in Ulaanbaatar, Mongolia*. A technical study report. Draft Final Report to the Promotion of Renewable Energy, Energy Efficiency and Green House Gas Abatement (PREGA) program. Report to the Asian Development Bank.

Sehmel, G.A., (1980). *Particle resuspension: A review*, Environmental International, Vol. 4, pp 107–127

World Bank (2008): *Small boiler improvement in Ulaanbaatar*. Part of the UB Clean Air Program mission related to the Clean Air Action Plan for Ulaanbaatar, Mongolia. World Bank Consultant Mission Report.

World Bank (2009). Air Pollution in Ulaanbaatar. Initial Assessment of Current Situation and Effects of Abatement Measures. Sustainable Development Series, Discussion Paper, East Asia and Pacific Region. December 2009.

Appendix 1

Emission factors for the power plants (CHPs)

The emission factor for PM10 for coal burning power plants used in the Discussion Paper (World Bank 2010) was 19.5 kg/ton (Reference: Guttikunda, 2007), for uncleaned emissions.

The US EPA AP-42 publication uses the equation for uncleaned emissions: EF=2.3*A lb/ton, where A is ash contents of the coal. For an ash content of 15%, about what it is in Nalaikh and Baganuur coal, this comes to 16 kg/ton, uncontrolled.

The JICA results from their testing of the emissions in the stacks of the CHPs no. 2 and 4, where:

- No. 2: 14.4 kg/ton
- No. 4: 0.55 kg/ton.

Comparing the AP-42 uncleaned EFs with the JICA measurements of cleaned emissions, the JICA results corresponds to a cleaning efficiency of the cleaning equipment of about 26% for CHP no. 2 (water scrubber) and 95% for CHP no. 4 (Electrostatic precipitator).

The AP-42 EF may not be quite representative for the uncleaned emissions of the UB CHPs. Still, the comparison indicates that the JICA measurement was carried out with the cleaning equipment performing poorly on CHP no. 4 and rather good on CHP no. 4. JICA assumed that the EF of CHP no. 3 was similar to that of CHP no. 2.

JICA's estimate of the CHP emissions during their measurements where:

- CHP no. 2: Coal consumption: 183,437 tons; PM10 emissions: 2,641.5 tons
- CHP no. 3: Coal consumption: 1,007,508 tons; PM10 emissions: 14,508.1 tons
- CHP no. 4: Coal consumption: 2,616,962 tons; PM10 emissions: 1,439.3 tons

The JICA calculations of total annual emissions from the 3 CHPs resulted in a total of 18,589 tons.

The rather limited amount of data on the emissions from the UB CHPs means that the CHP emissions are fairly uncertain. Since the cleaning equipment was operating poorly during the JICA measurements, it can be said that the emissions calculated by JICA, and which were used in the present report, should represent a rather high estimate of the CHP annual emissions. Still, the emissions could even be higher in periods when the cleaning equipment might not be in operation at all.

Ulaanbaatar, Mongolia, Air Monitoring and Health Impact Baseline (AMHIB) Report

Annex D

Analysis on Estimating the Effects of Air Pollution on Mortality and Hospitalization in Ulaanbaatar[1]

D1 Introduction

This chapter presents the results of the analysis of the association between air pollution and both premature death (mortality) and hospitalization (morbidity) in Ulaanbaatar (UB). Similar epidemiological studies, conducted over the last decade on five different continents, have demonstrated associations between short-term (i.e., daily) changes in air pollution and premature death (U.S. EPA 2009). Many other adverse health outcomes from daily, multi-day, or long-term (one year to several years) changes in ambient air pollutants, including particulate matter (PM), have been reported (Brook et al., 2010).

PM is a mixture of liquid and solid particles of different chemical constituents and sizes. PM is typically designated as either PM_{10} or $PM_{2.5}$ (particles less than 10 or 2.5 microns in diameter, respectively) or as the difference between PM_{10} and $PM_{2.5}$ (known as "coarse particles" or CP). $PM_{2.5}$ (known as "fine particles") is generated from many sources, including fuel combustion by mobile sources (cars, trucks and buses), stationary sources (power plants and industrial boilers), and residential sources (home heating and cooking). CP can also be generated by mechanical grinding during industrial processing, by construction debris, and by natural sources such as sea salt and blowing dust. Fine particles are often thought to be more toxic on a weight-adjusted basis than coarse particles, since they are more likely to penetrate deeply into the lung. However, the evidence is somewhat mixed and may depend on the concentrations and the patterns of exposure and population characteristics (Malig and Ostro, 2009). The various particulate matter metrics—including PM_{10}, $PM_{2.5}$, black smoke, and sulfates—appear to show fairly consistent associations with both premature mortality and morbidity. The latter includes outcomes such as hospital admissions, emergency room visits, heart attacks, asthma exacerbation, respiratory symptoms, work and school loss, and reduction in lung function (U.S. EPA, 2009).

Similarly, associations in epidemiologic studies have been observed between NO_2 and both mortality and morbidity (U.S. EPA, 2008). The primary sources for NO_2 are fuel combustion by mobile sources, and combustion of fossil fuels by power plants, factories, and residences. The epidemiologic studies indicating effects of PM and NO_2 are also supported by findings from toxicological and clinical studies (U.S. EPA 2008, 2009).

Because of data limitations, most studies to date have examined the effects of relatively short-term (i.e., single- or multi-day) exposure. Specifically, time-series or case crossover studies examine the correlation of daily changes in air pollution, typically over several years, with daily changes in mortality. These studies control for other potential confounding factors (i.e., other variables that might explain daily mortality) that vary over time and may be associated with mortality, so that an independent effect of pollution can be quantified. With increasing statistical sophistication, these studies have shown that either one-day or multi-day PM average concentrations are associated with both total mortality and cardiopulmonary mortality. Among the first of the multi-city studies

[1]The report is drafted by the following World Bank consultants under the AMHIB project: Bart Ostro and Stephen Rauch with support from Enkhjargal Altangerel, Suvd Batbaatar and Burma Badrakh, who provided data sets, suggestions and insights into the current situation in Ulaanbaatar. As part of the AMHIB project, Enkhjargal, Suvd and Burma had first drafted a report "*Health Impact Assessment*" in 2009 that this report builds upon. Peer reviewers were Carlos Marcelo Bortman, the World Bank and Jordi Sunyer Deu, the Centre for Research in Environmental Epidemiology, Barcelona. World Bank Task Team Leaders are Jostein Nygard and Gailius Draugelis.

on mortality, Schwartz et al. (1996) examined data from the Harvard Six Cities study. This database included monitors sited specifically to support ongoing epidemiological studies and to be representative of local population exposures. Consistent associations were reported between daily mortality and daily exposures to both PM_{10} and $PM_{2.5}$, with a 0.8% (95% confidence interval (CI) = 0.5, 1.1) increase in daily total mortality per every 10 $\mu g/m^3$ change in PM_{10}.

Since this effort, several other multi-city studies have been published for both PM_{10} and $PM_{2.5}$. For example, in a study of 10 USA cities, Schwartz (2000) examined the daily effects of PM_{10} and reported that a 10 $\mu g/m^3$ change in PM_{10} (measured as a two-day average of lag 0 and lag 1) was associated with a 0.7% increase in all-cause, daily mortality. In another multi-city study, Burnett et al. (2000) analyzed total mortality data for 1986–1996 from the eight largest Canadian cities and found that both PM_{10} and $PM_{2.5}$ were associated with daily mortality. For PM_{10}, a 10 $\mu g/m^3$ increase was associated with a 0.7% (CI = 0.2, 1.2) increase in daily mortality. Another study involving 29 European cities reported an association between daily mortality and PM_{10}, with an overall effect estimated at 0.6% per 10 $\mu g/m^3$ (Katsouyanni et al., 2001). Dominici et al., (2002) analyzed the 88 largest cities in the USA (NMMAPS) and found an association of about 0.27% per 10 $\mu g/m^3$ of PM_{10}. Meta-analyses of earlier mortality studies suggest that, after converting the alternative measures of particulate matter used in the original studies to an equivalent PM_{10} concentration, the effects on mortality are fairly consistent. A recent meta-analysis of European studies suggested a mean increase of the risk of 0.6% per 10 $\mu g/m^3$ PM_{10} (WHO, 2004). In addition, a meta-analysis of Asian studies indicated a mean increase of the risk of 0.4% to 0.5% per 10 $\mu g/m^3$ PM_{10} (Wong et al. 2008).

More recently, data on $PM_{2.5}$ have become available to support analyses of effects on health. For example, Ostro et al. (2006) analyzed nine large counties in California and reported an effect of 0.6% increase in mortality (CI = 0.2, 1.0) per 10 $\mu g/m^3$ $PM_{2.5}$. Fine particles were also associated with cardiovascular and respiratory mortality, as well with all-cause deaths for those above age 65. In a study of 25 U.S. cities, Franklin et al. (2007) found an effect of 1.2% (CI = 0.3, 2.1) for a similar change in $PM_{2.5}$. Finally, in a study of 112 (for $PM_{2.5}$) and 47 (for PM_{10}) U.S. cities, Zanobetti et al. (2009) reported effects of 1% (CI = 0.8, 1.2) and 0.5% (CI = 0.2, 0.7) for 10 $\mu g/m^3$ changes in fine and coarse particles, respectively.

It is important to note that much larger effects have been detected from the few studies that have examined long-term exposures to PM on cohort survival. In this type of study, a sample of individuals are selected and followed over time. For example, Dockery et al. (1993) followed approximately 8,000 individuals in six cities in the eastern USA over a 15-year period (the Harvard Six Cities study); and Pope et al. (1995) followed mortality rates over a 7-year period in approximately 550,000 individuals in 151 cities in the USA. These studies used individual-level data so that other factors that affect mortality could be characterized and adjusted for in the analysis. Once the effects of individual-level factors were determined, the models examined whether longer-term citywide averages in PM (measured as PM_{10}, $PM_{2.5}$ or sulfates) were associated with different risks of mortality and life expectancies. The estimated mortality effects of long-term exposure to fine particles (approximately 7 to 13% per 10 $\mu g/m^3$ of $PM_{2.5}$) are much larger than those associated with daily exposure. Importantly, these study results imply large differences in life expectancy. Specifically, 24 $\mu g/m^3$ difference in $PM_{2.5}$ between the cleanest and dirtiest cities is associated with an almost 1.5-year difference in life expectancy for the city populations (Pope, 2000). The difference for people who actually died from diseases associated with air pollution was estimated to be about 10 years. This is because air pollution-related deaths make up only a small fraction of the total deaths in a city. Since these earlier studies were published, several additional and supportive studies, involving other cohorts, have been completed (Eftim et al., 2008; Puett et al., 2008; Miller et al., 2007; Ostro et al., 2010). A comprehensive review of the existing studies and a discussion of the underlying biological mechanisms that underlie these effects are provided by Brook et al. (2010).

In the following sections, the results of an analysis of daily changes in PM_{10}, $PM_{2.5}$, CP and NO_2 for one year of data in UB are presented. This includes the effects of exposure to these pollutants on both disease-specific mortality and hospital admissions.

Table of Contents

D2 Data and Methods

Exposure data

All pollution data was obtained from the Air Monitoring and Health Impacts Baseline (AMHIB) study, sponsored by the World Bank and based on recommendations from several Mongolian representatives. Data cover the period from June 2008 to May 2009. The PM_{10} and $PM_{2.5}$ data come from a network of 8 monitoring stations (see Figure D.1 and Table D.1).

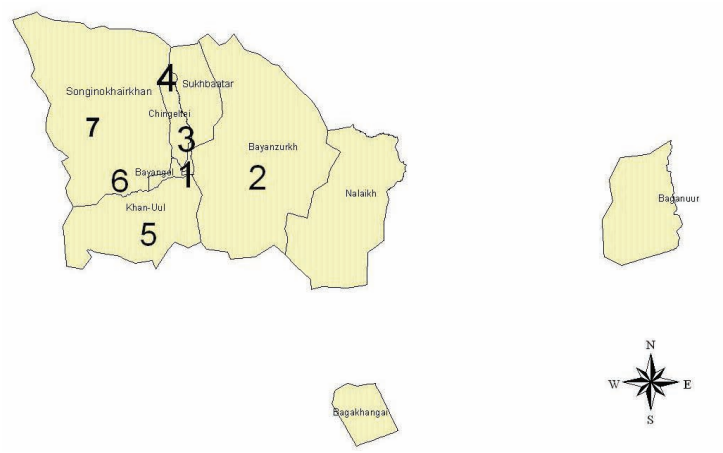

Figure D.1 Administrative zones and AMHIB stations, Ulaanbaatar, Mongolia.

Table D.1 PM monitor stations and associated hospital districts

Station #	Station Name	Sampler Method	PM Size Fraction	Monitor Operating Period
1	NAMHEM	Kosa Monitor	PM10, PM2.5	6/08 – 5/29
2	NRC	GENT Sampler	PM10, PM2.5	6/08 – 5/29
3	100 ail	GENT Sampler	PM10, PM2.5	6/08 – 5/29
4	buudal	Dust-Trak 8520	PM2.5	6/08, 9/08-5/
5	CLEM	Rotary Bebicon	PM10	6/08 – 5/29
6	3r_khoroolol	Partisol FRM-Model 2000	PM10	6/08 – 5/29
7	SKHD_7 (Bayanhoshuu)	Dust-Trak 8520	PM2.5	6/08 – 5/29
8	NISEH_8 (Airport)	Dust-Trak 8520	PM2.5	6/08, 9/08-5/09

Pollution data included 24-hour averages of PM_{10}, $PM_{2.5}$, CP and NO_2. CP was calculated by subtracting $PM_{2.5}$ from PM_{10}. Data were sampled twice a week, on Wednesday and Sunday. In addition, there were 6 weeks during which data was taken every day: 10/26/2008–11/1/2008, 11/24/2008–11/30/2008, 12/28/2008–1/3/2009, 1/25/2009–1/31/2009, 2/28/2009–3/4/2009, and 3/25/2009–3/30/2009. Unfortunately, very different sampling methods were used for $PM_{2.5}$ and PM_{10} and comparisons among instruments show large discrepancies (World Bank, Appendix C, 2009). In addition, humidity has a differential impact on the measurements of each of the monitors. These differential measurement errors may reduce the likelihood of observing a health effect, given that one exists or may result in a reduced estimate of risk. Unfortunately, the actual effect on the confidence interval cannot be determined. Data for NO_2 were provided as an average of 4 monitors in UB that measure this pollutant.

Weather/meteorology data

Daily temperature data are determined from an average of several monitors in UB and include information on average temperature (in °C), relative humidity (%) and wind speed (in meters/sec).

Mortality and hospitalization data

UB is divided into nine administrative districts, but only the westernmost districts (1 through 6) have nearby PM-monitoring stations (see Figure D.1 and Table D.2). These six districts had a total population of approximately 930,000 in 2008. The other 3 districts are very small (total population under 60,000) and spatially distinct from the rest of the urban area of UB. Health data are identified by the administrative district of residence. Therefore, to minimize exposure misclassification, the analysis was restricted to the more populated and contiguous six districts. For morality, both "natural" and cardiovascular deaths were examined where natural mortality is defined as total mortality minus deaths due to injuries, accidents, violence, and suicides (and labeled, in this analysis, as all-cause mortality).

Table D.2 Administrative district with associated PM monitor and population

District*	Name	$PM_{2.5}$ Monitor Used	PM_{10} Monitor Used	2008 Pop
1	Bayangol	1	6	160,818
2	Bayanzurkh	2	2	211,614
3	Songino Khairkhan	7	6	211,056
4	Sukhbaatar	3	3	123,041
5	Khan Uul	1	5	90,925
6	Chingeltei	4	3	132,883

*Districts 7, 8 and 9 did not have a nearby PM monitor and were excluded from the analysis.
Source of population data: World Bank (2009) Air Pollution in Ulaanbaatar: Initial Assessment of Current Situation and Effects of Abatement Measures.

For hospitalization, both cardiovascular and respiratory admissions were examined. The coding of cause of death and hospitalization was based on the tenth version of the International Classification of Diseases, (ICD-10), codes S through Z. In addition, for both mortality and morbidity, cases due to either cardiovascular or respiratory disease were examined. Cardiovascular deaths and hospitalizations were assigned ICD codes starting with "I", while respiratory cases' ICD codes began with "J".

Assigning exposure

In order to estimate the exposure of the population to ambient concentrations of studied pollutants, the population distribution needs to be superimposed on the distribution of these ambient concentrations. The level of accuracy depends on resources and data availability. Two methods of assigning exposure for PM_{10}, $PM_{2.5}$ and CP were tested. First, the administrative district of residence (and presumed location of the deaths and hospitalizations) was matched with the closest PM monitor (see Figure D.1). This was undertaken in order to minimize the misclassification of pollution exposure given the distinct spatial orientation of the city and surrounding ger areas. Table D.2 displays the matching between event location and monitor. Of the eight monitors that were initially available for the analysis, only monitors #8 (NISEH) and #5 (CLEM) were not used. The former was not used since it is located at the airport, a significant distance away from the center city, and the latter was not used since it only measured PM_{10} and these measurements had unexplainable variations—i.e. they were much lower than those of all of the other monitors, and even lower than the $PM_{2.5}$ measurements for that district (from a different monitor). Note that the monitor corresponding to Administration District 1 (AMHIB station 6, 3-r khoroolol) only measures PM_{10}. However, AMHIB station #1 also matches up with Administrative District 1, so District 1 residents were assigned $PM_{2.5}$ data from that monitor. Likewise station #6 only measures PM_{10} for district 3, so $PM_{2.5}$ data were taken from nearby station # 7. Similar substitutions were made in other districts using nearby monitors.

The study team noted that four of the $PM_{2.5}$ monitors (# 1, 4, 7, and 8) had readings that were highly correlated ($r > 0.6$, see Table D.3). Therefore, as an alternative measure of exposure, an average PM measure from those four monitors was calculated. In cases of missing observations at a monitor, the average was taken of the remaining monitors in the set (in the analysis, controls were only included if their average $PM_{2.5}$ value was taken from the same monitors as the case). Subsequent analysis indicated very difference between the different exposure assessments so only results using the first method are presented below.

Table D.3 Pairwise correlations among $PM_{2.5}$ monitors and NO_2

	NAMHEM (1)	NRC (2)	ail100 (3)	buudal (4)	SKHD (7)	Niseh (8)	NO_2
NAMHEM (1)	-	0.15	0.34	0.64	0.66	0.84	0.38
NRC (2)	0.15	-	0.13	0.03	-0.04	0.12	0.07
ail100 (3)	0.34	0.13	-	0.33	0.42	0.30	0.26
Buudal (4)	0.64	0.03	0.33	-	0.64	0.70	0.49
SKHD (7)	0.66	-0.04	0.42	0.64	-	0.77	0.51
Niseh (8)	0.84	0.12	0.30	0.70	0.77	-	0.54
NO_2	0.38	0.07	0.26	0.49	0.51	0.54	-

None of the PM_{10} monitors were highly-correlated (largest r = 0.34) (see Table D.4), so an average PM_{10} measure was not created. The lack of correlation among PM_{10} monitors is expected, given the amount of coarse particles in UB. These particles tend to be generated and experienced at the more local level.

Table D.4 Pairwise correlations among PM_{10} monitors and NO_2

Variable	NAMHEM (1)	NRC (2)	ail_100 (3)	UB_1 (5)	r_khoroolol (6)	NO_2
NAMHEM (1)	-	0.04	0.32	0.17	0.30	0.37
NRC (2)	0.04	-	0.02	0.08	0.06	-0.17
ail_100 (3)	0.32	0.02	-	0.10	0.34	0.21
UB_1 (5)	0.17	0.08	0.10	-	0.14	0.08
r_khoroolol (6)	0.30	0.06	0.34	0.14	-	0.30
NO_2	0.37	-0.17	0.21	0.08	0.30	-

Method

As in previous studies (Malig and Ostro, 2008), a time-stratified case-crossover study design was used. In this method, temperature on the date of the case is compared to several control days (referent periods) occurring within the same month and year. Each individual in the study design serves as his or her own control, thus matching on a wide range of individual-level characteristics. For the analysis, a case-crossover dataset was created, with controls taken from the same month as the case date (i.e. the patient's record) and from the same monitor. In order to preserve independence of controls from cases, only controls at least 3 days apart from the case date were included in the dataset. To prevent overlap between different control days, only controls using Sunday or Wednesday measurements were included in the analysis. When average $PM_{2.5}$ was used, controls were only included if their average $PM_{2.5}$ value was taken from the same monitors as the case.

Regression analysis was used to estimate the impact pollution exposure has on health (morbidity and mortality) and the accuracy (predictive value) of the model's estimate. Each of the study's regression models included the pollution exposure, two terms for temperature, one for relative humidity, and 6 indicator variables for day of week. The temperature data were designed to control for non-linear relationships with mortality and morbidity. Therefore, a cold temperature variable was developed which was assigned to equal the actual temperature value when it was less than 65°F (18.33°C) (and 65°F otherwise) and a warm apparent temperature variable assigned when temperature was equal to or greater than 65°F (and zero otherwise). A dataset was generated to measure same-day PM exposure (lag 0) as well as up to 3 days previous (lag1, lag2 and lag3). The case-crossover analysis was carried out using matched logistic regression (PROC PHREG in SAS version 9.1). The resulting estimated beta coefficient is provided and the odds ratio (OR) is calculated relative to the inter-quartile range (i.e., IQR or the difference between the 75th percentile and 25th percentile of the distribution).

Given the large seasonal differences in concentrations and sources of PM, as a sensitivity analysis for mortality was conducted after stratifying the year by cool and warm season. The latter was defined as May through September.

D3 Results

Tables D.5 and D.6 summarize the descriptive statistics of data used in the mortality and morbidity analyses. These are based on measurements for both cases and controls included in the analysis, except for age statistics, which include only cases. For example, for the mortality analysis, based on all of the districts, the average temperature was –2°C, and the mean pollution concentrations of NO_2, PM_{10}, $PM_{2.5}$ and CP (in $\mu g/m^3$) were 29, 486, 301 and 206, respectively. Median PM_{10}, $PM_{2.5}$ and CP are much lower at 227, 95, and 112 $\mu g/m^3$, respectively, due to skewed distribution and the very high concentrations that occur in the winter. As expected, PM concentrations vary widely among districts. For example, median $PM_{2.5}$ ranges from 42 $\mu g/m^3$ in District 6 to 256 $\mu g/m^3$ in District 3. In addition, the use of two different monitors to represent $PM_{2.5}$ versus PM_{10} in a given district led to some implausible results such as $PM_{2.5}$ being greater than PM_{10} in one district. We subsequently tested the regression results with and without this monitor and there were no significant quantitative differences. As a result, the results are presented using the monitors as shown in Table D.2.

Table D.7 summarizes the mortality and hospital data. The mean age at death was 56.3, with 1,425 cases of all-cause mortality, 568 cardiovascular (40% of the total), and 53 respiratory (4% of the total). Males made up about 57% of all mortality. Due to the small amount of respiratory-specific mortality, it was dropped from subsequent analysis. Regarding hospitalizations, there were 6,291 cardiovascular-specific and 21,991 respiratory-specific admissions. Males made up 44.7% of the cardiovascular plus respiratory hospital admissions.

Table D.5 Descriptive statistics of data used in mortality analysis

District (number of cases)	Statistic	Temperature (°C)	NO_2 ($\mu g/m^3$)	PM_{10} ($\mu g/m^3$)	$PM_{2.5}$ ($\mu g/m^3$)	CP ($\mu g/m^3$)
All	Median	-2	28	227	95	112
	Mean	-2	29	486	301	206
(n = 1,425)	IQR	26	14	301	119	266
All, warm season	Median	15	25	125	26	104
	Mean	15	27	200	65	152
(n = 462)	IQR	10	16	144	30	143
All, cool season	Median	-10	29	276	141	122
	Mean	-10	30	609	388	225
(n = 963)	IQR	16	14	136	161	150
1	Median	-2	28	220	38	159
	Mean	-1	29	401	68	343
(n = 200)	IQR	22	12	263	84	236
2	Median	-2	28	184	63	105
	Mean	-1	29	264	136	153
(n = 346)	IQR	26	12	196	97	130
3	Median	-5	28	229	244	0
	Mean	-3	28	432	713	-217
(n = 304)	IQR	24	12	410	1099	589
4	Median	-2	28	275	144	171
	Mean	-3	29	785	409	386
(n = 178)	IQR	24	12	735	375	297
5	Median	-2	28	214	39	155
	Mean	-1	29	401	69	343
(n = 161)	IQR	24	12	271	92	231
6	Median	-5	28	275	198	74
	Mean	-3	29	778	403	402
(n = 236)	IQR	24	11	732	552	506

*IQR = interquartile range (75%tile - 25%tile of the distribution). IQR for “All” districts based on difference between case and control days.

Table D.6 Descriptive statistics of data used in hospital analysis

District (number of cases)	Statistic	Temperature (°C)	NO_2 ($\mu g/m^3$)	PM_{10} ($\mu g/m^3$)	$PM_{2.5}$ ($\mu g/m^3$)	CP ($\mu g/m^3$)
all	Median	-8	28	273	85	189
	Mean	-6	28	534	233	330
(n = 28,282)	IQR	23	14	389	101	289
1	Median	-6	28	287	42	230
	Mean	-6	27	465	74	396
(n = 11,664)	IQR	21	10	438	91	365
2	Median	-11	30	215	95	105
	Mean	-9	30	285	177	151
(n = 6,079)	IQR	20	11	231	107	152
3	Median	8	28	129	248	6
	Mean	5	28	301	754	-225
(n = 2,336)	IQR	30	14	259	1212	816
4	Median	-9	28	393	198	213
	Mean	-7	28	895	493	405
(n=6,015)	IQR	17	11	726	361	347
5	Median	-5	28	287	39	244
	Mean	-2	29	473	67	405
(n = 1,235)	IQR	28	11	431	81	340
6	Median	-12	28	671	198	344
	Mean	-7	28	1262	441	806
(n = 843)	IQR	24	12	1396	615	995

*IQR = interquartile range (75%tile - 25%tile of the distribution). IQR for "All" districts based on difference between case and control days

Table D.7 Descriptive statistics for mortality and hospitalization data used in analysis

	All-cause	Cardio	Resp	Other	Female	Male	Mean Age
Mortality	1,425	568	53	804	613	812	56.3
Hospitalization		6,291	21,991	-	15,637	12,645	41.0

Table D.8 summarizes the basic logistic regression results for 1,379 deaths (based on all-cause mortality for lag0 PM_{10}) occurring in approximately 126 days with pollution data between June 2008 and May 2009. For particulate matter using the full year of data, the only significant associations observed were between cardiovascular mortality and lag 1 CP ($p < 0.05$) and lag3 CP ($p < 0.10$). Using the IQR of exposures on the case versus control days, the odds ratio (OR) was 1.07 (95% confidence interval (CI) = 1.00 – 1.15) which amounts to a 0.25% (95% CI = 0, 0.5) change in mortality per 10 μg/m^3 of CP As displayed in Table D.9, modest associations were also observed for lag1 NO_2 with both all-cause and cardiovascular mortality. For all-cause mortality, the OR = 1.12 (95% CI = 0.99, 1.28) while for cardiovascular morality, the OR = 1.22 (95% CI = 0.97 – 1.49) for the IQR of 14 μg/m^3.

Table D.8 Regression results for mortality and particulate matter, June 2008–May 2009

Outcome	Variable	Beta	s.e	p-value	IQR*	OR	OR(low)	OR(high)	cases
All-cause	pm25_lag0	0.05	0.10	NS	119	1.01	0.98	1.03	1305
All-cause	pm25_lag1	-0.10	0.11	NS	118	0.99	0.96	1.01	1293
All-cause	pm25_lag2	0.09	0.09	NS	127	1.01	0.99	1.04	1254
All-cause	pm25_lag3	0.03	0.11	NS	135	1.00	0.98	1.03	1193
Cardio	pm25_lag0	0.07	0.17	NS	119	1.01	0.97	1.05	525
Cardio	pm25_lag1	-0.21	0.18	NS	118	0.98	0.94	1.02	520
Cardio	pm25_lag2	0.02	0.17	NS	127	1.00	0.96	1.05	511
Cardio	pm25_lag3	0.02	0.21	NS	135	1.00	0.95	1.06	469
All-cause	pm10_lag0	-0.10	0.09	NS	301	0.97	0.92	1.03	1393
All-cause	pm10_lag1	0.06	0.08	NS	321	1.02	0.97	1.07	1369
All-cause	pm10_lag2	0.06	0.08	NS	339	1.02	0.97	1.08	1332
All-cause	pm10_lag3	0.08	0.09	NS	325	1.03	0.97	1.08	1274
Cardio	pm10_lag0	0.08	0.14	NS	301	1.02	0.94	1.11	554
Cardio	pm10_lag1	0.10	0.12	NS	321	1.03	0.96	1.12	556
Cardio	pm10_lag2	0.01	0.13	NS	339	1.00	0.92	1.10	549
Cardio	pm10_lag3	0.21	0.14	NS	325	1.07	0.98	1.17	501
All-cause	CP_lag0	-0.09	0.08	NS	266	0.98	0.94	1.02	1273
All-cause	CP_lag1	0.12	0.08	NS	280	1.03	0.99	1.08	1241
All-cause	CP_lag2	0.00	0.07	NS	295	1.00	0.96	1.04	1215
All-cause	CP_lag3	0.08	0.08	NS	296	1.02	0.98	1.07	1164
Cardio	CP_lag0	0.03	0.13	NS	266	1.01	0.94	1.08	511
Cardio	CP_lag1	0.25	0.13	< 0.05	280	1.07	1.00	1.15	496
Cardio	CP_lag2	0.00	0.13	NS	295	1.00	0.93	1.07	497
Cardio	CP_lag3	0.25	0.15	< 0.10	296	1.08	0.99	1.17	458

Note: Estimated beta and standard error are × 1000 and can be interpreted as the percent change in mortality per 10 μg/m^3.
NS = not significant at $p < 0.10$. * Interquartile range in μg/m^3

Table D.9 Regression results for mortality and nitrogen dioxide, June 2008–May 2009

Outcome	Variable	Beta	s.e	p-value	IQR*	OR	OR(low)	OR(high)	cases
All-cause	NO2_lag0	1.14	4.80	NS	14	1.02	0.89	1.16	1288
All-cause	NO2_lag1	8.35	4.70	<0.10	14	1.12	0.99	1.28	1267
All-cause	NO2_lag2	-3.78	5.01	NS	15	0.94	0.82	1.09	1214
All-cause	NO2_lag3	-1.89	5.06	NS	14	0.97	0.85	1.12	1169
Cardio	NO2_lag0	12.78	7.54	< 0.10	14	1.20	0.97	1.47	520
Cardio	NO2_lag1	12.26	7.39	< 0.10	14	1.22	0.97	1.49	508
Cardio	NO2_lag2	6.68	7.69	NS	15	1.10	0.89	1.36	504
Cardio	NO2_lag3	0.92	8.06	NS	14	1.01	0.81	1.26	457

Note: Estimated beta and standard error are × 1000 and can be interpreted as the percent change in mortality per 10 μg/m^3.
NS = not significant at $p < 0.10$. *Interquartile range in μg/m^3

Table D.10 summarizes the significant effects for mortality after stratifying by the warm and cool seasons. For the warm season, associations were observed for all-cause mortality and both lag2 $PM_{2.5}$ ($p < 0.01$) and lag2 PM_{10} ($p < 0.10$). The result indicated a 1.4% increase in mortality per 10 μg/m^3 of $PM_{2.5}$. For the IQR of the difference in concentrations between cases and controls during the warm season, this result indicates an OR of 1.04 (1.01, 1.07). For the cold season, associations were observed between CP and cardiovascular mortality ($p < 0.05$ for lag1 and $p < 0.10$ for lag3). The effect was about 0.27% per 10 μg/m^3 of CP and for the IQR the OR was 1.10 (95% CI = 1.00, 1.21).

Table D.10 Regression results for mortality and particulate matter by season

Season	Outcome	Variable	Beta	s.e	p-value	IQR*	OR	OR(l)	OR(h)
Warm	All-cause	pm25_lag2	1.38	0.48	< 0.01	31	1.04	1.01	1.07
	All-cause	pm10_lag2	0.53	0.31	< 0.10	143	1.08	0.99	1.17
Cold	Cardio	CP_lag1	0.2659	0.1324	< 0.05	367	1.10	1.00	1.21
	Cardio	CP_lag3	0.2792	0.1538	< 0.10	361	1.11	0.99	1.23

Note: Estimated beta and standard error are × 1000 and can be interpreted as the percent change in mortality per 10 μg/m^3.
*Interquartile range in μg/m^3

Table D.11 presents the results for hospital admissions for both cardiovascular and respiratory disease. For $PM_{2.5}$, robust associations were observed with cardiovascular admissions and all lags ($p < 0.001$), with the strongest associations for lag3. At that lag, the OR for the IQR was 1.09 (95% CI = 1.07, 1.11) based on 5,400 cases. This amounts to a 0.82% (95% CI = 0.64, 1.0) increase in admissions per 10 μg/m^3 of $PM_{2.5}$. Associations were also observed between lag2 and lag3 $PM_{2.5}$ and respiratory admissions. For lag3, the OR for the IQR was 1.03 (95% CI = 1.02, 1.04) owing to a 0.24% change per 10 μg/m^3 of $PM_{2.5}$. For PM_{10}, strong associations were also observed between cardiovascular admissions and all lags ($p < 0.001$). Again, the strongest association was for lag3 with an OR for the IQR of 1.09 (95% CI = 1.05, 1.13). This amounts to a 0.2% increase in admissions per 10 μg/m^3 of PM_{10}. Some positive associations were also observed with respiratory admissions but the results were less robust. CP demonstrated a weak and varied association with respiratory admissions.

Table D.11 Results of logistic regressions for hospitalization and particulate matter, June 2008–May 2009

Outcome	Variable	Beta	s.e	p-value	IQR	OR	OR(low)	OR(high)	cases
Cardio	pm25_lag0	0.56	0.08	< 0.001	101	1.06	1.04	1.08	5,642
Cardio	pm25_lag1	0.41	0.07	< 0.001	104	1.04	1.03	1.06	7,213
Cardio	pm25_lag2	0.59	0.08	< 0.001	109	1.06	1.05	1.08	6,238
Cardio	pm25_lag3	0.82	0.09	< 0.001	109	1.09	1.07	1.11	5,398
Resp	pm25_lag0	-0.03	0.03	NS	101	1.00	0.99	1.00	20,848
Resp	pm25_lag1	0.02	0.03	NS	104	1.00	1.00	1.01	25,708
Resp	pm25_lag2	0.07	0.03	< 0.05	109	1.01	1.00	1.01	24,240
Resp	pm25_lag3	0.24	0.05	< 0.001	109	1.03	1.02	1.04	20,319
Cardio	pm10_lag0	0.15	0.04	< 0.001	389	1.06	1.03	1.09	6,090
Cardio	pm10_lag1	0.11	0.03	< 0.001	395	1.05	1.02	1.07	7,846
Cardio	pm10_lag2	0.17	0.04	< 0.001	421	1.07	1.04	1.10	6,790
Cardio	pm10_lag3	0.21	0.05	< 0.001	406	1.09	1.05	1.13	5,668
Resp	pm10_lag0	0.01	0.02	NS	389	1.01	0.99	1.02	21,581
Resp	pm10_lag1	-0.02	0.02	NS	395	0.99	0.98	1.01	26,813
Resp	pm10_lag2	0.04	0.02	< 0.05	421	1.02	1.00	1.03	25,049
Resp	pm10_lag3	-0.08	0.03	< 0.01	406	0.97	0.95	0.99	20,955
Cardio	CP_lag0	0.05	0.04	NS	289	1.01	0.99	1.04	5,441
Cardio	CP_lag1	0.01	0.04	NS	286	1.00	0.98	1.03	6,832
Cardio	CP_lag2	0.07	0.04	NS	294	1.02	1.00	1.05	6,051
Cardio	CP_lag3	-0.03	0.07	NS	283	0.99	0.96	1.03	5,184
Resp	CP_lag0	0.05	0.02	< 0.10	289	1.01	1.00	1.03	20,438
Resp	CP_lag1	-0.03	0.02	NS	286	0.99	0.98	1.00	25,161
Resp	CP_lag2	0.02	0.02	NS	294	1.01	0.99	1.02	23,749
Resp	CP_lag3	-0.18	0.03	< 0.001	283	0.95	0.93	0.97	19,904

Note: Estimated beta and standard error are × 1000 and can be interpreted as the percent change in hospitalization per 10 μg/m^3.
*Interquartile range in μg/m^3 NS = not significant at p < 0.10

Finally, Table D.12 summarizes the results for hospitalization and NO2. Cardiovascular admissions were strongly associated with lags of 1 and 3 days with the latter generating an OR of 1.21 (95% CI = 1.13, 1.30) for the IQR. Respiratory effects were also observed but again were quite variable. For a 3-day lag, the OR = 1.18 (95% CI = 1.13, 1.23).

Table D.12 Results of logistic regressions for hospitalization and nitrogen dioxide, June 2008–May 2009

Outcome	Variable	Beta	s.e	p-value	IQR	OR	OR(low)	OR(high)	cases
Cardio	NO2_lag0	-2.88	2.34	NS	14	0.96	0.90	1.02	5633
Cardio	NO2_lag1	**3.20**	**1.88**	**<0.001**	14	1.05	0.99	1.10	7368
Cardio	NO2_lag2	1.07	2.15	NS	15	1.02	0.95	1.08	6174
Cardio	NO2_lag3	**13.77**	**2.67**	**< 0.001**	14	1.21	1.13	1.30	5319
Resp	NO2_lag0	-1.37	1.53	NS	14	0.98	0.94	1.02	20613
Resp	NO2_lag1	-2.00	1.24	NS	14	0.97	0.94	1.01	25515
Resp	NO2_lag2	**-2.25**	**1.34**	**< 0.10**	15	0.97	0.93	1.01	23736
Resp	NO2_lag3	**12.00**	**1.56**	**< 0.001**	14	1.18	1.13	1.23	20246

Note: Estimated beta and standard error are × 1000 and can be interpreted as the percent change in hospitalization per 10 μg/m^3.
*Interquartile range in μg/m^3
NS = not significant at p < 0.10

D4 Summary and discussion

UB's population is exposed to high concentrations of PM from different sources, each with different chemical constituents and size fractions. Thus, the findings from the limited available data support the conclusion that there are significant public health implications related to air pollution in UB. Since most studies similar to this one involve several years of data, however, it would be important to repeat this study once more data are available. Nevertheless, several important associations were observed between daily changes in PM and NO_2 and mortality and morbidity. This is particularly noteworthy given the sparsity of data, i.e. only one year of data generally collected on an every 3rd or 6th day basis. The data sparsity also could lead to inaccurate or unstable results.

For mortality, the strongest associations using the full year of data were observed for coarse particles. Specifically, a 1-day lag in CP was associated with cardiovascular mortality. Exposure to CP was associated with an increase of approximately 0.3% per 10 μg/m^3. However, given the very high exposures to these pollutants in UB, effects associated with a range equal to the IQR generate a daily increase in mortality of about 7%. In addition, a strong effect was observed between $PM_{2.5}$ and mortality during the warm season. For hospital admissions, the strongest associations were observed for $PM_{2.5}$ and PM_{10} with cardiovascular disease.

While no associations were observed for PM_{10} or $PM_{2.5}$ using the full year, the analysis of the warm season revealed associations for these pollutants with all-cause mortality. Regarding PM_{10}, a 10 μg/m^3 change was associated with a 0.5% (95% CI = –0.08, 1.14) change in mortality. The magnitude of effects per μg/m^3 of PM_{10} observed in UB is similar to those observed in studies in the Western industrialized nations. For example, in a study of PM_{10} in ten cities in the United States, Schwartz (2000) reported that a 10 μg/m^3 change in PM_{10} (measured as a two-day average of lag 0 and lag 1) was associated with a 0.7% increase in daily mortality. In another multi-city study, Burnett et al. (2000) analyzed mortality data for 1986–1996 from the eight largest Canadian cities and found that PM_{10} was associated with a 0.7% (95% CI = 0.2, 1.2) increase in daily mortality. Another study involving 29 European cities reported an association between daily mortality and PM_{10} of 0.6% per 10 μg/m^3 (Katsouyanni et al., 2001). Likewise, in a study of 88 largest cities in the U.S., Dominici et al., (2002) found an association of about 0.27% per 10 μg/m^3 of PM_{10}. Studies where PM_{10} has a large share of coarse particles tend to show effects at the lower end of the range. For example, studies in three Chinese cities that were part of the PAPA project reported a combined effect estimate of 0.37% per 10 μg/m^3 of PM_{10} (versus 0.3% in UB). The estimates ranged from 0.5%, 0.3% and 0.4% for Hong Kong, Shanghai and Wuhan, respectively.

For $PM_{2.5}$, no associations were observed in the full year analysis of data. However, in the analysis of the warm season, there was a relationship between a two-day lag in $PM_{2.5}$ and all-cause mortality. Specifically, a 10 μg/m^3 change in $PM_{2.5}$ was associated with a 1.38% change in mortality. This estimate is similar to those reported from studies of $PM_{2.5}$ in the U.S. Specifically, in an analysis of 27 U.S. cities, Franklin et al. (2007) found an effect of 1.2%, Burnett et al. (2003) reported a 1.1% increase in mortality in eight Canadian cities and a recent study of 112 U.S. cities (Zanobetti et al., 2009) reported an effect of 1.0% per 10 μg/m^3. In the analysis of nine California counties, Ostro et al. (2006) reported a significant association with a risk of 0.6% per 10 μg/m^3 of $PM_{2.5}$. Coupled with the high concentrations of $PM_{2.5}$ observed in the warm season, the estimated odds ratios were elevated, indicating a 4% increase in mortality for exposures equal to the IQR of 30 μg/m^3.

There are several possible explanations for the lack of an effect of $PM_{2.5}$ in the full year analysis. The most obvious might be the differential pattern of sources and exposures through the season. It is possible that during the winter exposure to $PM_{2.5}$ is easier to avert for the majority of the population living in houses and apartments in the central city. About half of the population of UB lives in apartments located in the central areas of the city. About 80% of these apartments are supplied with central heating and hot water from three power plants located to the west. The remainder of the apartments is supplied by local boilers. During the warmer months, residents will spend more time outdoors and incur greater exposures. In addition, unlike $PM_{2.5}$ in most urban areas in the western industrialized nations where mobile sources typically generate at least half of the $PM_{2.5}$, in UB the dominant source s appear to be blowing dust and coal combustion. As described in Annex B, based on data from 2008 to 2009 at the AMHIB site 2 (NRC) 47% of the $PM_{2.5}$ comes from crustal sources and only 13% comes from mobile sources. Coal combustion makes up most of the remaining share of $PM_{2.5}$ (35%) with biomass contributing 4%. At site 3 (Zuun Ali), mobile sources generate only 3 % of the $PM_{2.5}$. Fine particles from mobile sources are important since they generate important elements such as black carbon and metals, but also because of the immediacy of exposures for a typical urban population that live,

drive, walk and work along the traffic corridors. Thus, the lack of a major contribution from mobile sources may help explain the lack of a mortality effect in the analysis of the full-year of data. It is unclear, however, how representative sites 2 and 3 are for the full urban population of UB.

It is important to note, however, that the full-year mortality results may also be due to low statistical power in the study. Given the strong associations between $PM_{2.5}$ and hospital admissions for cardiovascular disease where there are many more cases, the low number of cases of daily mortality makes it much more difficult to detect an effect. Another factor is the increased sampling (daily for six weeks) during the winter when concentrations of coarse particles are very high, thereby increasing the chances of finding a CP effect. Measurement error may also play a role since clogging in the monitors may occur during days of higher concentrations. In addition, for those monitors that first extract coarse particles and then report fine particles as the remainder, there can be greater errors in measurement of the fine fraction. Specifically, measured concentrations of coarse particles may then be too high and fine particles too low (World Bank, 2009). Differences in diurnal patterns for fine and coarse particles may play a role as well as $PM_{2.5}$ is very low between the morning and later afternoon peaks (World Bank 2009). Finally, the mortality results could have been due solely to chance given the sparseness of the data.

It should be noted that the results were somewhat sensitive to the assignment of monitors to administrative districts. While the general findings were not significantly altered, there were changes in specific results when a different monitor was assigned to given district (data not shown). This sensitivity analysis was necessary since for some districts, there was not an obvious choice of a monitor that would clearly represent exposure.

The effects of coarse particles observed for UB, about 0. 3% per 10 $\mu g/m^3$ (95% CI = 0.0, 0.5) is similar to effects found in other studies of coarse particles. For example, Malig and Ostro (2009) reported an effect of 0.7% for a similar change for 15 California counties. In this study, $PM_{2.5}$ and CP were uncorrelated, making it easier to determine an independent effect of CP. In an analysis of 112 U.S. cities, Zanobetti et al. (2009) also reported an association for CP and mortality with a risk estimate of 0.46% per 10 $\mu g/m^3$. Other studies in Palm Springs, California (Ostro et al., 2000), Phoenix (Mar et al., 2000) and Mexico City (Castillejos et al., 2000) have reported relatively similar effect estimates. The association in UB appears to be driven by exposures in the cold season since no associations were observed during the warm season. During the cold season, a robust association was observed between cardiovascular mortality and lags of 1 and 3 days of CP.

In contrast to mortality, consistent associations were observed in the full year analysis between the cardiovascular hospitalization and both $PM_{2.5}$ and PM_{10}. The fewer associations for mortality may be due to the limited number of days where PM measurements were obtained (126 days) coupled with the relatively small number of average deaths per day. This may serve to significantly reduce the statistical power necessary for the study to detect an effect. Most studies of daily mortality include three years or more of data. In addition, as noted earlier, the wide variation in monitoring techniques and subsequent difference in measurement errors would likely make it more difficult to detect a health effect, given that one exists. The likelihood of finding stronger or more consistent associations with PM and mortality with more data is supported by the strong associations with hospital admissions for cardiovascular disease, some of which are extremely likely to result in mortality. It should also be noted, however, that the sparse data available for the analysis could also lead to inaccurate and highly variable results. This can lead to variability in the estimated coefficients for some of the outcomes observed when different lags were employed. Note, also, that given the every 3rd day data, a different mortality data set is employed for each different lag. For example, if PM is measured on day one, lag0 refers to mortality on day one, but lag1 would consider mortality on day 2 and lag2 would use mortality on day 3. Therefore, some variation in the results by day of lag may be due to the difference in the mortality data on each day.

The associations between $PM_{2.5}$ and PM_{10} and hospital admissions for cardiovascular disease were strong and consistent. For $PM_{2.5}$, a 10 $\mu g/m^3$ increase was associated with a 0.8% increase in cardiovascular admissions. Again, this magnitude is similar to that found in many other studies conducted in the North American and Western Europe.

In summary, the population of UB is exposed to high concentrations of PM from different sources and with different chemistry and size fractions. There is existing scientific literature to suggest that many of these sources—coal

combustion, local boilers, motor vehicles, biomass and even crustal material—can contribute to adverse health effects, especially at the concentrations experienced in UB. The findings of our analysis of the limited available data support the conclusion that there is a significant public health burden related to exposure to air pollution in UB.

References

Brook RD, Rajagopalan S, Pope CA, III, Brook JR, Bhatnagar A et al. (2010) Particulate Matter Air Pollution and Cardiovascular Disease. An Update to the Scientific Statement From the American Heart Association. Circulation 121: 2331–2378.

Burnett RT, Brook JR, Dann T, Delocla C, Philips O, Calmak S, Vincent R, Goldberg MS, Krewski D (2000). Associations between particulate- and gas-phase components of urban air pollution and daily mortality in eight Canadian cities. *Inhalation Toxicology* 12(Suppl. 4):15–39.

Castillejos M, Borja-Aburto VH, Dockery DW, et al. (2000) Airborne coarse particles and mortality. *Inhalation Toxicology* 12:61–72.

Dockery DW, Pope CA III, Xu X, Spengler JD, Ware JH, Fay ME, Ferris BG, Speizer FE (1993). An association between air pollution and mortality in six US cities. *New England Journal of Medicine* 329:1753–1759.

Dominici F, McDermott A, Zeger SL, Samet SM (2002). On the use of generalized additive models in time-series studies of air pollution and health. *American Journal of Epidemiology* 156:193–203.

Eftim SE, Samet JM, Janes H, McDermott A, Dominici F (2008) Fine particulate matter and mortality: a comparison of the six cities and American Cancer Society cohorts with a Medicare cohort. *Epidemiology* 19:209–216.

Franklin M, Zeka A, Schwartz J (2007) Association between PM2.5 and all-cause and specific-cause mortality in 27 US communities. *Journal of Exposure Science and Environmental Epidemiology* 2007;17:279–287.

Katsouyanni K, Touloumi G, Samoli E, Gryparis A, Le Tertre A, Monopolis Y, Rossi G, Zmirou D, Ballester F, Boumghar A, Anderson HR, Wojtyniak B, Paldy A, Braunstein R, Pekkanen J, Schindler C, Schwartz J (2001). Confounding and effect modification in the short-term effects of ambient particles on total mortality: results from 29 European cities within the APHEA2 project. *Epidemiology*, 12:521–531.

Malig B, Ostro B (2009) Coarse particles and mortality: evidence from a multi-city study in California. *Occupational and Environmental Medicine* 66:832–839.

Mar TF, Norris GA, Koenig JQ, et al. (2000) Associations between air pollution and mortality in Phoenix, 1995–1997. *Environmental Health Perspectives* 108:347–53.

Miller KA, Siscovick DS, Sheppard L, Shepherd K, Sullivan JH, Anderson GL, Kaufman JD (2007) Long-term exposure to air pollution and incidence of cardiovascular events in women. *New England Journal of Medicine* 356:447–458.

Ostro BD, Broadwin R, Lipsett MJ (2000) Coarse and fine particles and daily mortality in the Coachella Valley, California: a follow-up study. *Journal of Exposure Analysis and Environmental Epidemiology* 10:412–9.

Ostro B, Broadwin R, Green S, Feng WY, Lipsett M (2006) Fine particulate air pollution and mortality in nine California counties: results from CALFINE. *Environmental Health Perspectives* 114:29–33.

Ostro B, Lipsett M, Reynolds P, Goldberg D, Hertz A, Garcia C, Henderson KD, Bernstein L (2010) Long-Term Exposure to Constituents of Fine Particulate Air Pollution and Mortality: Results from the California Teachers Study 118:363–369.

Pope CA III (2000). Epidemiology of fine particulate air pollution and human health: biologic mechanisms and who's at risk? *Environmental Health Perspectives*, 108(Suppl. 4):713–723.

Pope CA III, Thun MJ, Namboodiri MM, Dockery DW, Evans JS, Speizer FE, Health CW Jr. (1995). Particulate air pollution as a predictor of mortality in a prospective study of US adults. *American Journal of Respiratory and Critical Care Medicine*, 151:669–674.

Puett RC, Schwartz J, Hart JE, Yanosky JD, Speizer FE, Suh H,, Paciorek CJ, Neas LM, Laden F (2008) Chronic particulate exposure, mortality, and coronary heart disease in the nurses' health study. *American Journal of Epidemiology* 168:1161–1168.

Schwartz J, Dockery DW, Neas LM (1996). Is daily mortality associated with specifically with fine particles? *Journal of the Air and Waste Management Association*, 46:927–939.

Schwartz J (2000). Assessing confounding, effect modification, and thresholds in the association between ambient particles and daily deaths. *Environmental Health Perspectives*, 108(6):563–568.

U.S. EPA (2008). Integrated Science Assessment for Oxides of Nitrogen—Health Criteria (Final Report). EPA/600/R-08/071.

U.S. EPA (2009) Integrated Science Assessment for Particulate Matter. EPA/600/R-08/139F

Wong CM, Vichit-Vadakan N, Kan H, Qian Z, the PAPA Project Teams(2008) Public Health and Air Pollution in Asia (PAPA): A Multicity Study of Short-Term Effects of Air Pollution on Mortality. *Environmental Health Perspectives* 116:1195–1202.

World Bank (2009) Air Pollution in Ulaanbaatar: Initial Assessment of Current Situation and Effects of Abatement Measures. Washington DC.

WHO (2004) Meta-analysis of time-series studies and panel studies of Particulate Matter (PM) and ozone (O_3): Report of a WHO Task Group.

Zanobetti A, Schwartz J (2009) The effect of fine and coarse particulate air pollution on mortality: a national analysis. *Environmental Health Perspectives* 117:898–903.

Ulaanbaatar, Mongolia, Air Monitoring and Health Impact Baseline (AMHIB) Report

Annex E

The Willingness to Pay for Mortality Risk Reductions in Mongolia[1]

Abstract

This paper reports on the results from a stated preference survey designed to estimate the willingness to pay for mortality risk reductions in Ulaanbaatar, Mongolia. The survey includes both contemporaneous and latent risk reductions of a magnitude typically achievable through clean air policy. The study looks at mortality risk reductions of the magnitude and types typically resulting from air pollution management policy. While the prime objective of the study is to estimate the willingness to pay for mortality risk reductions in Ulaanbaatar in order to support the work in the AMHIB project, an additional intention is to build a more solid bridge for benefits transfer between developed and developing countries. The survey was conducted in winter 2010. Estimates of willingness to pay passed external and internal scope tests. Study results imply a value of statistical life of $221,000 (319 million tugrug) for contemporaneous 5-in-10,000 annual risk reduction using the official exchange rate to convert tugrug to U.S. dollars.

Introduction

This paper reports on the first Mongolian study estimating willingness to pay (WTP) for mortality risk reductions. The study estimates willingness to pay for reductions in mortality risk and its population level equivalent, value of statistical life. The estimates are based on results from a stated preference survey of Ulaanbaatar residents, conducted in January and February 2010. In addition to providing Mongolia-specific VSL estimates, this survey is designed to help build a stronger empirical basis for transfer of environmental health valuation estimates among countries, particularly between developed countries where many such studies have been conducted and developing countries, where there have been far fewer. It does this by administering the same survey instrument used in studies in seven other countries: the U.S. and Canada (see Krupnick et al. 2002; Alberini et al. 2004), the U.K., France, and Italy (see Alberini et al. 2006b), and Japan (see Itaoka et al. 2005) and China (World Bank 2011). As in the China study, this survey uses a payment card/screen rather than the dichotomous choice approach to eliciting respondents' WTP that was used in the other six studies. This approach was used to address problems with dichotomous choice elicitation found in recent stated preference studies conducted in China (World Bank 2011, Zhongmin et al. 2003) and in India (Bhattacharya et al. 2007). The risk reductions offered respondents in the Mongolian survey are of the kind and size that are expected from air pollution policy (contemporaneous (e.g., respiratory) and latent (cancer), ranging from 5 to 10 in 10,000 annual risk.

Section 2 of the paper reviews contingent valuation studies of WTP for mortality risk reduction in eastern Asia, including one conducted in Inner Mongolia, and methodologically focused literature comparing dichotomous choice and payment card elicitation methods. Section 3 briefly describes the theoretical model underlying statistical analysis in this study. Section 4 describes the survey design, adaptation, and administration. Section 5 describes the characteristics of our sample, estimation methods and results, including estimates of WTP for current and future risk reductions. Section 6 compares our estimates with those from other countries using the same basic survey instrument. Finally, Section 7 offers a discussion and conclusions.

[1]This report is drafted by the following World Bank consultants under the AMHIB–project: Sandra Hoffmann, Qin Ping, Alan Krupnick, Sereeter Lodoysamba, Burmaa-jar Burmaa, Altangerel Enkhjargal and Batbaatar Suvd. Peer reviewers were Hua Wang and Giovanni Ruta, both from the World Bank. World Bank task team leaders were Jostein Nygard and Gailius Draugelis.

Table of Contents

Figures

Tables

E1 Literature review

The study team is aware of no prior studies estimating willingness to pay for reduction in health risks in Mongolia. Five such studies have been conducted in China (Hammitt and Zhou 2006; Li et al. 2002; Wang et al. 2001; Zhang 2002; Zhang et al. 2004; World Bank 2011), but the study team is aware of none conducted in other countries bordering Mongolia. Cultural and socioeconomic conditions in and Mongolia point to a need for specifically Mongolian VSL estimates rather than use of estimates based on those from China or other countries.

This study uses a payment card/screen to elicit willingness to pay. Payment cards are one of the two standard approaches to eliciting willingness to pay using closed ended questions. The other is dichotomous choice. With payment cards, respondents are asked to choose the amount they are willing to pay for a benefit from values written on a card. In dichotomous choice questions respondents are asked whether they are willing to pay a specified amount with a second follow-up WTP question. Champ and Bishop (2006) review the relative merits of each approach and conclude that, independent of the study context, neither method is clearly superior to the other. World Bank 2011 provides a more detailed discussion of the literature comparing payment card and dichotomous choice elicitation methods and their application in China.

Prior stated preference studies in China, including one in Inner Mongolia, found respondents tended to agree to pay the amount presented in dichotomous choice questions even when those values were raised to very high levels. This tendency toward "yea saying" has been seen in other settings and may be a common form of survey bias in which respondents seek to please the surveyors. These Asian studies found that payment cards were an effective means of overcoming this problem. In a study in Chinese cities that used the instrument on which this Mongolia survey is based, World Bank 2011 found excessive "yea saying" even though the survey instrument had been successfully administered in six industrialized countries (World Bank 2011). This problem was not found when the same survey was administered substituting a "payment screen" elicitation format for the dichotomous choice format (World Bank 2011). Zhongmin et al. (2003) encountered a similar problem with excessive "yea saying" when using a dichotomous choice question to elicit riverine ecosystem services in Inner Mongolia. They also found that use of a payment card resolved this problem.

E2 Conceptual model

The conceptual model underlying this study as well as the other seven studies which use this survey instrument is a life-cycle model of consumption with uncertain lifetime explained fully in Alberini et al. (2004). This work draws on a long line of similar models dating back to the 1960s (see Yari 1965, Arthur 1981, Shepard and Zeckhauser 1982, 1984, and Cropper and Sussman 1990). The life-cycle model assumes that an individual of age *j* maximizes expected lifetime utility by choosing a future consumption stream:

$$V_j = \sum_{t=j}^{T} q_{j,t}(1+\rho)^{j-t} U_t(C_t) \tag{1}$$

where V_j is the present value of expected utility lifetime consumption, $U_t(C_t)$ is utility of consumption at age t, $q_{j,t}$ is the probability that the individual who is now age j survives to age t, and ρ is the subjective rate of time preference. V_j is maximized subject to the constraint that the present value of expected consumption cannot exceed current wealth W_j plus the present value of expected lifetime earnings, y_t:

$$L_j = \sum_{t=j}^{T} q_{j,t}(1+\rho)^{j-t} U_t(C_t) + \lambda_j \left[\sum_{t=j}^{T} q_{j,t}(1+r)^{j-t}(y_t - C_t) + W_j \right] \tag{2}$$

where λ_j is the marginal value of an increase in wealth at time j and r is the riskless rate of interest.

Policies, like air pollution control, which reduce the probability of dying, D_t, in any period, *t*, *will* thus affect V_j. Since reducing the probability of dying increases the likelihood of surviving in that and all subsequent periods, the life cycle model can be used to determine the amount of current wealth that an individual would be willing to pay to reduce the probability of dying in any period or periods. The willingness to pay for a small change in probability of dying in any year *k* can be expressed as the marginal rate of substitution between wealth, W_j and the probability of dying in year *k* times the change in D_k (Alberini et al. 2006).[2]

$$WTP_{j,k} = -\frac{dV_j / dD_k}{dV_j / dW_j} dD_k \equiv VSL_{j,k} dD_k \tag{3}$$

Or, inversely, VSL is the WTP for a small change in mortality risk divided by the change in the risk. Alberini et al. (2004, 2006) show that under standard assumptions regarding individuals' ability to borrow through their lifetime, (2) and (4) imply that:

$$WTP_{j,k} = \frac{dD_k}{(1-D_k)} \sum_{t=k+1}^{T} q_{j,t} \left[\lambda_j^{-1} (1+\rho)^{j-t} \frac{u_t(C_t)}{\partial u_j / \partial C_j} + (1+r)^{j-t} (y_t - C_t) \right] \tag{4}$$

Equation (4) then serves as the basis for empirical estimation in this study, as it did in other studies conducting using the survey instrument adapted for this study in Ulaanbaatar. In particular, WTP is increasing in wealth and income, in reductions in the risk of death, and aversion to mortality risks. Because the literature on gender and risk aversion generally finds women more averse to physical risks than men, one would also expect that gender would help explain WTP to reduce mortality risks (Finucane et al. 2000 and Flynn et al. 1994). Alberini (2004) shows that (4) implies a theoretically ambiguous relationship between age and WTP, and between health status and WTP to reduce mortality risks. Baseline risk presented in the survey is the mortality risk of someone of the respondent's age and gender living in Ulaanbaatar. This suggests that theoretical findings regarding the ambiguous relationship between health status, age and WTP may also hold for baseline risk. Past studies have not found baseline risk to have an independent effect on WTP.

E3 Survey design and administration

E3.1 The survey instrument

The survey questionnaire begins with demographic questions. Questions about the health history of the respondent and the respondent's parents are used to remind respondents that they face mortality risks. Responses to these questions are also used to test for the influence of health status on WTP to reduce mortality risks. The second section of the survey introduces the concept of chance and the probability of dying. Simple probability concepts are introduced using virtually universal games of chance including coin tosses (Figure E.1) and die throws.

[2] D_k is considered as the altered probability of dying at age *k*. By definition, $q_{j,t} = (1 - D_j)(1 - D_{j+1})....(1 - D_{t-1})$

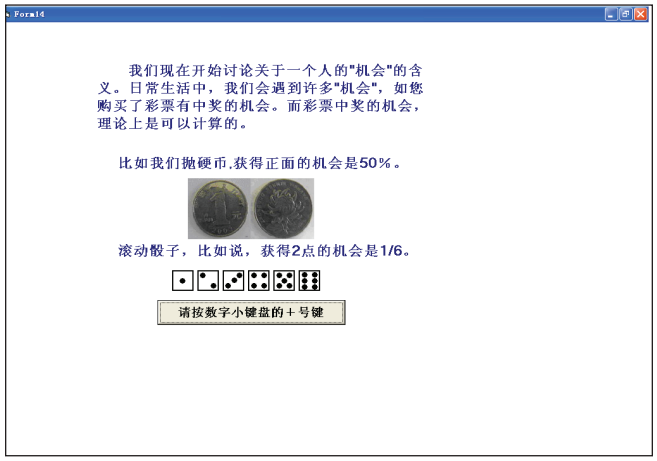

Figure E.1 Introduction to probability concepts using coin tosses. (Chinese version used to develop Mongolian survey.)

Because mortality risks associated with air pollution and other environmental hazards are typically much smaller than those seen on a die toss, a representation using a much larger denominator is needed. The original version of the survey instrument worked towards this by first presenting a grid of 36 squares motivated by a discussion about roulette wheels. It then presents the risk communication device used in the survey to elicit WTP for a mortality risk reduction—a 1,000-square grid in which risks are represented using red squares (Figure E.2). To test their comprehension, respondents are asked to compare grids depicting mortality risks for two hypothetical people (person A and person B) and to determine which of the two has the higher risk of death. They are also asked to select which of the two people they would rather be. The results of these questions are used to identify respondents' ability to understand the survey instrument and are used in cleaning the survey data.

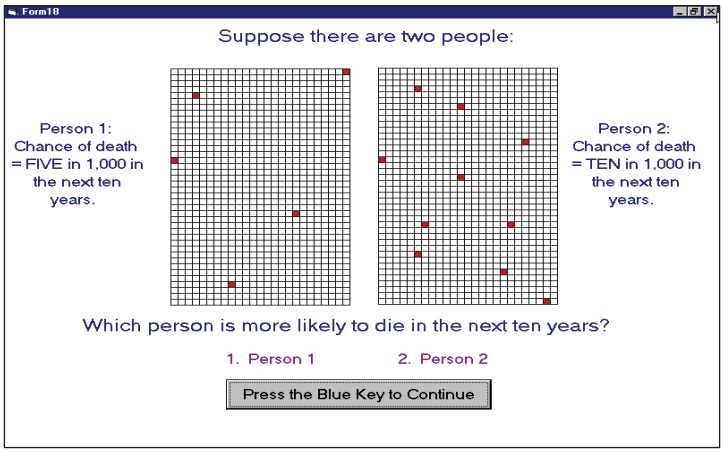

Figure E.2 The survey risk communication device: The 1,000-square grid. (American version used to develop Mongolian survey.)

The third section of the survey is designed to increase the saliency of mortality risk and mortality risk reduction efforts to respondents. It first presents respondents with age- and gender-specific leading causes of death and then introduces common risk-mitigating behaviors, illustrative risk reductions, and qualitative costs of reducing risks. These screens remind respondents that people regularly take actions that have real costs as a means of reducing their chance of dying. We present respondents with information on the effectiveness of common actions taken to reduce mortality risk and describe their relative cost qualitatively.

The survey then presents respondents with information on baseline mortality risks for someone of their own age and gender living in Ulaanbaatar and asks them to accept this risk as their own for the purpose of the survey. Respondents' acceptance of the baseline risk is tested in debriefing questions.

Respondents are next told about a product that would reduce their risk of dying over a specified period. The description of the product is purposefully left as generic as possible so as not to have the characteristics of the product unnecessarily affect respondents' WTP. A product is used as the means of reducing the risk rather than

air pollution policy because the purpose of the survey is to cleanly estimate WTP to reduce mortality risk. Having respondents think that the risk reduction was due to an improvement in air quality would evoke a wide range of benefits in addition to mortality risk reduction. These might include the aesthetic benefits of clearer air, the altruistic utility respondents gain from protecting others' health or the benefits respondents themselves might experience from reductions in morbidity, rather than mortality, associated with reduced air pollution. The 1000 square grid is used to show respondents their own baseline mortality risk and the reduction in their baseline risk that would result from use of this product (Figure E.3). Finally, respondents are asked about their WTP for this product using a payment screen approach (see below).

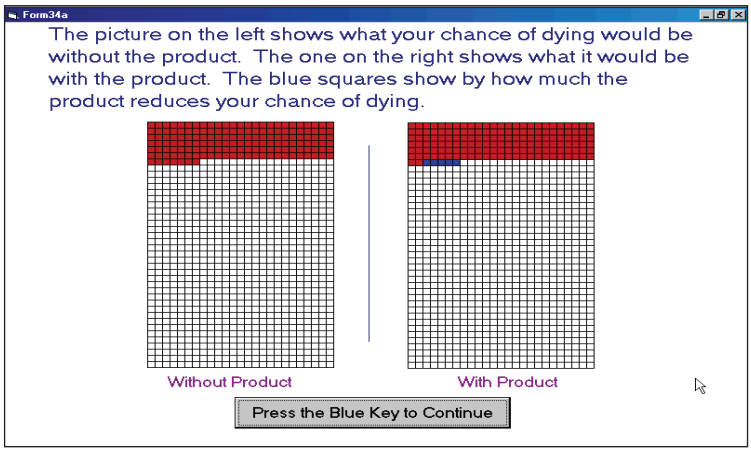

Figure E.3 Depiction of risk change (American version used to develop Mongolian survey).

At the time the survey was conducted it was unknown how large a risk reduction might be possible from air pollution policy in Ulaanbaatar. As a result, we considered use of mortality risk reductions of a magnitude typically seen from air pollution policies, i.e., in the range of 1 in 10,000 to 10 in 10,000 per year. As the survey was originally being developed in the U.S., it became clear that respondents had a difficult time understanding very small changes in risk such as these. As a result, a devise was developed to convey this magnitude of risk reduction in a way comprehensible to respondents. Instead of a risk reduction of x in 10,000 over 1 year, respondents were offered a risk reduction of x in 1,000 annually over 10 years. As discussed below, focus group results in Ulaanbaatar led to us using two levels of annual risk reduction, 5 in 10,000 and 10 in 10,000.

The sample design has two waves or treatments. Respondents in the first wave receive a 5 in 1,000 annual risk reduction over 10 years as the initial WTP question and a 10 in 1,000 annual risk reduction over 10 years as a second WTP question. Respondents in the second wave receive a 10 in 1,000 annual risk reduction for 10 years followed by a question offering a 5-in-1,000 annual risk reduction over 10 years (Table E.1). The initial WTP question offers a contemporaneous risk reduction to all respondents. The second WTP question offers a latent risk reduction to respondents age 40 to 65 and a contemporaneous risk reduction to respondents over age 65. This structure allows testing for ordering effects among those over 65.

Table E.1 Study design

Group of Respondents	*Initial current risk reduction valued*	*Second risk reduction valued*	
		Future risk reduction	*Current risk reduction*
		Age 40–65	> 65
Wave 1 (N = 309)	5 in 1,000	10 in 1,000	
Wave 2 (N = 320)	10 in 1,000	5 in 1,000	

Note: Respondents over 65 did not get a latency question.

The basic form of the contemporaneous risk question is how much the respondent would be willing to pay for a product that, when used and paid for annually over the next 10 years, would reduce their baseline risk by *x* in 1,000 each year during the same period. A timeline is used to illustrate the payment period and the period during which the benefit is experienced. The latency risk reduction questions ask respondents how much they would be willing to pay for a product that, when used and paid for annually over the next 10 years, would reduce their annual mortality risk by x in 1,000 for a ten-year period beginning at age 70. Figure E.4 illustrates elicitation of WTP for latent, 5 in 1,000 annual risk reductions over 10 years for a 46 year-old respondent. Prior to receiving questions about WTP to reduce latent risks, respondents are asked what probability they think they have of surviving to age 70. A variety of surveys have shown that individuals are reasonably good at estimating future survival probabilities (Hamermesh 1985; Hurd and McGarry 1996).

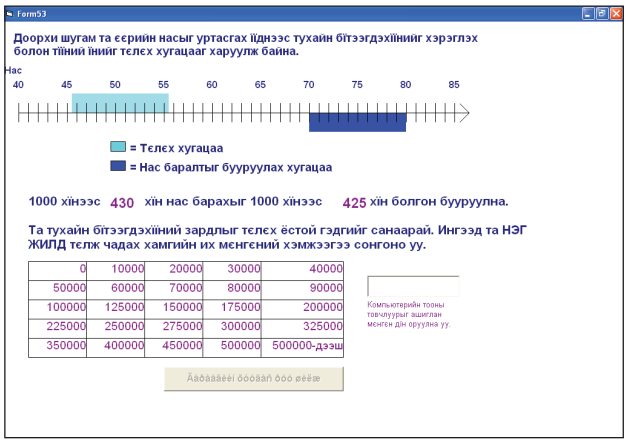

Figure E.4 Payment card elicitation of willingness to pay.

An extensive series of debriefing questions follows the risk valuation questions. These questions test respondents' understanding of concepts presented in the survey, acceptance of various elements of the risk reduction scenario and baseline risk, and the presence of other factors that call the credibility of answers into question.

E3.2 Adaptation of the survey instrument

The survey instrument used in this study is based closely on one first developed for use in the United States (Alberini et al., 2004) and more recently adapted for use in China (Krupnick et al. 2010). In adapting the survey for use in Mongolia, we had two, sometimes conflicting, goals. The primary goal was producing a survey that Mongolian respondents would understand and find credible. The secondary goal was to maintain as much consistency as possible with versions of the survey that had been administered successfully in other countries. This consistency enables results of this study to be used to as a basis for transferring environmental health benefits estimates among countries.

After translating the survey into Mongolian and back translating to English to verify the accuracy of the translation, a series of focus groups were held in Ulaanbaatar in fall 2009 to help adapt the survey. Several changes were needed to assure that the survey reflected Mongolian circumstances. These included the structure of health care delivery, causes of mortality, gender-specific life expectancy, and activities individuals engage in to protect their health. Focus group participants found the use of a generic product to reduce mortality risks credible, but they also suggested that describing the product as being approved by U.S. and European, as well as Mongolian, health authorities would enhance its credibility. As in many developing countries, households in Ulaanbaatar often have multiple sources and types of income. The income question was revised to ask respondents to include all of these sources in reporting their household income.

Focus groups also disclosed that there is a culture in Ulaanbaatar of not disclosing a small portion of one's income, which participants referred to as "secret income". As a result, income figures reported in this survey should be viewed as underestimating real household income. This would have the effect of inflating estimates of WTP as a percent of household income but it cannot be known by how much. Focus group participants recommended changing the reference to roulette wheels in the probability tutorial to a reference to a better known,

but similar, wheel used on a popular Mongolian TV game show to select possible prizes. Few other changes in risk communication were needed. A risk attitude question referring to air and train travel to measure aversion to safety hazards was changed to one related to crossing busy streets.

Focus groups were also used to test the appropriate size of risk changes. Participants in the focus groups found it difficult to understand or distinguish the magnitude of the smallest risk reduction, 1 in 10,000. Results from the original U.S. version of the survey indicated that U.S. respondents also had difficulty comprehending the 1 in 10,000 risk reduction (although the results passed an external scope test, i.e., WTP increased with the size of the risk reduction). The response of focus group participants as well as results from pretests of the survey indicated that Ulaanbaatar respondents did understood the meaning of 5 in 10,000 and 10 in 10,000 annual reductions in mortality risk and believed that the product offered in the survey would reduce mortality risks by these magnitudes.

E3.3 Survey design and validity testing

The survey's design permits testing for consistency of responses with the underlying theoretical model and good survey design standards. The structure of the contemporaneous risk reduction questions allows tests of whether WTP is increasing with the size of the risk reduction by comparing responses between samples (external scope tests) (Figure E.5) and, for those 65 and above, within samples (internal scope test). The external scope test can also be performed for the latent risk reductions. The Mongolian survey design does not permit testing for the influence of the latent risk reductions question being preceded by a contemporaneous risk reduction question. An alternative form of the external scope test is to combine the subsamples and use a dummy variable to identify which sample got the larger risk reduction. This test is more difficult to pass that a split sample means test because of the *ceterus paribus* conditions imposed by the regression framework (although by doubling the number of observations, power is increased). Comparison of responses to contemporaneous and latent risk reductions questions allows tests for positive discounting. Finally the study design allows for tests of whether question order affects responses (Figure E.5).

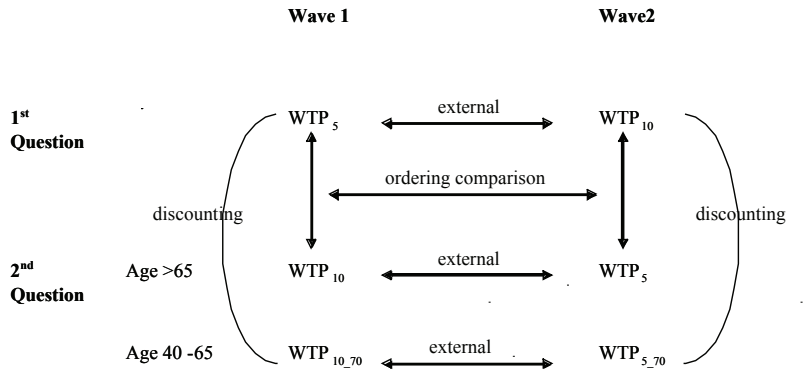

Figure E.5 Scope tests.

E3.4 Interpretation of the payment card/screen[3]

The payment card/screen elicitation approach (Figure E.4) presents respondents with a matrix of ordered numbers and asks them to pick one corresponding to their maximum willingness to pay for the risk reduction. The chosen "stated" number can be thought of 1) as an appropriate estimate of WTP, 2) as the top end of an interval between the chosen number and the next lowest number (which we estimated using a Weibull distribution), or 3) as the bottom end of an interval between this number and the next highest number (which we did not estimate). In order of conservativeness, what we will call the Weibull estimate is more conservative (lower) than use of the stated value as an estimate. We also set WTP at the value in the matrix immediately below the chosen number, which in this context is similar to a Lower Turnbull estimate. This would be the most conservative of the three estimates used in our analysis.

[3]While the visual presentation of the payment card used in this survey is similar to that used in the China study, it is functionally different. In the China study, the computer cursor randomly appeared within the matrix of numbers. Respondents choose their bid by moving the cursor to choose their desired bid level. Krupnick et al. (2010) explains the advantages of this functionality. Project constraints did not permit use of this functionality in the Mongolian survey instrument. As a result, the Mongolian survey is closer to a conventional payment card WTP elicitation even though it continues to appear on a computer screen.

The values presented in the payment card/screen range from 0 to 500,000 tugrug per year for 10 years. Focus group results suggested that WTP in Ulaanbaatar would generally not exceed 500,000 tugrug per year. The range also includes the range of WTP values seen in other countries where this survey instrument was administered, PPP-corrected. This helps assure that study results can be compared to those of previous studies. As shown in Figure E.4, numbers were set up in a matrix, rather than a list for compactness and to mitigate visual starting point bias. Range intervals were designed to be roughly constant in percentage terms. Psychometric studies and experimental economics suggest this as a means of reducing response error (see Rowe, Schulze, and Breffle 1996 and Ready, Navrud and Dubourg 2001 for discussions of this literature). In the Mongolian survey, a box with a flashing cursor was placed to the side of matrix. The survey enumerator asked respondents which value in the matrix they would be willing to pay for the risk reduction.

E3.5 Administration of the survey

The survey was administered in Ulaanbaatar, the capital of Mongolia using random sampling stratified by neighborhood. Respondents came to a neighborhood center. The survey was administered on weekends to accommodate respondents' work schedules and was administered on laptop computers operated by enumerators who entered participants' responses. Enumerators all received very explicit training regarding the level of interaction with respondents that was permissible to maintain consistency in administration across respondents. Participants were also given an inexpensive gift to thank them for participating. A sample of 629 respondents completed the survey.

E4 Sample characteristics, estimation methods and results

E4.1 Cleaning the sample

Table E.2 provides descriptive statistics on indicators that a respondent may not have understood the survey. Four of these indicators were ultimately used to clean the sample. Six respondents were dropped because they responded incorrectly to questions testing their understanding of probability or the way it was presented in the survey (FLAG1). Respondents over 80 are unlikely to survive to realize the benefits provided by the product. One respondent was over 80 and dropped, as were respondents over 80 in prior studies using this survey. A total of 131 respondents (or 20% of the full sample) said they did not understand probability well (FLAG6). WTP estimates did not pass scope when FLAG6 respondents were included in the sample, suggesting that more work may need to be done to overcome innumeracy when conducting this or similar surveys in developing countries. Finally, 26 respondents indicated that they were willing to pay more than 90% of their stated income for the indicated risk reduction. This indicates a failure to take the budget constraint seriously, a failure to understand the question being asked, or a protest bid. Use of this cleaning criterion was also important to WTP estimates passing scope tests. None of the cleaning variables were strongly correlated; correlation coefficients were all less than |0.05|.

Table E.2 Descriptive statistics for cleaning criteria variables

Variable	Number obs.	% of total obs.
FLAG1[1]	6	0.95
OVER80[2]	1	0.16
FLAG6[3]	131	20.82
WTP/income $\geq$ 0.9	26	4.13

[1] FLAG1 is a categorical variable indicating that a respondent failed to pass one or more probability comprehension tests in the survey.
[2] OVER80 identifies respondents who were over 80 years of age.
[3] FLAG6 is a categorical variable indicating that a respondent answered that they did not understand probability well.

We applied three alternative cleaning approaches in our analysis. Cleaning approach A eliminates respondents who failed tests of understanding of probability and the respondent over 80. Cleaning approach B eliminates these same respondents plus those who state they do not understand probability well. Cleaning approach C drops those in cleaning approach B plus respondents who expressed a willingness to pay that is 90% or more of their per capita income. In general, we report the results of cleaning approach A because it is the least restrictive. We do not report results for cleaning approach B as they were in general quite similar to those for cleaning approach A. We report results for cleaning approach C because with this cleaning, WTP estimates behave in ways more

consistent with the underlying theoretical model. We also found no statistically significant difference on major demographic variables between the sample remaining after cleaning approach C was applied and the sample as a whole (Table E.3).

Table E.3 Comparison of demographic variables by cleaning and place of birth

	Whole Sample	Cleaning approach C[1]	Comparison of means
Variable Definition	*Mean*	*Mean*	*Wald tests (p value)*
Socio-demographics			
Age	54.37	53.99	-0.61*(0.54)*
Age distribution (%)			
40–49	38	39	0.32 (0.75)
50–59	31	31	1.05 (0.29)
60–69	21	21	0.48 (0.63)
70 and older	10	9	0.32 (0.75)
Gender (1 = male, 0 = female)	0.38	0.40	0.71*(0.48)*
Share of respondents with university education (%)	0.46	0.48	0.66*(0.51)*
Monthly Income (tugrug)			
Household Income	390,063	402,118	0.88 (*0.38)*
Per Capita Income	103,113	106,548	0.75 (*0.45*)
Observations	629	472	

[1]Cleaning approach C drops Flag1, Flag6, Over80, WTP/income <0.9

E4.2 Sample characteristics

Descriptive Statistics

Table 4 reports descriptive statistics for the full sample. The study sample is also somewhat more female than male (38% male). In Mongolia as a whole, 51% of the population is male (National Statistical Office of Mongolia 2009). Ulaanbaatar residents account for 65% of the Mongolian population (National Statistical Office of Mongolia 2009). 45% of the sample has some college education, which is clearly an overestimate for the population. Mean monthly household income in the sample, 390,063 tugrug or 103,113 tugrug per capita, is roughly comparable to the national average household income of 399,096 tugrug per month, and much lower than Ulaanbaatar average of 547,825 tugrug (National Statistical Office of Mongolia, Feb. 2009). Mongolia has a young population and a low life expectancy compared to other countries studied using this survey instrument. The sample similarly is skewed toward a younger population despite an effort to oversample in the older age categories. 83% of respondents expect to live to age 70. This may seem optimistic in light of the fact that 23% of respondents report having problems with bronchitis, 44% have heart disease. But in 2005, an average 60-year-old Mongolian woman could expect to live to age 78, a man to age 75 (United Nations 2010). Life expectancy has risen rapidly in Mongolia and is projected to continue to increase in the coming years. While the average life expectancy at birth of Mongolians is currently 68, it was only 42 in 1950 and is projected to reach 73 by 2030 (United Nations 2010).

Table E.4 Descriptive statistics

	Whole Sample			
Variable Definition	*Mean*	*Std Deviation*	*Min*	*Max*
Socio-demographics				
Age	54.4	10.3	40	81
Age distribution (%)				
40–49	38			
50–59	31			
60–69	21			
70 and older	10			
Share of respondents with university education (%)	0.45	0.49	0	1
Health status (%)				
Respondent with bronchitis	0.23	0.42	0	1
Respondent with cancer	0.07	0.26	0	1
Respondent with heart disease	0.44	0.49	0	1
Chance to live to age 70	83	22	0	100
Monthly income (1000 tugrug)				
Household Income	390,063	223,358	150,000	850,000
Per Capita Income	103,113	75,680	12,500	42,5000
Number of observations	629			

E4.3 Estimation methodology

To estimate WTP for the assumption that the chosen value is the respondents' actual WTP and for the Lower Turnbull estimates, we use a Tobit model. For the interpretation of the stated WTP as the lower bound of an interval (the Weibull model), the underlying econometric model is

$$\log \mathrm{WTP}_i^* = \mathrm{X}_i\beta + \varepsilon_i \tag{1}$$

where *WTP** is the underlying willingness to pay for a selected risk reduction; *X* denotes a vector of age, health, and other attributes; β is a vector of coefficients; and ε is an extreme value Type I error term. Effectively, equation (1) describes a survival time model based on the Weibull distribution. The log-likelihood function of the data is

$$\log \mathrm{L} = \sum_{i-1}^{n} \left\{ \mathrm{F}\left[\log\left(\mathrm{WTP}_i^{\mathrm{H}} - \mathrm{X}_i\beta\right)/\sigma\right] - \mathrm{F}\left[\log\left(\mathrm{WTP}_i^{\mathrm{L}} - \mathrm{X}_i\beta\right)/\sigma\right] \right\} \tag{2}$$

where *F* is the type I extreme value distribution with scale σ, $WTPi^H$ and $WTPi^L$ are upper and lower bounds for WTP, and *X* is a vector of age, health, and other attributes with β as the corresponding coefficients. σ is the scale

parameter of ε, as well as the reciprocal of the shape parameter of the Weibull distribution describing WTP. The scale parameter for the Weibull distribution is exp*(Xβ)*.

E5 Results

E5.1 WTP estimates, and scope, discounting and ordering tests

Tables E.5, E.6, and E.7 present results for respondents aged 40 to 65. Analysis reported in Table E.5 assumes that the values respondents choose from the payment card represent their true WTP.

Table E.5 Stated value: External scope tests under alternative data cleaning approaches (Respondents 40 to 65)

Cleaning Criteria	Sample A Flag1 & Over80		Sample B Flag1, Flag6, Over80		Sample C Flag1, Flag6, Over80, WTP/income <0.9	
	N	Mean	N	Mean	N	Mean
WTP5	303	265,402	232	256,362	221	221,067
WTP10	319	286,802	260	297,434	251	256,665
WTP5_70	238	130,299	189	132,474	184	132,376
WTP10_70	270	206,394	223	213,361	210	178,902
	t-tests for significance of difference in means					
		p[1]		p		p
5 vs 10	-0.63	0.26	-1.04	0.15	-1.67	0.05
5_70 vs 10_70	-3.92	0.00	3.59	0.00	-2.76	0.00
5 vs 5_70	6.20	0.00	5.52	0.00	4.80	0.00
10 vs 10_70	2.36	0.01	2.08	0.02	3.79	0.00

WTP5 means WTP for a 5 in 1000 risk reduction beginning immediately. WTP5_70 means WTP for a 5 in 1000 risk reduction beginning at age 70. WTP10 is WTP for a 10 in 1000 risk reduction.
[1]Ho: wtp5=wtp10; Ha: wtp5<wtp10

Analysis presented in Tables E.6 and E.7 assume a Weibull and a Lower Turnbull model, respectively. Under cleaning approach C, WTP responses pass external scope tests (at the 90% level) for both contemporaneous and latent risk reductions for all distributional assumptions (Tables E.5, E.6 and E.7). WTP for a contemporaneous 5 in 10,000 annual risk reduction ranged from 159,457 tugrug using a Lower Turnbull estimation to 221,067 assuming stated WTP is respondents' true WTP. Results show positive and statistically significant discounting for all cleaning approaches and the stated value and Weibull models (Tables E.5, E.6 and E.7).

Table E.6 Weibull: External scope tests under alternative datacleaning approaches (Respondents 40 to 65)

	A			B			C		
Cleaning criteria	Flag1 & Over80			Flag1, Flag6, Over80			Flag1, Flag6, Over80, WTP/income <0.9		
	N	Mean		N	Mean		N	Mean	
WTP5	299	200,192		229	202,175		218	182,624	
WTP10	317	213,851		258	222,279		249	211,664	
WTP5_70	210	127,291		168	129,622		164	129,622	
WTP10_70	248	176,732		204	180,612		192	165,945	
	t-test for significance of difference in means								
			p^1			p		p	P
5 vs 10		-16.18	0		-18.75	0		-28.78	0
5_70 vs 10_70		-54.79	0		-45.91	0		-34.26	0
5 vs 5_70		86.52	0		67.20	0		51.39	0
10 vs 10_70		41.07	0		37.77	0		42.72	0

[1]Ho: wtp5=wtp10; Ha: wtp5<wtp10

Table E.7 Lower Turnbull (lower bound value): External scope tests under alternative data cleaning approaches (Respondents 40 to 65)

	Sample A			Sample B			Sample C		
Cleaning Criteria	Flag1 & Over80			Flag1, Flag6, Over80			Flag1, Flag6, Over80, WTP/income <0.9		
	N	Mean		N	Mean		N	Mean	
WTP5	303	169,274		232	173,772		221	159,457	
WTP10	319	185,721		260	194,481		251	185,717	
WTP5_70	238	101,933		189	105,053		184	104,647	
WTP10_70	170	143,315		223	145,538		210	136,857	
	t-tests for significance of difference in means								
			p^1			p			p
5 vs 10		1.35	0.09		-1.49	0.07		-1.96	0.03
5_70 vs 10_70		3.41	0.00		-3.17	0.001		-2.58	0.01
5 vs 5_70		5.84	0.00		2.04	0.02		4.36	0.00
10 vs 10_70		3.41	0.00		3.55	0.00		3.63	0.00

[1]Ho: wtp5=wtp10; Ha: wtp5<wtp10

Tables E.8 and E.9 present results for respondents over 65. The survey design allows for internal scope tests to be run only on those over 65. Table E.8 treats stated WTP as respondents' true WTP. Table E.9 assumes a Weibull distribution. WTP estimates pass internal scope for all cleaning approaches for both models (Tables E.8 and E.9). Tests for the influence of question order on responses can only be tested for respondents over 65. An ordering affect was only found with cleaning approach A, either when treating the stated value as respondents' true WTP or when using a Lower Turnbull model (Table E.10). While no statistically significant ordering effect is found with

cleaning approach C, this is probably due to the small sample size. When respondents received a 10 in 1000 risk reduction over 10 years as the first question, they were willing to pay less for a 5 in 1000 risk reduction over 10 years than those who were asked the willingness to pay for a 5 in 1000 risk reduction over 10 years as their first question. Correspondingly, those who received the 5 in 1000 risk reduction over 10 years as the first question were willing to pay more for a 10 in 1000 risk reduction over 10 years than those presented with it as a first question. These results are evidence for a question ordering effect that would have implications for interpreting an internal scope test (but not an external scope test).

Table E.8 Stated value: Internal scope tests under alternative data cleaning approaches (Respondents over 65 years old)

Cleaning Criteria	Sample A Flag1 & Over80			Sample B Flag1, Flag6, Over80			Sample C Flag1, Flag6, Over80, WTP/income <0.9		
	N	Mean	*p*	N	Mean	*p*	N	Mean	*p*
First WTP5	49	217,551		37	205,000		36	204,027	
Second WTP10	49	325,673		37	322,378		36	321,333	
		-1.66	0.05		-1.61	0.06		-1.57	0.06
First WTP10	65	249,400		43	264,116		42	263,262	
Second WTP5	65	118,230		43	123,488		43	123,488	
		3.92	0.00		3.22	0.00		3.16	0.00

Table E.9 Weibull: Internal scope tests under alternative data cleaning approaches (Respondents over 65 years old)

Cleaning Criteria	Sample A Flag1 & Over80			Sample B Flag1, Flag6, Over80			Sample C Flag1, Flag6, Over80, WTP/income <0.9		
	N	Mean	*p*	N	Mean	*p*	N	Mean	*p*
First WTP5	47	175,138		36	169,258		35	167,552	
Second WTP10	48	246,530		37	242,583		36	239628	
		-12.4	0		-10.43	0		-9.89	0
First WTP10	65	189,736		43	201,559		42	199,509	
Second WTP5	53	120,913		35	128,747		34	131,261	
		20.78	0		14.19	0		12.81	0

Table E.10 Test of ordering effect with data cleaning approach A (Respondents over age 65)[1]

	Stated Value			*Weibull*			*Lower Turnbull*		
	N	*Mean*	*(p)*	*N*	*Mean*	*(p)*	*N*	*Mean*	*(p)*
WTP5 *First Question*	49	217,551		47	175,138		49	148,775	
WTP5 *Second Question*	65	118,231	2.44 (0.02)	48	120,913	13.52 (0.00)	65	88,231	-2.59 (0.01)

	Stated Value			*Weibull*			*Lower Turnbull*		
	N	*Mean*	*(p)*	*N*	*Mean*	*(p)*	*N*	*Mean*	*(p)*
WTP10 *First Question*	65	249,400		65	189,736		65	159,153	
WTP10 *Second Question*	49	325,674	-1.38 (0.17)	48	246,530	30.07 (0.00)	49	204,286	-1.56 (0.12)

[1]2-tailed test

E5.2 Regression analysis on contemporaneous WTP

Regression analysis provides further evidence about construct validity, that is, whether the survey is measuring WTP. Again, consistent with basic economic theory, one would expect WTP to increase with income and risk reduction. The life-cycle model also implies an inverted U-shape relationship between age and WTP. This relationship was found in other studies conducted using this survey instrument (see, for example, Alberini et al (2004) for Canada and Alberini et al (2006) for the U.S.), though not in Japan (Itaoka et al (2005). Krupnick (2008) surveys the stated preference literature on the relationship between age and WTP for mortality risk reductions. Theoretically, the effect of health status on WTP is indeterminate (Alberini et al. 2004). Alberini et al. (2004) reported that a family history of chronic heart or lung disease increases WTP by 26% in Canada, and 37% in the USA.

Table E.11 presents results from regression analysis of construct validity for contemporaneous risk reductions pooling the entire data set. We show results for cleaning methods A and C only. Results for cleaning approach B are quite similar to those for cleaning approach A. The coefficient for income is both highly significant and positive. Regardless of cleaning approach, wealthier respondents are WTP more to reduce mortality risk. With cleaning approach C, but not A, a risk reduction of 5 in 1000 over 10 years is significant and negative, again indicating the results pass scope, even controlling for observable sample characteristics. For cleaning approach A, we find an inverted-U shaped relationship between age and WTP and find that more risk averse respondents are WTP more to reduce mortality risk. Existing health conditions do not influence WTP. As in most past studies

that use this survey instrument, baseline risk is also not a significant predictor of WTP when substituted for age and gender. Being born in Ulaanbaatar and having a University education result in higher WTP, independent of reported income in cleaning approach A. These variables could be standing in for unreported income. Also, those who are more risk averse are willing to pay more, although this affect is not significant with Cleaning Criteria C. Use of robust variance estimators does not change regression results for either contemporaneous or latent WTP indicating that heteroskedasticity is not playing a strong role.

Table E.11 Weibull: Construct validity of WTP for the current risk reduction

	Sample A		Sample C	
Variable	Coef.	s.e.	Coef.	s.e.
Intercept	5.05***	(1.42)	2.19	(1.56)
Age	0.08*	(0.04)	0.07	(0.04)
Age square	-0.001*	(0.0004)	-0.001*	(0.0004)
University Education (=1)	0.19**	(0.08)	0.12	(0.08)
Gender dummy (1=male)	0.05	(0.08)	-0.02	(0.08)
Per capita monthly income (log form)	0.38***	(0.06)	0.60***	(0.06)
Born in Ulaanbaatar (=1)	0.19**	(0.08)	0.13	(0.08)
Risk averse (=1)	0.17**	(0.08)	0.02	(0.08)
Heart Disease dummy	-0.08	(0.08)	-0.05	(0.08)
Bronchitis dummy	0.06	(0.09)	0.07	(0.09)
Cancer dummy	0.09	(0.15)	0.05	(0.15)
If the risk variable is 5 in 1000 reduction	-0.03	(0.08)	-0.13*	(0.07)
Scale parameter	1.08	(0.04)	1.26	(0.05)
Number of Observations	616		468	

Sample A cleaning approach: drop Flag1, Flag6 and >80 years old.
Sample C cleaning approach: drop Flag1, Flag6, >80, and WTP/income ≥ 0.9.
* significant at 10% level; ** significant at the 5% level; *** significant at the 1% level.

Table E.12 shows results for regressions on WTP for latent risk reduction. Again, income has a significant and positive influence on WTP. The coefficient on the 5 in 10,000 annual risk reduction relative to that of 10 in 10,000 is negative and significant indicating that WTP estimates pass scope with both cleaning approaches A and B. The relationship between age and WTP is not significant. Again baseline risk was not significant when substituted for age and gender and use of robust variance estimation did not affect results.

Table E.12 Weibull: Construct validity of WTP for the latent risk reduction

Variable	Sample A Coef.	Sample A s.e.	Sample C Coef.	Sample C s.e.
Intercept	3.15	(2.67)	1.63	(2.76)
Age	0.12	(0.09)	0.11	(0.09)
Age square	-0.001	(0.001)	-0.001	(0.001)
University Education (=1)	0.11	(0.09)	0.03	(0.09)
Gender dummy (1=male)	-0.001	(0.09)	-0.02	(0.10)
Per capita monthly income (log form)	0.38***	(0.08)	0.52***	(0.08)
Born in Ulaanbaatar (=1)	0.18**	(0.09)	0.05	(0.10)
Risk averse (=1)	0.12	(0.09)	-0.08	(0.10)
Heart Disease dummy	-0.12	(0.09)	0.01	(0.09)
Bronchitis dummy	0.11	(0.11)	0.18	(0.12)
Cancer dummy	0.28	(0.17)	0.21	(0.18)
If the risk variable is 5 in 1000 reduction	-0.47***	(0.09)	-0.32*	(0.09)
Chance to survive to 70	0.005**	(0.002)	0.002	(0.002)
Scale parameter	1.06	(0.04)	1.16	(0.04)
Number of Observations	458		356	

Sample A cleaning approach: drop Flag1, Flag6 and >80 years old.
Sample C cleaning approach: drop Flag1, Flag6, >80, and WTP/income $\geq$ 0.9.
* significant at 10% level; ** significant at the 5% level; *** significant at the 1% level.

In choosing a value of statistical life to use in policy analysis, we consider construct validity (performance on split sample tests and regressions) and the appropriateness of the risk reduction type and magnitude to the application. In other countries studied, a 5 in 10,000 risk reduction has been the most robust for use in assessing policies that reduce conventional air pollution and roughly matches the health risk reductions one could expect from application of air pollution policies. An issue for further investigation is whether this is also appropriate for Ulaanbaatar. For this preliminary analysis we assume that 5 in 10,000 annual risk reduction would be the most appropriate for Ulaanbaatar based on experience in other countries.

Mongolia's relatively short life expectancy raises a question about the validity of including older respondents in the Ulaanbaatar study and about the validity of results for WTP for latent risks. Average life expectancy at birth in Mongolia is 68.1 years compared to 79.9 in the U.S. or 83.1 in Japan (U.N. 2010). For those who survived to age 65 in 2005, life expectancy in Mongolia was 15 years for women and 12 for men. This compares to a life expectancy of 20 for 65 year-old women in the U.S. and 15 for U.S. men. In part for this reason and in part because current policy proposals focusing on reducing particulate matter pollution will primarily provide contemporaneous rather than latent health benefits, we recommend relying on estimates of WTP for contemporaneous risk reduction in evaluating current air pollution policy proposals in Ulaanbaatar. However, investments in pollution control and sanitation in Ulaanbaatar should lead to increased life expectancy over time. Other changes that are part of the process of development that Mongolia expects, such as improved sanitation, improved health care, increased educational levels and economic growth, are expected to increase life expectancy during the life times of survey

respondents (U.N. 2010). As a result, from a policy perspective, it should also be of interest to understand these respondents WTP to reduce their own annual mortality risk in their old age.

Tables E.11 and E.12 present results of Weibull regressions on both current and latent risk reductions. Results for the Lower Turnbull regressions were virtually identical to those run assuming a Weibull distribution. Models defining stated WTP as "true" WTP did not perform as well.

Critics often claim that stated preference studies overstate WTP because respondents do not actually have to expend their own money and do not receive actual benefits. To address this tendency, it is useful to explore whether policies are still rational assuming lower bound estimates of WTP from stated preference studies. In this study, that means relying on Weibull or Lower Turnbull estimates rather than stated WTP as a measure of true WTP.

Construct validity on both Weibull and stated value under both cleaning methods A and C is good, though the Weibull assumption with cleaning approach C performs best. Estimates based on a Weibull distribution and cleaning method C pass split sample scope tests as well as within sample scope tests and show that latent risk reductions are valued less than current risk reductions, a result consistent with a positive rate of time preference (Tables E.9 and E.6). The Weibull regressions on the pooled sample created by using cleaning approach C also had a negative and significant coefficient on the 5 in 10,000 risk reduction in both the contemporaneous and latent risk reduction equations, indicating that even in a pooled sample, respondents were willing to pay less for a smaller risk. This is a stronger test for scope than that comparing split sample means, since it controls for other differences in the samples. Lower Turnbull with cleaning approach C performs comparably to the Weibull regression.

As explained above, the Lower Turnbull estimate of WTP as applied in this analysis is a more conservative measure of willingness to pay than either the stated value or the Weibull estimate. In China, a Lower Turnbull estimate was used for policy analysis, although in other countries where this survey was administered the Weibull estimates were used. To be conservative, and for use in cost-benefit analyses or less formally developing materials depicting the strength of preferences for mortality risk reduction in the population, we recommend use of a VSL based on the Lower Turnbull estimate and cleaning criteria C for Ulaanbaatar. The WTP estimate is 159,000 tugrug divided by 5 in 10,000, which is 319 million tugrug. With reported monthly household income of 402,118 tugrug, WTP is 3.3 percent of annual household income. Using the 2009 official exchange rate, this implies a VSL of $221,000 U.S. (World Bank 2010).

E6 Comparisons of results from other countries using the "same" survey

As already noted, the survey reported on above is very similar to surveys administered to respondents in other countries, including the U.S., Canada, Japan, France, Italy the U.K. and China. Key results from all these surveys are compared in Table E.13. This comparison is based on the only risk changes and statistical assumptions that are common to all eight studies: a 5/10,000 annual risk reduction and the Weibull distribution. Purchasing power parity (PPP) exchanges rates are used in this study to facilitate comparisons across countries because they provide a more realistic comparison of the tradeoffs consumers face in making expenditures in difference countries. PPP exchange rates are based on the price of a similar basket of consumer goods in relative countries rather than exchange rates that may be set by government policy for macro economic reasons. Official exchange rates are also reported because of greater uncertainty regarding exchange rates in small economies like Mongolia than in large industrial countries.

Table E.13 Mean VSL by country and study for 5 in 10,000 annual risk change (conversion to $US using PPP and official exchange rates for Mongolia; PPP for all other countries)

	Mongolia	**China**	**Canada**	**U.S.**	**Japan**	**UK**	**France**	**Italy**
	Ulaanbaatar	Shanghai, Juijiang, Nanning	Hamilton, Ontario	Entire country	Shizuoke	Bath	Strasbourg	5 cities
WTP (Current 5 in 10,000) as a % of Average Household Income	3.3%	1.68 %	1.00%	1.45%	0.81%	1.59%	7.71%	3.50%
Current VSL: 5/10,000 $ US (millions)	0.25[1] 0.57[2]	0.44	0.93	1.54	0.66	1.17	4.56	2.28
Scope test: Ratio of VSLs for 10 vs. 5 in 10,000 risk reduction	1.15	1.21	1.3	1.6	1.5	NA	?	NA
Latent VSL: 5/10,000 $US (Millions)	0.18[1] 0.40[2]	0.39	0.53	0.69	0.48	0.51	1.25	0.87
Ratio of Future to Contemporaneous VSL 5 in 10,000 risk reduction	0.61	0.90	0.57	0.45	0.73	0.44	0.27	0.38

mil. = millions
[1]official exchange rate: 1446.52 tugrug/$ 2009
[2] PPP exchange rate: 635 tugrug/$

While significant effort was made to make certain that the studies were as similar as possible, there are some unavoidable differences. WTP was elicited using a payment screen format in China, a payment card format in Mongolia and a dichotomous choice (DC) approach in the other six countries. The U.S. study used a nationally representative sample. All other studies reflect WTP in urban areas in each country.

The top row of Table E.13 gives mean WTP for a 5 in 10,000 risk reduction as a percentage of respondents' average household income in the various country studies. Because Mongolia is considerably poorer than the other countries studied, we would expect a lower VSL, but not necessarily a lower WTP as a percentage of household income. The Ulaanbaatar study implies a VSL of $575,000 U.S. for contemporaneous risk reduction, and $408,000 U.S. for latent risk reductions based on a 2009 purchasing power parity exchange rate. These are in the low to mid-range of VSL estimates in studies using this survey instrument (Table E.13). However, WTP is higher as a percentage of household income in the Mongolian study than in all other study countries except France and Italy. Sensitivity to scope for Mongolia, represented as the ratio of WTP for 10 to 5 in 10,000 risk reduction (1.15) is lower than, but roughly in the range of those found in other studies, from 1.21 for China to 1.6 in the U.S. study. Time preferences, expressed as the ratio of WTP for contemporaneous to future risk reduction, is also in the mid-range of those found in other study countries. Mongolia (with a ratio of 0.61) appears to be less future-oriented than other Asian countries in the set, namely China (0.90) and Japan (0.73) and more like Canada (0.57) and the U.S. (0.45). It must be remembered that time preferences and subjective discount rates reflect not only individuals' attitudes but also the macroeconomic conditions and institutional environment they face (Horika et al. 2006). For example, individuals with little access to credit will have a much higher savings rate than those in a country with ample consumer credit.

E7 Discussion

This study presents the results of a new stated preference study of WTP to reduce mortality risk conducted by the Mongolian Ministry of Health and Resources for the Future, funded by the World Bank. To the best of our knowledge it is the first such study to be conducted in Mongolia. The study estimates willingness to pay for mortality risk reduction in the Mongolian capital of Ulaanbaatar. The risk reduction scenarios include both a contemporaneous risk reduction and a future risk reduction because conventional air pollution causes both immediate and delayed increases in mortality risk. The study uses a survey instrument adapted from one that has been used in seven other countries, including China. This was done to permit international comparisons and, ultimately, examine benefits transfer issues. The survey also uses a payment card/screen to elicit willingness to pay. This was done because our administration of the survey in China and another stated preference study in Inner Mongolia found a payment card or "payment screen" was a useful means of overcoming excessive "yea-saying" encountered with use of a dichotomous choice payment vehicle in these studies.

The survey was fielded in Ulaanbaatar in December and January of 2009–2010. Several analyses were conducted: evaluation of respondents' understanding of the survey instrument, estimation of WTP, analysis of the robustness of WTP estimates to different approaches to data cleaning, tests for response to the scope of the risk reduction and to latency of the risk reduction, and regressions to check for construct validity.

The relationships between WTP for risk reductions of various sizes and WTP for contemporaneous and future risk reductions were generally in the direction expected by theory. These relationships were also statistically significant with appropriate sample cleaning and estimation procedures. Though we did find a higher than usual percentage of respondents who exhibited some form of problem in understanding or accepting the survey. In general regression analysis checking for construct validity also performed well. Given the appropriate performance of the instrument, a VSL of 319 million tugrug for a contemporaneous 5 in 10,000 annual risk reduction is justified by this study for use in cost-benefit analyses. This value translates into a VSL in US$ of $221,000 on the basis of the official exchange rate or $575,000 on a PPP basis. These values should be interpreted as only valid for Ulaanbaatar, not outlying rural areas of Mongolia.

References

Alberini, A., M. Cropper, A. Krupnick, and N. Simon. 2004. Does the Value of Statistical Life Vary with Age and Health Status? Evidence from the U.S. and Canada. *Journal of Environmental Economics and Management* 48: 769–792.

Alberini, A., M. Cropper, A. Krupnick, and N. Simon. 2006. Willingness to Pay for Mortality Risk Reductions: Does Latency Matter? *Journal of Risk and Uncertainty* 32: 231–245.

Alberini, Anna, Alistair Hunt, and Anil Markandya. 2006. Willingness to Pay to Reduce Mortality Risks: Evidence from a Three-country Contingent Valuation Study. *Environmental and Resource Economics* 33(2): 251–264.

Banister, Judith and Kenneth Hill. 2004. "Mortality in China 1967–2000." Population Studies 58(1): 55–75.

Boyle, K.J., and R.C. Bishop. 1988. Welfare Measurements Using Contingent Valuation: A Comparison of Techniques. *American Journal of Agricultural Economics* 70(1): 20–28.

Brown, Thomas C., Patricia A. Champ, Richard C. Bishop, and Daniel W. McCollum. 1996. Which Response Format Reveals the Truth about Donations to a Public Good? *Land Economics* 72(2): 152–66.

Chestnut, L., R. Rowe, and W. Breffle. 2004. Economic Valuation of Mortality Risk Reduction: Stated Preference Approach in Canada. Report for Health Canada prepared by Stratus Consulting, Dec. 23.

Cropper, Maureen, and F. G. Sussman. 1990. Valuing Future Risks to Life. *Journal of Environmental Economics and Management* 19: 160–174.

Desvousges, William H., V. Kerry Smith and Matthew P. McGivney. 1983. A Comparison of Alternative Approaches for Estimating Recreation and Related Benefits of Water Quality Improvements. EPA-230-05-83-001. Office of Policy Analysis, U.S. Environmental Protection Agency. Washington, DC.

Melissa L. Finucane, Paul Slovic, C. K. Mertz; James Flynn Theresa A. Satterfield. 2000. Gender, Race, and Perceived Risk: The 'White Male' Effect. Health, Risk and Society. 2:159–172.

Flynn, James, Paul Slovic, and C.K. Mertz. 1994. Gender, Race, and Perception of Environmental-Health Risks. Risk Analysis 14: 1101–1108.

Haefele, M., R. Kramer, and T. Holmes. 1992. Estimating the total value of forest quality in high-elevation spruce-fir forests. In *The Economic Value of Wilderness*. General Technical Report SE-78, Southern Forest Experiment Station, Research Triangle Park, NC.

Hammitt, J.K. and Y. Zhou. 2006. The Economic Value of Air-Pollution-Related Health Risks in China: A Contingent Valuation Study. *Environmental and Resource Economics* 33: 399–423.

Hamermesh, D. 1985. Expectations, Life Expectancy, and Economic Behavior. *Quarterly Journal of Economics* 100: 389–408.

Holmes, T.P., and R.A. Kramer. 1995. An Independent Sample Test of Yea-Saying and Starting Point Bias in Dichotomous-Choice CV. *Journal of Environmental Economics and Management* 29: 121–23.

Horioka, Charles Yuji and Junmin Wan. 2006. The determinants of household saving in China: A dynamic panel analysis of provincial data, NBER Working Paper Series12723 http://www.nber.org/papers/w12723, National Bureau of Economic Research (December)

Hurd, M., and K. McGarry. 1996. The Predictive Validity of the Subjective Probabilities of Survival in the Health and Retirement Survey. Economics Department, SUNY Stony Brook. March.

Itaoka, K., A.J. Krupnick, M. Akai, A. Alberini, M. Cropper, and N.B. Simon. 2005. Age, Health, and the Willingness to Pay for Mortality Risk Reductions: A Contingent Valuation Survey in Japan. Discussion paper 05-34. Washington DC: Resources for the Future.

Krupnick, A., and A. Alberini. 2000. Cost of Illness and WTP Estimates of the Benefits of Improved Air Quality in Taiwan. *Land Economics* 76 (1): 37–53.

Krupnick, A.J., A. Alberini, M. Cropper, N. Simon, B. O'Brien, R. Goeree, and M. Heintzelman. 2002. Age, Health and the Willingness to Pay for Mortality Risk Reductions: A Contingent Valuation Study of Ontario Residents. *Journal of Risk and Uncertainty* 24: 161–186.

Li, Y., M. Bai, W. Zhang, K. Yang, X. Wang. 2002. Analysis on the influence factors of residents' willingness to pay for improving air quality in Beijing, *China Population, Resources and Environment* 12(6): 123–126.

Mitchell, R.C., and R.T. Carson. 1981. An Experiment in Determining Willingness to Pay for National Water Quality Improvements. Draft report to the U.S. Environmental Protection Agency, Washington, DC.

Mitchell, R.C., and R.T. Carson. 1984. A Contingent Valuation Estimate of National Freshwater Benefits: Technical Report to the U.S. Environmental Protection Agency. Resources for the Future Press, Washington, DC.

National Oceanic and Atmospheric Administration. 1993. Natural Resource Damage Assessments under the Oil Pollution Act of 1990. *Federal Register* 58(10): 4601–4614.

National Statistical Office of Mongolia. 2009. Yearbook.

Ready, R., J. Buzby, and D. Hu. 1996. Differences between Continuous and Discrete Contingent Value Estimates. *Land Economics* 72: 397–411.

Ready, R.C., S. Navrud, and W.R. Dubourg. 2001. How Do Respondents with Uncertain Willingness to Pay Answer Contingent Valuation Questions? *Land Economics* 77(3): 315–26.

Reaves, D.W., R.A. Kramer, and T.P. Holmes. 1999. Does Question Format Matter? Valuing an Endangered Species. *Environmental and Resource Economics* 14: 365–83.

Rowe, R., W. Schulze, and W. Breffle. 1996. A Test for Payment Card Biases. *Journal of Environmental Economics and Management* 31: 178–185.

Smith, V.K., and W.H. Desvousges. 1987. An Empirical Analysis of the Economic Value of Risk Changes. *Journal of Political Economy* 95: 89–113.

United Nations. UNdata: A World of Information. Life expectancy at birth and life expectancy at age x. http://data.un.org. Accessed Oct. 20, 2010.

Wang, H., J. Mullahy, D. Chen, L. Wang, and R. Peng. 2001. Willingness to pay for reducing the risk of death by improving air quality: a contingent valuation study in Chongqing, China. Paper presented at the Third International Health Economic Association Conference in York, UK.

Wang H., and D. Whittington. 2005. Measuring Individuals' Valuation Distributions Using a Stochastic Payment Card Approach. *Ecological Economics* 55: 143–54.

Welsh, M., and G. Poe. 1998. Elicitation Effects in Contingent Valuation: Comparisons to a Multiple Bounded Discrete Choice Approach. *Journal of Environmental Economics and Management* 36: 170–185.

World Bank. 2010. World Development Indicators.

World Bank 2011: 2010. Willingness to Pay for Mortality Risk Reductions. Draft working paper. Prepared by Krupnick, A., S. Hoffmann, and Q. Ping under contract with the World Bank.

Zhang, X. 2002. *Valuing mortality risk reductions using the contingent valuation methods: evidence from a survey of Beijing Residents in 1999*. Beijing, China: Centre for Environment and Development, Chinese Academy of Social Sciences.

Zhang, M., J. Fan, C. Hu, B. Zhang (2004), "Assessment of Total Economic Value of Improving Atmospheric Quality of Lanzhou," *Journal of Arid Land Resources and Environment* (in Chinese), 18, 3: 28–32.

Zhongmin, X., C. Guodong, Z. Zhiqiang, S. Zhiyong, and J. Loomis. 2003. Applying Contingent Valuation in China to Measure the Total Economic Value of Restoring Ecosystem Services in Ejina Region. *Ecological Economics* 44: 345–358.

Ulaanbaatar, Mongolia, Air Monitoring and Health Impact Baseline (AMHIB) Reports

Annex F

Air Pollution Abatement Options and their Costs in Ulaanbaatar

Table of Contents

General note on emissions from stoves

Traditional stoves emit the bulk of their PM during the start-up phase, as measured in SEET laboratory. These stoves emit, over an entire burning cycle, 300–350 mg $PM_{2.5}$ per MJ heat produced. During the first 30 minutes of the burning cycle ("start-up"), PM emissions are as high as 10 g/m^3, but quickly reduce to 10s of micrograms/m^3 during the regular burning or coking phase. Clean stoves have a start-up phase of several minutes (1–5) instead of 30 minutes, and emission levels are less than 1 g/m^3. Total emissions over a burning cycle are 3–10 mg/MJ of heat. Refueling with a hot fire does briefly increase emissions, but by far less than during the start-up. Thus, PM emissions relate mainly to the cold-start of the fire. Therefore, the emissions comparison between the different stoves should depend on the number of cold starts, which varies during the heating season. The following matrix was used.

		cold starts							
	Total/season	*Sept*	*Oct*	*Nov*	*Dec*	*Jan*	*Feb*	*Mar*	*Apr*
Ger	840	1	2	4	5	6	6	3	1
Home without Heating wall	840	1	2	4	5	6	6	3	1
Home with heating wall	600	1	2	3	3	4	4	2	1
Home with LPB	360	1	2	2	2	1	1	2	1

The total number of cold starts has been multiplied by the estimated emissions over a burning cycle for each heating system. This is a conservative estimate, since the burning cycle for clean stoves is considerably longer, requiring even less cold-starts. This has not been reflected in the analysis because there are no hard data. The emissions over a burning cycle were measured at SEET, and these are confirmed.

Backlighting

Cost of traditional stoves: $30 Source: ASTAE 2009 (USD 2009).

Emissions reductions (PM) from better ignition without changing the stove: 50 percent, Source: S. Lodoysamba, C. Pemberton-Pigott. 2010. "The Contribution of Domestic Stoves to Poor Air Quality in Ulaanbaatar."

Fuel cost savings: 0 percent, Source: SEET, 2011.

Emissions reductions (PM) from better ignition with stove modifications: 60 percent, Source: S. Lodoysamba, C. Pemberton-Pigott. 2010. "The Contribution of Domestic Stoves to Poor Air Quality in Ulaanbaatar."
Fuel savings: 10 percent; estimation, C. Pemberton-Pigott
Stove modification cost: $10 (insert more bricks into the stove)
Added benefit, not valued: stove burn time is longer, up to 5 hrs compared to 3 for traditional stove

Cleaner stoves

Cost of traditional stoves: $30 Source: ASTAE 2009 (USD 2009).
Cost of low-pressure boiler systems: $120 Estimate (USD 2009).
Cost of certified stoves: $100 Source: MCA Proposal July 2009.

Proposed level of subsidy: 70 percent. Higher levels of subsidies may be necessary for the poorest households.

Cost of subsidy to Project: $70.00
Cost to beneficiary household: $30.00
Cost of consumer financing to project: 10 percent, Fees and terms of consumer loans need to be negotiated with banks; MCC.

Annual MCC target: certified stoves: 22,500 Disseminated to replace traditional stoves in any condition and all 'improved' stoves that would have been replaced. It is assumed that certified stoves would not generally replace low-pressure boiler heating systems, so LPB replacement rates are unaffected.

Life of cleaner stoves: 10 years after which, the household reverts to the type of stove originally replaced. Fuel savings by cleaner stoves: 10 percent This assumption is well below some claims, but is in line with reasonable expectations for stoves that provide both cooking and space heating services.
Emissions reductions by certified stoves: 90 percent, source: SEET, 2011
Fuel saving certified stoves: 20 percent, source: SEET, 2011

Semi-coked coal

Cost of traditional stoves: $30 Source: ASTAE 2009 (USD 2009).
Cost of low-pressure boiler systems: $120 Estimate (USD 2009).
Cost of certified stoves: $ 100 Source: MCA Proposal July 2009.

Proposed level of subsidy: 70 percent. Higher levels of subsidies may be necessary for the poorest households.

Cost of subsidy to Project: $70.00
Cost to beneficiary household: $30.00
Cost of consumer financing to project: 10 percent, Fees and terms of consumer loans need to be negotiated with banks; MCC.

Annual MCC target: certified stoves: 22,500 Disseminated to replace traditional stoves in any condition and all 'improved' stoves that would have been replaced. It is assumed that certified stoves would not generally replace low-pressure boiler heating systems. As a result, LPB replacement rates are unaffected.

Life of certified stoves: 10 years after which, the household goes back to the type of stove originally replaced. Fuel savings by certified stoves: 10 percent This assumption is well below some claims, but is in line with reasonable expectations for stoves that provide both cooking and space heating services.

Emissions reductions by certified stoves: 70 percent. The certification target is 50 percent reduction in PM emissions or better and such performance is necessary to clean up the air in UB.
Additional emission reduction from the use of SCC: 10 percent However, this is not certain and there is no proof that SCC will reduce emission; it may increase emissions and possibly a new stove will also be needed.

Investments for SCC plant: $11.2 million; Source: Smokeless UB proposal
Equalization subsidy as per Operational Framework, source: EBRD

Electric heating

Source: Heating in poor, peri-urban Ger areas of Ulaanbaatar—ASTAE October '09, Annex 6

Average non-heating electricity demand per family: 0.9 kW
Heating capacity (W) needed to heat one square meter: 150 W
Average heating area (small house, 5 × 6 m): 30 m^2
Total heating capacity needed for a detached house (150 × 30 m^2 = 4,500 W): 4.5 kW
Total heating capacity needed for a ger (150 × 22 m^2 = 3,300 W): 3.3 kW
(An apartment is considered to have the same assumptions as those for the detached house, because the detached house uses small house information)
Average capacity needed for electric heating: 4 kW
Average tariff day time: Tg 51.6/kWh
Average tariff night time: Tg 12/kWh
Transmission system rehabilitation and upgrade: $150 million
Electric heaters, 150,000 × $300: $45 million
Internal wiring, special meter, envelope renovation, 150,000 × $1000: $150 million
Heating hours per day: 18 hours/day

For 2010–2014, it is assumed that feasibility study, environmental impacts assessment and other safeguard issues, financial mobilization, construction periods will be conducted.

By 2023, households with electric heating require total additional capacity MW (total of 2015–2023): 1,122 MW
By 2023, the capital costs for the total additional capacity MW (total costs of 2015–2023): $1,683 million
Cost data for new apartment buildings: the Government's Smokeless UB proposal, 2010
Number of new apartments installed: the Government's Smokeless UB proposal, 2010

Apartment buildings

Cost data for new apartment buildings: the Government's Smokeless UB proposal, 2010
Number of new apartments installed: the Government's Smokeless UB proposal, 2010
Other information: Heating in poor, peri-urban ger areas of Ulaanbaatar-ASTAE October '09, Annex 6

Average non-heating electricity demand per family: 0.9 kW
Heating capacity (W) needed to heat 1 square meter: 150 W
Average heating area (small house, 5 × 6 m): 30 m^2
Total heating capacity needed for a detached house (150 × 30 m^2 = 4,500 W): 4.5 kW
Total heating capacity needed for a ger (150 × 22 m^2 = 3,300 W): 3.3 kW
(Apartment is considered to have the same assumptions as those for the detached house, because the detached house uses small house information.)
Average capacity needed for electric heating: 4 kW
Average tariff day time: Tg 51.6/kWh
Average tariff night time: Tg 12/kWh
Transmission system rehabilitation and upgrade: 150 US$ million
Electric heaters, 150,000 × $300: $45 million
Internal wiring, special meter, envelope renovation, 150,000 × $1000: $150 million
Heating hours per day: 18 hours/day
For 2010–2014, it is assumed that a feasibility study, environmental impacts assessment and other safeguard issues, financial mobilization, construction periods will be conducted.
By 2023, households with electric heating require total additional capacity MW (total of 2015–2023): 1,122 MW
By 2023, the capital costs for the total additional capacity MW (total costs of 2015–2023): $1,683 million

Reduction of road dust

In the ger areas of Ulaanbaatar (including city center, mid-tier, and fringe ger areas), the combined length of earthen and paved road is 80,929 km with the majority,, 72,313 km or 89.4 percent, being earthen road (Kamata et al. 2010). Under this scenario of reducing dust from road, it is assumed that 500 km of these roads will be paved and sidewalk constructed between 2016–23. Also, it is expected that these newly paved roads will be swept. In addition, it is also expected that existing paved and unpaved roads will be swept, with an annual increase of 1,000 km for each category of road. Based on the above assumptions, PM_{10} reduction from roads are estimated to come from (i) newly paved roads and the sidewalk along the newly paved roads; (ii) sweeping of these newly paved roads; and (iii) sweeping of existing paved and unpaved roads. Only hard surfaced unpaved roads are supposed to be swept. It is assumed that the dustiest roads will be paved and swept first. For the 2010–15, feasibility study, it is also expected that environmental impacts assessment and other safeguard issues, financial mobilization, construction periods will be conducted. Unpaved road in the city center and nearby are assumed to have less traffic. Other data used for this analysis are the following.

Road pavement capital cost: 28 mil MNT/km (Kamata et al. 2010)
Sidewalks capital cost: 21 mil MNT/km (Kamata et al. 2010)
Road O&M cost: 5 percent of capital cost
Calculated emission factor unpaved road (g/km travelled): 2312.2 (Guttikunda 2007)
Calculated emission factor paved road (g/km travelled): 700.6 (Guttikunda 2007)
Max PM10 dust as per Inventory (t) paved: 5,142 (2008 value, Table 4.3 of this study) Max PM_{10} dust as per Inventory (t) unpaved: 4,812 (2008 value, Table 4.3 of this study)
Paved road length: 8,616 km (Kamata et al. 2010)

Unpaved road length: 72,313 km (Kamata et al. 2010)
PM_{10} per km paved: 0.60 ton/km
(Equivalent for unpaved road in the city center or nearby assumed to be 0.4 ton/km)
PM_{10} per km unpaved 0.07 ton/km
(This is low despite the high emission factor because many unpaved roads have low traffic)
PM_{10} reduction by sweeping: 33 percent (based on 33 percent reduction by wet cleaning (Guttikunda 2007) and 36.27 percent reduction by sweeping (World Bank 2007))
Paving the unpaved road and constructing sidewalk along the road: 500 km/year
Existing paved road sweeping: 1,000 km/year
Existing unpaved road sweeping: 1,000 km/year
Road sweeping cost (MNT mil/ton of PM_{10} reduction): 0.647 (World Bank 2007)

Greening of the city

Number of areas to be vegetated is based on the smokefree Ulaanbaatar national program 2010–16. In this program, 0.7 percent (about 952 hectares) of Ulaanbaatar's land is to be annually vegetated during the period. This value of vegetation of 952 hectare per year is assumed to continue from 2011 to 2023. This includes reforestation, planting broad-leafed trees upstream of the Tuul and Selbe rivers, greenbelt establishment, land reclamation, among other things. Other initiatives include a ger district garden, a garden near power plant number four, national park, dust reduction through the re-vegetating of city public spaces and roads,. These actions are additional and are not included in the assumption of annual vegetation of 952 hectares.

It is assumed that half of the annual increase of vegetation cover will die per year.

Mongolia's data on PM_{10} deposition rate to trees or any types of vegetation was not available. Since PM_{10} deposition to any types of vegetation is very specific to each situations (e.g, wind speed, surrounding building, climate, temperature, latitude, type of vegetation, and so forth), the estimation is made conservatively, taking the middle value of an estimated range of PM_{10} deposition rates in the United Kingdom (Hewitt 2010) and changes depending on the value of the deposition rate used. Also, data on the prevention of suspension by vegetation cover is not available for Mongolia/UB. Thus, secondary data in Mojave Desert in the United States was used to make a conservative estimate (Grantz et al. 1998). Thus, this analysis should be interpreted as an exercise.

PM_{10} deposition rates to trees: 5.0 kg/ha/yr (Hewitt 2010)
(Average of an estimated range of 1–10 kg/ha/yr by Hewett (2010) is used)
PM_{10} reduction by fugitive dust stabilization by vegetation:80 percent
(estimated from Grantz et al. (1998) at 83 percent reduction)
Cost of reforestation capital cost:0.5 mil MNT/ha/yr
(estimated from the smokefree Ulaanbaatar national program 2010–16)
Vegetation cover increase (ha): 0.70 percent per year
(estimated from the smokefree Ulaanbaatar national program 2010–16)
Reforestation O&M cost: 5 percent of capital cost

Total soil dust suspension PM10 emissions (ton/year) 13,557 ton/year

Estimate of the total soil dust suspension PM_{10} emissions: Due to the way PM suspension from soil is introduced into the model (see Annex C), a figure for the total soil suspension of PM is not easily available. An estimate of the total soil suspension of PM_{10} is calculated based upon the total ger stove emissions: 19,731 tons/year. The spatial distribution of the soil suspension is similar to the spatial distribution of the ger stove emissions. Thus, the ratio between soil suspension PM and ger stove PM emissions is equal to the ratio between the contributions to the PWE (population-weighted exposure) from these two sources. The contribution from ger stove emissions to the PWE in 2007 was 195.6 $\mu g/m^3$ (see table 4.4), while the contribution from soil dust suspension was 134,4 $\mu g/m^3$ (see Table 4.4). Multiplying the ger stove emissions, 19,731 tons/year by the ratio 134.4/195.6 gives 13,557 tons/year, which is the estimate for soil suspension emissions of PM_{10}.

Sweeping cost of new road pavement (mil MNT) is estimated as:

[Road pavement and sidewalks PM_{10} Dust reduction (ton)+ Sweeping PM_{10} Dust reduction of new paved road (ton)] * [Road Sweeping cost MNT mil/ton of PM_{10} reduction]

Sweeping PM_{10} dust reduction of new paved road (ton) is estimated as:

[New Road pavement and sidewalk/year (km)]* [PM_{10} per km paved (an equivalent for unpaved road in the city center or nearby assumed to be 0.4 ton/km see above assumption)]* [Sweeping reduction of the dust PM_{10} by 33 percent]

PM_{10} reduction by sweeping existing paved road (ton) is estimated as:

[Sweeping of existing paved road (km)]*[PM_{10} per km paved]*[[Sweeping reduction of the dust PM_{10} by 33 percent]

Sweeping cost of paved roads (mil MNT) is estimated as:

[PM_{10} reduction by sweeping existing paved road (ton)]*[Road Sweeping cost MNT mil/ton of PM_{10} reduction]

O&M cost (mil MNT) of vegetation is estimated as:

[Vegetation remains alive, cumulative (ha)]*[Cost of reforestation capital cost/ha]*[O&M cost/ha]

Scenarios seven and eight—Road dust reduction and greening the city

Two additional scenarios of fugitive dust reduction in terms of PM_{10} are included: (i) paving of unpaved roads with construction of sidewalk and sweeping the newly paved roads and existing paved roads; and (ii) increasing vegetation in the city.

Table F.1 Impact and costs of the different scenarios for PM reduction

	2009	2010	2011	2012	2013	2014	2015	2016	2017	2018	2019	2020	2021	2022	2023
Scenario 1a: backlighting															
total costs/benefits (US$ million)	0.2	0.3	0.7	1.2	1.3	1.3	1.3	1.4	1.3	1.4	1.4	1.5	1.5	1.6	1.6
total investment costs	0.2	0.2	0.2	0.2	0.1	0.1	0.1	0.1	-	-	-	-	-	-	-
costs program	0.2	0.2	0.2	0.2	0.1	0.1	0.1	0.1	-	-	-	-	-	-	-
costs propellant	-	0.1	0.5	1.0	1.2	1.2	1.3	1.3	1.3	1.4	1.4	1.5	1.5	1.6	1.6
firewood savings	-	-	-	-	-	-	-	-	-	-	-	-	-	-	-
emission reduction	0%	3%	19%	40%	45%	45%	45%	45%	45%	44%	44%	44%	44%	43%	43%
Scenario 1b: modifications															
total costs/benefits (US$ million)	0.20	0.13	(0.39)	(1.46)	(2.25)	(2.50)	(2.58)	(2.65)	(2.78)	(2.86)	(2.94)	(3.03)	(3.12)	(3.21)	(3.30)
total investment costs	0.20	0.26	0.59	0.70	0.27	0.08	0.09	0.09	0.04	0.04	0.04	0.04	0.04	0.04	0.04
costs program	0.20	0.20	0.20	0.15	0.10	0.05	0.05	0.05	-	-	-	-	-	-	-
costs modification	-	0.06	0.39	0.55	0.17	0.03	0.04	0.04	0.04	0.04	0.04	0.04	0.04	0.04	0.04
savings of fuel	-	(0.14)	(0.98)	(2.15)	(2.51)	(2.59)	(2.66)	(2.74)	(2.82)	(2.90)	(2.98)	(3.07)	(3.16)	(3.25)	(3.35)
emission reduction	0%	4%	31%	67%	75%	75%	75%	75%	74%	74%	74%	73%	73%	73%	72%
Scenario 2: clean stoves															
total costs/benefits (US$ million)	-	-	0.87	(0.11)	(1.09)	(1.90)	(2.94)	(3.98)	(5.96)	(6.19)	(6.77)	(7.00)	(6.52)	(6.75)	(6.98)
total investment costs	-	-	1.84	1.83	1.82	1.97	1.90	1.82	0.06	0.04	(0.32)	(0.34)	0.35	0.34	0.32
- costs program	-	-	1.6	1.6	1.6	1.6	1.6	1.6	0.4	0.4	-	-	-	-	-
- costs stoves	-	-	0.3	0.3	0.2	0.4	0.3	0.2	(0.3)	(0.3)	(0.3)	(0.3)	0.4	0.3	0.3
- costs fuel	-	-	(1.0)	(1.9)	(2.9)	(3.9)	(4.8)	(5.8)	(6.0)	(6.2)	(6.4)	(6.7)	(6.9)	(7.1)	(7.3)
emission reduction	0%	0%	16%	30%	44%	56%	68%	79%	80%	80%	80%	80%	80%	80%	79%

continued

	2009	2010	2011	2012	2013	2014	2015	2016	2017	2018	2019	2020	2021	2022	2023
Scenario 3: SCC + clean stoves															
total costs/benefits (US$ million)	-	0.31	10.13	11.35	12.75	13.79	1.50	1.11	0.63	0.46	0.30	0.13	0.66	0.49	0.31
total investment costs	-	0.66	10.99	12.73	14.64	16.19	4.42	4.55	4.21	4.19	4.18	4.16	4.85	4.84	4.82
- equalization costs	-	-	3.2	8.9	14.4	15.8	4.1	4.3	4.5	4.5	4.5	4.5	4.5	4.5	4.5
- costs stoves	-	-	0.3	0.3	0.2	0.4	0.3	0.2	(0.3)	(0.3)	(0.3)	(0.3)	0.4	0.3	0.3
- costs fuel	-	(0.4)	(0.9)	(1.4)	(1.9)	(2.4)	(2.9)	(3.4)	(3.6)	(3.7)	(3.9)	(4.0)	(4.2)	(4.4)	(4.5)
- cost SCC production plant	-	0.7	7.5	3.6	-	-	-	-	-	-	-	-	-	-	-
-	-	-	-	-	-	-	-	-	-	-	-	-	-	-	-
emission reduction	0%	0%	11%	9%	10%	17%	35%	59%	59%	60%	60%	60%	60%	59%	59%
Scenario 4: electric heating															
total costs/benefits (US$ million)	-	206.00	300.08	346.74	376.35	258.73	101.67	83.27	86.59	90.06	93.71	97.53	101.54	105.76	47.46
total investment costs	-	204.56	295.61	335.94	358.78	233.92	72.55	53.10	55.33	57.66	60.12	62.70	65.42	68.28	8.56
- program	-	0.2	0.2	0.1	0.1	-	-	-	-	-	-	-	-	-	-
- stoves	-	1.7	3.7	7.7	8.2	8.7	5.2	1.2	1.3	1.3	1.4	1.5	1.5	1.6	1.6
- energy	-	1.4	4.5	10.8	17.6	24.8	29.1	30.2	31.3	32.4	33.6	34.8	36.1	37.5	38.9
- develop infrastructure	-	202.6	291.7	328.2	350.5	225.2	67.4	51.9	54.0	56.3	58.7	61.3	63.9	66.7	6.9
Emission reduction	0%	5%	15%	35%	55%	75%	85%	85%	85%	85%	85%	85%	85%	85%	85%
Scenario 5: relocation into apartments															
total costs/benefits (US$ million)	-	-	-	-	-	-	260.90	354.85	529.75	613.91	814.38	842.82	1,028.93	1,256.48	1,534.70
total investment costs	-	-	-	-	-	-	261.61	356.97	533.95	620.72	824.53	856.78	1,047.30	1,280.22	1,565.00
- apartments							195.5	265.5	398.8	460.6	621.2	645.5	787.7	961.2	1172.9
- energy							-0.7	-2.1	-4.2	-6.8	-10.2	-14.0	-18.4	-23.7	-30.3
- develop infrastructure							66.1	91.5	135.1	160.1	203.4	211.3	259.6	319.0	392.1
emission reduction	0%	0%	0%	0%	0%	0%	3%	7%	13%	20%	28%	36%	45%	56%	69%

Table F.2 Results of HOB scenario

Scenario	**2010**	**2011**	**2012**	**2013**	**2014**	**2015**	**2016**	**2017**	**2018**	**2019**	**2020**	**2021**	**2022**	**2023**
efficient boilers installed	36	38	46	56	65	70	75	80	85	90	90	90	90	90
medium efficient ,,,,	18	16	10	4	0									
inefficient,,,,	36	36	34	30	25	20	15	10	5	0				
boilers replaced (med-> eff)		2	6	6	4	0	0	0	0	0	0	0	0	0
boilers replaced (in eff-> eff)		0	2	4	5	5	5	5	5	5	0	0	0	0
consumption (t/season)	66,526	66,033	63,569	60,120	56,670	54,206	51,743	49,279	46,815	44,351	44,351	44,351	44,351	44,351
reduction in consumption	0%	1%	4%	10%	15%	19%	22%	26%	30%	33%	33%	33%	33%	33%
emission (normative/season)	91,806	90,870	85,893	78,747	71,454	66,033	60,613	55,192	49,771	44,351	44,351	44,351	44,351	44,351
reduction in emissions	0%	1%	6%	14%	22%	28%	34%	40%	46%	52%	52%	52%	52%	52%
cost of investments (million US$)	-	0.24	1.02	1.32	1.23	0.75	0.75	0.75	0.75	0.75	-	-	-	-
energy savings (million US$)	-	0.02	0.11	0.23	0.35	0.44	0.53	0.62	0.70	0.79	0.79	0.79	0.79	0.79
total costs	-	0.22	0.91	1.09	0.88	0.31	0.22	0.13	0.05	(0.04)	(0.79)	(0.79)	(0.79)	(0.79)
NOTE: emissions are relative to the consumption of coal for HOB use only														
total costs/benefits (US$ million)	0.20	0.62	1.31	1.29	1.08	0.51	0.42	0.33	0.15	0.06	(0.79)	(0.79)	(0.79)	(0.79)
total costs (US$ million)	0.20	0.64	1.42	1.52	1.43	0.95	0.95	0.95	0.85	0.85	-	-	-	-
- program management	0.20	0.40	0.40	0.20	0.20	0.20	0.20	0.20	0.10	0.10				
- investments	-	0.24	1.02	1.32	1.23	0.75	0.75	0.75	0.75	0.75	-	-	-	-
- energy	-	(0.02)	(0.11)	(0.23)	(0.35)	(0.44)	(0.53)	(0.62)	(0.70)	(0.79)	(0.79)	(0.79)	(0.79)	(0.79)
emission reduction	0%	1%	6%	14%	22%	28%	34%	40%	46%	52%	52%	52%	52%	52%

NPV costs	$5.9	million
average emission reduction	32%	
US$ million needed for 1% reduction	$18.2	million

Please note that emission reduction is relative to the emissions from HOB only, not to the overall emissions in UB.

Table F.3 Paving roads and greening the city

	2010	2011	2012	2013	2014	2015	2016	2017	2018	2019	2020	2021	2022	2023
New road pavement and sidewalk/year (km)							500	500	500	500	500	500	500	500
Capital cost (mil MNT)							24,500	24,500	24,500	24,500	24,500	24,500	24,500	24,500
O&M cost of new road pavement and sidewalk (mil MNT)							1,225	2,450	3,675	4,900	6,125	7,350	8,575	9,800
Sweeping cost of new road pavement (mil MNT)							276	553	829	1,106	1,382	1,659	1,935	2,212
Road pavement and sidewalks PM_{10} Dust reduction (ton)							362	723	1,085	1,447	1,808	2,170	2,532	2,893
Sweeping PM10 Dust reduction of new paved road (ton)							66	164	263	361	460	558	657	755
Sweeping of existing paved road (km)							1,000	2,000	3,000	4,000	5,000	6,000	7,000	8,000
PM_{10} reduction by sweeping existing paved road (ton)							197	394	591	788	985	1,182	1,379	1,576
Sweeping cost of paved roads (mil MNT)							127	255	382	509	637	764	891	1,019
Max PM_{10} dust as per Inventory (t) paved and unpaved road						9,954	9,954	9,954	9,954	9,954	9,954	9,954	9,954	9,954
Total PM_{10} reduction (ton)							625	1,282	1,939	2,596	3,253	3,910	4,567	5,224
Reduction						0.0%	6.3%	12.9%	19.5%	26.1%	32.7%	39.3%	45.9%	52.5%
Total costs (US$ million)						-	19	20	21	22	23	24	26	27

	2010	2011	2012	2013	2014	2015	2016	2017	2018	2019	2020	2021	2022	2023
New plantings (ha)		951.6	952	952	952	952	952	952	952	952	952	952	952	952
Cumulative Vegetation cover increase (ha)		952	1,903	2,855	3,806	4,758	5,709	6,661	7,612	8,564	9,516	10,467	11,419	12,370
Remains alive, cum (ha)		476	952	1,427	1,903	2,379	2,855	3,330	3,806	4,282	4,758	5,234	5,709	6,185
planting capital cost (mil MNT)		476	476	476	476	476	476	476	476	476	476	476	476	476
O&M cost (mil MNT)		12	24	36	48	59	71	83	95	107	119	131	143	155
PM_{10} Dust reduction by deposition to vegetation (ton)		2	5	7	10	12	14	17	19	21	24	26	29	31
PM_{10} reduction by fugitive dust stabilization by vegetation (t)		76	152	228	304	380	456	532	608	684	760	836	912	988
Total PM_{10} reduction (t)		78	157	235	313	392	470	549	627	705	784	862	940	1,019
Max total PM_{10} dust in UB (t)	13,557	13557	13557	13557	13557	13557	13557	13557	13557	13557	13557	13557	13557	13557
Reduction	0.00%	0.58%	1.16%	1.73%	2.31%	2.89%	3.47%	4.05%	4.62%	5.20%	5.78%	6.36%	6.94%	7.52%
Total costs (US$ million)	-	0.3	0.4	0.4	0.4	0.4	0.4	0.4	0.4	0.4	0.4	0.4	0.4	0.5

continued

	2010	2011	2012	2013	2014	2015	2016	2017	2018	2019	2020	2021	2022	2023
Scenario 7: road dust														
- investments	0.0	0.0	0.0	0.0	0.0	0.0	18.7	19.8	21.0	22.2	23.3	24.5	25.6	26.8
PM reduction	0.0%	0.0%	0.0%	0.0%	0.0%	0.0%	6.3%	12.9%	19.5%	26.1%	32.7%	39.3%	45.9%	52.5%
NPV costs	$66.73	million												
average emission reduction	16.8%													
US$ million needed for 1% reduction	398	million												
Scenario 8: greening														
- investments	0.0	0.3	0.4	0.4	0.4	0.4	0.4	0.4	0.4	0.4	0.4	0.4	0.4	0.5
PM reduction	0.00%	0.58%	1.16%	1.73%	2.31%	2.89%	3.47%	4.05%	4.62%	5.20%	5.78%	6.36%	6.94%	7.52%
NPV costs	$2.51	million												
average emission reduction	3.76%													
US$ million needed for 1% reduction	67	million												

Ulaanbaatar, Mongolia, Air Monitoring and Health Impact Baseline (AMHIB) Report.

Annex G

PM measurement data[1]

Table of Contents

[1]This report was written by the following World Bank consultants under the AMHIB project: Steinar Larssen, Sereeter Lodoysamba, Dagva Shagjjamba and Gunchin Gerelmaa. It was peer reviewed by Dick van den Hout, Netherlands Organization for Applied research/TNO, Sameer Akbar, World Bank, M. Khaliquzzaman, World Bank consultant and Taizo Yamada, JICA. World Bank Task Team Leaders were Jostein Nygard and Gailius Draugelis.

A: AMHIB data quality assessment

Section 1 of Annex G shows results of inter-comparison campaigns between instruments participating in the AMHIB measurement network. Section 2 presents the data correction procedures resulting from the inter-comparisons.

1. Comparison between the instruments in the AMHIB monitoring network

The PM measurement equipment of the AMHIB network was provided by various institutions, and differs between the various stations. The instruments utilize different measurement principles and operate under very varying pollution and meteorological conditions, which affects data quality. The following is a comparison of the PM concentration data provided by these instruments.

The comparison has been made through co-located comparison sampling that was carried out three times in 2008, each of 4–5 days duration: 4–5 and 17–20 April, 1–6 July and 17–22 November 2008. The first two campaigns were carried out at the NAMHEM monitoring station on the roof of the NAMHEM building, while the last one in November was carried out at the meteorology station UB3 located in a ger area to the west and north of UB centre. During the last campaign, NILU provided a GRIMM 107 PM monitor.

The AMHIB team carried out calibration of the air flow through the instruments used, and of the filter weighing procedure at NUM, where all the filters are weighed. The accuracy of the air flow and particle weight determinations was generally on the order of 10% or better. These uncertainties are acceptable, and cannot explain the larger instrument discrepancies. However, larger weighing errors have been detected occasionally; therefore, there can be larger discrepancies for individual data.

None of the instruments can be considered a reference instrument. The GRIMM 107 monitor, which was included in the last inter-comparison campaign in November, is a state-of-the-art monitor using optics to detect particles. It has a built-in filter that can be used to calibrate the instrument response to the local conditions. It is known, and it was demonstrated in the UB campaign, that the GRIMM instrument response is affected by the relative humidity, in that hygroscopic particles grow at high relative humidity which again increases the instrument optical response. Due to the built-in filter, this effect could be corrected for to provide PM concentration data comparable to well controlled filter samplers. In the absence of a reference instrument, the GRIMM 107 was used in this case as the instrument against which the other instruments are compared.

Table G.1 gives characteristics of the instruments in the AMHIB network.

Table G.1 Characteristics of the instruments in the AMHIB network

Instrument/Institution	Measurement principle	Characteristics/Reference
Gent sampler w/10 μm PM inlet. NUM. Stations 2 and 3 (Sampler is denoted NUM and NRC at stations 2 and 3 respectively)	Filtering. Gravimetric analysis	The sampler has two filters in series, separating the particles in 2 size fractions. The instrument has sampling artifacts explained below (1). http://www.informaworld.com/smpp/content~db=all~content=a779035212
C-20 sampler w/ special inlet. CLEM. Station 5	Filtering. Gravimetric analysis	Japanese instrument. The inlet to the sampler is designed to cut particles larger than 10 μm. The performance of the inlet is not tested.
Ecotech monitor CLEM Station 5	Beta absorption	State-of-the-art PM monitor http://www.ecotech.com.au/
Partisol 2000. NAMHEM. Station 6	Filtering. Gravimetric analysis	State-of-the-art PM sampler, USA. PM_{10} During the comparison sampling, the sampler was run with standard filters (glass fiber) except on 17–20 November, when nuclepore filters (pore size 1.2 μm) were used. http://thermoscientific.com/wps/portal/ts/products/detail?navigationId=L10405&categoryId=89579&productId=11960560
KOSA NAMHEM. Station 1	Beta absorption	Japanese instrument. Measures $PM_{2.5}$ and PM_{10}.
Dusttrak 8520 Stations 1,4,7,8	Light scattering	State-of-the-art monitor, USA. Measures $PM_{2.5}$ or PM_{10}. The response of the instrument, in UB conditions, increases significantly during high relative humidity (RH) conditions, when hygroscopic particles (containing sulfate) grow in size. http://www.ecoenvironmental.com.au/eco/dust/dustrak_8520_am.htm
GRIMM 107	Light scattering	State-of-the-art monitor, Germany. The same problem as above with increased response during high RH. http://www.grimm-aerosol.com/en/Environmental-Dust-Monitors/1/7/index.html#

1. The GENT sampler is a so-called 2-filter sampler, where particles are collected on two filters in series, the top filter (Nuclepore filter, pore size 8 μm) collects the coarse particle fraction ($PM_{10-2.5}$) and the bottom filter (Nuclepore filter, pore size 0.4 μm) collects the smaller (fine) particle fraction ($PM_{2.5}$). The separation between coarse and fine particles is acceptable for this sampler at fairly low PM concentrations, while it is not ideal when concentrations are high. Two features occur: dry coarse particles will to some extent penetrate the top (coarse PM) filter and end up on the bottom ($PM_{2.5}$) filter when the coarse fraction is large, while on the other hand, the top filter tends to clog on highly polluted days, leading to fine particles being retained on the top filter. The clogging also leads to reduced air flow through the sampler which again changes the particle cut-off diameter of the top filter towards larger diameter. These non-ideal features result in inaccuracies in the $PM_{2.5}$ determination, while they do not affect the PM_{10} determination. To avoid the filter clogging effect, the GENT

samplers were, particularly after November 2008, run intermittently (e.g. 15 minutes each hour) so that most of the hours of the day could be covered without the sampler clogging. Still, $PM_{2.5}$ determination with this sampler is uncertain in the generally very polluted UB atmosphere. The degree of uncertainty cannot be well estimated based on the data at hand.

Tables G.2 and G.3 provides specific data from the comparison campaign in November 2008, when the GRIMM 107 instrument was included. Table G.4 gives data from calibration of the GRIMM 107 response, based upon the weighing of the built-in calibration filter. Table G.4 also includes relative humidity and temperature data for the days of the November campaign.

Table G.2 PM_{10} concentrations from comparison sampling during 18–22.11. 2008, for pairs of instruments over the same operating period

Location	**NAMHEM station UB 3**						**Rel. hum. %**[2]
Date	**GRIMM 107**	**NUM**	**NRC**	**Partisol**[1]	**CLEM C-20**	**Kosa**	
18-19.11	799	525					60
	874		571				60
	426			218			54
	1290				100	149	73
19-20.11	509	352					38
	500		376				38
	131			73			45
	487				-	233	46
20-21.11	592	472	928				43
	189			44			40
	619				212	153	58
21-22.11	430	434					37
	674		707				40
	703			355	241	85	56

[1]Partisol was run with Nuclepore 1.2 µm pore size filter, except for the last day, when it was run with standard glass fiber filter
[2]RH during the most PM exposed periods during each sampling period. NAMHEM data.

Table G.3 $PM_{2.5}$ concentrations from comparison sampling during 18–22.11.2008, for pairs of instruments over the same operating period

Location	**NAMHEM station UB 3**					**NAMHEM**
Date	**GRIMM**	**NUM**	**NRC**	**Dusttrak 1**	**Dusttrak 2**	**KOSA**
18-19.11	454	181				
	502		195			
	953			915	1080	133
19-20.11	241	270				
	237		224			
	272			338	398	194
20-21.11	248	337	615			
	363			411	469	132
21-22.11	137	288				
	286		337			
	418			-	528	80

Table G.4 Calibration of the GRIMM instrument response relative to the built-in filter. PM_{10}

Location		NAMHEM station UB 3				
Date	GRIMM response, optical	GRIMM, filter	Ratio Filter/ optical response	Rel. hum. average	Rel. hum. Most exposed hours	Temp Degrees C average
17-18.11	884	431	0.49	75	79	-17
18-19.11	1290	741	0.57	68	73	-12
19-20.11	487	325	0.67	50	46	-5
20-21.11	619	445	0.72	60	58	-7
21-22.11	703	486	0.67	49	55	-7

Figure G.1 shows the results of the comparisons between the Gent (NUM), the Partisol, the CLEM (C-20) sampler and the KOSA instrument, for PM_{10} and $PM_{2.5}$, from the April and July campaigns. There are at times discrepancies, some large, between many of the samplers. Some of the discrepancies are partly the result of the characteristics of the instruments described in Table G.1. However, many discrepancies are not easily explained, e.g. the low concentrations measured by the C-20 (CLEM) sampler and by the KOSA instrument (although the KOSA has increased response during the November comparison, shown in Figure G.2).

Figure G.2 shows the results from the November campaign with also the GRIMM 107 results included. In each of the plots, each point represents an instrument pair operated over exactly the same time period, so results from the two instruments in the pair are comparable. Figure G.3 shows the hourly day-by-day PM measurements by the GRIMM 107 instrument, from 17 to 22 November 2008, together with the RH and temperature measurements carried out by NAMHEM. The extremely high PM concentrations during this week are evident, as is its strong variation across the day and between days, with the highest concentrations during the morning and evening hours of ger area heating.

Comparison of KOSA, CLEM (C-20) and Partisol with GRIMM 107

Figure G.2 confirms the results from the April and July campaigns. For PM_{10}, the KOSA, CLEM (C-20) and Partisol instruments give very low values compared to the GRIMM 107, although the GRIMM's response is too high due to the RH effect. Also for $PM_{2.5}$, the KOSA give very low response. The Dusttrak instruments give results comparable to the GRIMM 107 results, which is to be expected since they use the same physical measurement principle (optical light scattering); see also below.

Comparison of Gent samplers (NRC and NUM) with GRIMM 107

Figure G.2 shows, for PM_{10}, that the GRIMM generally gives higher concentrations than the Gent samplers (NUM and NRC), except for NRC on the 20–21.11, which could be an outlier. The data in Table G.4 provide the possibility for assessing the effect of the relative humidity (RH) on the GRIMM 107 instrument response. The increased response at high RH is due to growth of hygroscopic particles. The ratio between GRIMM filter mass and its optical response are plotted in Figure C.4 against the relative humidity. With GRIMM results adjusted using Figure G.4, the results are shown in Figure G.5. The adjusted GRIMM and the Gent sampler results agree quite well, except for the mentioned outlier.

For $PM_{2.5}$, the Gent sampler results varied widely compared to the GRIMM, sometimes much higher, sometimes similar, sometimes much lower. It is difficult to explain this large variation. However, the Gent sampler, with its so-called 'tandem filter' system (two filters in series) is not an ideal system for separating coarse from fine particles, as explained above. The results of this comparison sampling are that $PM_{2.5}$ results from the Gent samplers cannot be trusted in terms of mass concentration. Results of source apportionment (SA) based upon chemical analysis of the $PM_{2.5}$ Gent filters (see Annex B) should also be interpreted with caution, because of the mixing of fine and coarse particles on the filters.

Comparison of Dusttrak instruments with the GRIMM 107

Figure G.2 shows that there is a close relationship between the Dusttrak and GRIMM results. This is an expected result since they use the same physical measurement principle (optical (laser) light scattering, detection at 90 degrees angle). Figure G.6 shows that the two Dusttrak instruments agree well. Dusttrak 1 has an about 15% lower response than Dusttrak 2.

Summarizing the observations from the comparison sampling:

1. The inclusion of the GRIMM 107 instrument during the November campaign lead to the following observations:
   - The GRIMM results could be adjusted for RH influence.
   - With GRIMM results adjusted, the Gent results for PM_{10} compared well with the GRIMM results.
   - Based upon this comparison, the Gent PM_{10} results can be considered trustworthy.
   - $PM_{2.5}$ results from the Gent samplers do not compare well with the GRIMM results, also not after RH correction. Gent gives sometimes higher, sometimes lower $PM_{2.5}$ than the GRIMM. Gent $PM_{2.5}$ values are uncertain.
   - The Dusttrak results compared well with the results from the GRIMM instrument, using the same measurement principle. Dusttrak results adjusted for RH the same way as for the GRIMM give a good representation of the $PM_{2.5}$ mass concentration at the concentration levels measured in UB. We assume then that the effect of RH on the Dusttrak response is similar to that on the GRIMM response, since the light scattering optics detection principle is similar for the two instruments.
2. The KOSA instrument somehow gave much too low PM concentrations compared to the GRIMM, Gent and Dusttrak instruments, during the inter-comparisons. During the November campaign, the Kosa response was still low, but increased and its results were not so low compared to the others. This increased response continued during the winter season. These results cannot be explained by the available data.
3. The CLEM (C-20) sampler also gave very low values compared with the other samplers during the inter-comparison campaigns. This low response cannot be explained by the data at hand.
4. The sampler comparisons did also show that the Partisol sampler, measuring PM_{10} at station 6, generally gave concentrations considerably lower than could be expected compared to the Gent samplers. The Partisol sampler gave sometimes spurious results compared to the Gent and other samplers. The average factor between Partisol and Gent results was 0.71, based upon the 10 parallel measurements when the Partisol was run with its standard fiber filter. This result is surprising, since the Partisol is considered to be a state-of-the-art instrument for PM sampling. For the 3 samples when Partisol was run with Nuclepore filter, the ratio was even lower, about 0.45. During the AMHIB period after October 2008, the Partisol was run with Nuclepore filters, to enable chemical analysis of the filters for source apportionment analysis. It was not possible for the AMHIB team to check the operation of the Partisol sampler technically during the AMHIB period.

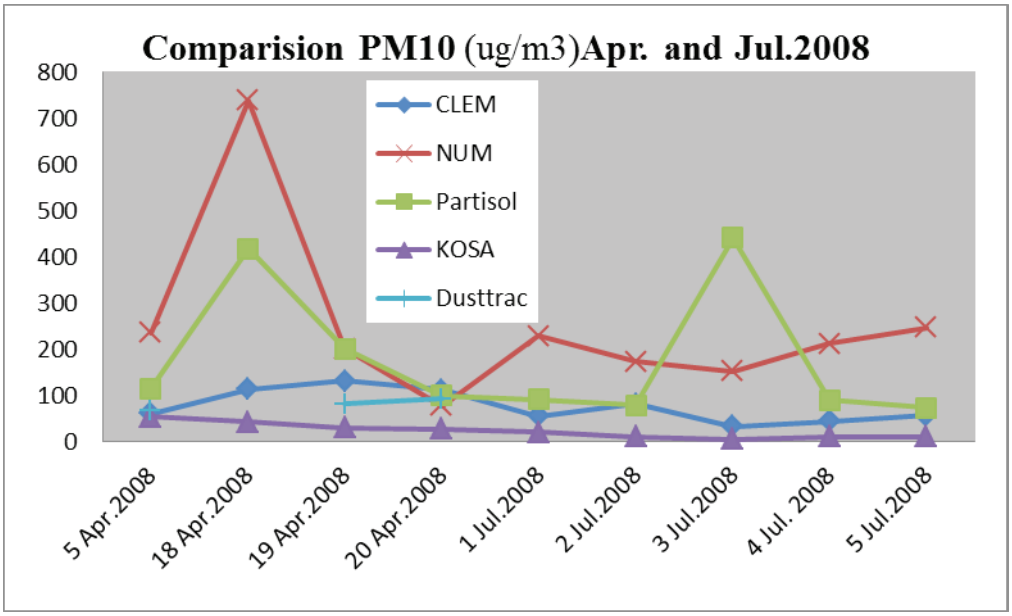

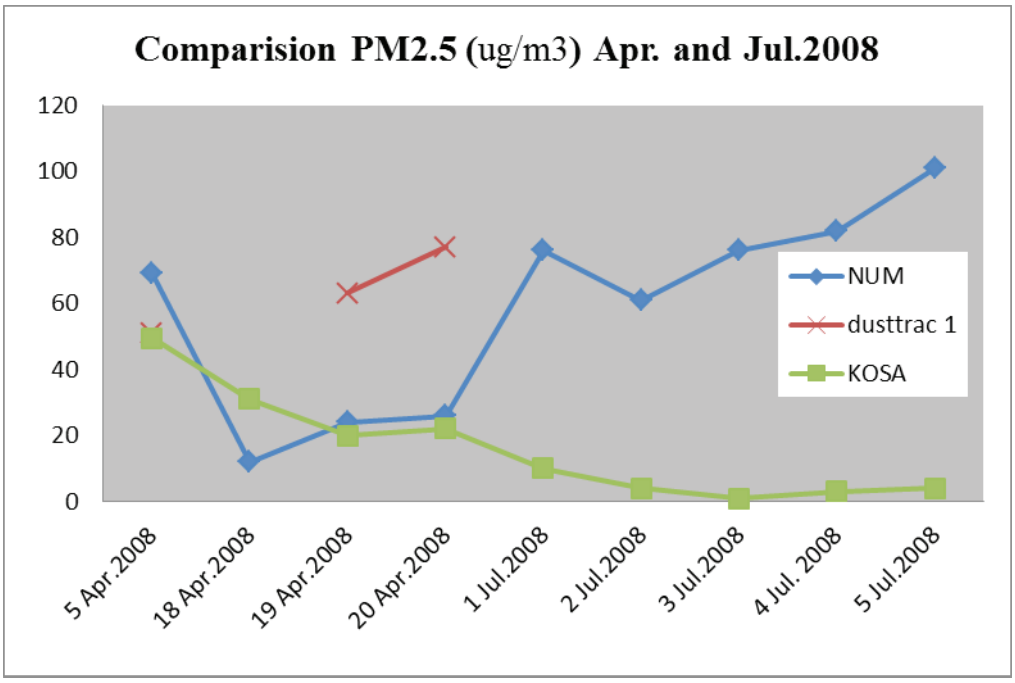

Figure G.1 Results from PM sampler and monitor comparisons in Ulaanbaatar, for PM_{10} and $PM_{2.5}$, April and July, 2008.

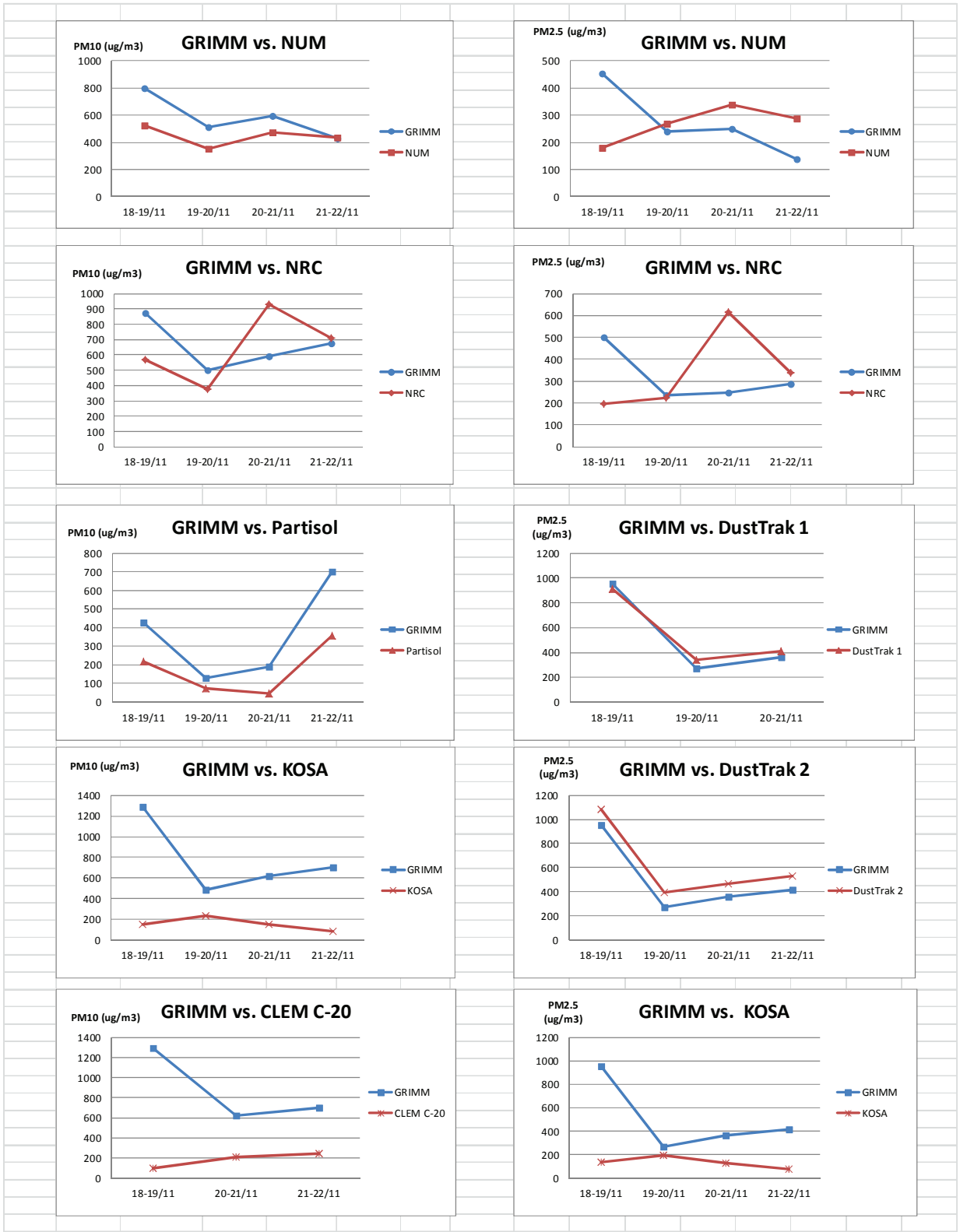

Figure G.2 Results from PM sampler and monitor comparisons at the UB3 station in Ulaanbaatar, for PM_{10} and $PM_{2.5}$, during November 2008.

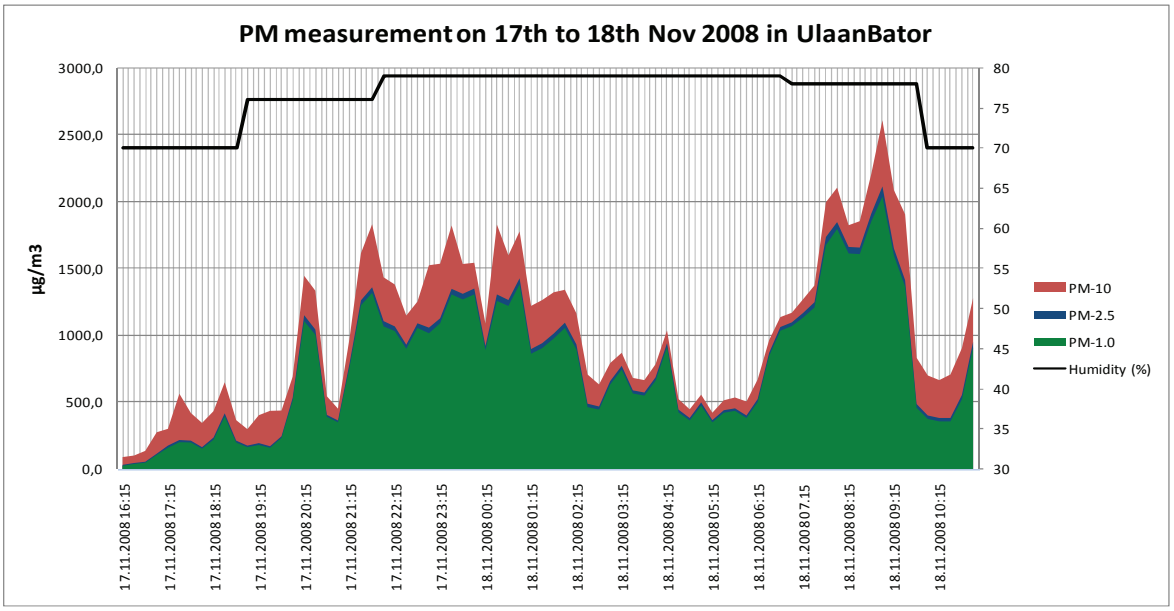

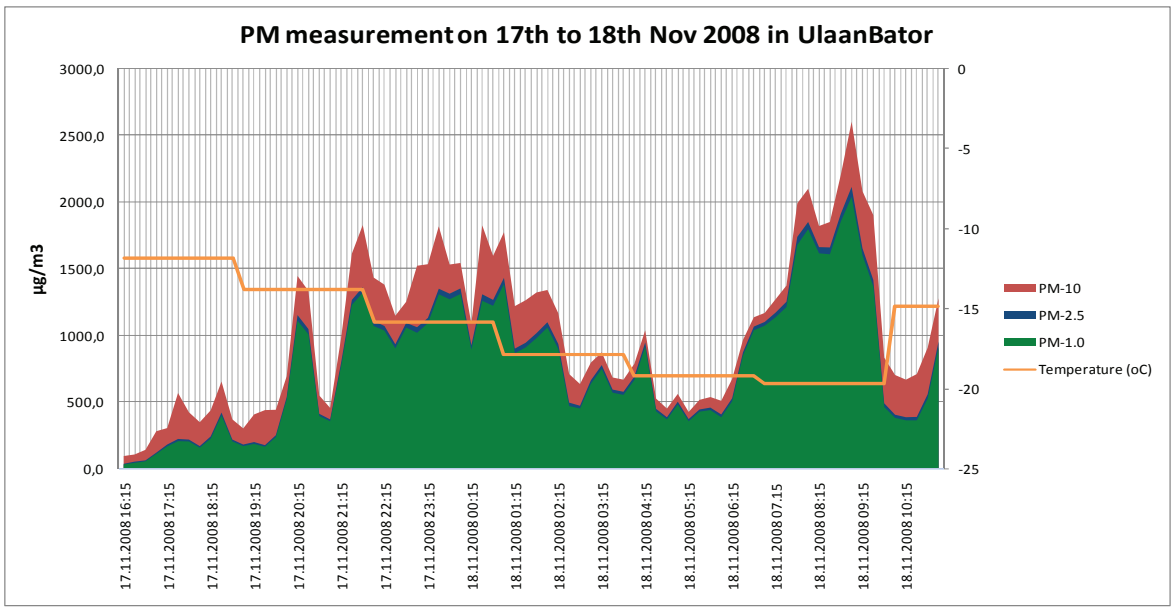

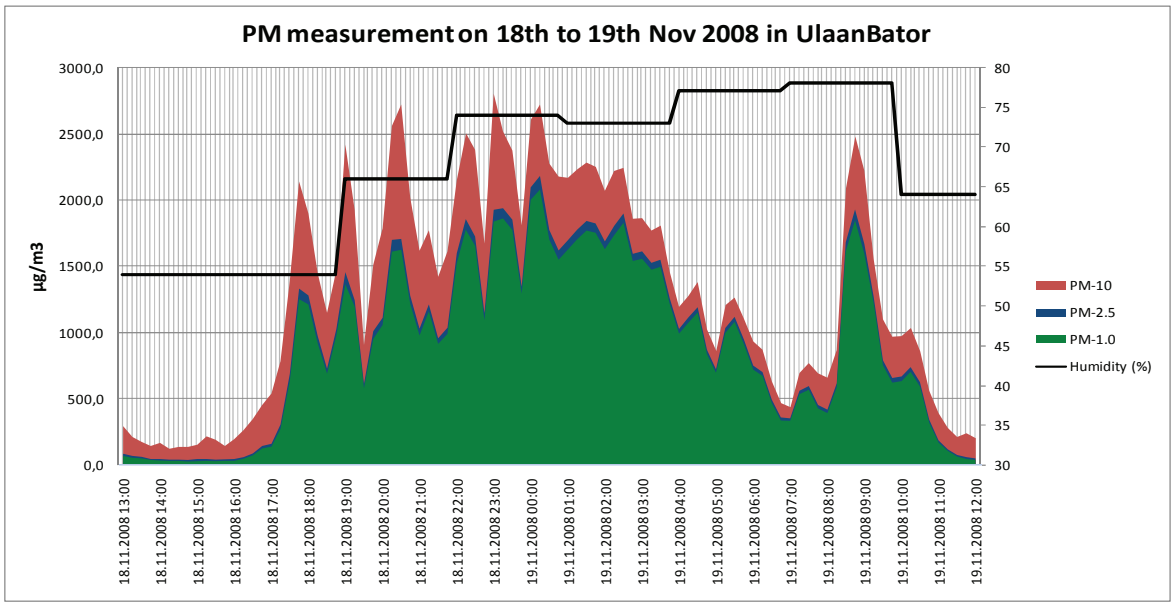

Figure G.3 PM concentrations measured with the GRIMM 107 monitor in UB 17–22 November, 2008.

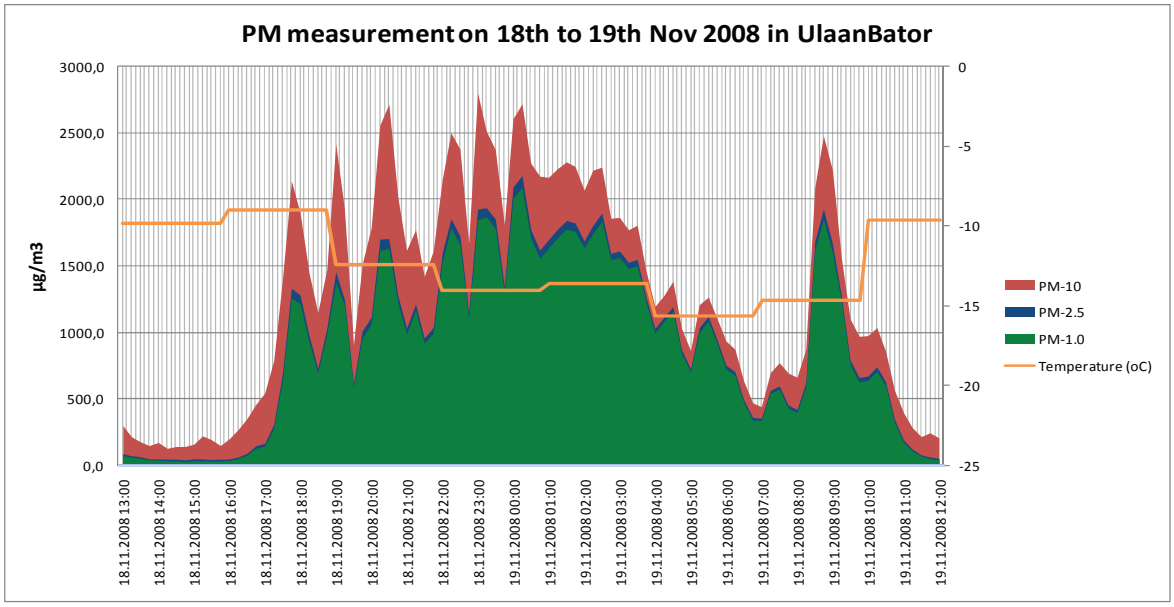

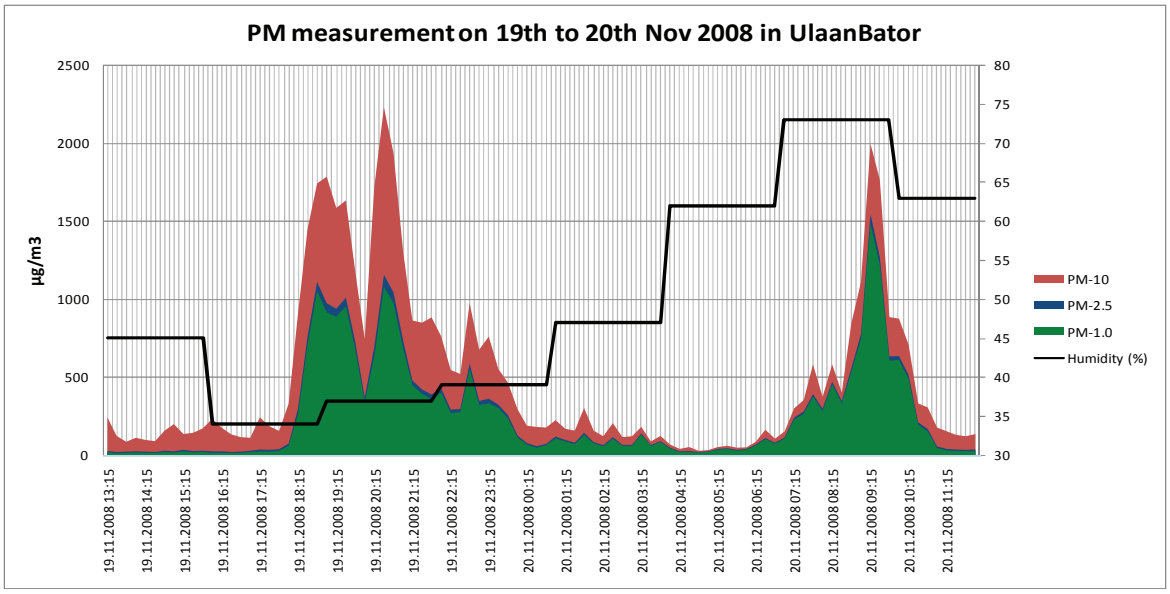

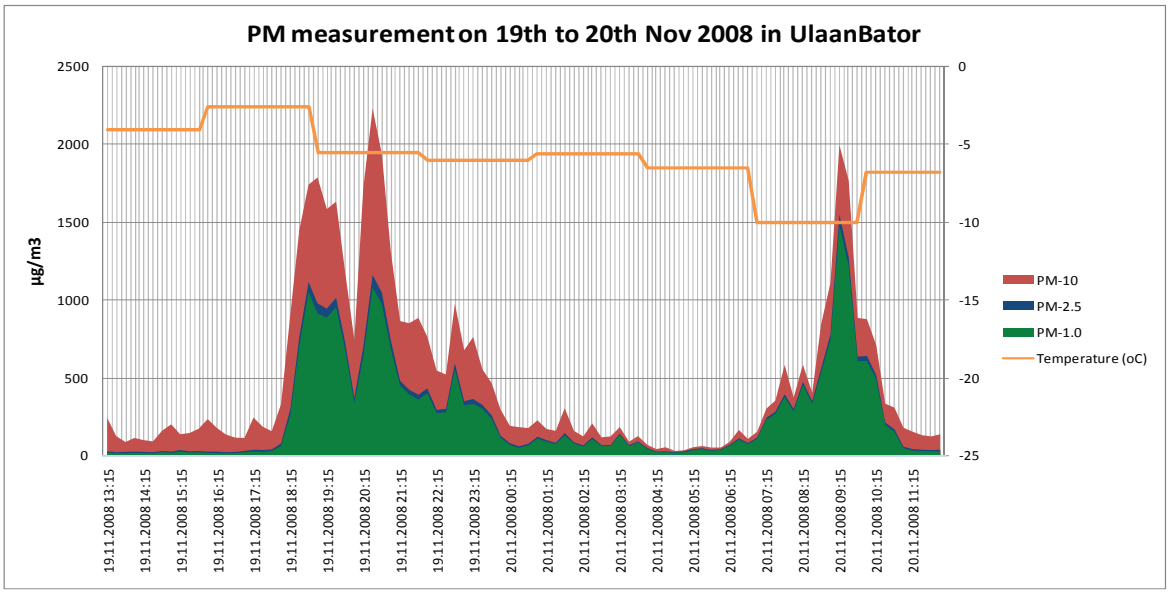

Figure G.3 *continued*.

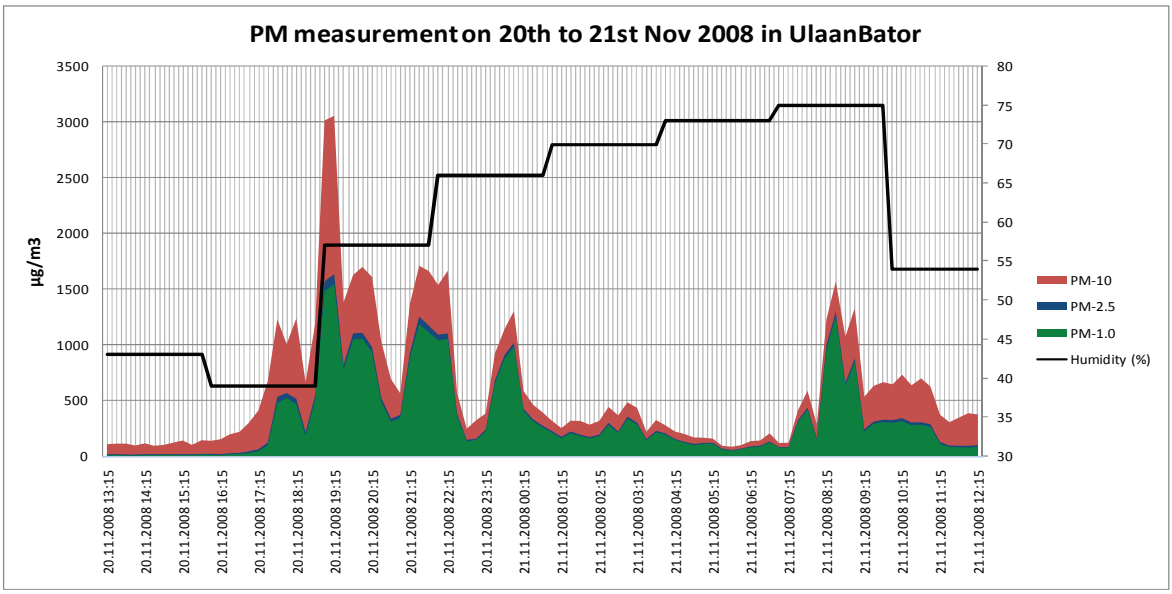

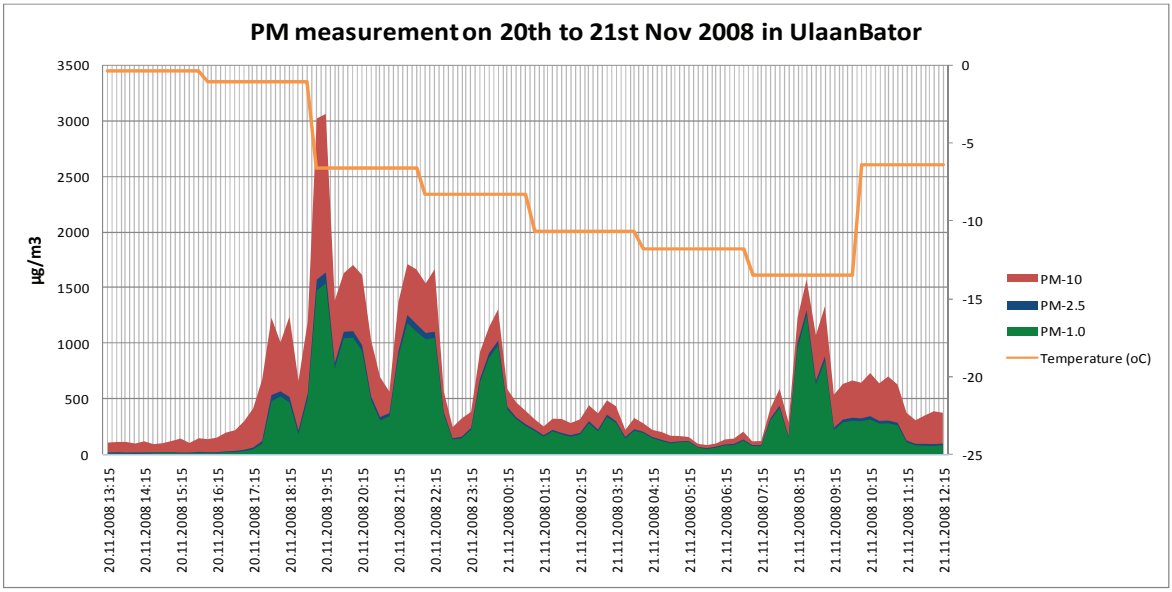

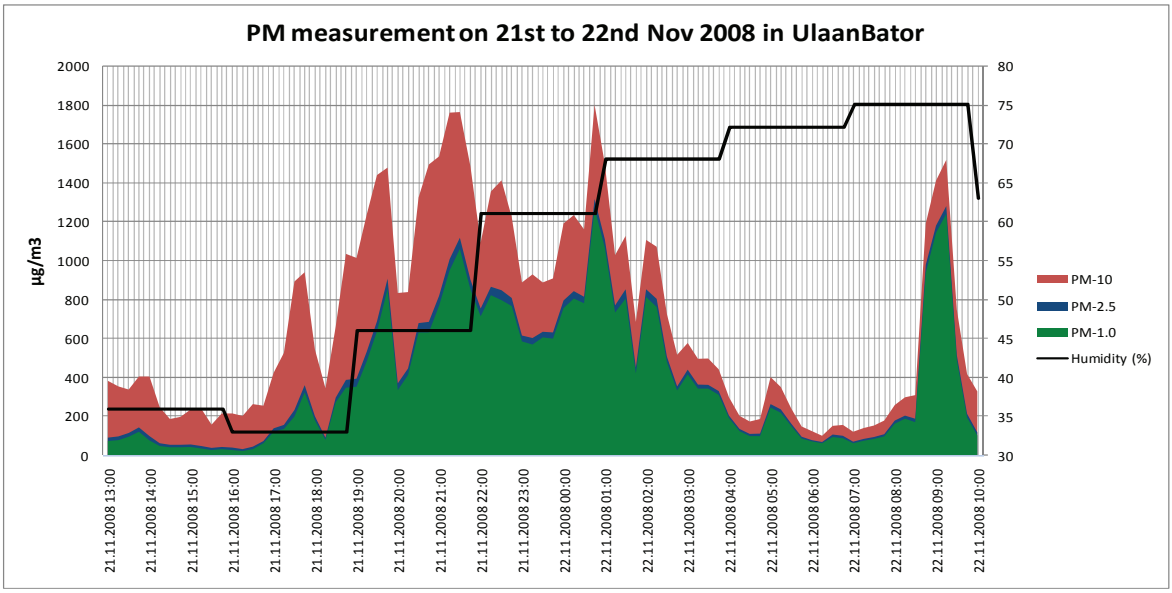

Figure G.3 *continued*.

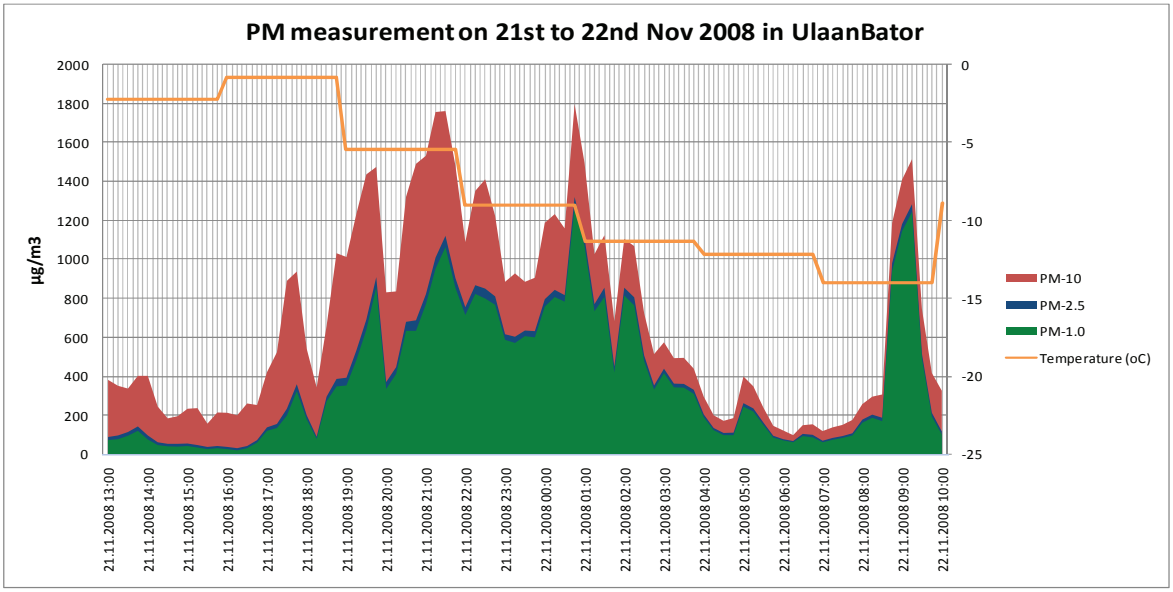

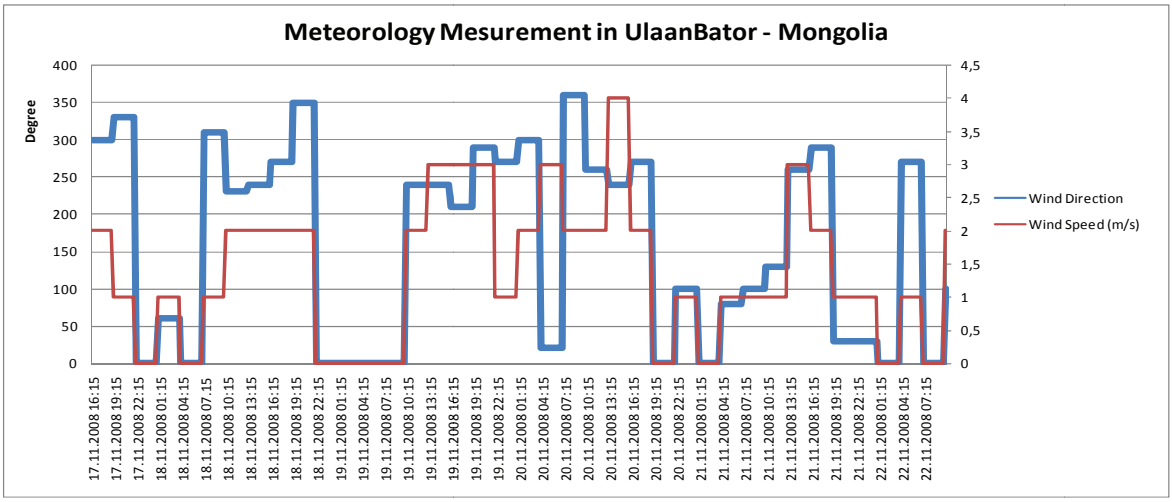

Figure G.3 *continued*.

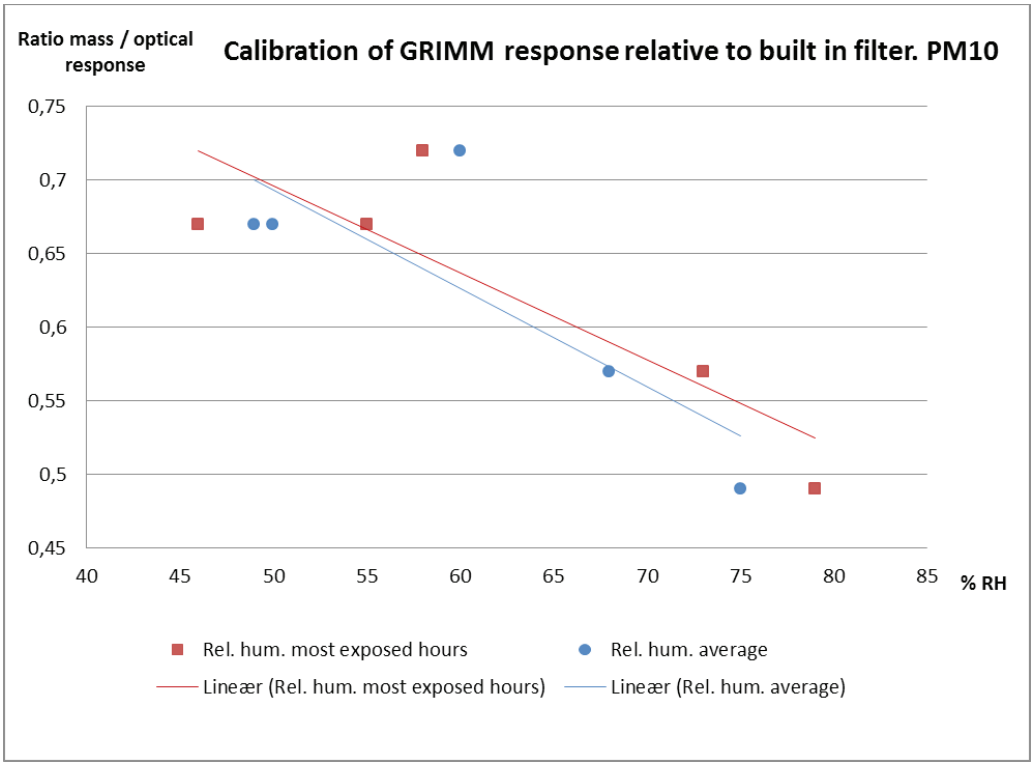

Figure G.4 PM Ratio between GRIMM 107 filter vs. optical response (both in μg/m^3) as a function of relative humidity, UB 17–22 November, 2008.

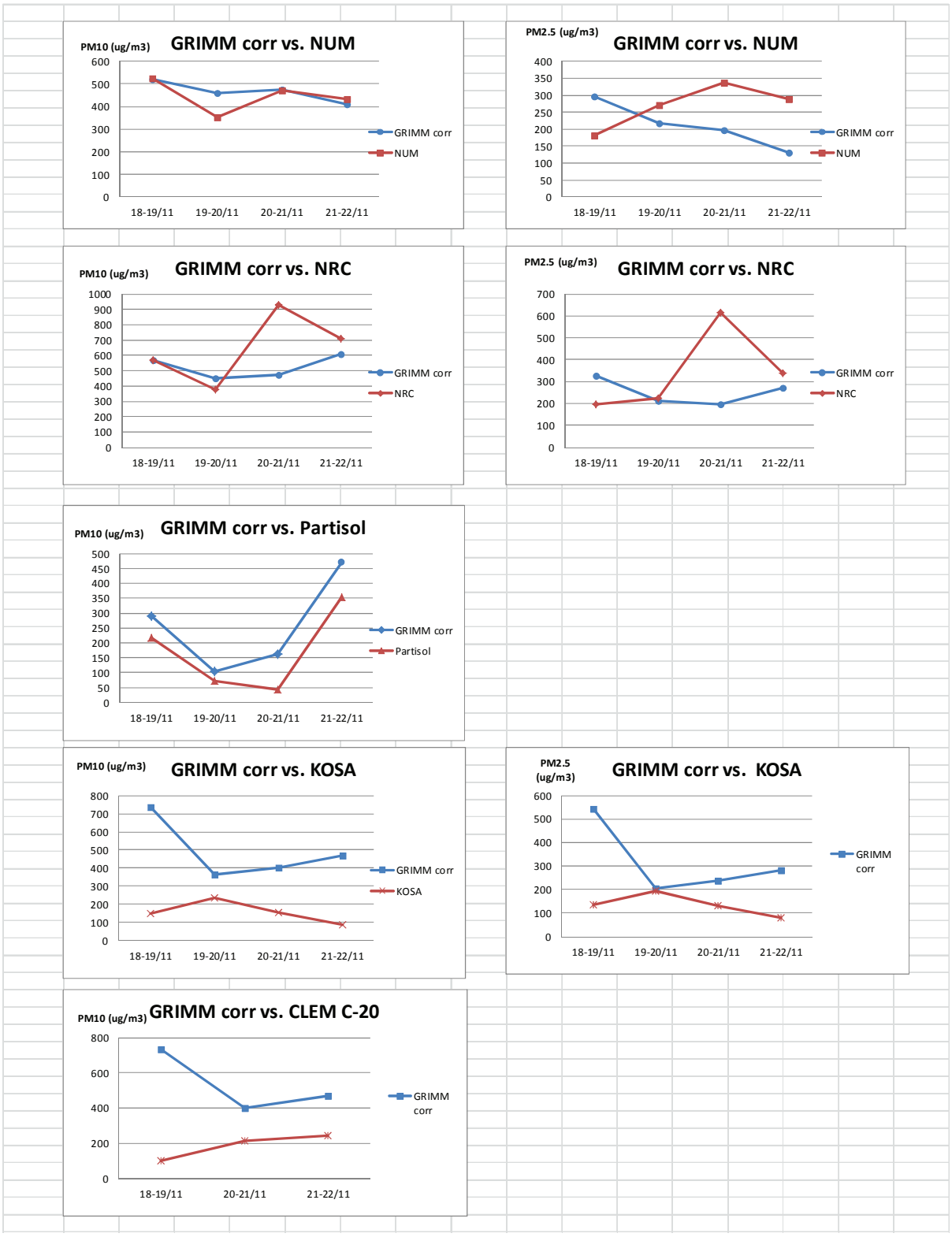

Figure G.5 Results from PM sampler and monitor comparisons at the UB3 station in Ulaanbaatar, for PM_{10} and $PM_{2.5}$ during November 2008, when the GRIMM response has been adjusted for the RH effect.

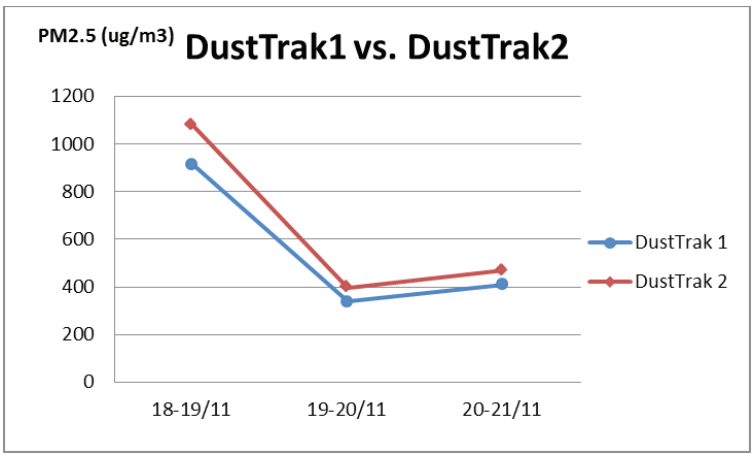

Figure G.6 Comparison of the two Dusttrak instruments.

2. Correction procedure based upon the sampler comparisons

Due to the discrepancies between the various instruments used, as well as other sampling artifacts, as described above, some of these data need to be corrected, to give a more correct representation of the PM concentrations in UB. The comparison measurement campaigns were rather brief, covering a total of up to 20 days dependent upon the instrument. Sometimes good indications of correction factors could be given, but there are uncertainties coupled to the correction factors.

Correction of the data from the various stations

PM_{10} at stations 2 (NRC) and 3 (Zuun ail):
Gent samplers were used here. They compare well with results from the GRIMM 107 instrument when its response was corrected for the RH effect. No corrections are applied to the PM_{10} from the Gent samplers.

$PM_{2.5}$ at stations 2 and 3:
It is clear that the Gent samplers do not separate the particles ideally between the fine and coarse fraction in the very polluted conditions in UB. The comparison with the RH adjusted GRIMM 107 results showed significantly variable results. On the average, the Gent sampler gave about 25% higher $PM_{2.5}$ concentration than the RH adjusted GRIMM 107, based upon 7 samples (one strong outlier excluded), corresponding to penetration of a certain part of the coarse fraction particles through the coarse filter and down to the fine filter. This factor can be used as a first order correction applicable to the UB conditions experienced, but it is uncertain.

PM_{10} at station 6 (3 Khoroolol):
The Partisol sampler is used here. In the period June–October it was used with the standard glass fiber filter. For this filter, the comparison sampling (10 samples) gave a correction factor of about 1.7 with one large outlier excluded. During November–May, Nuclepore filters were used to allow source apportionment (SA) analysis of the data from this station. For three days of comparison with the GRIMM sampler when the Partisol was run with Nuclepore, the correction factor varied between 1.8 and 4.3 for the individual days, with an average of 2.7. This is obviously a very uncertain correction factor. Still, it seems clear that the Partisol should be corrected. Based upon the limited data at hand, we correct the Partisol data, run with the Nuclepore filter, with a factor 2.0, although the factor has a relatively large uncertainty.

$PM_{2.5}$ at stations 4, 7 and 8 (6 Buudal, Bayanhoshuu, and Airport):
The Dusttrak instrument is used on these stations. The Dusttraks agree well with the GRIMM 107 results. Data from the Dusttraks needs to be corrected for the effect of the RH on the instrument response. The November experiments with the GRIMM 107 instrument gave the following correction factors for RH:

- RH> 65%: correction factor: 0.55
- RH of 50–65%: correction factor: 0.65
- RH<50%: correction factor: 1.0.

During the October–February period, 55% of the days had average RH>65%, and 38% of the days had RH of 50–65%.

This leads to a correction factor for $PM_{2.5}$ data from the Dusttraks, of 0.68, to be applied to the average $PM_{2.5}$ concentration measured during that period. The underlying assumption is that the PM composition is affected by RH similarly on all days. This appears to be an acceptable assumption, since the same dominating sources are active in the ger areas every day. Outside the October–February period, the RH is generally low, and no correction is applied.

B: AMHIB PM concentration data

A. $PM_{2.5}$

Equipment type	KOSA-1	GENT	GENT	Dust track	Dust track	Dust track
Method	Light scatter	Gravimetric	Gravimetric	Optic	Optic	Optic
Location	NAMHEM (Site No.1)	NRC (Site No.2)	Zuun Ail (Site No.3)	6 buudal (Site No.4)	Bayanhoshuu (Site No.7)	Airport (Site No.8)
Date	**Concentration µg/m³**					
4-Jun-08	14	8	Filter damaged	73		98
8-Jun-08	97	131	64	21		557
11-Jun-08	2		Filter damaged	393		87
15-Jun-08	3	20	2	34		78
18-Jun-08	7	18	16	29		128
22-Jun-08	3	13	20	70		193
25-Jun-08	5	3	power off	26		
29-Jun-08	4	10	power off	31		44
2-Jul-08		40	power off			
6-Jul-08		15	power off			
9-Jul-08	1	46	power off			
13-Jul-08	0	63				
16-Jul-08	1	6	24			
20-Jul-08	2	3	power off			
23-Jul-08	1	3	15			
27-Jul-08	1	3	1			
30-Jul-08		16				
3-Aug-08	8	power off	62			
6-Aug-08	6	79	2			
10-Aug-08	5	91	1			
13-Aug-08	5	86	55			
17-Aug-08	4	9	49			
20-Aug-08	6	60	75			
24-Aug-08	6	power off	77			
27-Aug-08		119	31			
31-Aug-08		10	86			
3-Sep-08	7	5	16	21	25	21
7-Sep-08	7	6	26	19	23	18
10-Sep-08	4	33	75	47	35	19
14-Sep-08	6	18	58	27	26	17

17-Sep-08	4	34	40	22	19	35
21-Sep-08	13	29	76	52	43	52
24-Sep-08	13	9	5	46	72	48
28-Sep-08	10	16	7	64	133	91
1-Oct-08	12	41	56	157	64	62
5-Oct-08	27	101	115	439	229	156
8-Oct-08	8	31	60	114	4060	
12-Oct-08	32	60	31	124	212	192
15-Oct-08	37	8	9	635		81
19-Oct-08	35	5	6	642	196	144
22-Oct-08	14	1426	4	44	51	79
26-Oct-08	66	100	17	176	104	389
27-Oct-08	58	34	54	273	347	307
28-Oct-08	63	55	11	314	298	311
29-Oct-08	48	28	65	34	65	149
30-Oct-08	82	Filter damaged	26	423	256	
31-Oct-08	13	Filter damaged	49		98	162
1-Nov-08	12	60	19	156	441	126
5-Nov-08	44	77	12	556	756	65
9-Nov-08	78	203	74	357	193	110
12-Nov-08	71	140	91	300	347	280
16-Nov-08		250	43	300	239	466
24-Nov-08	128	122	222	713	777	845
25-Nov-08	141	45.1	198	928	714	238
26-Nov-08	59	105	114	468	755	594
27-Nov-08	49	86.2	1100	697	1100	340
28-Nov-08	84	107	430	561	188	682
29-Nov-08	148	3312	1196	735		767
30-Nov-08		141	468	556	733	362
3-Dec-08	88	136	471		145	886
7-Dec-08	133		958		1340	893
10-Dec-08	269	48	1749		3230	1210
14-Dec-08	372	407	1304	847	1820	1110
17-Dec-08	160	24	370	953	2150	1090
21-Dec-08	528	158	333	870	2160	1230
24-Dec-08	174		222	522	248	960
28-Dec-08	143	46	279	919	280	370
29-Dec-08	239	52	209	1480	1660	627
30-Dec-08	258	47	286	1410	1400	649
31-Dec-08	106	44	149	2640	1200	797
1-Jan-09	42	41	147	1080	904	329
2-Jan-09	99	75	133	591	207	376
3-Jan-09	212	48	161	919	2150	887
7-Jan-09	161	128	2434	867	2350	400
11-Jan-09	243	178	539	1100	2310	702

14-Jan-09	158	153	937	1330	2610	706
18-Jan-09	138	119	729	1340	2060	718
21-Jan-09	41	54	1029	117	101	54
25-Jan-09	123	213	1206	529	1580	621
26-Jan-09	170	88	5657	1360	1980	626
27-Jan-09	173	154	821	988	1450	418
28-Jan-09	119	224	1875	485	1350	71
29-Jan-09	140	144	846	683	1190	500
30-Jan-09	143	145	987	620	1410	650
31-Jan-09	113	55	1867	869	1390	659
4-Feb-09	145	269	1107	power off	2060	617
8-Feb-09	116	227	745	475	1290	488
11-Feb-09	51	111	387	348	434	180
15-Feb-09	157	235	189	348	1060	511
18-Feb-09	42	95	150	113	105	153
22-Feb-09	104	106	150	439	1100	328
27-Feb-09	85	22	93	325	948	490
28-Feb-09	97	66	44	349	773	539
1-Mar-09	85	57	63	289	736	398
2-Mar-09	74	36	64	266	724	353
3-Mar-09	72	50	113	198	472	298
4-Mar-09	49	28	58	187	205	163
8-Mar-09	85	58	35	153	415	269
11-Mar-09	21	103	200	67	145	77
15-Mar-09	57	122	212	195	power off	187
18-Mar-09	39	106	44	139	369	198
22-Mar-09	38	35	57	186	196	178
25-Mar-09	37	134	213	165	78	212
26-Mar-09	22	97	3343	155	200	171
27-Mar-09	29	112	178	148	power off	156
28-Mar-09	15	51	197	179	176	113
29-Mar-09	25	Filter damaged	273	165	240	154
30-Mar-09	32	131	133	198	217	183
1-Apr-09	42	158	193	259	114	88
5-Apr-09	23	193	162	88	244	111
8-Apr-09	39	39	19	106	179	179
12-Apr-09	22	88	40	68	154	51
15-Apr-09	32	86	16	102	138	145
19-Apr-09	22	45	18	78	115	91
22-Apr-09	10	35	144	32	69	42
26-Apr-09	18	22	79	60	85	51
29-Apr-09	19	493	405	52	power off	68
3-May-09		403	419	37	73	39
6-May-09		425	430	35	33	41
10-May-09		1085	440	30	54	49

13-May-09	17	153	189	55	78	52
17-May-09	27	161	212	55	82	62
20-May-09	53	31	359	44	68	119
24-May-09	21	36	257	42	71	45
27-May-09	16	102	495	48	32	23
31-May-09	12	118	536	31	39	46

B. PM_{10}

Equipment type	KOSA	GENT	GENT	Rotary Bebicon	Partisol
Method	Light scatter	Gravimetric	Gravimetric	Gravimetric	Gravimetric
Location	NAMHEM (Site No.1)	NRC (Site No.2)	Zuun Ail (Site No.3)	CLEM (Site No.5)	3 khoroolol (Site No.6)
Date	**Concentration µg/m³**				
4-Jun-08	26	200	147	59	
8-Jun-08	137	479	297	170	
11-Jun-08	10	82	114	77	181
15-Jun-08	12	264	227	319	249
18-Jun-08	18	136	114	148	132
22-Jun-08	6	33	27		
25-Jun-08	10	40	power off		39
29-Jun-08	12	47	power off		28
2-Jul-08		150	power off		
6-Jul-08		109	power off		
9-Jul-08	4	157	power off	10	8
13-Jul-08	1	230		4	38
16-Jul-08	10	132	140	42	102
20-Jul-08	9	126		17	83
23-Jul-08	10	81	60	20	54
27-Jul-08		42	16	5	29
30-Jul-08	9	113	234	25	81
3-Aug-08		power off	202	25	70
6-Aug-08		462	112	72	96
10-Aug-08		150	64	30	100
13-Aug-08		279	187	42	128
17-Aug-08		188	243	35	129
20-Aug-08		114	134	2	29
24-Aug-08		power off	158	10	43
27-Aug-08		289	165	19	107
31-Aug-08		184	347	16	67
3-Sep-08		36	79	12	25
7-Sep-08		982	115	109	60
10-Sep-08		172	223	63	62
14-Sep-08		47	131	10	17
17-Sep-08		151	152	45	125
21-Sep-08		119	207	6	73

24-Sep-08	5	79	38	27	58
28-Sep-08	11	185	106	38	143
1-Oct-08	6	276	214		95
5-Oct-08	23	410	393		323
8-Oct-08	5	95	178		68
12-Oct-08	32	406	138	131	200
15-Oct-08	35	87	41		117
19-Oct-08	37	114	43		179
22-Oct-08	3	1478	8	23	53
26-Oct-08	78	155	43	83	233
27-Oct-08	72	266	99	86	160
28-Oct-08	67	259	132	68	204
29-Oct-08	21	442	208	64	149
30-Oct-08	103		87	89	212
31-Oct-08	8		75	93	102
1-Nov-08	53	166	96	76	106
5-Nov-08	43	306	55	69	79
9-Nov-08	73	325	291	226	216
12-Nov-08	65	406	279	84	252
16-Nov-08	233	676	250	114	212
24-Nov-08	56	661	493		3800
25-Nov-08	190	149	411		350
26-Nov-08	91	298	212		1125
27-Nov-08	178	271	2235	78	1400
28-Nov-08	197	354	777	150	469
29-Nov-08	198	Filter damaged	2184	125	47000
30-Nov-08	165	411	799	94	
3-Dec-08	65	230	842	60	1567
7-Dec-08	214		1770	58	1452
10-Dec-08	326	102	1960	71	353
14-Dec-08	426	614	2587	116	692
17-Dec-08	205	65	807		1129
21-Dec-08	649	238	632		512
24-Dec-08	221		419		733
28-Dec-08	183	70	244	68	234
29-Dec-08	303	119	344	60	250
30-Dec-08	328	100	393	22	350
31-Dec-08	132	84	197	36	357
1-Jan-09	53	82	229	26	231
2-Jan-09	125	180	238	52	100
3-Jan-09	266	89	209	28	517
7-Jan-09	200	272	4360	77	860
11-Jan-09	307	284	867	88	1046
14-Jan-09	202	264	1687	43	2725
18-Jan-09	188	193	1307	118	633
21-Jan-09	20	108	2019	21	176
25-Jan-09	146	342	2328	113	220

26-Jan-09	215	111	10990	97	909
27-Jan-09	230	244	1817	65	610
28-Jan-09	146	305	3622	78	682
29-Jan-09	172	214	1634	58	1355
30-Jan-09	184	212	1889	55	933
31-Jan-09	151	100	3694	68	2985
4-Feb-09	185	546	2184	77	653
8-Feb-09	149	526	1450	86	power off
11-Feb-09	58	439	1375	51	377
15-Feb-09	165	394	311	39	405
18-Feb-09	38	122	930	112	174
22-Feb-09	114	174	1552	55	128
27-Feb-09	98	105	135	130	737
28-Feb-09	116	111	121	138	772
1-Mar-09	100	80	99	60	893
2-Mar-09	87	58	118	93	921
3-Mar-09	86	88	242	55	619
4-Mar-09	52	53	132	56	302
8-Mar-09	89	113	89	65	329
11-Mar-09	27	159	381	34	151
15-Mar-09	96	270	474	64	287
18-Mar-09	87	831	69	61	240
22-Mar-09	56	77	89	69	193
25-Mar-09	57	277	460	77	265
26-Mar-09	38	213	3612	58	262
27-Mar-09	43	236	349	power off	188
28-Mar-09	36	130	372	power off	142
29-Mar-09	43	Filter damaged	495	85	214
30-Mar-09	41	281	346	51	365
1-Apr-09	57	390	448	42	329
5-Apr-09	32	588	403	45	370
8-Apr-09	55	184	138	182	341
12-Apr-09	32	169	100	46	229
15-Apr-09	32	169	69	57	340
19-Apr-09	32	76	34	23	147
22-Apr-09	18	70	358	40	181
26-Apr-09	26	80	229		245
29-Apr-09	22	1118	923	43	
3-May-09		870	905	29	
6-May-09		861	968	38	273
10-May-09		1403	864	37	315
13-May-09	27	327	399	40	188
17-May-09	35	372	428	45	143
20-May-09	62	90	671	32	50
24-May-09	0	86	503	24	40
27-May-09	6	215	892	21	349
31-May-09	0	287	1024	36	107

C: Meteorology data and dependence of PM concentrations on the meteorology parameters

Table 1 Meteorology data on days of AMHIB measurements

Date	Temperature °C	Relative humidity (%)	Wind velocity (m/sec)
4-Jun-08	15	43.6	1.5
8-Jun-08	22.1	35	3.5
11-Jun-08	9.2	55.1	4.3
15-Jun-08	18.9	32.4	5.5
18-Jun-08	19.2	50.5	3.5
22-Jun-08	11.9	84.9	2.8
25-Jun-08	17.3	68.9	2.6
29-Jun-08	20.1	57.8	2
2-Jul-08	16.3	73.1	2.1
6-Jul-08	21.2	54.5	3.3
9-Jul-08	14.9	66.5	2.6
13-Jul-08	18.6	57.5	3.4
16-Jul-08	24.9	34.1	2.3
20-Jul-08	26.2	34.9	3
23-Jul-08	23.2	39.9	2.8
27-Jul-08	17.6	51.9	4.4
30-Jul-08	18.5	52.9	2.5
3-Aug-08	25.5	26.6	3.1
6-Aug-08	16.7	58.8	4
10-Aug-08	22.1	34.9	1.5
13-Aug-08	23.1	23.4	2
17-Aug-08	22.3	38.5	2.6
20-Aug-08	13.5	64.1	1.4
24-Aug-08	7	79	2.9
27-Aug-08	7.9	85.6	3.1
31-Aug-08	17.5	45.9	1.5
3-Sep-08	8.1	76.4	2.6
7-Sep-08	8.1	56.4	3.5
10-Sep-08	13.6	51.6	2.8
14-Sep-08	10	47.3	3.4
17-Sep-08	14	35.8	2.9
21-Sep-08	7.3	37.4	3.9
24-Sep-08	17.2	40.8	2.9
28-Sep-08	8	43.5	2.6
1-Oct-08	5.7	54	2.3
5-Oct-08	4.7	44.1	1.9
8-Oct-08	1.5	71.9	2
12-Oct-08	5.9	43.1	2.3
15-Oct-08	1.4	84.5	2
19-Oct-08	5.8	41.3	2.6
22-Oct-08	-6.8	79.1	3.3

26-Oct-08	-2.1	60	1.6
27-Oct-08	-0.6	60.5	1.5
28-Oct-08	-1.7	65.9	1.4
29-Oct-08	-1	64.9	2.5
30-Oct-08	-2.2	67.1	2.3
31-Oct-08	-1.9	62.9	2.5
1-Nov-08	-2.2	57.8	3
2-Nov-08	-5.6	68.6	2.6
5-Nov-08	-2.4	64	2
9-Nov-08	1.3	43.3	2
12-Nov-08	-8.9	51.1	2
15-Nov-08	-12.4	67.6	1.3
19-Nov-08	-6.8	50.8	2.1
23-Nov-08	-9.1	71.4	1.8
24-Nov-08	-9.1	61.9	1.1
25-Nov-08	-9	61.6	2.1
26-Nov-08	-10.2	67.3	1.5
27-Nov-08	-6.7	68.4	2
28-Nov-08	-8.8	76.9	1.5
29-Nov-08	-8.1	71.3	1.6
30-Nov-08	-8.3	76.3	2.6
3-Dec-08	-24.8	58.4	2.6
7-Dec-08	-15.5	70.6	1.5
10-Dec-08	-17.5	70.9	1.1
14-Dec-08	-15.6	72.3	0.6
17-Dec-08	-21.2	65.6	1
21-Dec-08	-25.5	62.6	1.3
24-Dec-08	-18.1	72.3	1
28-Dec-08	-18.9	74.3	2.1
29-Dec-08	-22.3	77.8	1.4
30-Dec-08	-23.2	72.1	0.6
31-Dec-08	-18.1	63.4	2.4
1-Jan-09	-18.1	70.5	1.9
2-Jan-09	-16.7	75.4	2.0
3-Jan-09	-21.2	74.6	0.5
7-Jan-09	-22.1	72.6	1.8
11-Jan-09	-22.1	77.4	0.8
14-Jan-09	-19.9	69.9	0.6
18-Jan-09	-18.8	68.0	1.4
21-Jan-09	-25.5	54.0	4.0
25-Jan-09	-22.3	61.3	1.3
26-Jan-09	-19.7	60.5	1.1
27-Jan-09	-15.8	72.9	1.5
28-Jan-09	-19.3	67.5	1.1
29-Jan-09	-18.9	61.8	1.6
30-Jan-09	-16.1	63.5	1.8

31-Jan-09	-12.9	62.2	1.0
4-Feb-09	-12.5	67.9	1.4
8-Feb-09	-10.9	55.0	1.6
11-Feb-09	-10.4	56.8	3.0
15-Feb-09	-27.5	57.8	1.6
18-Feb-09	-18.2	57.1	6.4
22-Feb-09	-21.5	58.4	1.8
27-Feb-09	-15.7	60.9	1.6
28-Feb-09	-12.7	58.0	1.8
1-Mar-09	-11.9	56.1	2.3
2-Mar-09	-11.1	58.4	1.4
3-Mar-09	-8.1	50.5	2.4
4-Mar-09	-10.4	57.1	3.0
8-Mar-09	-11.9	49.8	2.8
11-Mar-09	-11.9	62.4	6.0
15-Mar-09	-5.0	57.6	2.1
18-Mar-09	-5.7	50.5	2.6
22-Mar-09	-9.6	47.8	2.6
25-Mar-09	-3.9	33.6	2.5
26-Mar-09	-2.3	43.4	2.4
27-Mar-09	-5.4	57.1	2.6
28-Mar-09	-5.9	66.0	4.0
29-Mar-09	-6.0	59.9	1.9
30-Mar-09	-4.6	45.9	2.1
1-Apr-09	5.1	23.6	2.1
5-Apr-09	7.0	28.5	2.9
8-Apr-09	12.3	32.0	2.3
12-Apr-09	6.6	41.5	3.5
15-Apr-09	1.4	28.8	1.6
19-Apr-09	2.0	56.5	2.8
22-Apr-09	5.4	35.6	3.9
26-Apr-09	10.6	24.8	2.9
29-Apr-09	12.2	21.9	3.5
3-May-09	16.3	19.5	3.6
6-May-09	15.9	22.5	3.5
10-May-09	9.1	54.1	3.7
13-May-09	14.9	31.6	2.8
17-May-09	13.8	28	3.6
20-May-09	8.2	33.8	4
24-May-09	12.5	30.7	2.3
27-May-09	1.3	75.2	4.7
31-May-09	20.5	19.8	3.6

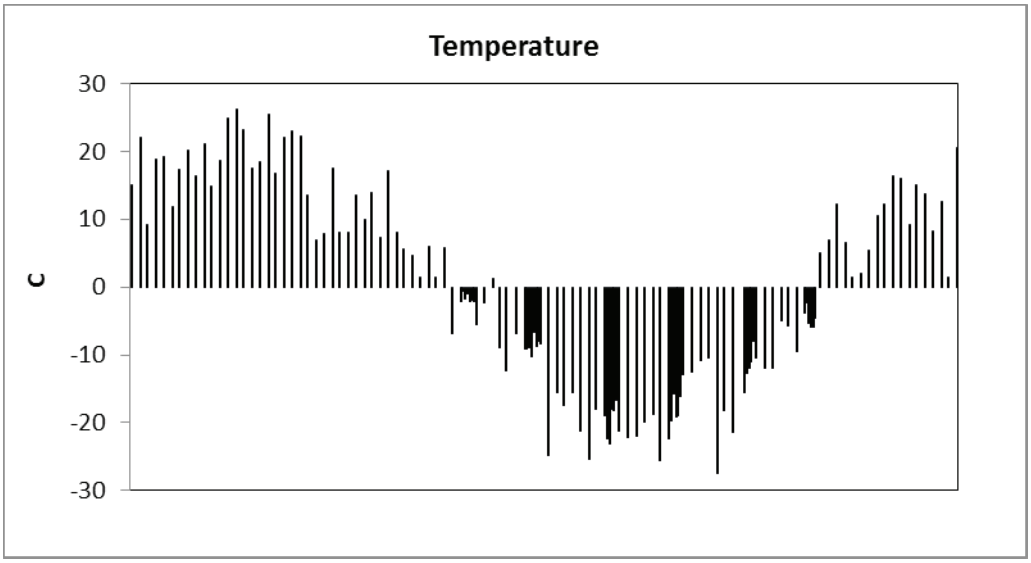

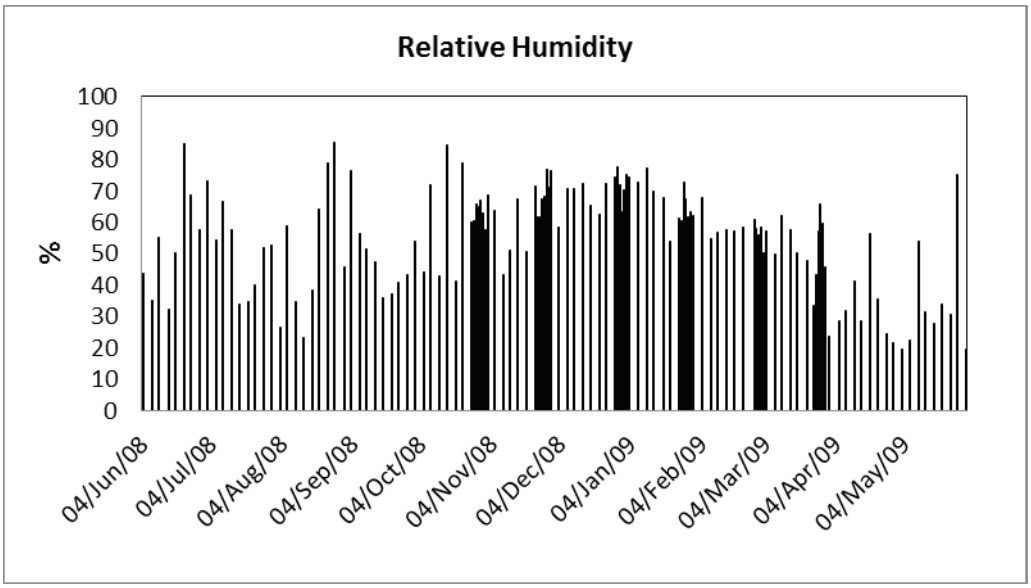

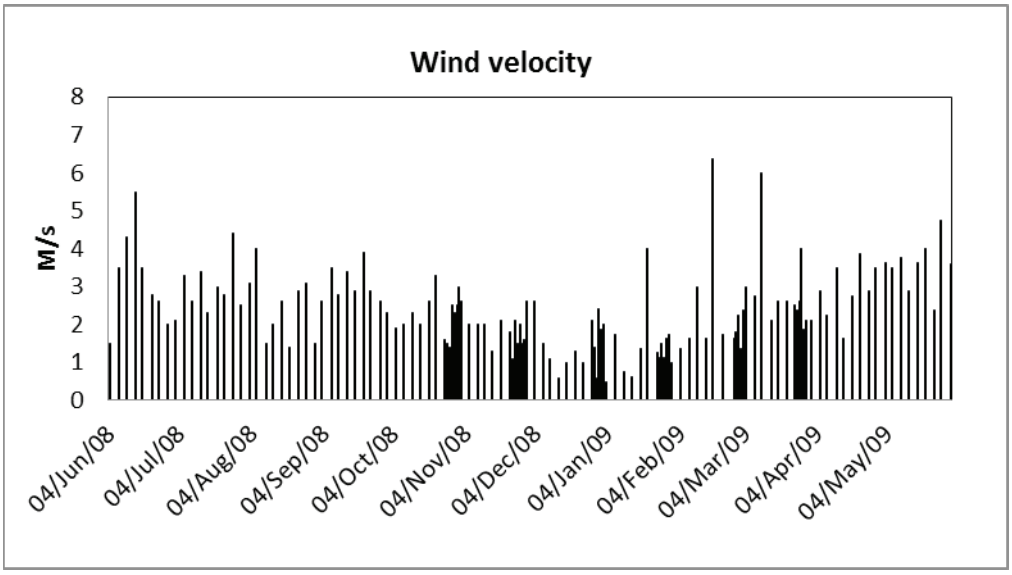

Figure 1 Time series of meteorology parameters.

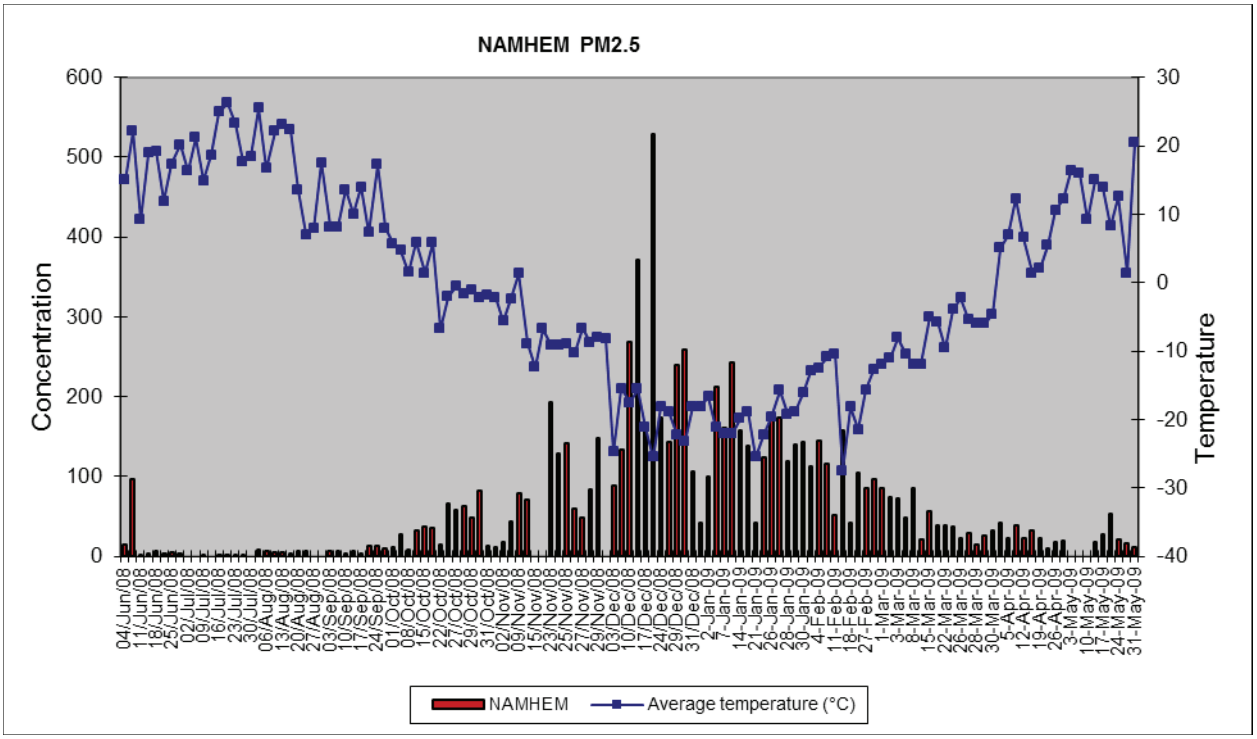

$PM_{2.5}$ concentration (µg/m^3) and temperature in NAMHEM site.

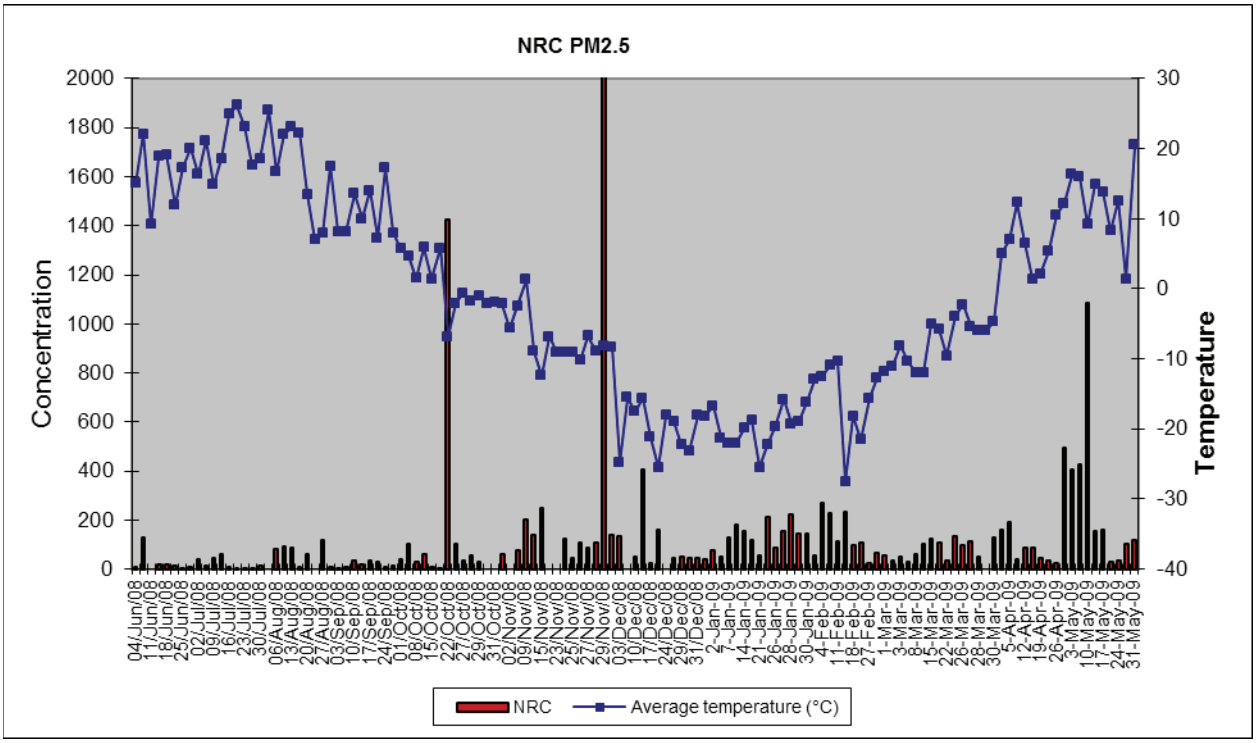

$PM_{2.5}$ concentration (µg/m^3) and temperature in NRC site.

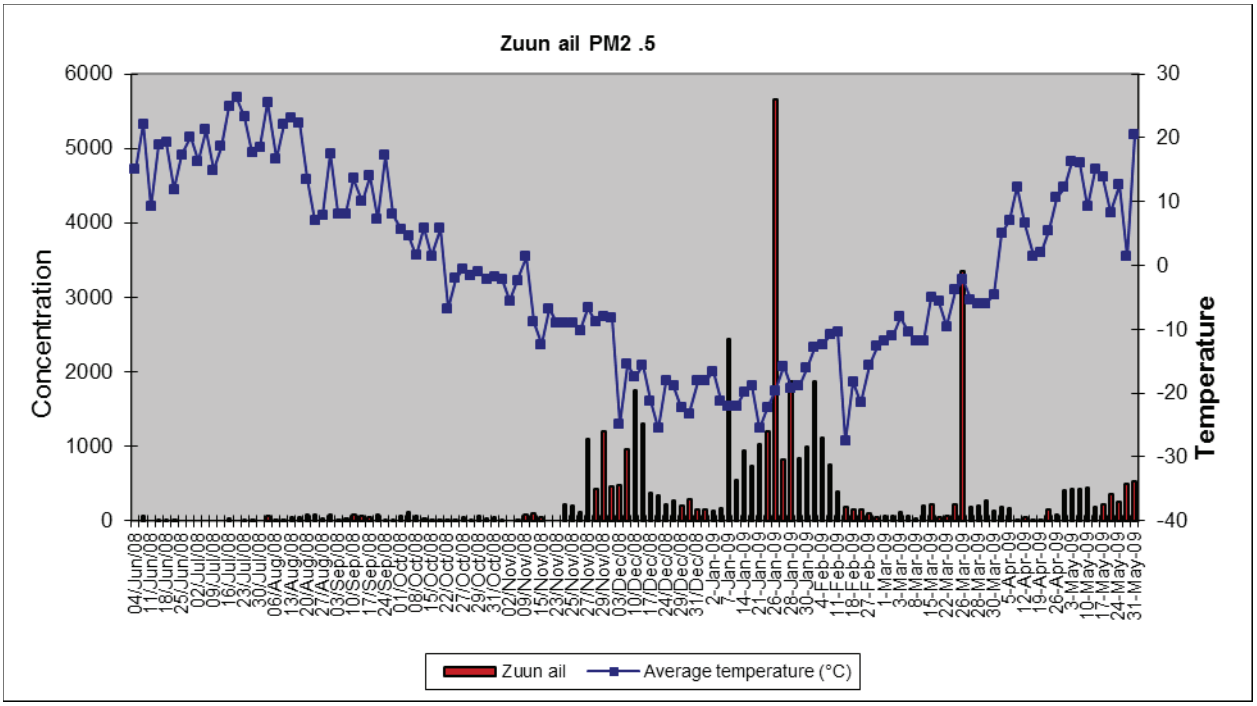

$PM_{2.5}$ concentration (µg/m^3) and temperature in Zuun ail site.

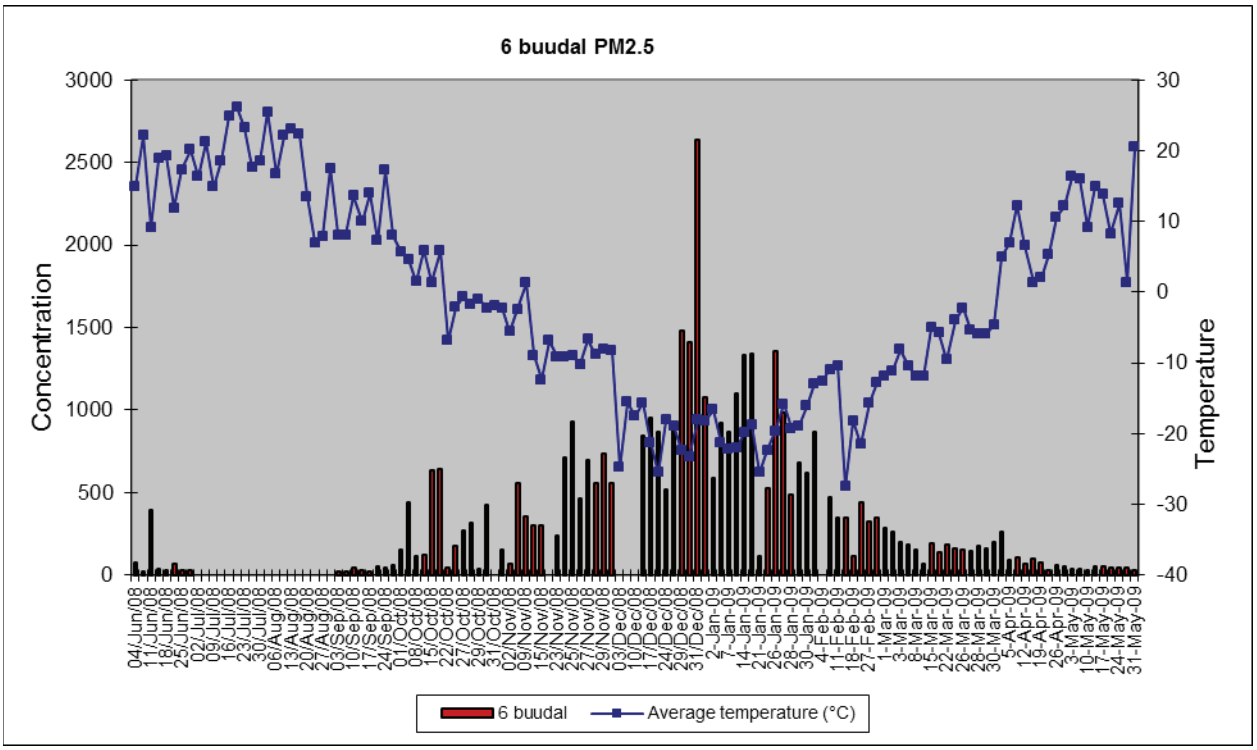

$PM_{2.5}$ concentration (µg/m^3) and temperature in 6 Buudal site.

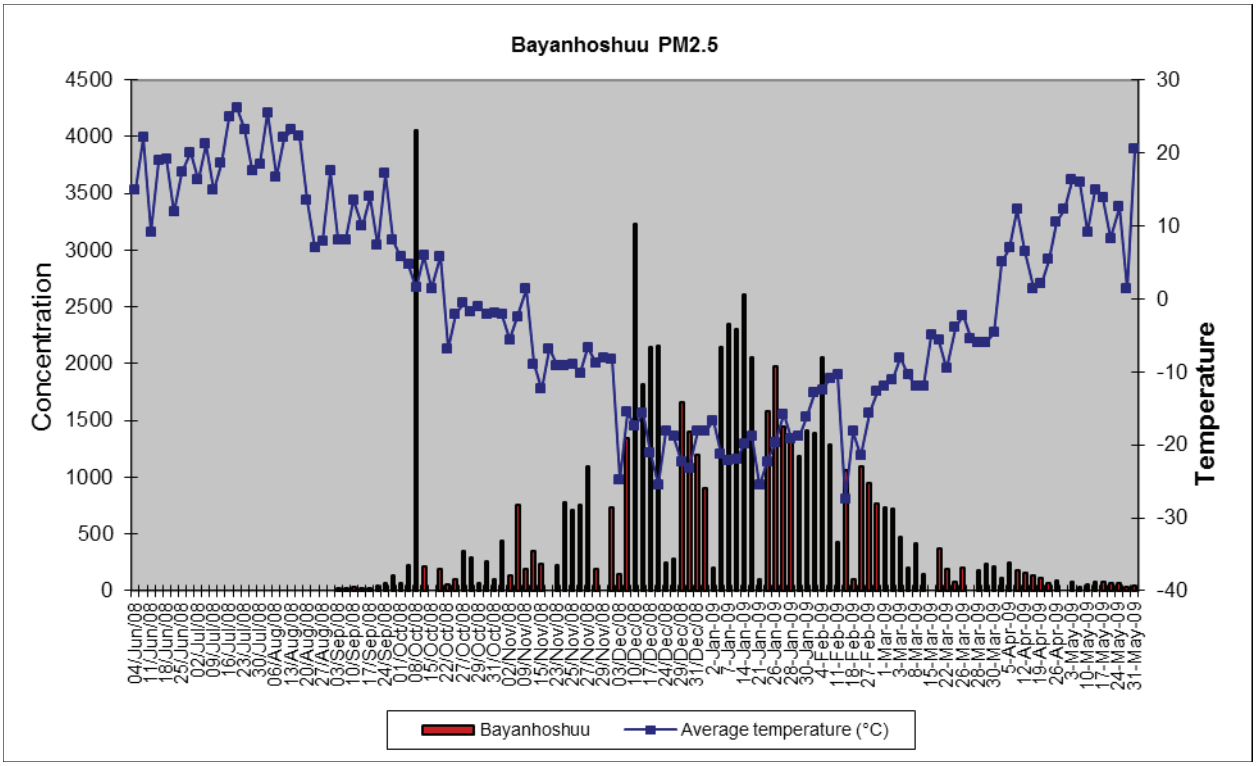

$PM_{2.5}$ concentration vs. temperature at the Bayanhoshuu site.

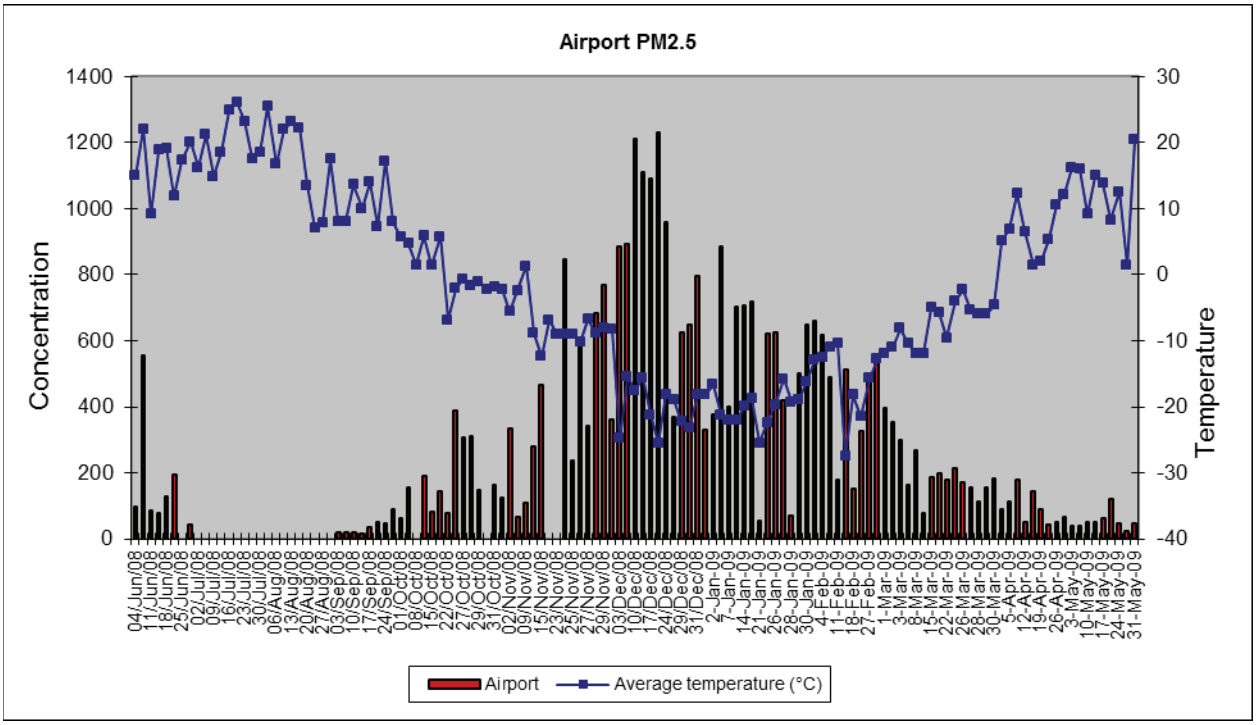

$PM_{2.5}$ concentration ($\mu g/m^3$) and temperature in Airport site.

$PM_{2.5}$/WIND VELOCITY

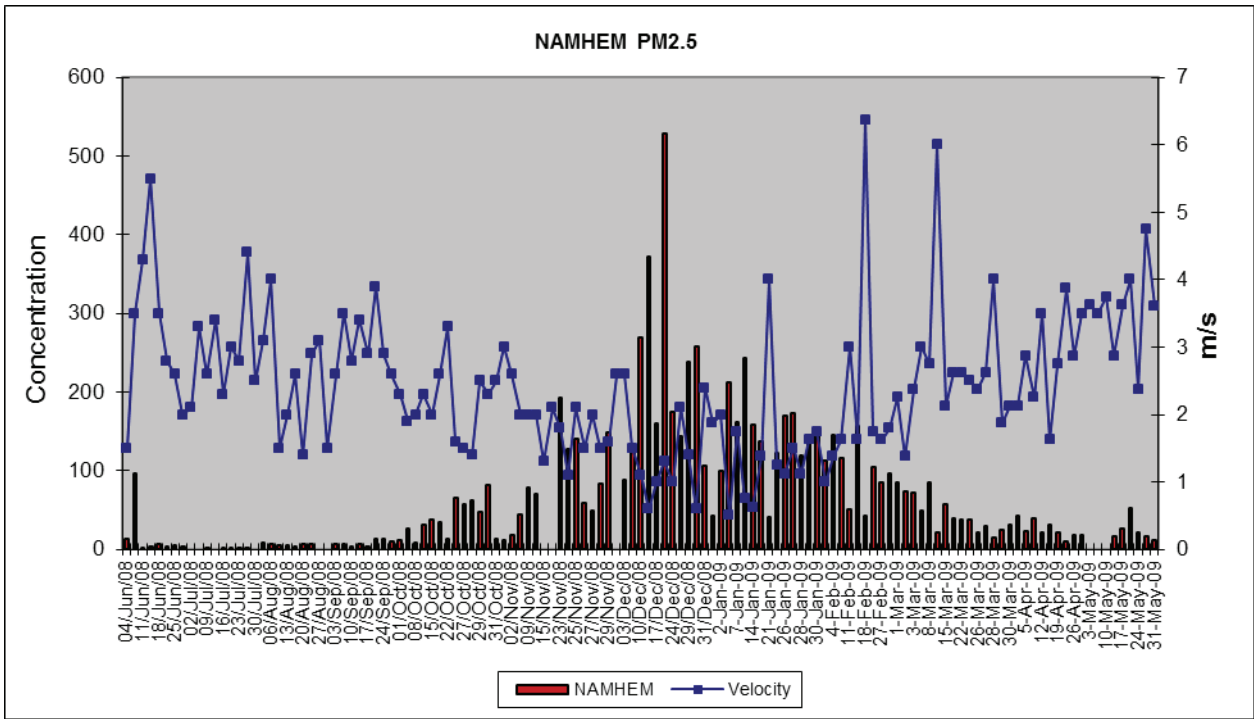

$PM_{2.5}$ concentration (µg/m^3) and wind velocity in NAMHEM site.

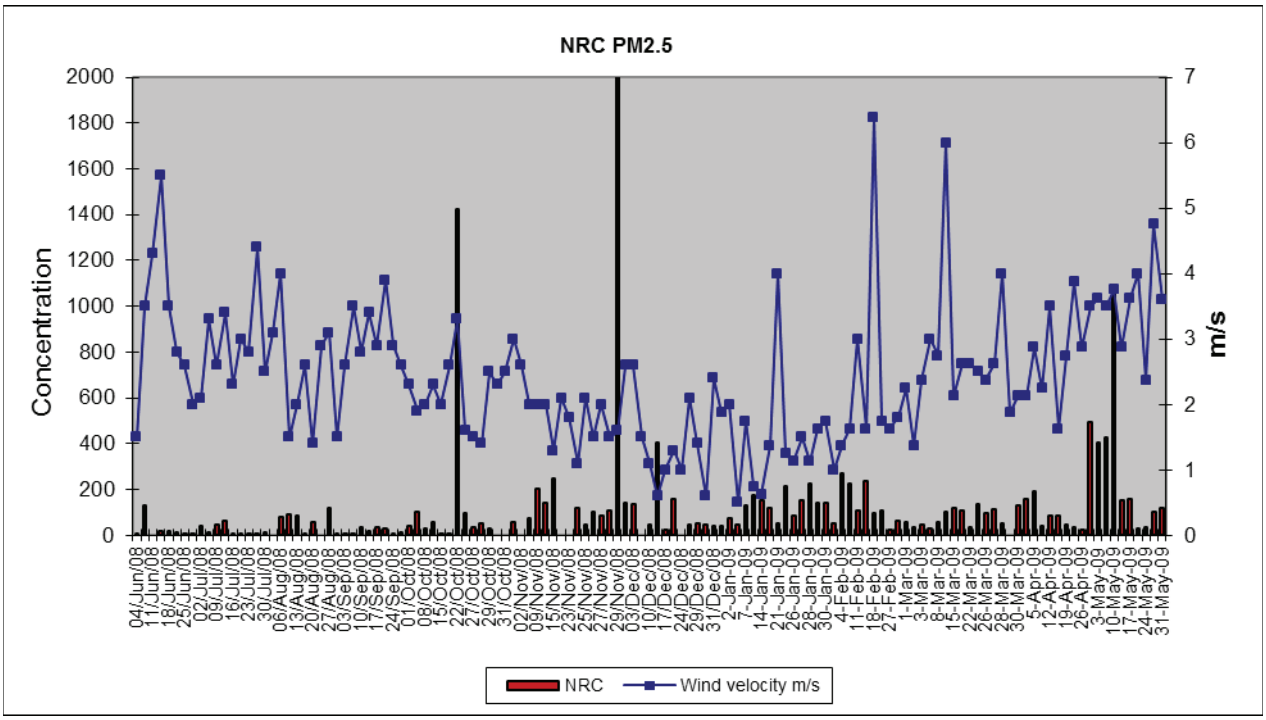

$PM_{2.5}$ concentration (µg/m^3) and wind velocity in NRC site.

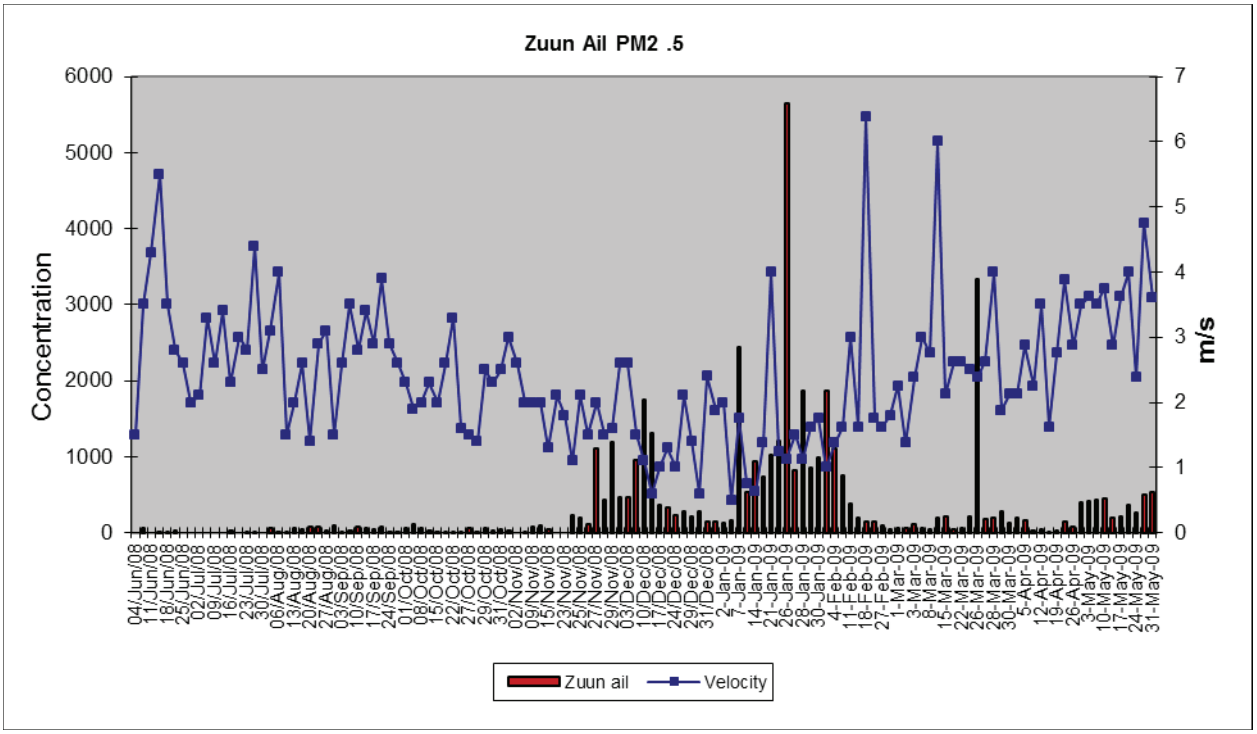

$PM_{2.5}$ concentration (µg/m^3) and wind velocity in Zuun Ail site.

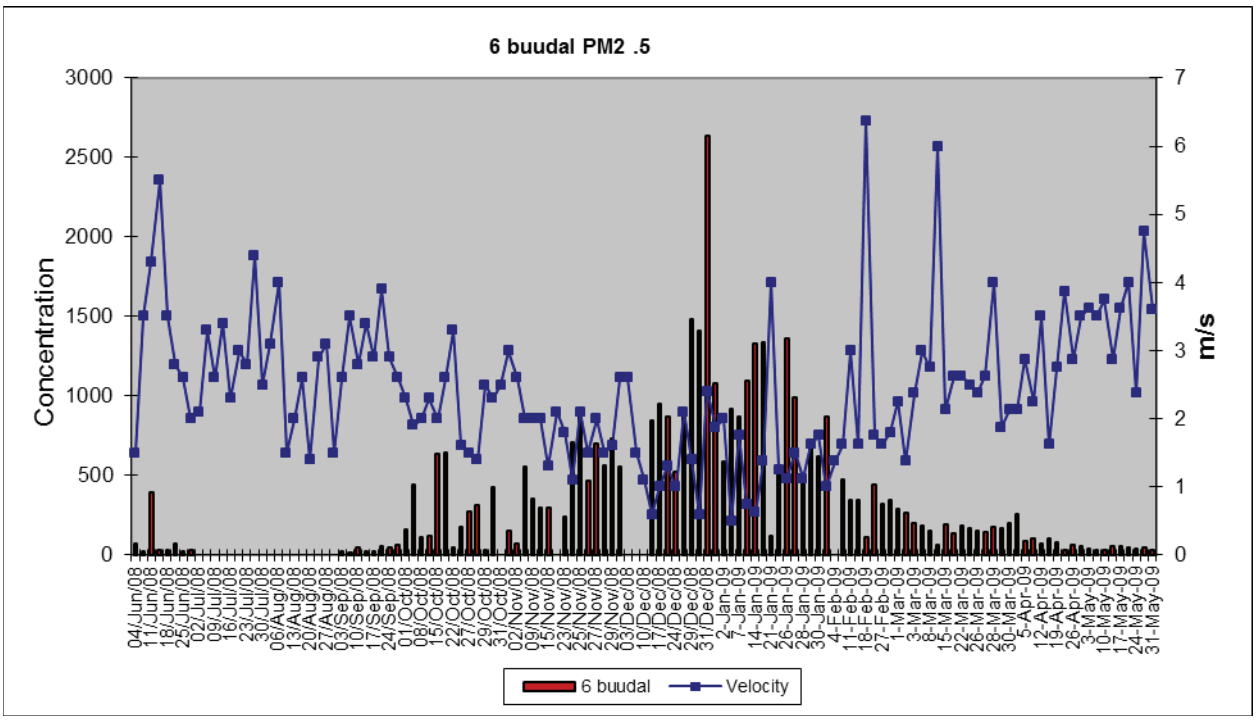

$PM_{2.5}$ concentration (µg/m^3) and wind velocity in 6 Buudal site.

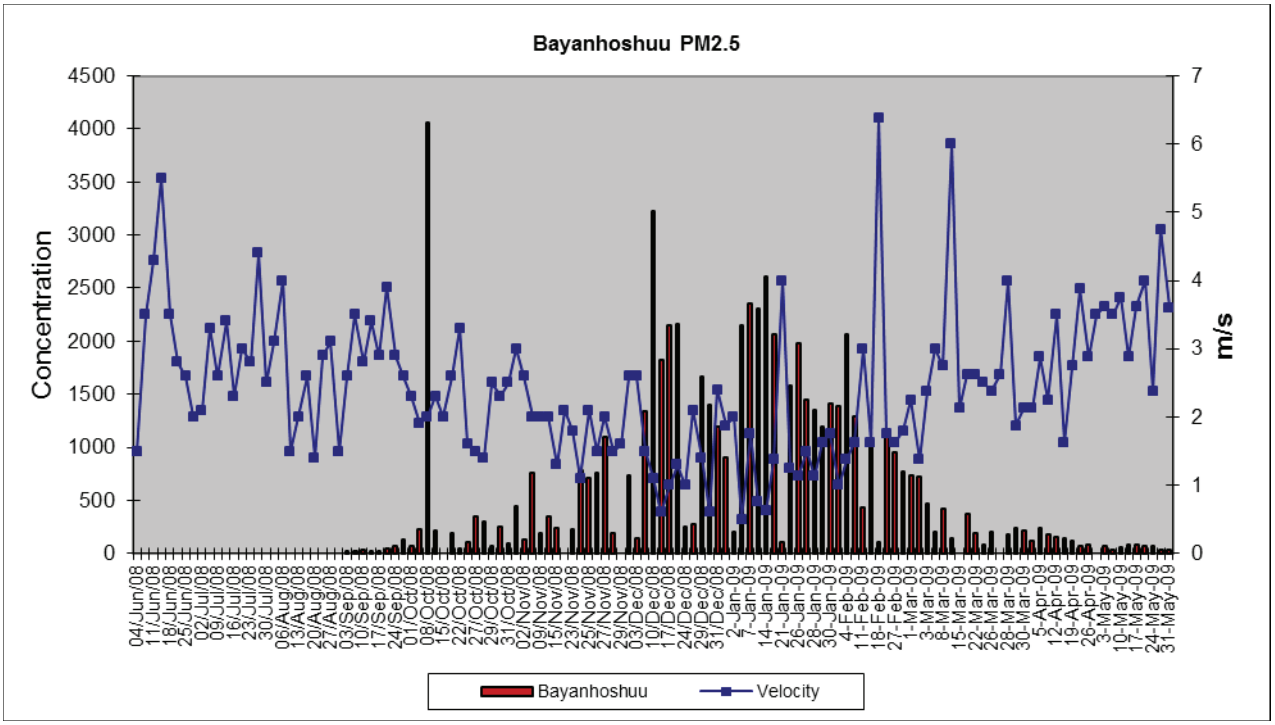

$PM_{2.5}$ concentration (μg/m^3) and wind velocity in Bayanhoshuu site.

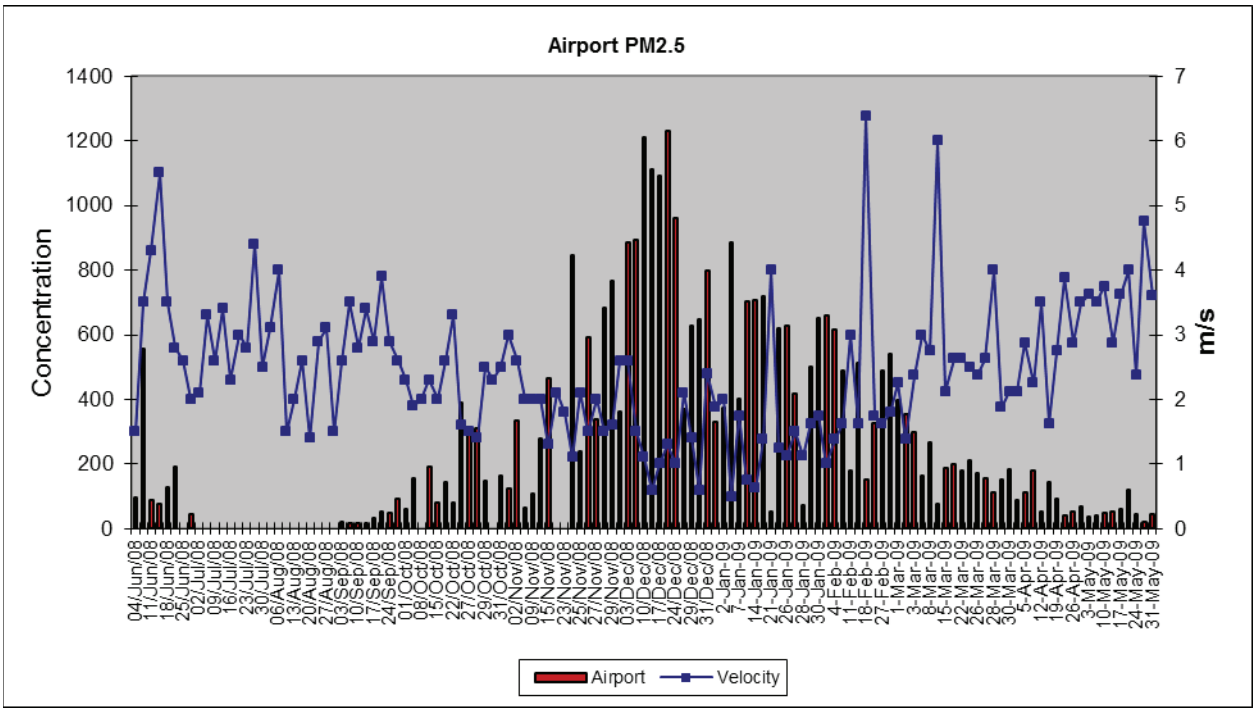

$PM_{2.5}$ concentration (μg/m^3) and wind velocity in Airport site.

$PM_{2.5}$/HUMIDITY

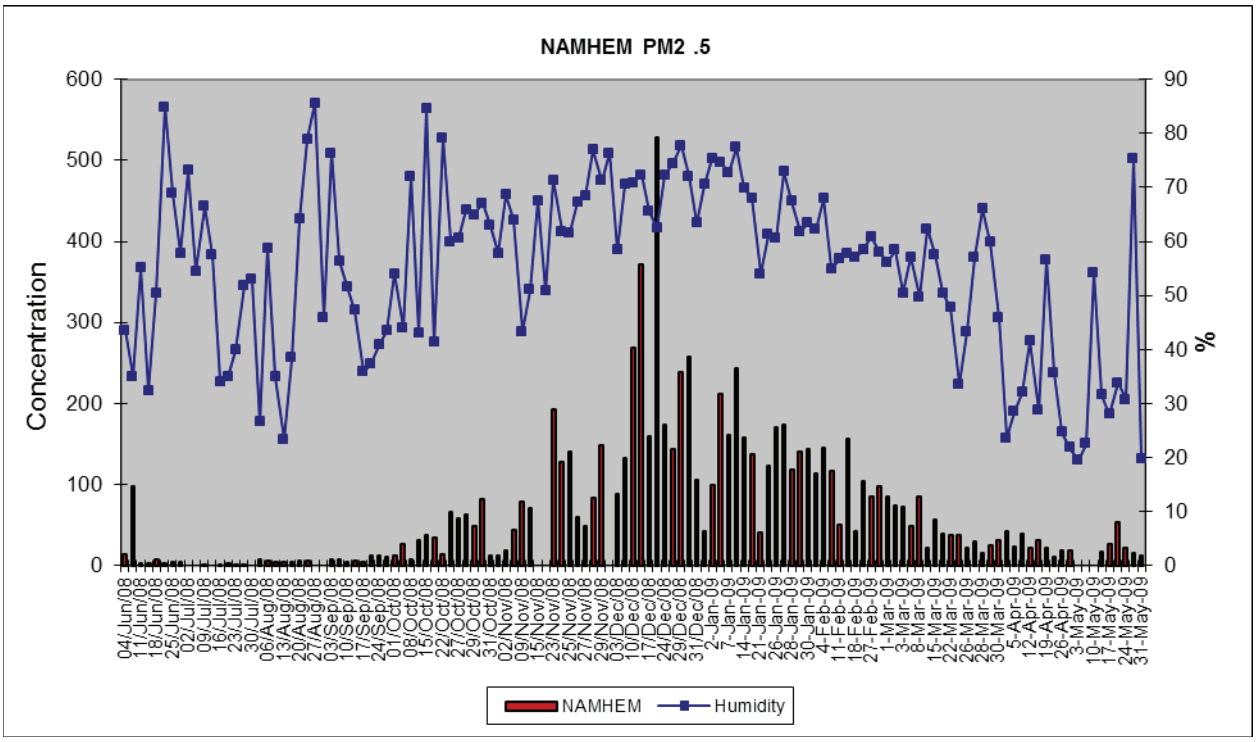

$PM_{2.5}$ concentration (µg/m^3) and humidity in NAMHEM site.

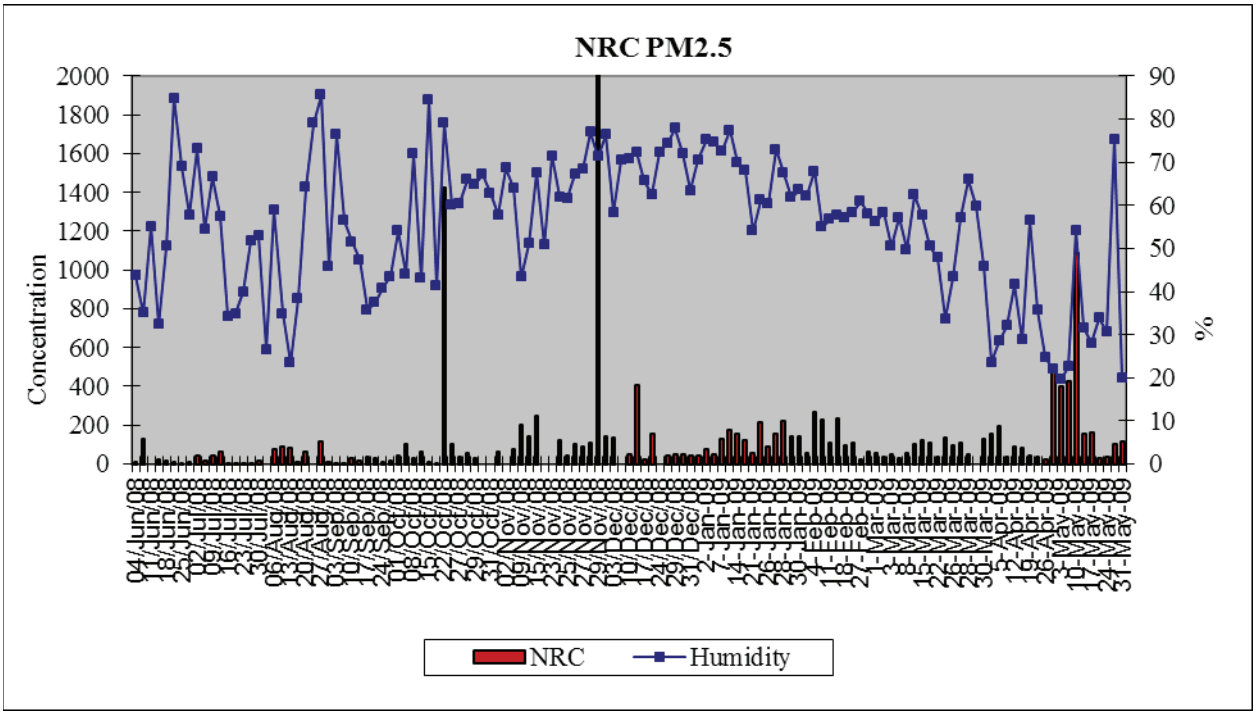

$PM_{2.5}$ concentration (µg/m^3) and humidity in NRC site.

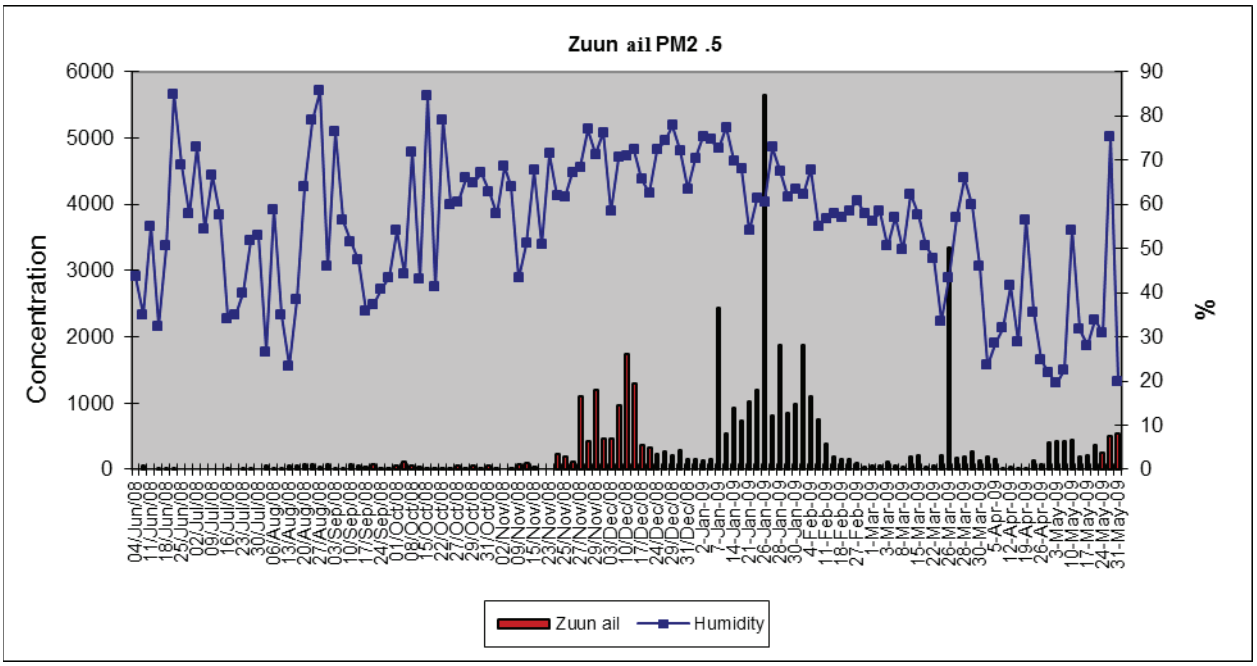

$PM_{2.5}$ concentration (µg/m^3) and humidity in Zuun Ail site.

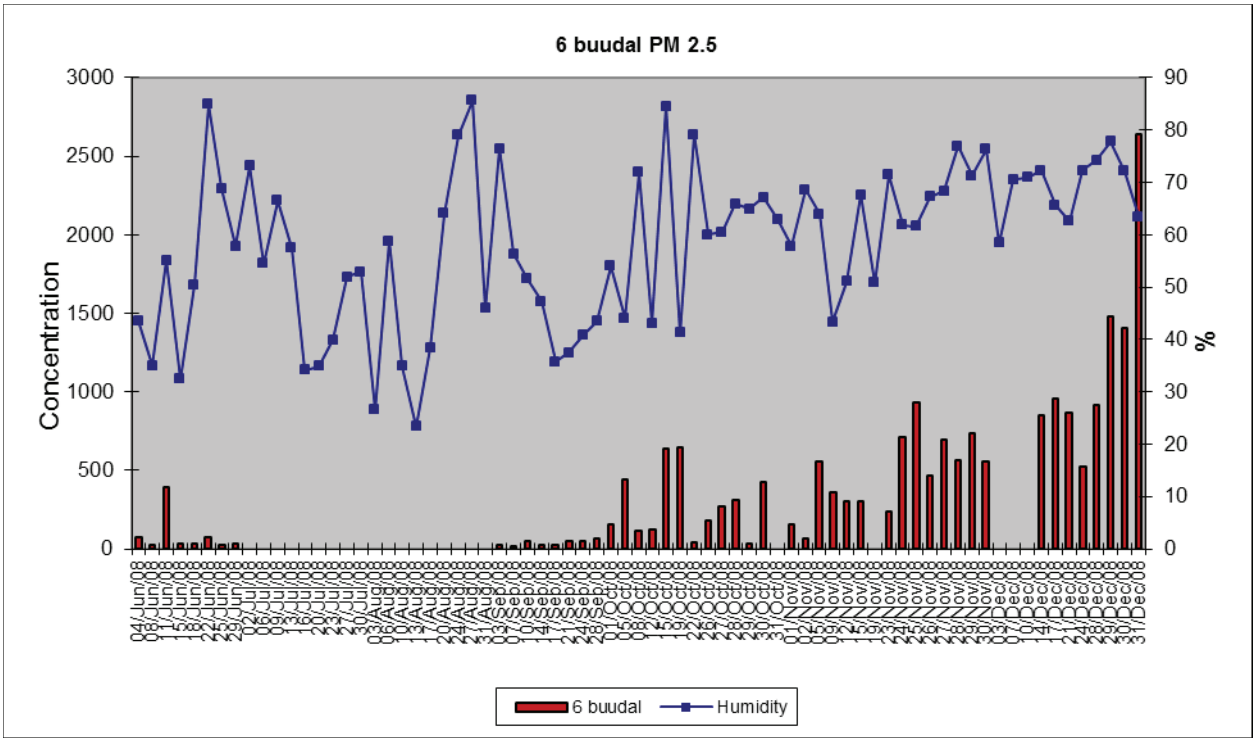

$PM_{2.5}$ concentration (µg/m^3) and humidity in 6 Buudal site.

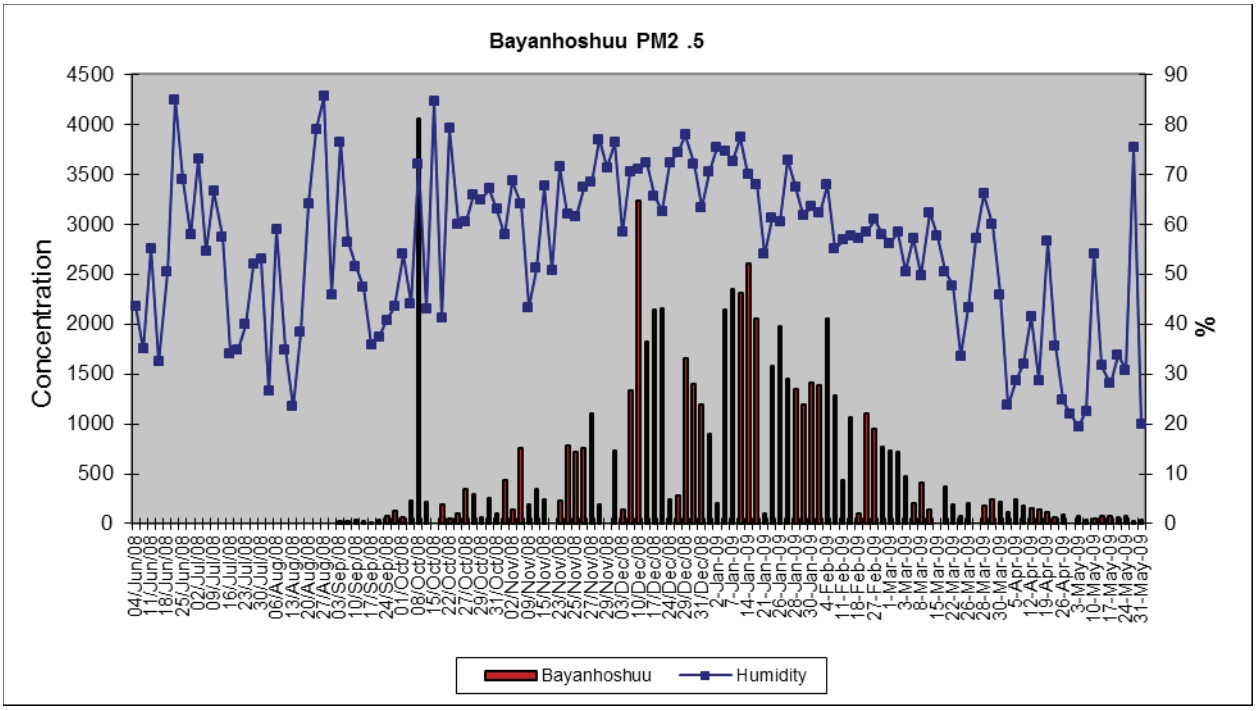

$PM_{2.5}$ concentration (µg/m^3) and humidity in Bayanhoshuu site.

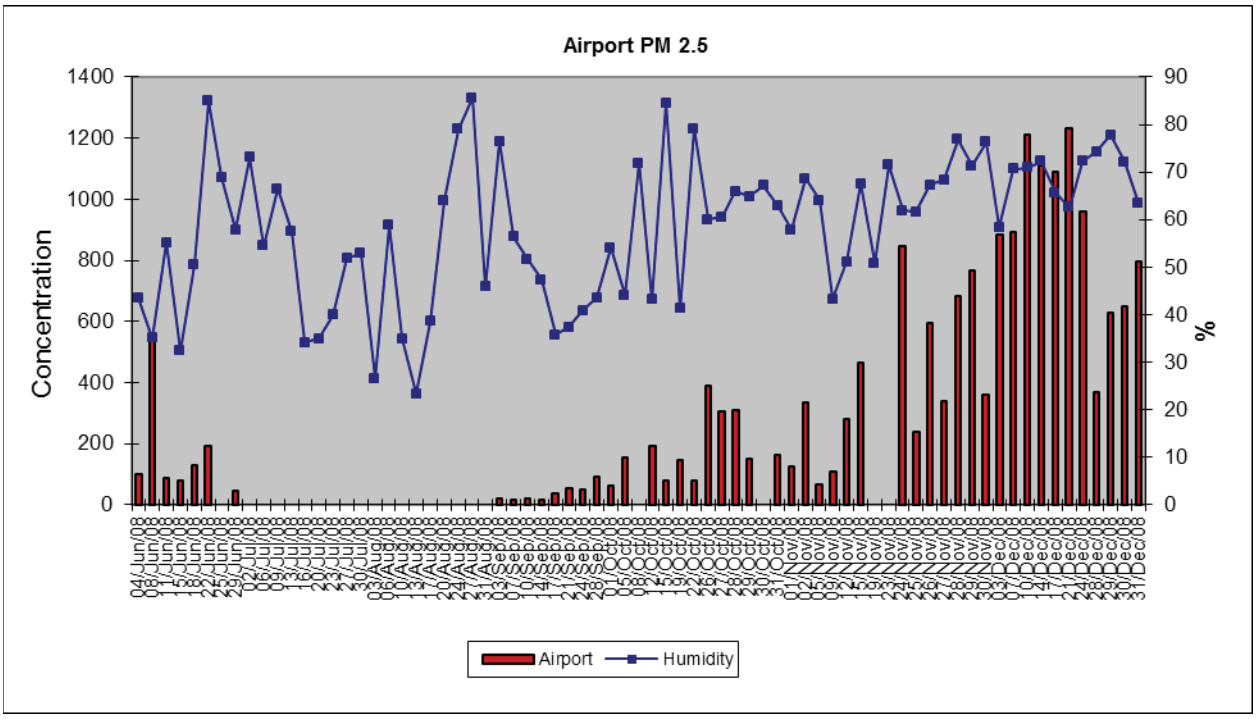

$PM_{2.5}$ concentration (µg/m^3) and humidity in Airport site.

PM_{10}/TEMPERATURE

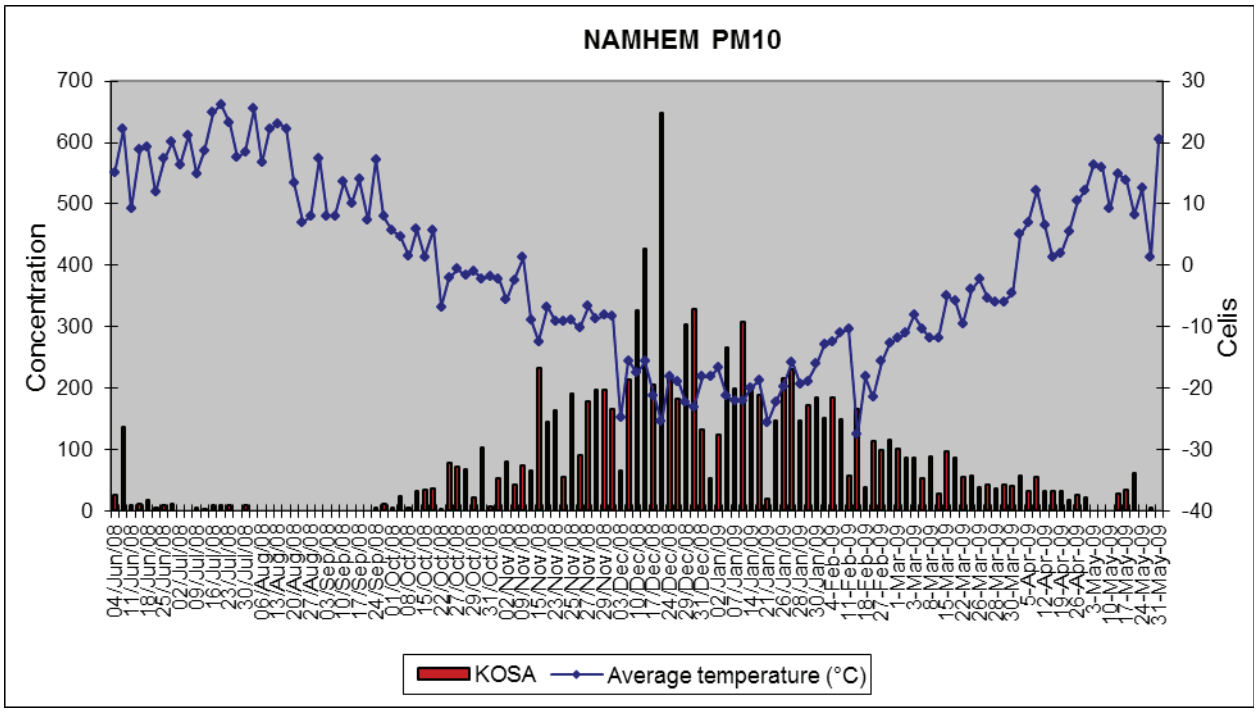

PM_{10} concentration (µg/m^3) and temperature in NAMHEM site.

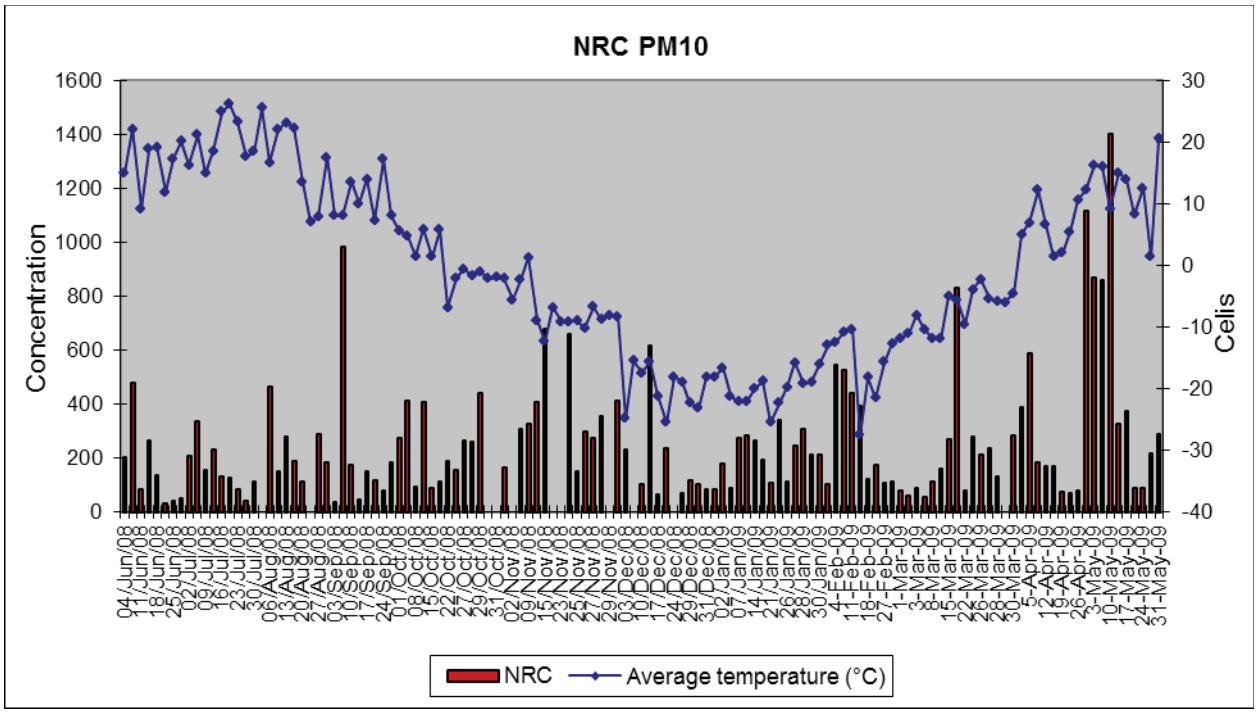

PM_{10} concentration (µg/m^3) and temperature in NRC site.

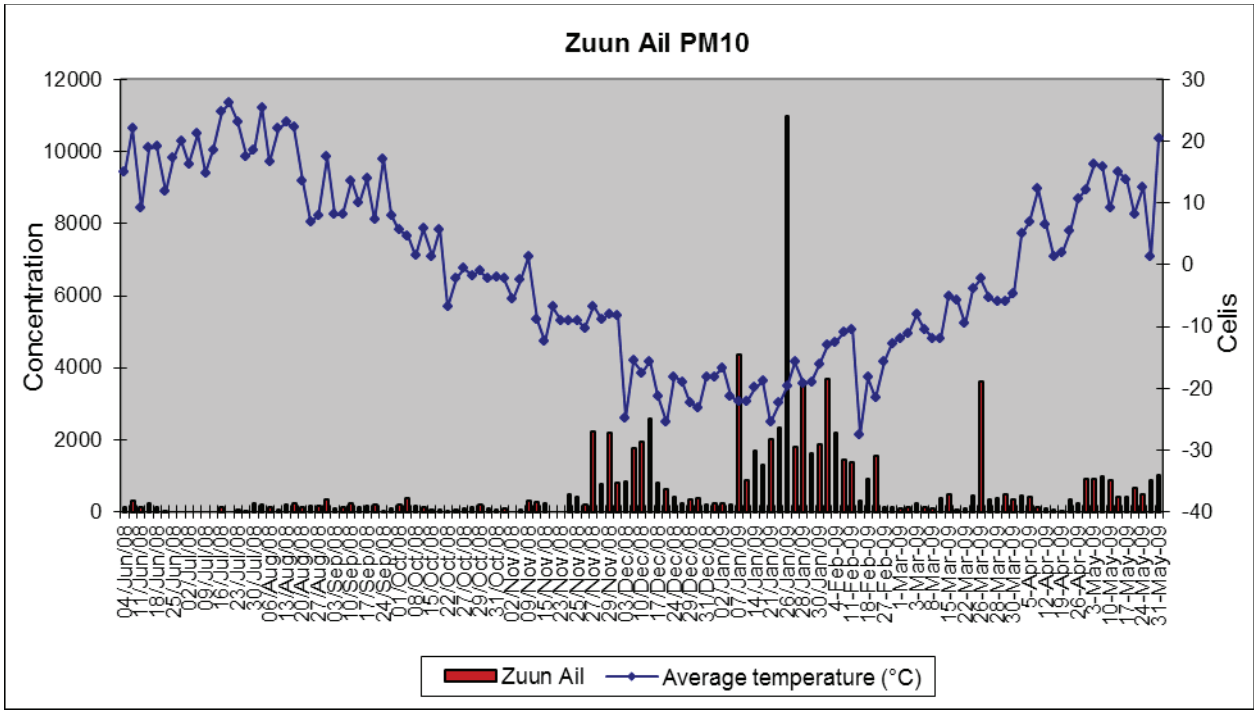

PM_{10} concentration (µg/m^3) and temperature in Zuun Ail site.

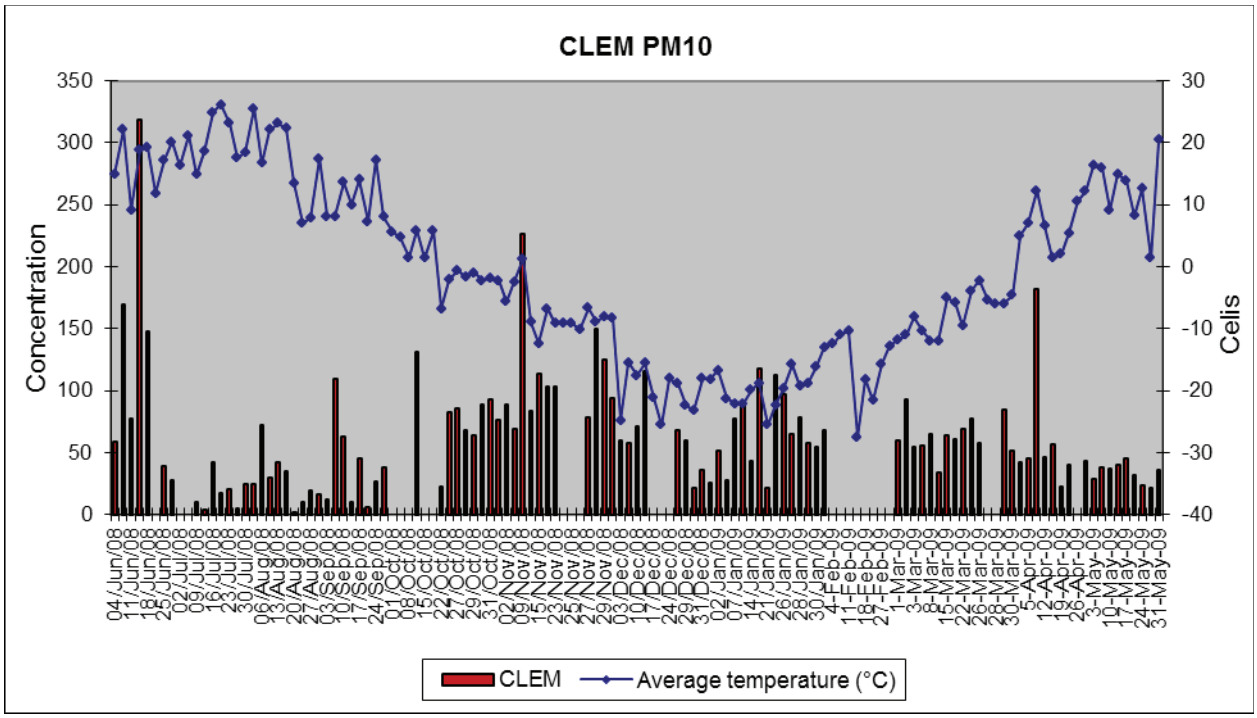

PM_{10} concentration (µg/m^3) and temperature in CLEM site.

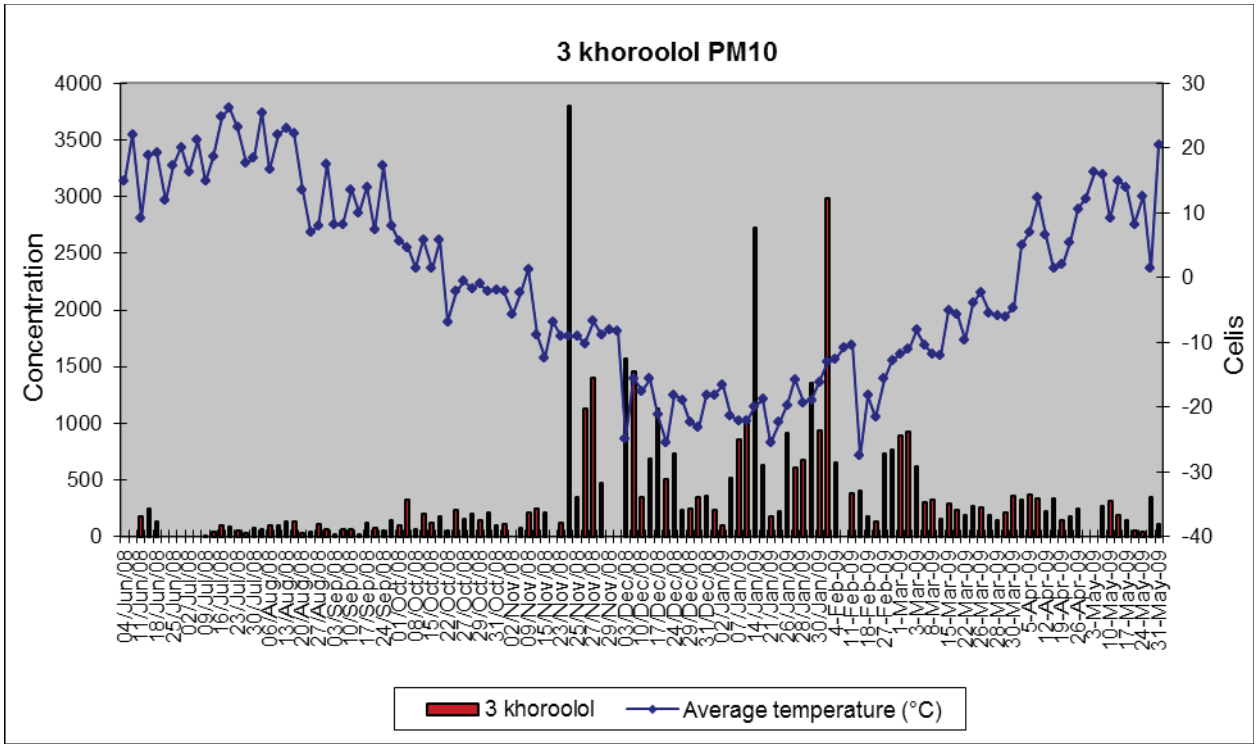

PM_{10} concentration (μg/m^3) and temperature in 3 khoroolol site.

PM_{10}/ WIND VELOCITY

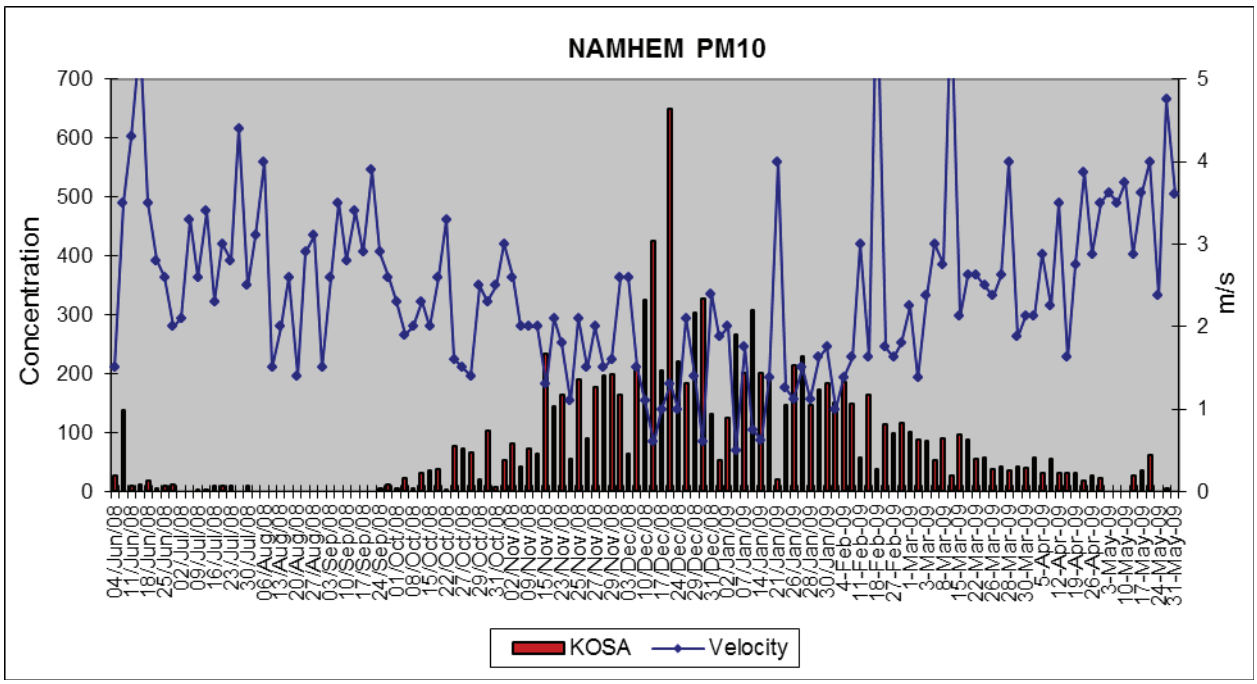

PM_{10} concentration (μg/m^3) and wind velocity in NAMHEM site.

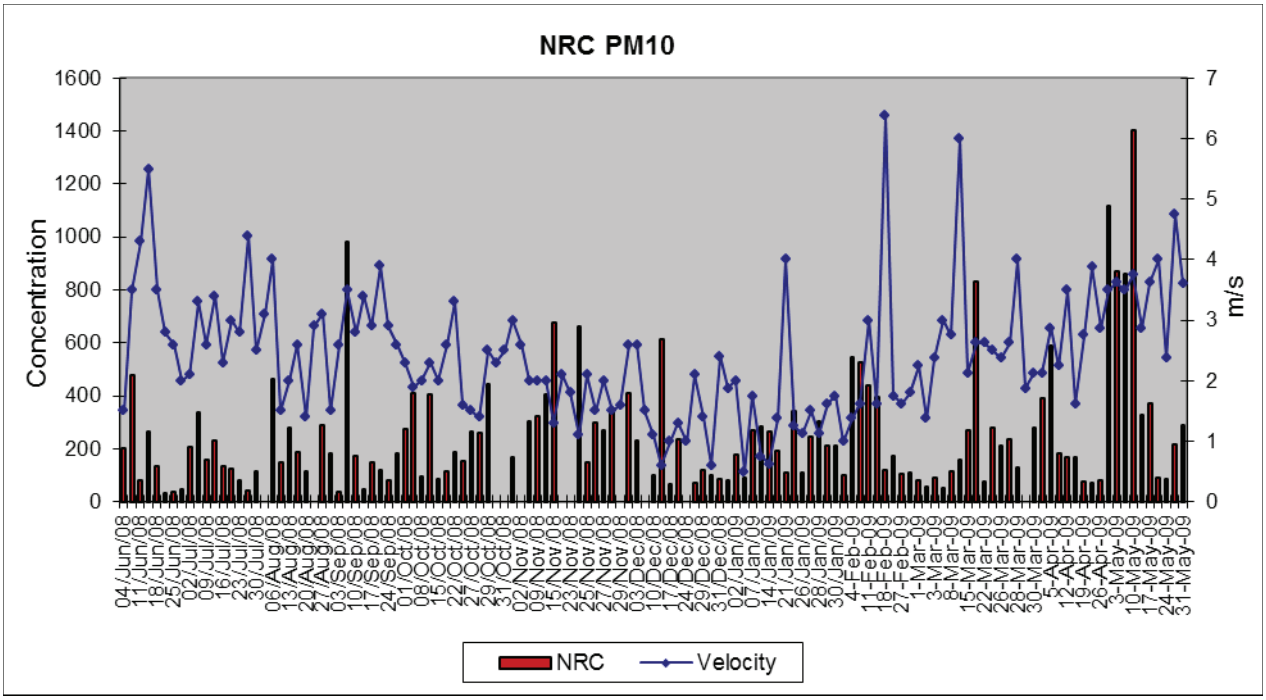

PM_{10} concentration (µg/m^3) and wind velocity NRC site.

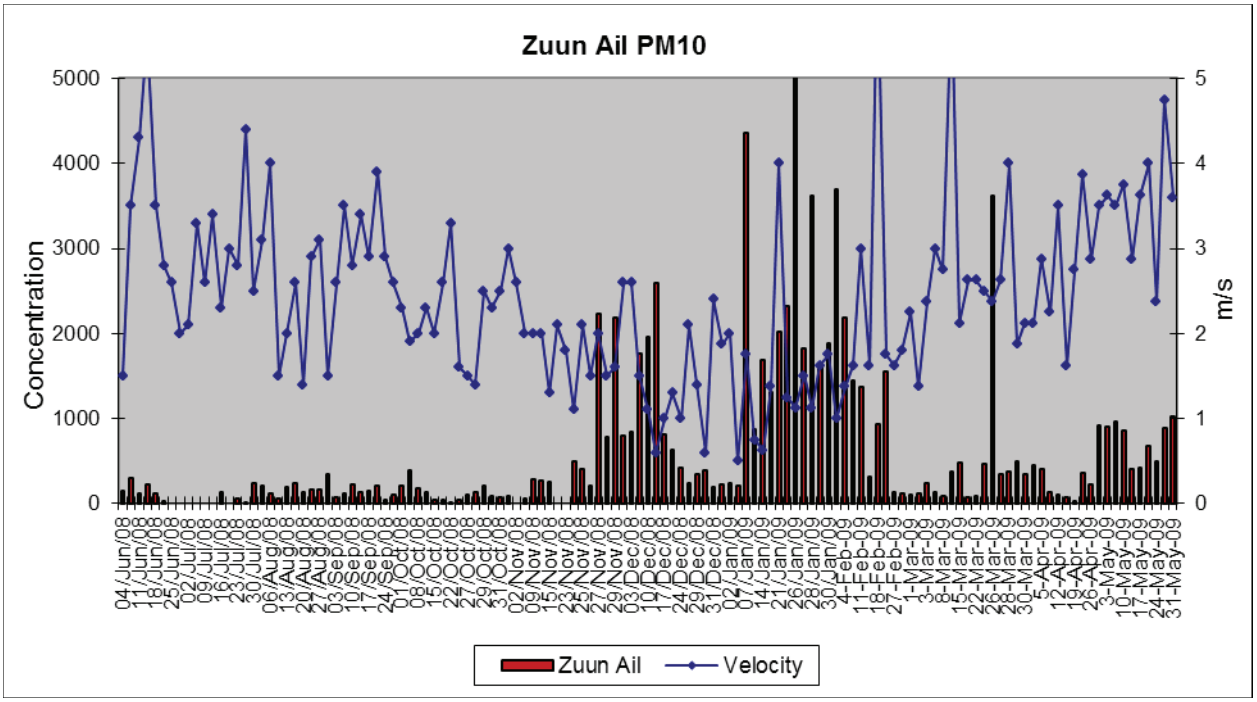

PM_{10} concentration (µg/m^3) and wind velocity in Zuun Ail site.

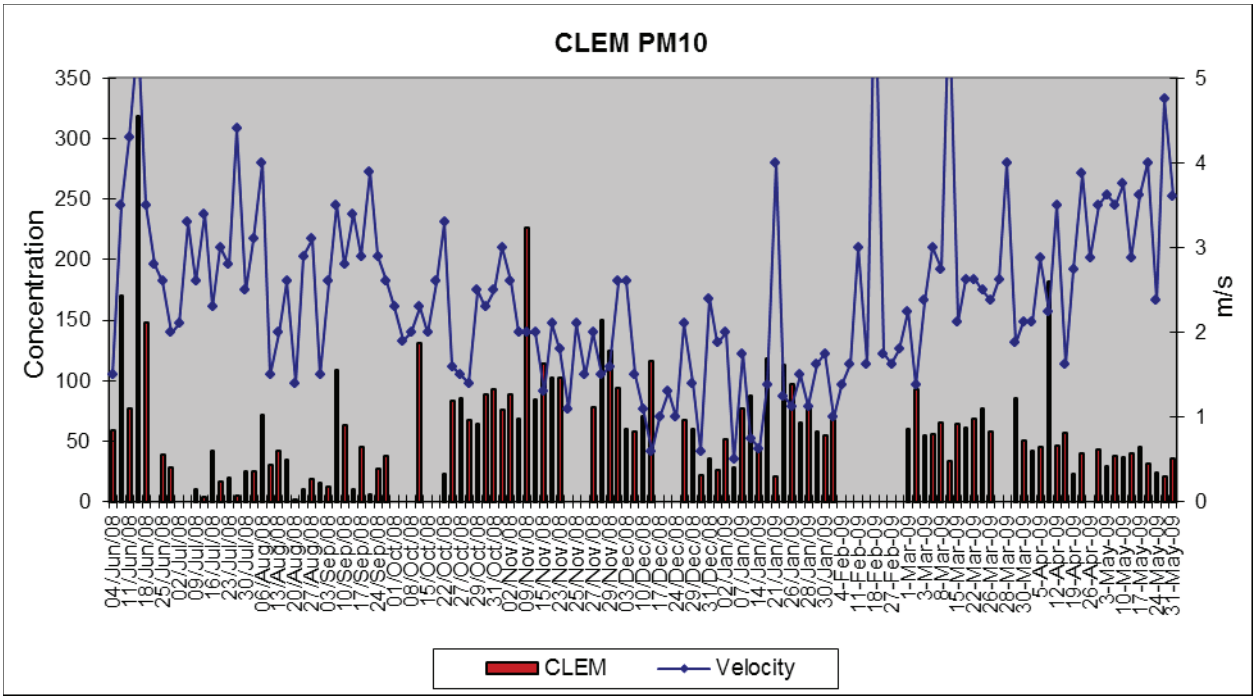

PM_{10} concentration (µg/m^3) and wind velocity in CLEM site.

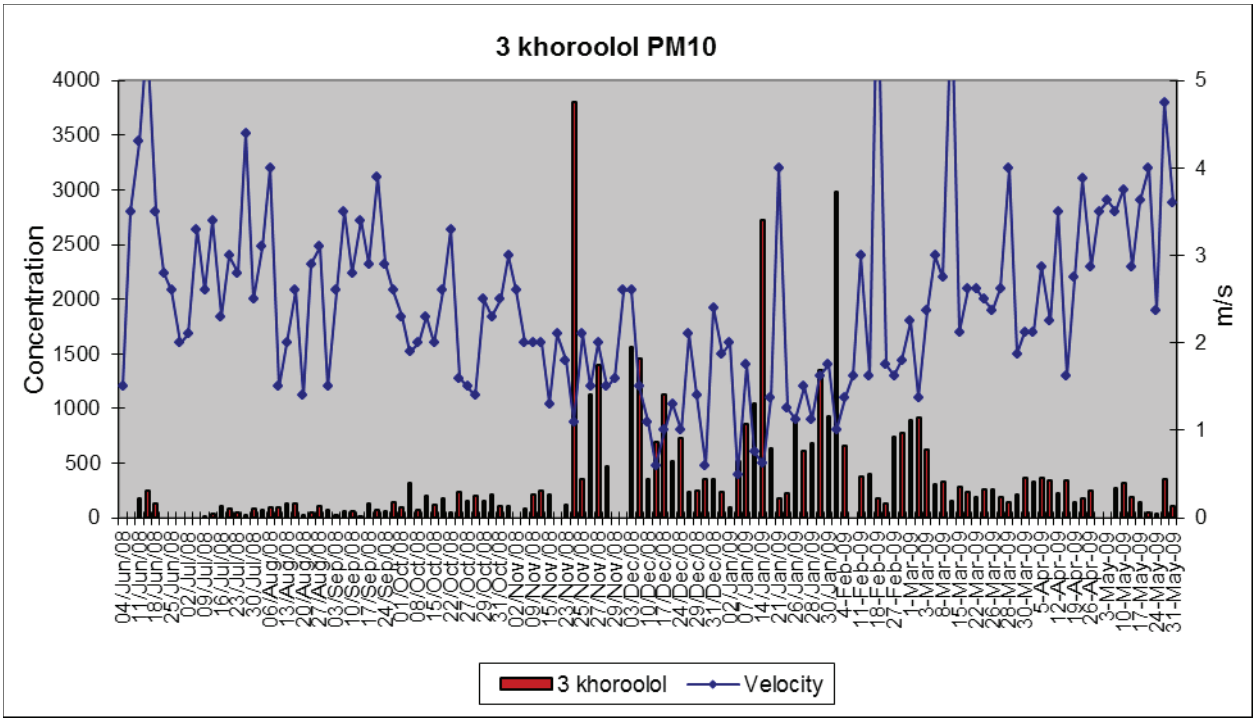

PM_{10} concentration (µg/m^3) and wind velocity in 3 khoroolol site.

PM_{10}/HUMIDITY

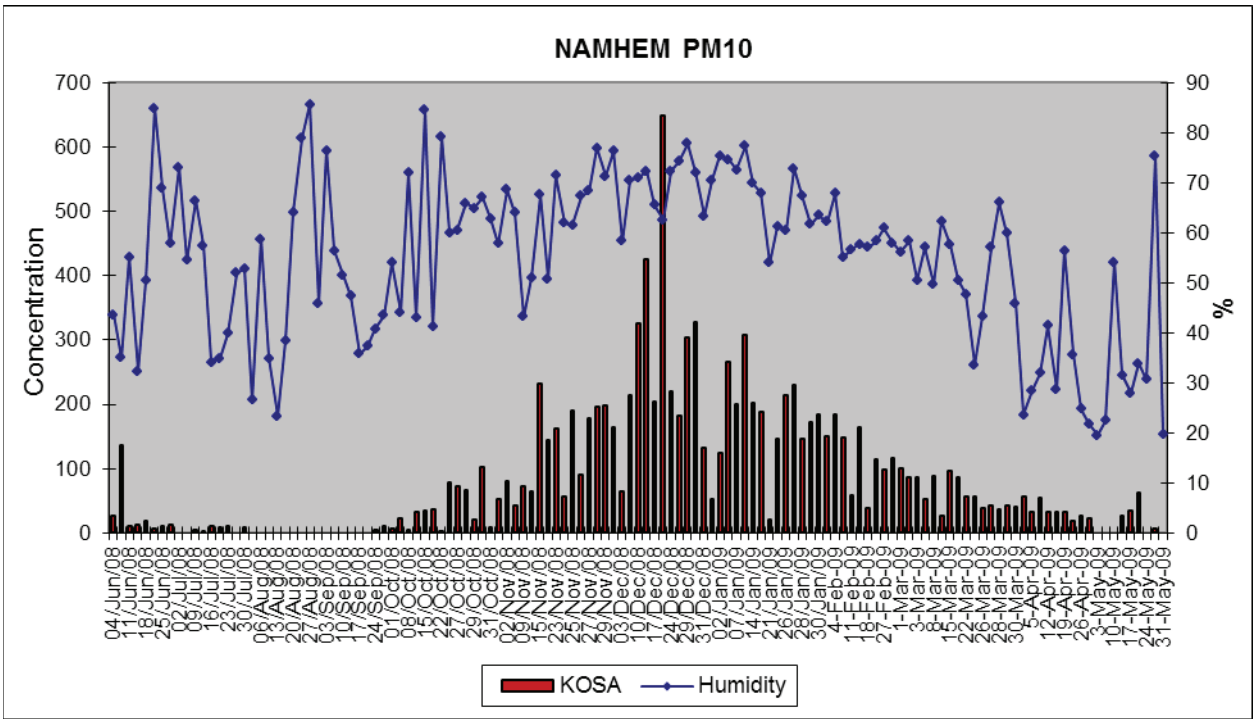

PM_{10} concentration (µg/m^3) and humidity in NAMHEM site.

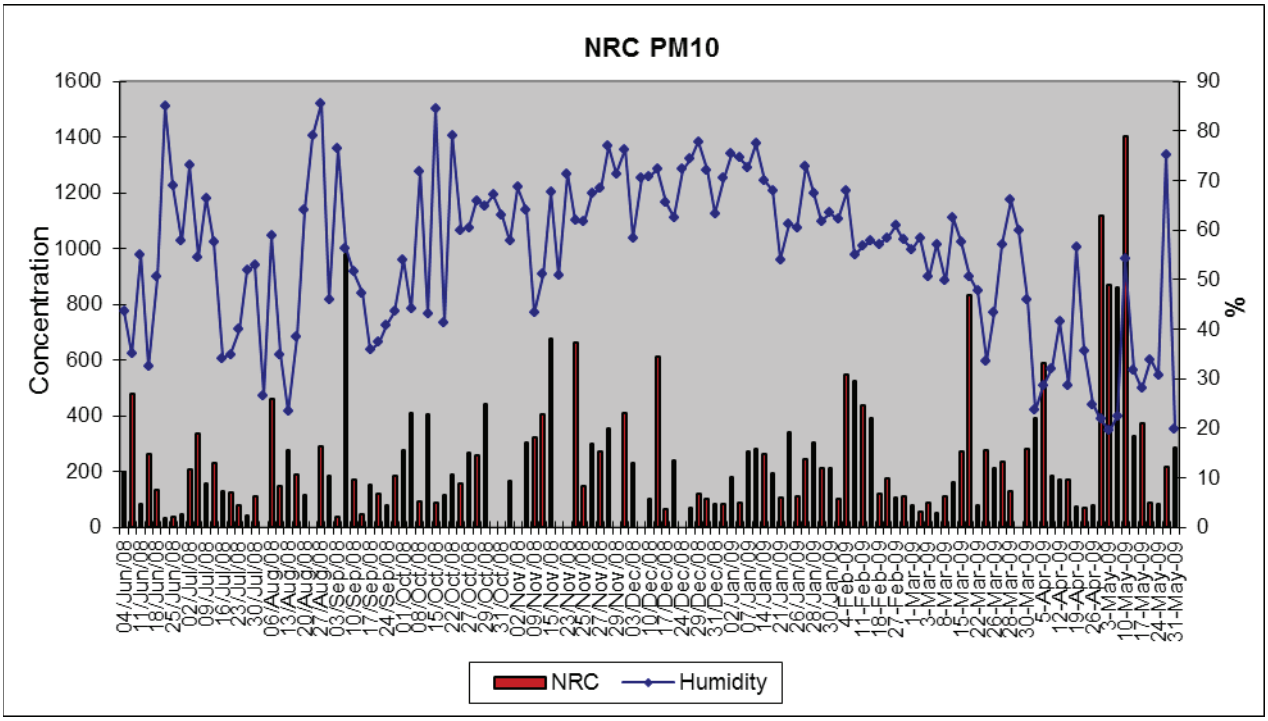

PM_{10} concentration (µg/m^3) and humidity in NRC site.

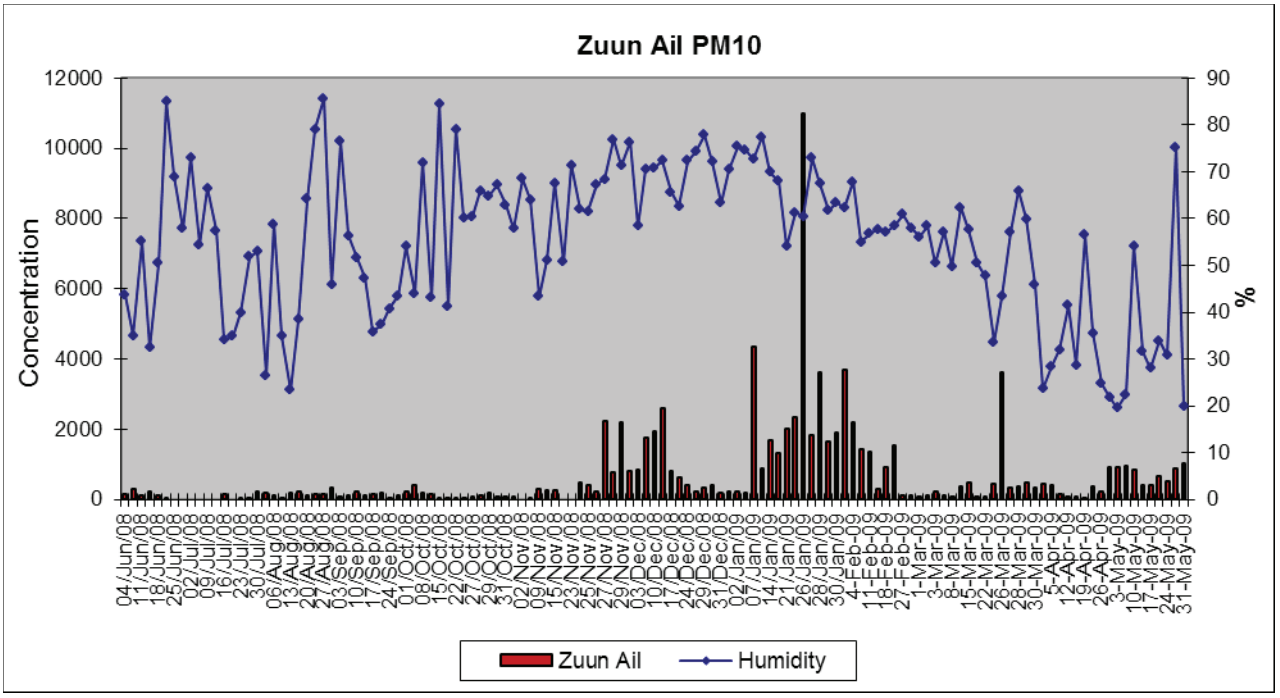

PM_{10} concentration (µg/m^3) and humidity in Zuun Ail site.

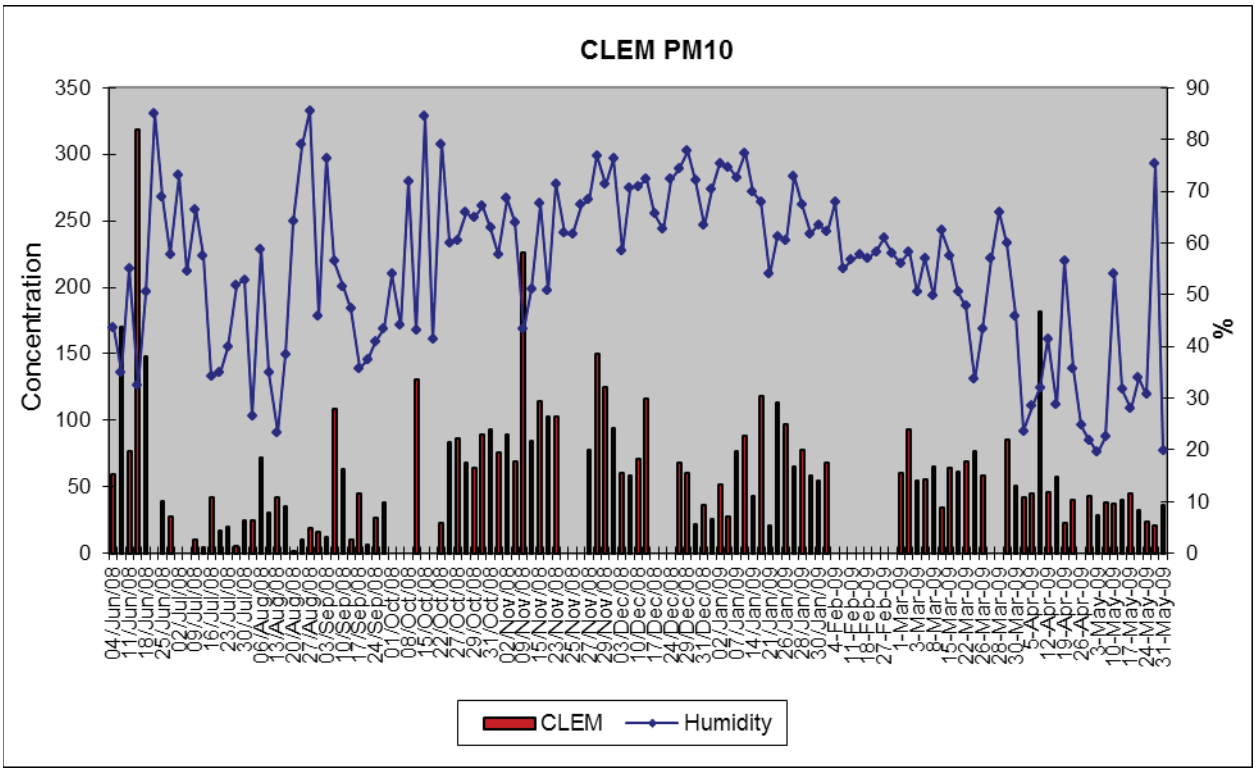

PM_{10} concentration (µg/m^3) and humidity in CLEM site.

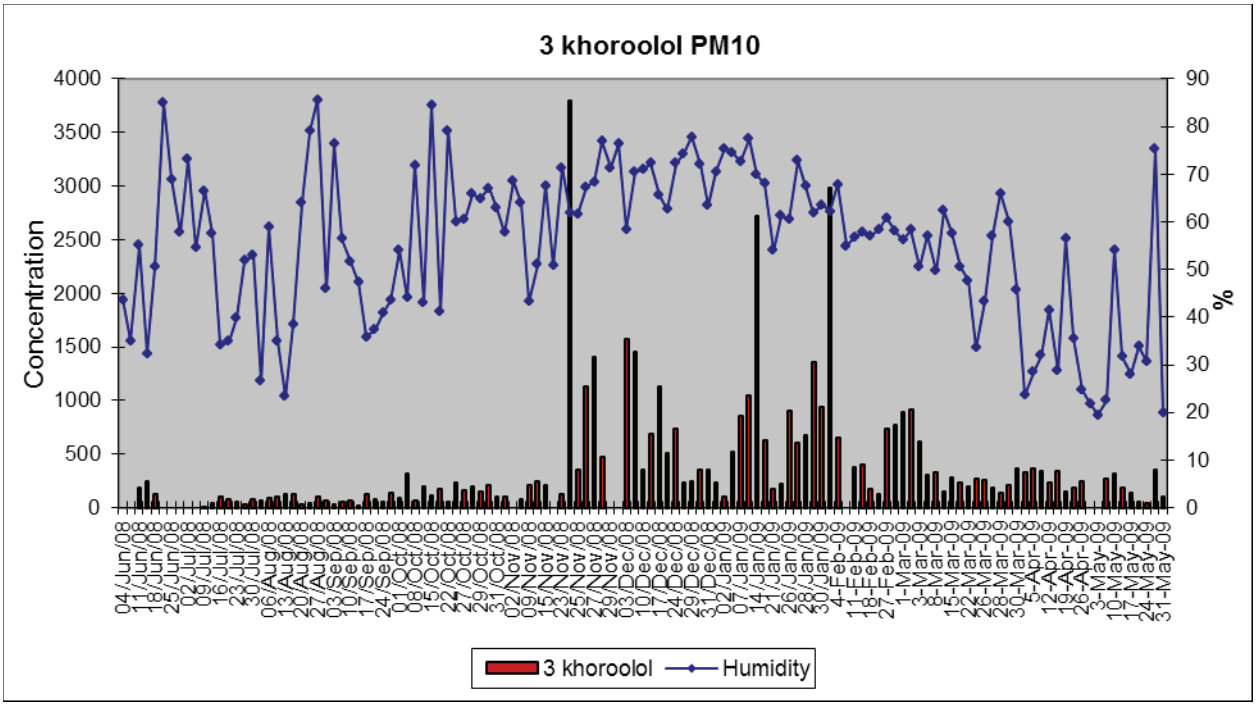

PM_{10} concentration (μg/m^3) and humidity in 3 khoroolol site.